Voltage-Based Backup Protection and Protection Performance Analysis using Wide-Area PMU data

Fangzhu Yu

A thesis submitted for the degree of Doctor of Philosophy to

Department of Electronic and Electrical Engineering

University of Strathclyde

April 2019

This thesis is the result of the author's original research. It has been composed by the author and has not been previously submitted for examination which has led to the award of a degree.

Abstract

This dissertation describes a system that analyses and summarises the operation of protection and provides backup protection functionality, using only voltage data from PMUs and wide-area communications infrastructure. The ability to rapidly identify the presence of faults, their locations and the presence of protection/circuit breaker failures, solely from voltage measurements, is the overarching contribution from this work. The scheme can operate in addition to existing backup schemes to provide a further, or alternative, relatively inexpensive, effective, simple, fast, wide-area backup protection to improve the resilience of power systems. Methods of power system model simplification for different types of fault have also been developed for establishing the capabilities and voltage thresholds of the scheme, and this simplification method is also claimed as a contribution arising from the work. It is shown how the system can operate for a wide range of fault levels, types and resistances – thereby addressing one of the key challenges for protection associated with concerns over protection in the context of reducing and more variable fault levels in future power systems.

To validate the developed scheme, case studies assessing scheme performance in several scenarios are presented. Variations of fault resistance, time of fault occurrence, fault location, and fault levels are simulated in Matlab (Simscape Power Systems) using the well-established and accepted IEEE 14-bus network.

Hardware in the loop tests are also conducted using an RTDS and actual PMU devices to test and validate the performance of the scheme and to demonstrate its ability to operate using actual hardware and in real time. Applicability of the developed system to large-scale power networks is also demonstrated. It is shown that the scheme is suited to interconnected power systems, and can operate with both reduced fault levels and for different types of faults with high resistances. Future work and suggestions for extensions to the developed system are also presented.

Acknowledgements

I would like to express my sincere gratitude to my supervisors Prof Campbell Booths and Dr Adam Dyśko for the continuous support of my PhD study and related research, for their patience, motivation, and immense knowledge. Their guidance helped me in all the time of research and writing of this dissertation.

Special thanks to Dr Qiteng Hong and Dr Steven Blair. I'm immensely grateful for their help and support to my PhD. I owe a lot of gratitude to others in our research group as well. There are many colleagues kept me carrying on, and they know who they are.

My gratitude extends to my friends that accompany me along the way of my research for the support. I would like to thank Xiaotong Li, Xuhui Duan, Mengran Yu and Xiaozuo Huang for their caring and understanding during my PhD study.

Finally, I would especially like to thank my parents, Yue Yu and Hua Feng and all the families and friends for all their supports and encouragements over the years. This dissertation is dedicated to them.

Contents

List of Figures

List of Tables

Glossary of Abbreviations

ANM	Active network management
ATM	Asynchronous transfer mode
CB	Circuit breaker
CBF	Circuit breaker fail protection
CT	Current transformer
DAR	Delayed auto-reclose
DFT	Discrete fourier transform
DG	Distributed generators
DT	Definite time
DTT	Direct transfer trip
EI	Extremely inverse
ETYS	Electrical ten year statement
FES	Future energy scenarios
FRT	Fault ride through
GB	Great Britain
GOOSE	Generic object oriented substation event
GPS	Global positioning system
HVDC	High voltage direct current
IDMT	Inverse definite minimum time
IP/MPLS	Internet protocol / multiprotocol label switching
IEC	International electrotechnical commission
KCL	Kirchhoff's current law
KVL	Kirchhoff's voltage law

LFDD	Low frequency demand disconnection
LOM	Loss of mains
NSG	Non-synchronous generation
NG	National Grid
OC	Open circuit
PDC	Phasor data concentrator
Ph-E	Single-phase to earth
Ph-Ph	Phase to phase
Ph-Ph-E	Phase-phase to earth
Ph-Ph-Ph-E	Three-phase to earth
PLC	Programmable logic controller
PMU	Phasor measurement unit
PNDC	The Power Networks Demonstration Centre
pu	Per-unit
RFT	Fault ride through
RoCoF	Rate of change of frequency
RTU	Remote terminal units
SC	Short circuit
SCADA	Supervisory control and data acquisition
SCL	Short circuit level
SDH	Synchronous digital hierarchy
SI	Standard inverse
SOF	System operability framework
SONET	Synchronous optical network
TCP/IP	Transmission control protocol/internet protocol
TDM	Time division multiplexing
TM	Time multiplier
UDP	User datagram protocol
URTDSM	Unified real time dynamic state measurement
UTC	Universal time coordination
VI	Very inverse

VISOR	Visualisation of real time system dynamics using enhanced monitoring
VT	Voltage transformers
WAMPAC	Wide-area monitoring, protection and control
WAMS	Wide-area monitoring system

Chapter 1

Introduction

1.1 Introduction and motivation for research

The motivation for this research and its contributions are twofold. Firstly, power systems are growing and changing significantly and this, as explained later, will result in significant reductions in fault levels in some parts of the system, and much greater volatility and variability in the magnitudes of faults currents compared to present levels. Furthermore, associated with the future power systems, many of the generation sources will be renewable in nature, many of them might be interfaced via power electronics converters and may not be as "resilient" during fault conditions, particularly on rare occasions when backup protection is required and the fault therefore remains on the system for longer – this may result in generators not being able to "ride through" fault situations – accordingly faster backup protection may be attractive in the future. Secondly, the proliferation of PMUs and high-performance wide-area communications systems is growing, which makes it easier to apply PMU measurements for monitoring, controlling and protection purpose – and therefore there is potential to carry out backup protection using a PMU/wide-area infrastructure which is already installed for other monitoring purposes – in addition to being able to summarise protection operations and failures, which could be great use to system operators, particularly in times of network stress where multiple faults may be occurring

within a very short time scale and there is a danger of data overload. Accordingly, these are the two main drivers for this work and these are considered in more detail in the following two subsections.

1.1.1 The changing nature of power systems

1.1.1.1 General challenges to power systems

The importance and mandated growth in the use of sustainable sources of energy is having a critical impact on future power systems [Ela17, YSWW10]. With increasing penetration of renewable sources and distributed generators (DGs), which are solutions to achieve decarbonisation of electrical energy systems, the inertia of future systems will be much lower and the "strength" of future power systems will be much weaker than that at present, which is depicted in detail in National Grid's (the operator of the power system in Great Britain) Future Energy Scenarios (FES) publications [Nat15a]. Figure 1.1 indicates a predicted generation mix for the future. The increasing trend of transferring power using converter-based sources (e.g. from renewable energy sources, embedded generation, HVDC interconnectors, storage and loads) brings various challenges to system operation, monitoring, protection and control.

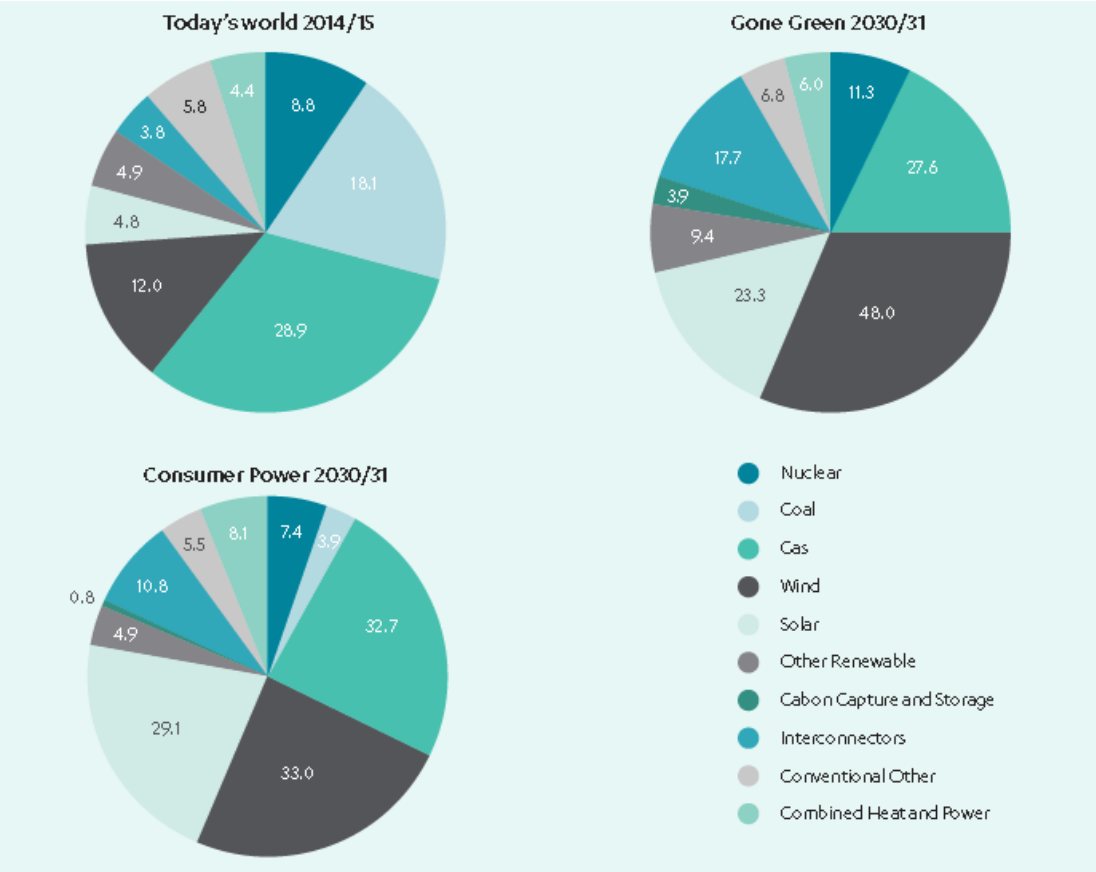

Figure 1.1: Generation mix of 2014/2015 and possible future scenarios (installed capacity (GW)) [Nat14]

The potential major issues caused by the future development of power systems are shown in Figure 1.2. Four major topics: system inertia, system strength and resilience, embedded generation and new technologies are discussed with a range of assessments conducted by National Grid. System inertia is proportional to the sum of stored energy in the rotating masses of generators and motors which are directly connected to the power systems. It is traditionally provided by transmission level synchronous machines with large rotating masses, mostly thermal power plants. However, there is a growing proliferation of non-synchronous sources, such as wind turbines, solar PV and HVDC interconnections which do not provide large amounts of natural inertia, and they are typically interfaced to the main grid via power electronics converters, which also do not inherently "transfer" or contribute any inertial responses (although they can provide "synthetic" inertia in some cases by adjusting power outputs to support frequency

response requirements [EME18]).

Topic	Assessment	Impact
System Inertia	Whole System Minimum Inertia	Decreasing whole system minimum inertia in future years
	Rate of Change of Frequency (RoCoF)	Trip of embedded generation protected by RoCoF relays
	Frequency Containment	Increase in volume of response required
System Strength and Resilience	Declining Short Circuit Levels and Protection	Difficulty detecting and clearing faults on weaker networks
	Voltage Dips	Widespread voltage dips and disconnection of embedded generation
	Voltage Management	Voltage containment and need for additional reactive compensation
	Power Quality	Power quality issues and need for additional filtering
	LCC HVDC Commutation Failure	Inability to operate LCC HVDC links in weak network conditions
	Demand Control by Voltage Reduction	Reduction in effectiveness of demand reduction by voltage control
	System Emergency Restoration	Reduction in black start plant and system restoration challenges
Embedded Generation	Regional System Stability	Stability issues associated with increase in embedded generation
	Low Frequency Demand Disconnection	Risk of cascade loss of generation should LFDD relays operate
	Active Network Management (ANM)	Uncoordinated TSO/DSO actions in constraint management
	Demand Forecasting	Increased demand forecasting error and increase in balancing actions
New Technology	Sub-Synchronous Resonance	Resonance issues and torsional shaft interaction
	Control System Interaction	Oscillations arising from uncoordinated control systems
	New Nuclear Capability	System flexibility and the impact of frequency response
	Demand Side Technologies	Changes in demand profile and impact of demand side technologies

Figure 1.2: Potential issues in future power systems [Nat15c]

This displacement of synchronous machines with non-synchronous sources and inverter-interfaced sources and interconnectors obviously leads to the reduction of system inertia (notwithstanding that synthetic inertia may be developed in the future), which will increase the potential risk of instability and various other undesirable behaviours of the system in terms of both voltage and frequency, especially during scenarios where there is maximum displacement of synchronous machines. Increasing volatility of the frequency following disturbances or other stressful scenarios (e.g. large load change) could lead to an increased change of rate of change of frequency (RoCoF), which could subsequently cause mal-operation of Loss of Mains (LoM) protection. Furthermore, higher levels of RoCoF could also lead to deeper frequency depressions following events, and, if the frequency drops below

certain thresholds, this could lead to generator or load trips on under-frequency, increasing the challenge of frequency containment (regulated for ±0.5 Hz in GB for no more than 60 seconds) and possibly increasing the risk of major or partial blackouts. The risk of voltage instability caused by a decline in system inertia is also a concern. Weaker systems will exhibit a larger and wider-ranging voltage depression (or collapse in severe cases) both during and following a disturbance, leading to consequent challenges in emergency restoration (black start) due to insufficient support from synchronous machines to maintain the voltage and frequency and general difficulties with voltage control and regulation, largely due to a decline of the reactive to real power ratio in systems (Q/P) [KOF+15]. Inadequate system inertia would also lower power quality due to increasing propagation of harmonics and potential resonance [RBJD, HTP+18]. Short circuit level is an indication of the amount of voltage support that can be provided to a specific point on the system. The reduced and often restricted current injection from converters decreases the short circuit levels, which could cause failure of existing protection, especially protection that relies solely on current magnitudes (which the majority of distribution protection systems are based upon), and increase risks of the failure of line commutated current (LCC) HVDC commutation due to the reduction of short circuit level (SCL) at the converter stations of LCC-HVDC links and voltage depressions during faults on the AC system around the area of the HVDC terminal [XZY18, PMR+15]. With increasing penetration of distributed generators changes the conventional radial topology of distribution networks, which enables the exchange of power between networks. In the future under low demand scenario, distributed generators could displace the power supplied from the bulk grid, which brings the challenge of visibility and control of voltages of which is current limited. With increasing penetration of embedded generation, especially during low demand summer scenarios, in the near future, power supplied from distributed generator might be able to meet the demand or even export the power to the power systems, which would cause disconnection of both demand side customer and the embedded generation due to operation of existing (Low Frequency Demand Disconnection) LFDD relays, which doesn't

take power flow level and direction into account. LFDD schemes are designed to automatically disconnect demand at distribution level on a stage by stage basis to limit the fall in frequency for extreme events beyond those defined as 'secured' events in the SQSS [The17] and Operating Code OC6 (Demand Control) of the Grid Code [Nat17]. It may thereby reduce the frequency support from distributed generators under disturbance. Active network management (ANM) is a scheme in distribution networks consisting of monitoring and control systems that connect the embedded generators connected to the power systems as soon as the capacity of the system is available. The immediate impact of ANM impacts brings uncertainty to the demand foresting and interaction between system operator and ANM actions. The above-mentioned new technologies including converter-based HVDC and other renewable energy and embedded generation would in general bring challenges for the existing control systems as aforementioned in this section. The impact of other clean energy to power systems, especially nuclear requires further investigation. Prevailing demand side technologies such as electric vehicles and energy storage changes the demand side profile and thereby bring challenge to the power systems [Nat15c].

1.1.1.2 Specific challenges to power system protection

Existing power system protection systems may encounter many challenges due to future development of the power system as outlined earlier, especially due to changes and a general decline in fault levels and variation of short circuit ratios caused by increasing amounts of converter-interfaced generation (particularly non-synchronous generation). In future power systems, individual source fault infeed is reducing and consequently, overall system fault levels may decrease significantly, potentially compromising system strength [Nat15a]. The reduction of short circuit level will lead to wider and deeper voltage depressions during and after faults, possibly compromising the operation of certain types of system protection and increasing challenges associated with low voltage ride through capability for all generators (particularly non-synchronous and those interfaced via converters), HVDC interconnectors and embedded HVDC links, which are

likely to grow in number significantly in the future. With the evolving topology of the power systems due to the transition from large-scale centralised to small-scale decentralised generation, short circuit ratios may be impacted negatively and therefore the existing settings of the power system protection may need to be adjusted (or possibly different types of protection may be required in some cases).

Protection systems minimise equipment damage, the risks of instability and wide-area blackouts and other undesirable conditions. This is achieved, typically within tens of milliseconds, by detecting power system conditions of an abnormal or dangerous nature and isolating faulted components from the power systems. For future power systems, if the primary protection was to fail, then existing backup protection based solely on current measurements (e.g. overcurrent protection) may fail to operate due to the aforementioned reductions in fault currents.

Furthermore, if, under a future "weaker system" scenario, the primary protection was to fail, then existing backup protection, which typically operates with approximately a 500 ms time delay (although circuit breaker fail may operate faster than this) [Nat11], could lead to "fault ride-through" problems for generators (both synchronous and converter based) and HVDC links. Ride-through for HVDC systems and all transmission-connected generation is usually only stipulated with respect to an assumed 140 ms maximum fault/severe voltage depression duration - primary protection clearance times (Mode A faults). The ride-through requirements of European countries are outlined in Figure 1.3 [KK10].

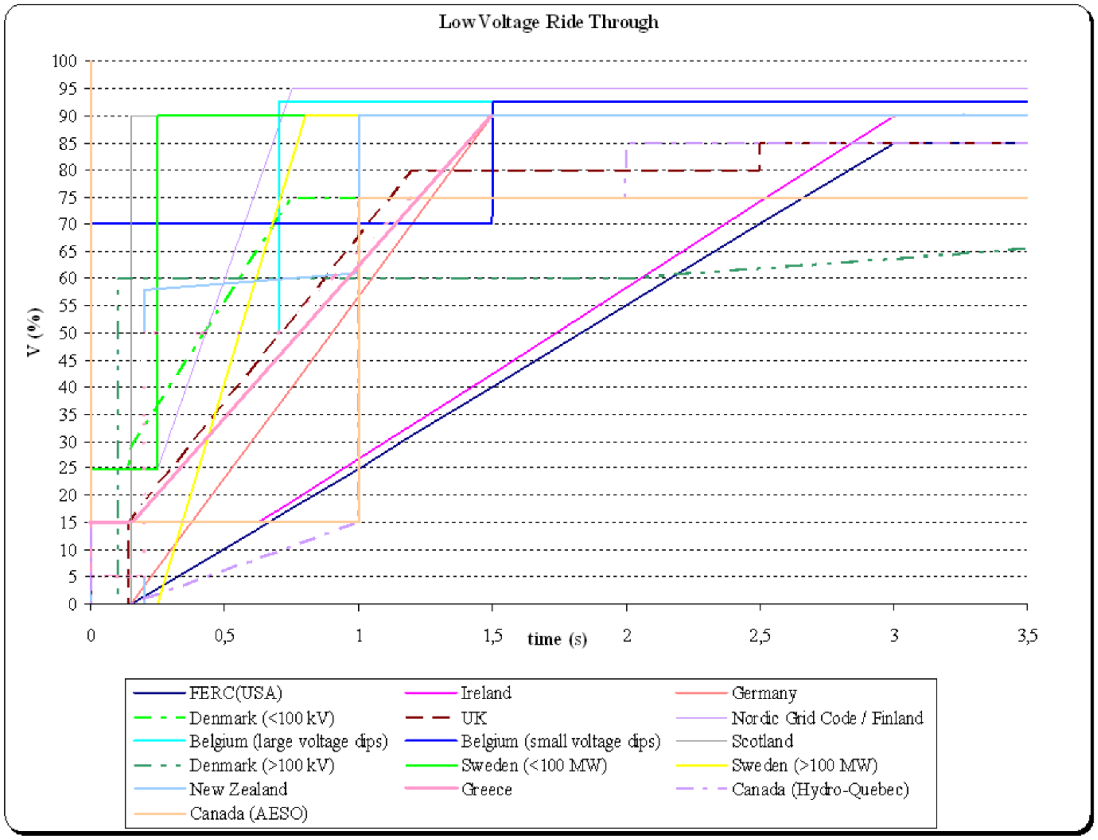

Figure 1.3: European countries voltage ride-through standards [KK10]

However, a number of synchronous generators may have difficulties in satisfying this requirement, particular under scenarios of voltage depressions between 15 – 50% of nominal voltage lasting up to several hundred milliseconds [Nat15b]. For faults/severe voltage depressions in excess of 140 ms (Mode B faults) – typically cleared by backup protection (with longer operating times), the ENTSO-E RfG Fault Ride Through Requirements do not address this issue specifically [ENT16]. This could be even more challenging in the future due to more severe and widespread voltage depressions in a weaker system. In such a scenario where primary protection (or circuit breakers) fail, although highly unlikely to occur in the first place, the risk of complete system collapse cannot be discounted.

Even for existing relatively strong power systems, if the main or backup protections do not operate correctly, it may cause significant disruption to power supplies to consumers. It has been noted that the root causes of a number of historical blackout events have been due to transmission backup protection not

operating correctly [HP06, ACA+12], particularly with reference to zone 3 protection within distance protection schemes. Significant reductions and increased variability in fault levels resulting from an increasing penetration of renewables introduces yet more challenges with respect to backup zones of distance and overcurrent protection, either rendering them prone to unwanted or nonoperation, or requiring complex evaluation and possibly adaption of settings based on prevailing system conditions [Nat15c]. This dissertation proposes a key solution to the issues addressed earlier in this section - a comprehensive backup protection scheme, which is not affected by fault level variation or reduction, and has the potential to operate quickly, while making effective and economic use of existing PMU and communications infrastructure that has already been installed for other purposes.

1.1.2 The growth in use of PMUs and wide-area communications

The number of PMUs installed in power systems throughout the world, and the investment in both the PMUs and associated high-performance communications infrastructure, has been increasing markedly in recent years and many "wide-area" monitoring, protection and/or control related projects have commenced in many countries, which evidences and supports the potential popularity and applicability of the work reported in this thesis; there are many related activities within both the research and industrial communities and examples of such activities are briefly introduced in this section – a comprehensive critical literature review of related work is presented in Chapter 3. For instance, in India, via the Unified Real Time Dynamic State Measurement (URTDSM) project [WDM+15], the Indian company Powergrid is installing 1,700 PMUs covering all 400 kV (and higher voltage where applicable) substations and major generating stations to strive for enhanced dynamic security monitoring and visualisation of the system. In the UK, SP Energy Networks led a major project entitled "Visualisation of Real Time System Dynamics using Enhanced Monitoring" (VISOR), that was

used to showcase and demonstrate the role of enhanced Wide-area Monitoring Systems (WAMS) in overcoming the challenges faced by the GB power system in the future as it moves towards a low carbon future [Pow12]. In 2013, over 2,300 PMUs had been commissioned in the Chinese power grid and all 500 kV (and higher voltage where applicable) substations and generation sites with a capacity of 100 MW or greater now have PMUs. In addition, many 220/110 kV sub-transmission substations are also equipped with PMUs. To manage this fleet of PMUs, more than 30 WAMS centre stations are in service, providing important dynamic information relating to power system state and operation [LSWS15].

To complement this PMU growth, there is an accompanying proliferation of research, investment and projects relating to wide-area communications, which provide favourable conditions for PMU-based wide-area applications for monitoring, control and protection. The telecommunications company Huawei submitted an ultra-bandwidth wireless automatic distribution communication networks that provide network services according to requirements stipulated by China Southern Power Grid. This solution is based on 4G eLTE technology to meet the needs of distribution automation, metering automation, and distribution network video surveillance services, and has high performance with high reliability and security, and low and repeatable latency and jitter, in order to satisfy the requirements for network operation applications [Hua15].

In summary, PMUs and communications technologies have been growing in popularity and this has led to increasing development of Wide-Area Monitoring, Protection and Control (WAMPAC) functions [KHL04a, Pow14]. The PMU-based wide-area backup protection scheme as reported in this dissertation is considered to be an effective alternative/extra layer to conventional backup protection schemes to meet the challenges of future power systems [HZC+11]. Accordingly, a relatively fast and inexpensive backup protection scheme with the additional functionality of summarising and reporting both correct protection operations and any failures is proposed. The proposed scheme of fault identification and location is based solely on voltage measurement data gathered from several PMUs. With a much faster reporting rate than Supervisory Control and Data Ac-

quisition (SCADA) systems, this wide-area measurement and protection system can be an additional method for providing enhanced monitoring and protection (in the form of wide-area backup protection) to power systems in the future. The system is initially targeted at transmission level but could potentially be applied at lower voltage levels as and when PMUs become more prevalent in such power systems (micro-PMUs have been developed and are becoming the subject of increasing attention by researchers [TGCR17]). This dissertation introduces the concept and theory of the scheme and configuration (applicability) of the scheme. Tests and validations of the scheme in both simulation and hardware in the loop are also included in this dissertation.

1.2 Contributions

This research has delivered a principal contribution to knowledge, which is the development and demonstration of a wide-area backup protection performance analysis scheme, which is capable of effectively summarising fault occurrences and locations, reporting on any failures of non-operation of circuit breakers or protection devices, and performing backup protection with requirements for solely voltage measurements from PMUs.

Associated with this main contribution are a number of associated secondary contributions:

- Design and demonstration of a voltage-based fault identification system to identify fault location (to the feeder level).
- Design and demonstration of a voltage-based fault categorisation system to identify fault type (e.g. phase-earth, three-phase).
- Identification of correct and incorrect/non-operation of protection and circuit breakers from analysis of voltage measurement.
- Development of a software tool that summarises graphically the operation/failure of protection to operate.

- A wide-area backup protection scheme that can identify failures of protection/circuit breakers and instruct the operation of appropriate circuit breakers to effect isolation of the fault.

- Design and demonstration a methodology of complex power system simplification that retains a high degree of accuracy, and can simplify any full multi-node power system model to a two-bus equivalent model for the purposes of determining and configuring the parameters of the protection performance analysis scheme.

- Investigation of the influence of fault levels, fault resistance, fault types and fault locations on the ability of a system to detect the presence of faults and protection failures using only measurement of voltage.

- Implementation of the scheme within an RTDS system to allow real time hardware in the loop testing, which demonstrates and validates the ability of the scheme to be applied in practical situations – this hardware arrangement has been and could be used by other researchers to test other types of monitoring, control and protection schemes.

1.3 Dissertation overview

Chapter 2 reviews the relevant background material through introducing the fundamentals of power system protection and emphasising challenges associated with future power system developments and the impact that they may have on conventional power system protection schemes. Chapter 3 presents an overview of the application of Phasor Measurement Units (PMUs) and contains a critical review of a number of existing and proposed wide-area protection schemes. The chapter highlights the contributions of the proposed scheme and the novelty of the scheme in the context of the other related and reviewed schemes. The principles of the proposed scheme are explained in detail in Chapter 4 using demonstrations of operation using relatively simple test cases (more complex case studies are included in later chapters). Both reporting and protection schemes are in-

cluded. The chapter also introduces the algorithm of fault type identification. In order to determine configuration of the scheme in a simple but effective way, a method of network simplification is discussed in Chapter 5. The chapter presents in a detailed overview of how any power system may be simplified into a two-bus equivalent circuit and shows how the corresponding parameters of the simplified model may be derived from the full power system. In Chapter 6, a method of automatically determining scheme configuration based on a range of different networks is presented. Simulation case studies that includes the impacts of different factors upon the scheme are presented in Chapter 7. Real time case studies for hardware in the loop tests are conducted in Chapter 8 for scheme validation. Chapter 9 concludes this dissertation by summarising the contributions and the novelty of the research. Recommendations for future research, which could carry on from and extend the work reported in this dissertation, are also made.

1.4 Publications

The following publications have been completed during the course of this PhD:

1.4.1 Journal Articles

Wide-Area Backup Protection and Protection Performance Analysis Scheme Using PMU

F. Yu, C.D. Booth, A. Dyśko, and Q,Hong

International Journal of Electrical Power&Energy Systems, Elsevier, volume 110, September 2019, pp. 630-641

1.4.2 Conference Papers

Backup protection requirements in future low-inertia power systems

F. Yu, C.D. Booth and A. Dyśko

2016 51st International Universities Power Engineering Conference (UPEC), Coimbra, Portugal, 2016, pp. 1-6

Voltage-based fault identification for a PMU-based wide area backup protection scheme
F. Yu, C.D. Booth and A. Dyśko
2017 IEEE Power And Energy Society General Meeting, Chicago, IL, US, 2017, pp. 1-5.

Chapter 2

Review of fundamentals of power system protection

2.1 Introduction

This chapter reviews the fundamentals of power system protection. While there is an introduction to protection systems in general, there are many textbooks available that provide detailed information relating to all aspects of power system protection, so there is no need to provide a detailed treatment of many of the more general aspects relating to the topic. In alignment with the topic of this research, focus is placed upon the topics associated with transmission level backup protection schemes. This chapter begins by providing an introduction to electrical faults, which are the main abnormal conditions that protection systems are required to mitigate and protect against and the key elements to consider during the designing of the proposed scheme. Section 2.3 provides an overview of sequence components, which is one of the fundamental theories which underpins the proposed scheme for detecting different types of faults. In Section 2.4, the protection schemes (both main and backup protection) used in transmission networks are introduced, along with discussions of the policies and regulations that are applicable to protection setting, the pros and cons of different schemes and the potential impact of future power scenarios (e.g. widespread introduction

of renewables leading to "weakening" of power systems) upon existing protection schemes.

2.2 Electrical faults

An electrical system fault is can lead to potentially catastrophic failures in power system equipment if not identified and responded to quickly. Faults can happen at any voltage level, although the consequences (and therefore the cost and complexity of protection) generally increase with increasing system voltage [IEE16]. At the basic level, based on current flow in the circuit, electrical faults can be mainly categorised as open circuit (OC) faults and short-circuit (SC) faults; although there can be other undesirable conditions (e.g. unbalance, loss of mains, overload) that can also require protection. This research work is focussing on the protection against SC faults (and a subsequent failure of the main protection systems to isolate these faults correctly). An OC fault occurs when a failure happens in the conduction path of electricity [SKS+00, RBM01], e.g. though a physically broken or severed conductor, and a SC fault may be caused by a failure of insulation (or other causes – e.g. an uninsulated conductor coming into contact with another – perhaps through conductor clashing in high winds, or through human error, vegetation touching conductors, etc.) leading to a short-circuit condition [IEE16].

In the context of power system protection and as the main topic of this dissertation, the vast majority of electrical faults are SC faults in nature (as opposed to OC faults which are, anecdotally, very much rarer), which are characterised by the presence of high currents in the power systems - the current only being limited by the impedance from the sources to the fault (and the return path) and the short circuit current provision capability of the sources supplying the current to the fault. SC faults, if not isolated in a timely fashion and in the proper fashion (i.e. ideally only isolating the faulted component or network section through opening circuit breakers), may cause severe damage to electrical equipment, system-wide disturbances, or even wide-area blackouts.

In three-phase AC power systems, SC faults can be mainly categorised as the following types (as illustrated in Figure 2.1): single-phase-to-earth (Ph-E) fault, phase-to-phase (Ph-Ph) fault, double phase-to-earth (Ph-Ph-E) fault, and three-phase (Ph-Ph-Ph) faults, which could also involve earth (Ph-Ph-Ph-E – not shown in the figure) [PB13]. Z_f is the fault impedance (typically associated with the arc or with some other resistive conducting path between the faulted phase(s) (and earth if it is an earth fault), and the faults with zero impedance are referred to as solid or bolted SC faults [GSO12]. Classified by the symmetry of power flow during the fault condition, SC faults can also be categorised as symmetrical or asymmetrical. Symmetrical faults are three-phase balanced (e.g. Ph-Ph-Ph faults), whereas asymmetrical faults are unbalanced across the three phases (e.g. all fault types except Ph-Ph-Ph faults as shown in Figure 2.1).

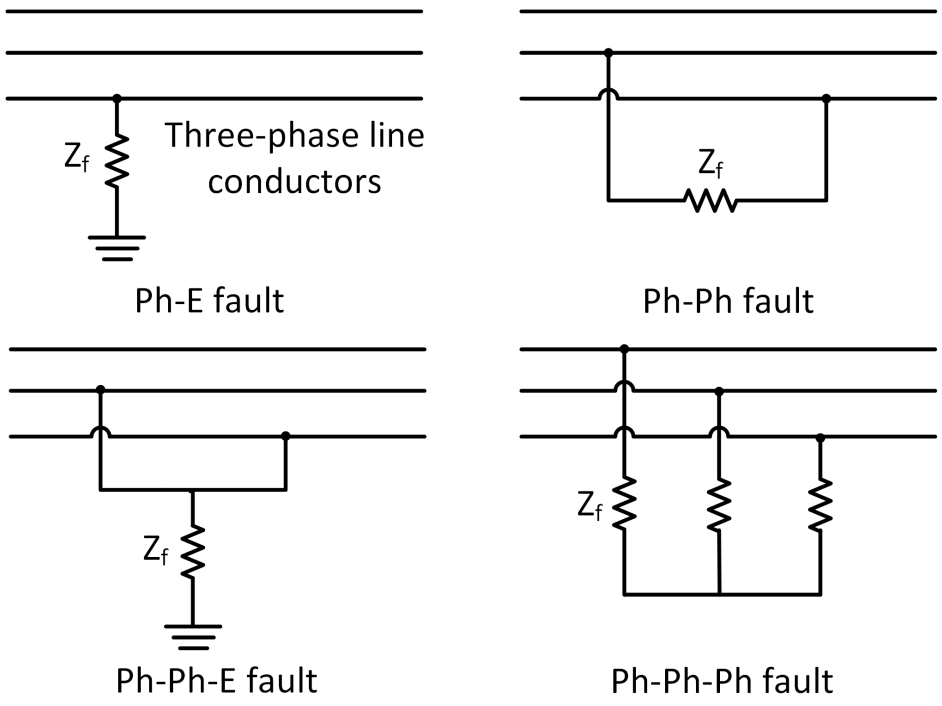

Figure 2.1: Main SC fault types in three-phase AC networks [PB13]

The majority of faults in three-phase AC power systems are PH-E in nature (80%); around 15% are either PH-PH faults or PH-PH-E faults and about 5% are PH-PH-PH/PH-PH-PH-E faults [Pre06].

2.3 Sequence components

The method of symmetrical components is well established and recently the centenary of the original publication [For18] was celebrated, and provides a tool to study systems with unbalanced voltages and/or currents, and these are used within the research reported in this dissertation to identify different types of faults, especially with regards to unbalanced faults. While extensive explanations of sequence components are available in many text books, an overview of their use is included here as it is fundamental to the operation of the fault identification and backup protection scheme operation reported later in the dissertation. Sequence components simplify fault analysis under unbalanced scenarios by synthesising phase domain components into three sets of sequence components: positive sequence, negative sequence, and zero sequence components. Once the system is solved in the symmetrical component domain, the results can be transformed back to the phase domain [Sch18].

$$\begin{cases} V_a = V_{a0} + V_{a1} + V_{a2} \\ V_b = V_{b0} + V_{b1} + V_{b2} \\ V_c = V_{c0} + V_{c1} + V_{c2} \end{cases} \tag{2.1}$$

The positive and negative sequence components are representative of balanced three-phase systems with the same phase sequence and the opposite phase sequence to the main system's (i.e. the unbalanced system) phase sequence respectively. The zero sequence component consists of three phasors that are equal in magnitude and phase [J.D11]. Using these three systems of balanced phasors, any unbalanced three phase system can be represented. The relationship between the actual phase components (in the physical unbalanced system being studied) and the various sequence components is demonstrated in Figure 2.2. The positive, negative and zero sequence components of phase a are denoted as V_{a1}, V_{a2}, V_{a0}. There are similar components for phases b and c. The physical domain quantities can be related to the sequence domain quantities as displayed in Figure 2.2 and

in Equation 2.1; in general, the actual unbalanced phasors are derived from a vector summation of the appropriate sequence components.

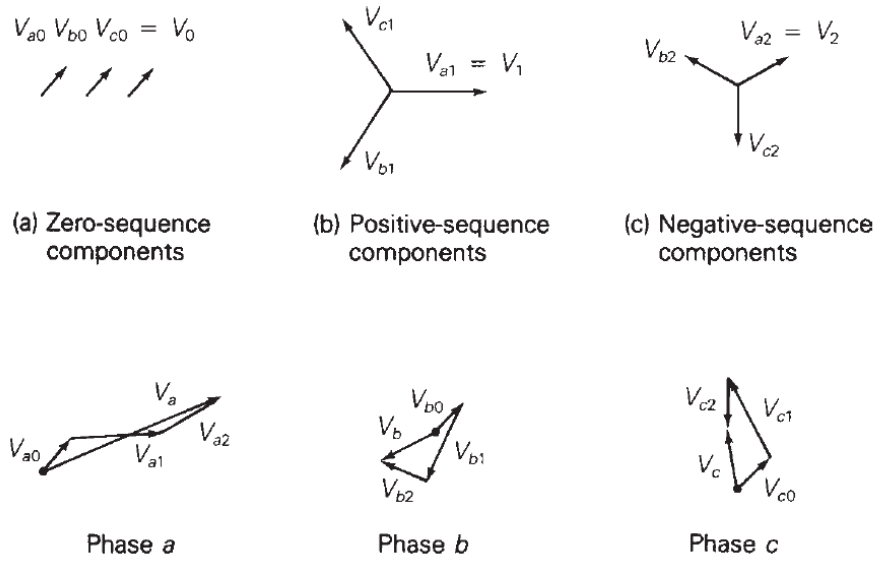

Figure 2.2: Resolving phase voltages into three sets of sequence components [GSO12]

To demonstrate, quantities V_0, V_1 and V_2 are defined in the sequence domain using phase a (or specifically V_a) as a reference and along with the "a" operator substitute the new "sequence" quantities into b and c phases, which is shown in (2). Quantity a-operator in Equation 2.2 is defined as a unit vector at an angle of 120°, written as a=1$\angle$120°. Mutual transformation between phase components and sequence components in matrix notation (of phase a) is shown in Equation 2.3 and Equation 2.3. Current phasor quantities have the same transformation form as voltage phasors and shown in Equation 2.3 and Equation 2.3.

$$\begin{cases} V_0 = V_{a0} \\ V_1 = V_{a1} \\ V_2 = V_{a2} \\ V_a = V_0 + V_1 + V_2 \\ V_b = V_0 + a^2 V_1 + a V_2 \\ V_c = V_0 + a V_1 + a^2 V_2 \end{cases} \tag{2.2}$$

$$\begin{bmatrix} V_a \\ V_b \\ V_c \end{bmatrix} = \begin{bmatrix} 1 & 1 & 1 \\ 1 & a^2 & a \\ 1 & a & a^2 \end{bmatrix} \begin{bmatrix} V_0 \\ V_1 \\ V_2 \end{bmatrix} \tag{2.3}$$

$$\begin{bmatrix} V_0 \\ V_1 \\ V_2 \end{bmatrix} = \frac{1}{3} \begin{bmatrix} 1 & 1 & 1 \\ 1 & a^2 & a \\ 1 & a & a^2 \end{bmatrix} \begin{bmatrix} V_a \\ V_b \\ V_c \end{bmatrix} \tag{2.4}$$

$$\begin{bmatrix} I_a \\ I_b \\ I_c \end{bmatrix} = \begin{bmatrix} 1 & 1 & 1 \\ 1 & a^2 & a \\ 1 & a & a^2 \end{bmatrix} \begin{bmatrix} I_0 \\ I_1 \\ I_2 \end{bmatrix} \tag{2.5}$$

$$\begin{bmatrix} I_0 \\ I_1 \\ I_2 \end{bmatrix} = \frac{1}{3} \begin{bmatrix} 1 & 1 & 1 \\ 1 & a^2 & a \\ 1 & a & a^2 \end{bmatrix} \begin{bmatrix} I_a \\ I_b \\ I_c \end{bmatrix} \tag{2.6}$$

Symmetrical components are widely used for fault study calculations. Normally, the positive, negative and zero-sequence impedance networks are given by the manufacturer. Depending on the type of fault being considered, each of the sequence networks are then connected together in various ways to calculate the fault currents and voltages [Mar16].

For a transmission line, the positive and negative sequence impedances are identical, because the phase sequence of voltages and currents have no effect on the line impedance. The zero sequence impedance, however, could include earth (or combined earth and neutral) conductors, the shields of conductors (sometimes used for earth/neutral return paths) and/or the resistance/impedance of earth itself, since the path of zero sequence currents for an unbalanced earth fault may consist of several paths depending on the design of the system [NPT18, Cas18].

For transformers, under unbalanced short circuit fault conditions, the shunt magnetising branch of transformers can be neglected due to the negligible magnitude of shunt magnetising branch currents when compared to the magnitude of any short circuit currents. Therefore, transformers could be modelled with an

equivalent series leakage impedance. Due to the static characteristic of transformers, the series leakage impedance will not change under circumstances of reversed applied phase voltages, which leads to the equal positive and negative sequence impedances of transformers [Cas18]. The zero sequence impedance of transformers varies according to winding connection, which is explained in detail in [NPT18, Hea98].

For generators, the positive sequence impedance of a synchronous generator is the ac resistance of the armature windings [Das17]. If apply negative sequence currents to the armature winding, and the generator is running at synchronous speed, the field winding shorted through generator exciter, then the negative sequence impedance equals to the ratio of the negative sequence fundamental frequency voltages to the currents. Negative sequence impedance (during unbalanced operation) is normally less than positive sequence impedance. The zero-sequence impedance is much less than the positive-sequence impedance [Cas18, MyT16].

The Thevenin equivalents for each sequence circuit is simplified and shown in Figure 2.3. Each of the sequence networks may be considered independently. Since each sequence circuit involves symmetrical currents, voltages and impedances in the physical model, each individual sequence network can be solved using a single-phase method [Mar16].

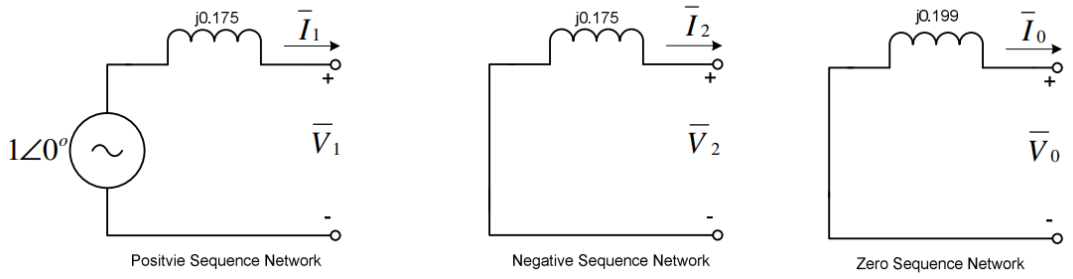

Figure 2.3: Resolving phase voltages into three sets of sequence components [Mar16]

Since fault analysis and calculation based on sequence components are based on fault types, it is very crucial to identify the connections of sequence networks corresponding to different types of faults – illustrated in Table 2.1. The diagrams

Fault types	Involved sequence networks	Connection type
Three-phase fault	Positive	-
Single line-to-earth fault	Positive, negative, zero	Series
Line-to-line fault	Positive, negative	Parallel
Double phase-to-earth fault	Positive, negative, zero	Parallel

Table 2.1: Sequence network connection based on fault types

for connections of different types of bolted faults are shown in Figure 2.4. Once the sequence network is connected, relatively simple calculations can be used to establish the voltage and currents for each of the sequence networks, which in turn can be used to establish the various quantities in the phases of the actual unbalanced system.

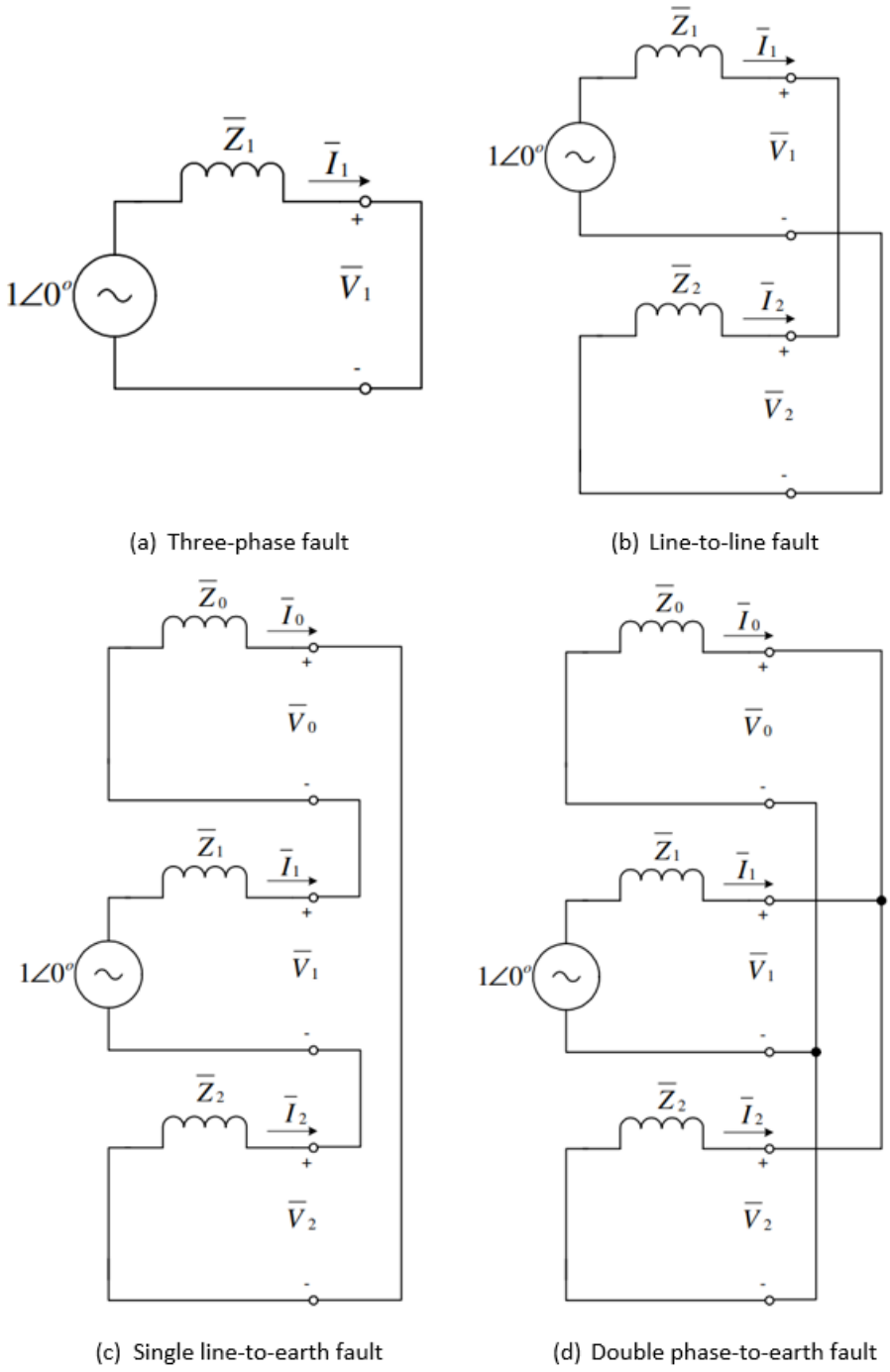

Figure 2.4: Sequence networks connections of different fault types [Mar16]

2.4 Power system protection

2.4.1 Overview

Short circuits happen in power systems due to mechanical or "natural" causes. Meticulous design, operation and maintenance can reduce the occurrence of short circuits in a large extend, but can never eliminate them. Thus, power system protection is needed to defend the system against the most potentially severe consequences of faulty conditions by detecting and isolating faults within milliseconds to avoid or minimise the damage to the power system and its components due to the very high levels of current typically associated with short circuit faults (which can easily be orders of magnitude larger than the normal maximum load currents). The purpose of system protection includes protecting the public, mitigating risks to system stability and minimising damage to the equipment arising from the fault condition. Power system protection is applied to generators, busses, transformers, lines and other power system equipment [IDA12]. Since the proposed scheme in this dissertation is related to power system protection on transmission lines, this section of the review is mainly focused on transmission line protection schemes. Voltage level for high voltage transmission systems in GB are 400 kV and 275 kV [Par11]. Transmission lines are a vital part of power systems, as they provide the path to transfer high amounts of power between generation and loads in the system [GE 07]. Once a fault on a transmission line is detected, the primary protection scheme will issue a tripping signal to associated circuit breakers (CBs) as quickly as possible (the decision to trip is normally made within one cycle – or 20 ms – in a 50 Hz system), which will then operate to isolate the faults from the system, with the total time from fault initiation through to isolation typically being less than 100 ms. If the protection scheme detects the fault but determines that the fault is remote, then it may delay its tripping output so that other protection systems closer to the fault location may react first (discrimination) - if the fault is detected as still being present on the system after a pre-determined time delay, then the protection schemes on the

adjacent parts of the power system to the faulted component may trip to provide backup. In this section, a brief review of protection schemes (both main and backup protection schemes) of transmission level used in transmission networks is undertaken. Categorised by whether a clearly defined zone of the power system is protected, protection systems can be classified as unit or non-unit. Unit protection schemes only detect and isolate faults with instantaneous operation within a clearly defined zone without reference to other sections. A non-unit scheme is intended to protect a specific area, but does not have a precisely fixed boundary of protection and protective zones can overlap into other areas apart from the main designated area, which offers a very important benefit of being able to provide backup to neighbouring system elements, which is not an inherent feature of unit schemes. In order to maintain stability of power systems, both types are required to give the benefits of unit, but also the backup properties of non-unit. Primary protection schemes include differential and distance protection schemes, which identify faults and isolate faults in a minimum period of time. Backup protection schemes including distance, overcurrent and circuit breaker failure protection coordinate with primary protection schemes to isolate faults with a time delay where primary protection scheme fails to operate, which ensures the priority of protection devices closets to the fault. The regulations and requirements for these schemes with regards to transmission line protection are discussed in the next sections, along with presentation and analyses of the challenges relating to backup protection schemes that may arise as a consequence of future power system developments and scenarios.

2.4.2 Existing primary protection schemes for high voltage networks

2.4.2.1 Overview

In this section, a brief review of primary protection schemes for transmission lines is conducted. In order to maintain the reliability of the system (ensure rapid fault clearance and isolation following fault inception), two primary protection schemes

(or "primary protection schemes") are applied in parallel [1], which are typically differential protection and distance protection (although in some cases, e.g. for very short lines, two differential schemes may be used as distance protection may not be applicable in such circumstances). To enhance brevity and relevance of this section, the concepts and principles of these protection schemes are briefly discussed and details can be found in [Als11].

2.4.2.2 Differential protection

Differential protection is a unit protection scheme. In the GB transmission network, it is one of the primary protection scheme for transmission lines. The underlying theory for differential protection is Kirchhoff's current law, which states that the vector sum of currents entering (and leaving) a point must be zero [And99]. The basic principle is to sense any difference in currents entering and leaving the unit being protected, which is the protected feeder in this case. The basic operating mechanism of differential protection (unbiased differential protection) is illustrated in Figure 2.5.

Ideally, with perfect CTs, the differential relay does not operate for an external fault Figure 2.5. (a)), since magnitude and phase of the current at End 1 and End 2 are identical, and therefore the secondary current I_{f1_sec} and I_{f2_sec} have the same magnitude and direction, which leads to zero differential current (i.e. I_diff =0 A). However, in practical scenario, even CTs in the same type and rating may be subject to various errors during external faults due to manufacturing differences, differences in pre-fault loading, and differences in saturation, etc. [GSO12], which may require other methods to deal with the asymmetry of the circuit, since these may cause a non-zero I_{diff} in the context of external faults or heavy loading conditions. Other means for the purpose of coping with these problems have been successfully developed and incorporated within differential protection systems, which are discussed in more details later in this section.

For scenarios of internal faults as show in (Figure 2.5.(b)), the direction of the current at the End 1 and End 2 would be different (as long as there are sources of fault current supplying each end of the protected line) and the possibility

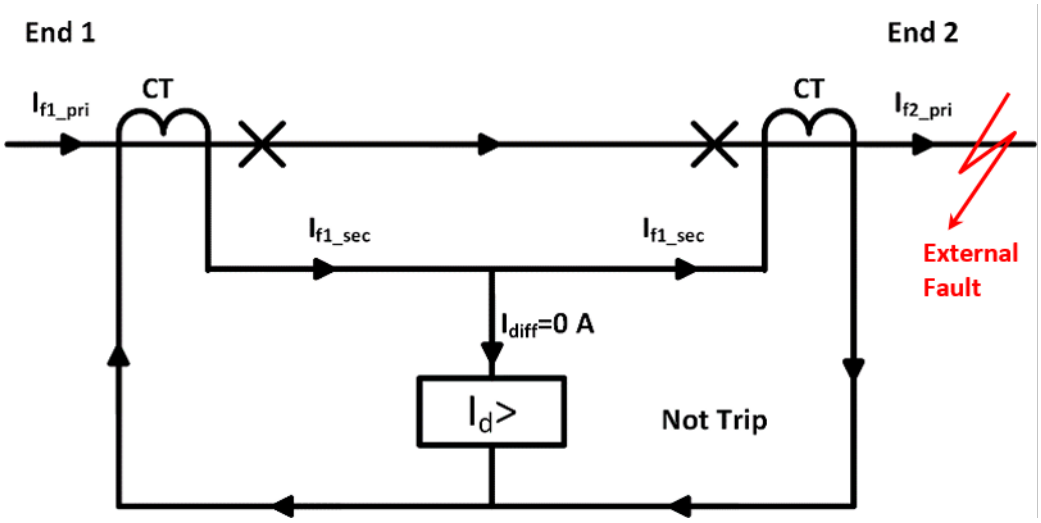

(a) External fault

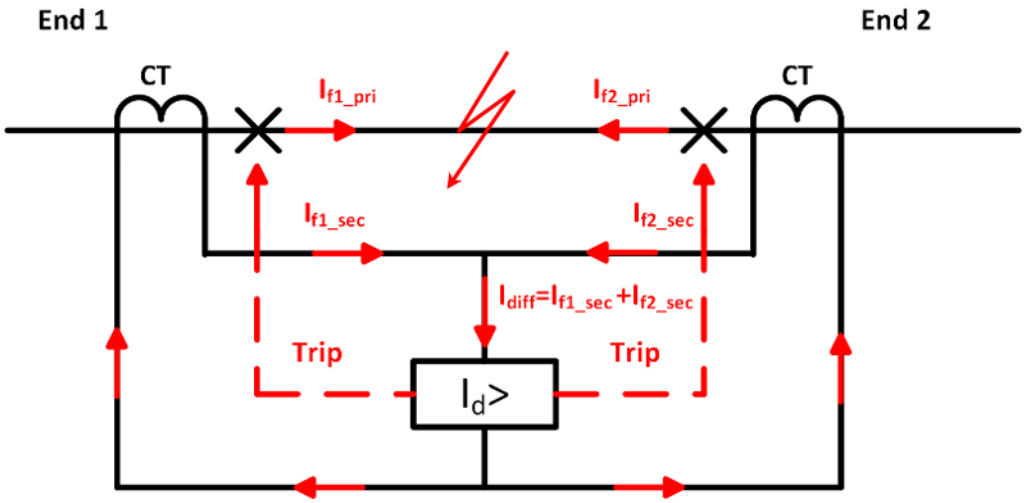

(b) Internal fault

Figure 2.5: Basic principle of differential protection

that they have different magnitudes would be high (indeed if there was only one end with a fault current infeed, then there would be zero current flowing to the fault from the end with no infeed), resulting in a non-zero value of I_{diff}, which, depending on the threshold setting of the relay, would normally trigger the protection operation due to a value of I_{diff} in excess of the threshold setting.

As the foregoing mentioned, rather than the basic operating mechanism based on Merz-Price principle [Als11], other methods are developed to compensate for asymmetry of the circuit during external faults and normal operating conditions to maintain security. For the scenarios of external faults or heavy loads, the current measured from terminals of the line could be different caused by various factors, such as errors of CTs and line charging current due to transmission line's shunt capacitance, which could be deducted from the current flowing "into" the line – i.e. in the direction of power flow, and the difference between the currents "flowing" into and out of the line is denoted as spill current.

To desensitise the asymmetry mentioned above during external faults, especially due to saturation of CTs (for example, CTs at one end of the line may completely or partially saturate, while the CTs at the other end of the line, which could have different specifications, may not saturate as much or may not saturate at all), biased differential protection is developed with restraint features (based on a value of current that represents the overall current magnitudes being measured – bias value will generally increase with increasing magnitudes of current – which increase the risk of increased spill currents) that are used in conjunction with the differential current values derived from the basic principle mentioned previously. Differential protection is biased when the operating threshold (i.e. the magnitude of differential current required to trip the protection) is dependent on the amount of current flowing through the protected circuit. A typical biased characteristic is shown in Figure 2.6, which is different from the unbiased characteristic. I_{s1} is the minimum pick-up current threshold; I_{s2} is the biased current threshold beyond which a different biased slope is used and k1 and k_2 are the settings to control the slopes of the biased characteristic. The biased differential characteristic has the advantage of providing high sensitivity for low fault currents and good security

for higher fault current levels, particularly for external faults, where the measured currents could be very high, but errors in CTs and other factors could result in errors in the currents measured at each end of the line due to CT saturation and generally increased CT errors at high current levels [GSO12].

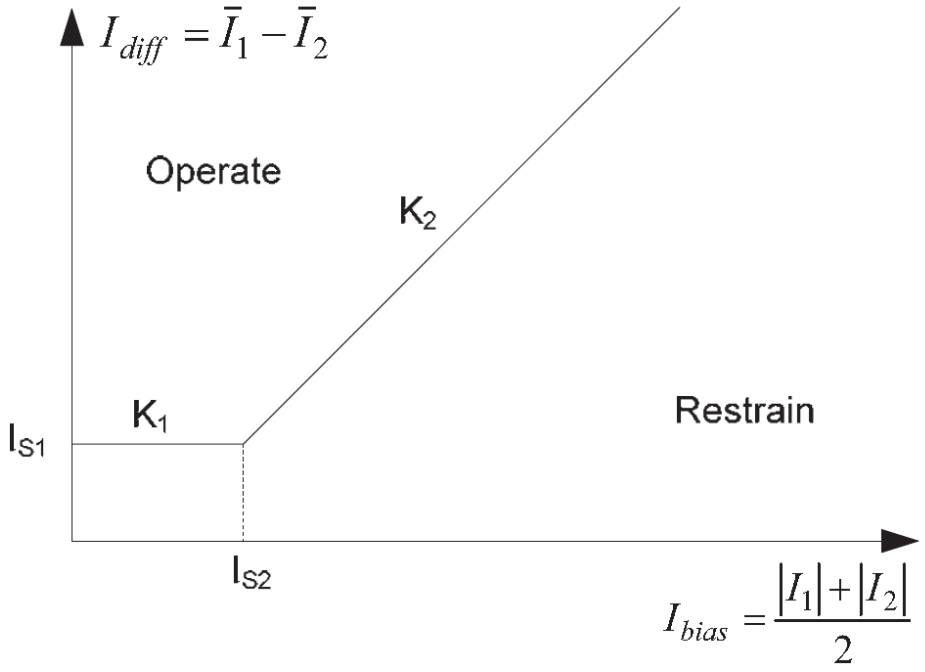

Figure 2.6: Biased differential operation characteristic[Als11]

A typical two-terminal differential protection for a feeder is shown in Figure 2.7, where communications between the local and remote end protection relays are used for the comparison of the measured current for determination of internal fault scenario.

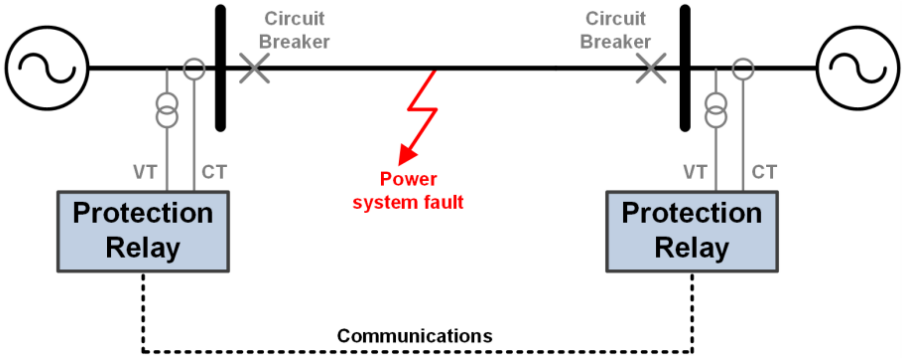

Figure 2.7: Typical two-terminal differential protection arrangement [Bla13]

In reality, communication delays should also be considered, for which either by use of different developed methods to compensate for the delay to ensure the synchronisation of the compared measurements or by the use of accurate GPS-based time tagging of measurements at the ends of the protected line [Als11].

2.4.2.3 Distance protection

The other primary protection scheme used for protection of transmission lines, often employed at transmission level and in parallel with differential protection schemes, is distance protection, a form of non-unit protection [Als11]. When a fault occurs on a line, the current rises significantly and the voltage collapses significantly at the point of fault and around the area of the fault. The level of voltage collapse in the vicinity of the fault – i.e. measured by distance protection relays around the location of the fault - depends on the fault level and the impedance, or distance, of the transmission lines around the fault location (with the distance relays typically taking measurements close to the line terminals. Distance protection calculates the complex ratio of the voltage and current measured by the CT (current transformer) and VT (voltage transformer) from the line respectively to determine the positive sequence impedance between fault locations and relay terminals. Since the positive sequence impedance is proportional to the distance from the measuring point to fault location, the distance relay (impedance relay) can be used to identify a fault up to the predetermined reach point (defined by the settings applied to the relay, which are calculated using known information relating to the impedance of the line(s) that are potentially protected by the relay. The approximate location of a fault can be ascertained by comparing the calculated impedance with the reach point impedance, which typically defines the boundary between the relay operating or not for a given zone of protection [And99]. This also has an important benefit of being insensitive to prevailing fault levels (unlike, for example, overcurrent protection), as if the system fault level reduces, the magnitudes of voltages and currents measured by the distance protection will change proportionately (e.g. for a lower fault level the current at the measurement point will reduce, while the voltage will increase

– their ratio (impedance) will remain constant) and therefore the relay will still observe faults at the same physical distance from the measuring point, regardless of source impedance/fault level.

As a non-unit protection scheme, distance protection is typically configured to have more than one protected zone and normally possesses three or more overlapped zones. The diagram of the reach of a three forward-looking zones of basic distance protection is shown in Figure 2.8. For the desired zone of protection which is shown in with a dotted line, Zone 1 is the primary protection which operates as fast as possible for a fault within Zone 1, while Zone 2 and Zone 3 are used to provide backup protection and typically faults detected in these zones are only reacted to by issuing a tripping signal after a user-configurable delay (during which the main protection responsible for clearing the faults in the remote zones should operate); if the fault is still present on the system after the delay time has passed, then the protection will trip as the remote protection (e.g. protecting the line B-C in Figure 2.8) will be deemed to have failed [HP08].

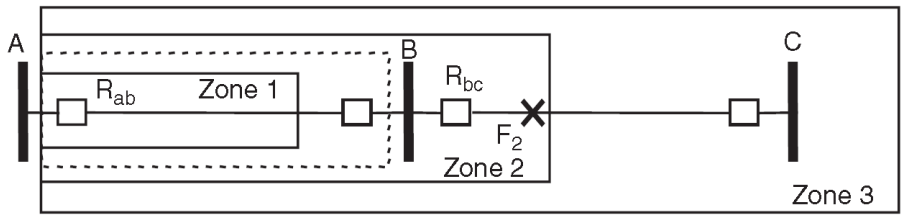

Figure 2.8: Three-zone step distance relaying to protect 100% of a line, and back up the neighbouring line [HP08]

Zone 1 is typically set up to be "under-reaching", where the relays at a given terminal (node A in Figure 2.8) do not operate for faults at on the protected line at or close to the remote locations (node B in Figure 2.8). These "under-reaching" setting policy is used to ensure that the relay will not trip "instantaneously" for a fault at or beyond the remote bus, which would of course be undesirable. The "under-reaching" design for primary protection is to cater for any uncertainty of reach caused by various factors such as transformer errors, other forms of measurements errors, changes in line impedance, fault resistance, etc. This is crucial for maintaining security (i.e. ensuring the protection does not operate when it

should not). Since Zone 1 alone does not protect the entire transmission line (the section between the end of Zone 1 and bus B is not protected), deliberately overreaching zones are needed. This "unprotected" Zone 1 area can also be protected by another distance relay at the remote end of the line which is "looking into" the line from the other end. Furthermore, accelerated schemes (utilising communications) can be used to overcome this, where a relay at one end of the line "seeing" a Zone 1 fault will send an "accelerate" signal to the remote relay at the other end of the line. If this relay is "seeing" the fault as a Zone 2 fault (i.e. it is close to the other end of the line), and receives an accelerate signal from the other relay, then it will over-ride the trip delay associated with Zone 2 and trip as fast as possible. Such accelerated schemes therefore ensure that faults close to line ends (i.e. in Zone 2 region for one of the relays) will be cleared quickly.

Zone 2 and Zone 3 are "overreaching protection", where the relays at one terminal (node A in Figure 2.8) operate for faults beyond the next terminal (node B for Zone 2 and node C for Zone 3 in Figure 2.8). They operate with a grading time delay to allow primary protection of the protected line to have the chance to operate. For the scenario in Figure 2.8, Zone 2 should operate with a time delay, so that for faults between node B and the end of Zone 2, Zone 1 of the next line is allowed to operate before Zone 2 of the relay at A. With coordination of different zones of distance protection [HP08], the desired protected zone (line section between node A and node B) can be protected, while ensure effective backup protection in the event of main protection/circuit breakers failing to operate for some reason.

Application of different distance relay characteristics depends on the specific requirements of power systems and upon policies applied by the operating company. R/X diagrams are normally used to describe these characteristics. Two widely used characteristic diagrams are shown in Figure 2.9. The "Offset Mho" scheme is capable of detection of close-up faults, but has an inherent risk of overreach of Zone 3 under very high load situations, where "load encroachment" may occur [SK00]. Quadrilateral schemes offer independent adjustment for forward reach and resistive settings, which provides more flexibility for short lines and

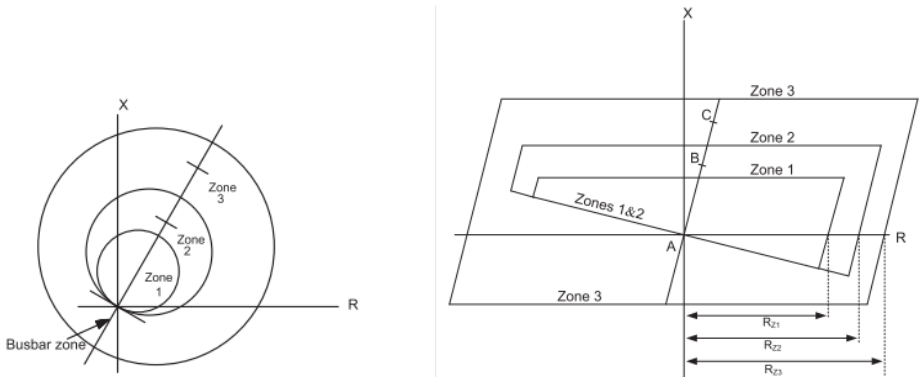

(a) Mho (b) Quad

Figure 2.9: Typical characteristics of distance protection [Als11]

earth fault impedance measurement [Als11].

Many distance protection schemes employ "pilot" functionality (e.g. they incorporate communication channels to assist with effective operation) [3] are developed to solve the problems of under-reaching zone 1 to protect the full length of the transmission line with less delays, such as direct under-reaching transfer trip (DUTT), permissive under-reaching transfer trip (PUTT), permissive over-reaching transfer trip (POTT), etc., which are discussed and introduced in detail in [Hea98].

2.4.3 Existing backup protection schemes for high voltage networks

2.4.3.1 Overview

This section focuses on reviewing existing backup protection schemes that are presently widely used in practice throughout the world, which are distance, over-current and circuit breaker failure protection. Emerging schemes and schemes proposed by other researchers are reviewed in the next section. Backup protection plays a key role in isolating faults in the events of failure in primary protection systems, thus offering an extra layer of assurance for overall power system reliability. Since the dissertation proposes a scheme, which aims to provide fault information for system operators and backup protection with data from already

installed PMUs, it is very crucial to understand the principles and GB standard of existing backup protection.

2.4.3.2 Distance protection

2.4.3.2.1 Principles

As introduced in Section 2.4.2.3, a distance (or impedance) protection scheme normally consists of three or more zones, each of which protects a predetermined area of the system from the relay's measuring point, which corresponds to an area spanning the first main protected feeder, and the subsequently-connected feeders from the remote substation(s), which are protected in back-up mode. If the measured impedance lies within the impedance corresponding to a zone of protection, the corresponding zone element will be triggered. The time setting for Zone 1 is "instantaneous", providing primary protection for the main protected line, and time delays for Zone 2 and Zone 3 (and in some cases other zones) are used to provide backup protection for other feeders in the vicinity of the protection relay [Als11] . Figure 2.10 illustrates a typical distance protection zone arrangement with the corresponding reaches/boundaries shown.

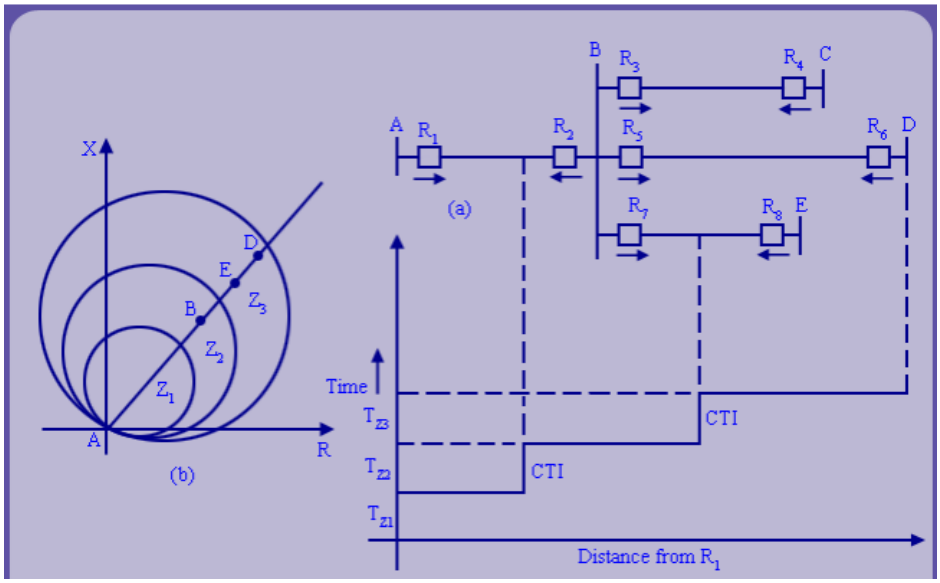

Figure 2.10: Typical distance protection zone arrangement[NPT18]

Zone 1 reach: Zone 1 typically provides instantaneous protection for all faults inside the Zone 1 reach boundary, which is normally 80-90% of the line length.

This is used rather than 100%, to avoid overreach due to various factors such as instrument transformer errors, line data errors and fault study data errors.

Zone 2 reach: The reach of Zone 2 will cover the section of the protected line outside the reach of Zone 1 as well as the initial section on the next adjacent lines to provide backup protection. Zone 2 normally covers 120% - 130% of the protected line (although the length of the next connected lines are also taken into account – see later in this section), which provides sufficient margin for non-zero fault impedance and other errors in relaying. With respect to the function of providing backup protection for the adjacent line, a large portion of the adjacent line needs to be covered without overlapping the Zone 2 reach of the other relays connected beyond the remote end of the "second" connected lines. Therefore, typically, Zone 2 is set to reach 50% of the shortest adjacent line for backup protection and to avoid such overlap. If the shortest adjacent line is too short, which leads to impedance of 50% of the shortest adjacent line less than 20% of the protected line. Zone 2 reach is then set to 120% of the protected line to ensure the full coverage of the protected line.

Zone 3 reach: Zone 3 elements perform backup function to Zone 1 and Zone 2 and also reverse direction backup function to adjacent infeeding circuit and the local bus. The reverse reach is normally set as 10% of the forward reach. Zone 3 element should not operate for the faults in the LV side or load encroachment.

Zone elements time setting: There is no intentional time delay for Zone 1 (primary protection). The time delay of Zone 2 and Zone 3 elements are set to coordinate with time-step protection at both the remote and local buses. The time delay for Zone 2 element is normally 400-500 ms, which taking into account of the priority of primary protection and circuit breaker operating time. Similarly, Zone 4 element is time delayed to discriminate with Zone 2 protection plus circuit breaker trip time for the adjacent line. A typical time delay setting for Zone 3 is about 1 s [And99].

2.4.3.2.2 GB standard for distance protection at transmission level

Distance protection scheme is only applied for transmission levels and should not

operate with a distribution fault. The typical GB distance protection setting requirements for 400 kV and 275 kV feeders is shown below (Z_1 is the impedance of protected line):

- Zone 1: Coverage = 80% Z_1 (forward). Time delay = 0 s
- Zone 2: Coverage = 150% Z_1 (forward). Time delay = 500 ms. The coverage of Zone 2 should be larger than 125% Z_1 under any circumstances. The reach of Zone 2 shall be at least 10% less than Zone 3, if possible.
- Zone 3: Coverage = $(0.8Z_1 + 1.5)$ % in per unit value on a 100 MVA base (forward). Time delay = 1000 ms.
- Zone 3 offset: Coverage = 10% Zone 3 setting or the next lower available setting (backward) [Nat11].

2.4.3.2.3 Discussion of practicalities of distance protection

The advantage of distance backup protection is that coverage of the protected line section is independent of internal impedance of the source compared to overcurrent protection (i.e. it is theoretically independent of fault level) and in general no communication system is required (although sometimes communications is used to enhance performance). The cost is relatively low as well, due to the widespread use of such protection and the fact that it can use the same measurement and tripping devices as other main protection systems [ATM07]. Also, use of distance protection along with other main protection schemes (e.g. differential) can benefit from the avoidance of common mode failures [Nor11].

The disadvantage of distance backup protection is the potential nuisance tripping/load encroachment of Zone 3, which could (and has in the past) cause cascading outages, and the difficulty for the setting of Zone 2 and Zone 3 protection to preserve and appropriate balance between sensitivity, security and dependability. Backup protection provided by distance protection tends to isolate additional elements from the power system which could potentially result in losing a larger proportion of the system and potentially placing more customers off supply. It is also more likely to falsely trip during stable system swings, as longer coverage and

more sensitivity is needed than local backup protection (circuit breaker failure protection – introduced more detailed in Section 2.4.3.4) [Nor11]. There is also a potential question over the efficacy of Zone 3, as it has just a significant time delay and there are questions (from the author) about when, if ever, it could be deployed.

2.4.3.3 Overcurrent protection

2.4.3.3.1 Principles

Overcurrent protection is a form of non-unit protection, which provides only remote backup protection for transmission level networks. Standard Inverse Definite Minimum Time (IDMT) relay characteristics defined by IEC 60255 are Definite Time (DT), Standard Inverse (SI), Very Inverse (VI) and Extremely Inverse (EI). For DT as shown in Figure 2.11, a fixed time delay is applied if measured current is higher than threshold. This is not used for power system protection, since discrimination and flexibility cannot be provided. For both high and low fault current, the operation time is the same which further limits its applicability, certainly in transmission power system protection. The other three characteristics can provide graded protection with discrimination of both current and time and can be used as backup protection. When fault current exceeds the predetermined current threshold, the operation time will be inversely proportional to the current magnitude and the equations that describe are discussed in [Als11].

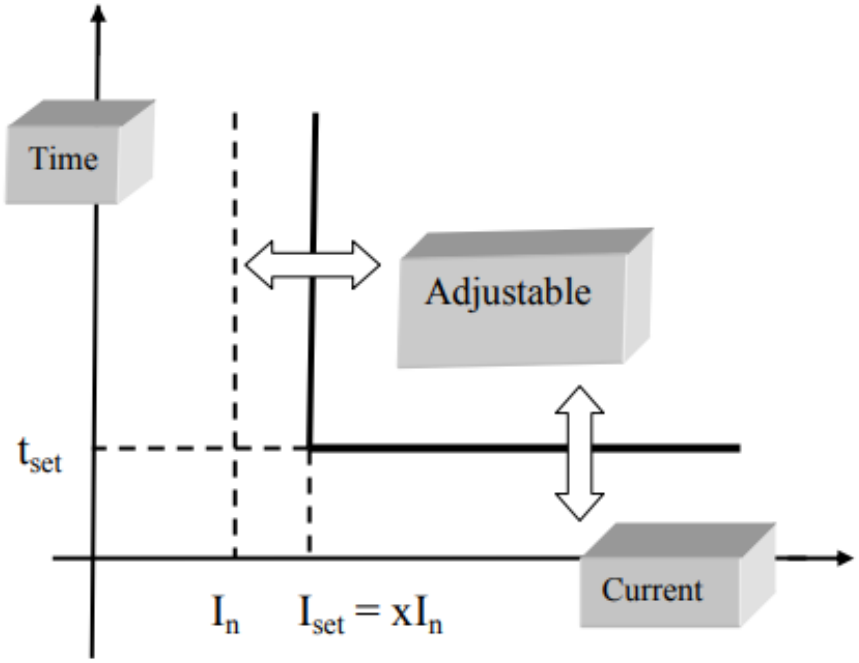

Figure 2.11: Definite Time Curve[Taw]

2.4.3.3.2 GB standard for overcurrent protection at transmission level

Overcurrent protection scheme serves transmission level only as backup protection. The overcurrent curve for transmission lines in GB is standard inverse (SI) curve [Nat11]. The overcurrent setting requirements for 400 kV and 275 kV transmission level feeders are shown below.

- The overcurrent setting is typically set to be 115% of the maximum loading – which is typically with respect to the thermal capability of the protected circuit.
- The maximum loading at 400 kV and 275 kV is 6.8 kA and 5.2 kA per phase respectively.
- Backup overcurrent protection operation time is at least 1 s for a three-phase fault at the remote end of the protected section with a fault infeed equivalent to 63 kA (maximum short circuit current) at 400 kV or 40 kA (maximum short circuit current) at 275 kV [Nat11].

2.4.3.3.3 Discussion of practicalities of overcurrent protection

The advantage of overcurrent protection as backup protection at the transmission level is that is inexpensive and independent of communication system. According to the principle of overcurrent protection, no additional hardware is required compared to circuit breaker fail (CBF) protection, which makes the expense relatively low. In addition, as no communication is needed, the security concerns about failure of communication system is not necessary.

The main disadvantage is the dependence on internal source impedance or fault level. According to the principle of the overcurrent protection, with the decrease of fault level in the future, the existing setting of overcurrent will perhaps not be sensitive enough to detect faults. If relays become more sensitive, there may be a risk of mal-operation. So, as with Zone 3 of distance protection, it is questionable whether overcurrent protection is beneficial, particularly in the future if fault levels decrease and/or become more variable.

2.4.3.4 Circuit breaker fail protection

2.4.3.4.1 Principles

Rather than installation of additional/redundant circuit breakers which need high expense and much space, circuit breaker fail protection is applied as a substitution to provide backup protection for failure of circuit breakers [KT11]. Although remote backup protection (distance and overcurrent protection) may be able to provide backup for a failed breaker, sometimes the time delay is too long which could cause damage to equipment due to the fault being on the system for a relatively long time, or the disconnected area would be so large that it could cause problems for system stability and performance [IEE82].

Circuit breaker fail (CBF) protection is extensively used as a local backup protection scheme which provides a relatively fast and secure means of backup protection. The block diagram which indicates basic logic of circuit breaker fail protection is shown in Figure 2.12. Circuit breaker fail protection is initiated by all relays tripping the breaker, but as a backup protection scheme, separate CT and AC wiring are normally used [XTTE12]. All initiation signals of CBF

from protection relays are hardware connected to dedicated circuit breaker fail relays [XTTE12]. When primary protection operates, the CBF function will be initiated, and if the circuit breaker that is tripped by the main protection operates, the fault will be cleared and current will be interrupted within a predetermined period of time. At the time of tripping, the breaker failure protection will be "armed" [ABB99]. If the monitored circuit breaker fails to operate within a predetermined period of time, the local circuit breaker fail relay will send a tripping signal to all adjacent circuit breakers, and in some cases to remote circuit breakers by direct transfer trip [IEE82].

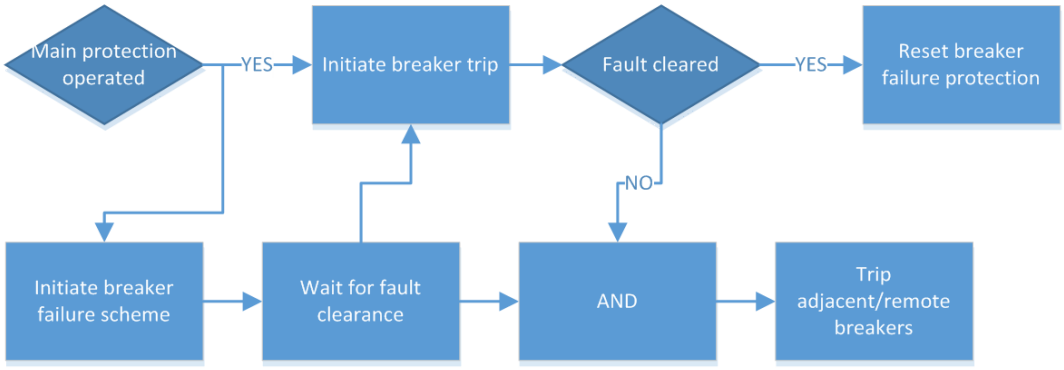

Figure 2.12: Basic logic diagram of circuit breaker fail protection

An example where a CBF relay sends tripping signal to adjacent circuit breaker is shown in Figure 2.13. For a fault between substation B and C, if circuit breaker 2 fails to operate within the expected time, CBF protection will operate to trip circuit breaker 1, 3 and 4 to clear the fault and to isolate failed circuit breaker (circuit breaker 2).

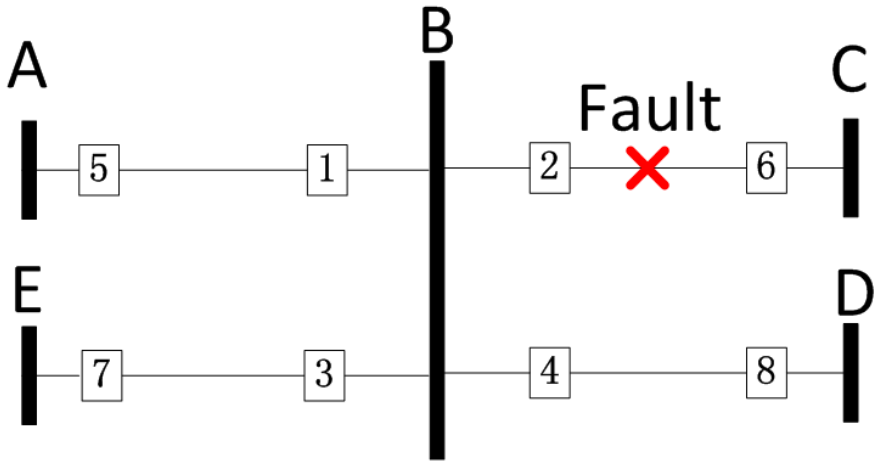

Figure 2.13: Example of breaker failure protection tripping adjacent circuit breakers

A circuit breaker scheme consists of three parts: CBF initiation circuits, fault detector and output circuit. In most of the cases, any operation of protection relays can initiate CBF except operation of CBF relays. Most CBF fault detectors are based on overcurrent relays but have variations depending on different schemes. Normally, a set of phase and ground instantaneous overcurrent elements are applied to detect current flow for transmission lines [ATM07]. For CBF output circuits, in most utilities, lockout relays are used to avoid automatic or manual reclosing of tripped circuit breakers tripped by CBF. In other cases, lockout relays are not applied in order to restore faster by remote control [XTTE12].

In transmission level, each breaker needs to be installed with one CBF scheme in all bus configurations to provide backup protection. The CBF scheme should attempt to re-trip the failed breaker before tripping adjacent or remote circuit breakers in case of losing large segment of system with spurious initiation if current threshold of CBF relay is below the threshold.

2.4.3.4.2 GB standard for circuit breaker fail protection at transmission level

Circuit breaker fail protection is typically the major and fastest backup protection scheme at transmission level networks. The setting requirements for GB 400 kV and 275 kV transmission CBF protection is to apply a current check threshold of 400 A and 240 A at 400 kV and 275 kV respectively to enable operation in the

first place [Nat11].

2.4.3.4.3 Discussion of practicalities of circuit breaker fail protection

In the event of a failure of main protection or circuit breaker(s), in many cases a smaller area of the transmission network will be isolated when CBF is used than by remote backup protection, with consequentially less disruption to the system (although the disruption caused by a protection failure and any form of backup operation will be severe at transmission level) [Nor11]. Furthermore, CBF has better operation than Zone 2 and Zone 3 distance protection whose operation may be influenced by many factors, including fault resistance, variable levels of remote limited by strong infeed effect [TH15]. Protection coordination and settings adjustment is simpler for CBF, as CBF only protects one specific zone with relatively simple logic, and does not need to take consideration of other factors such as fault levels and variability.

The primary disadvantage of CBF is that it may fail to operate because of common-mode failure which refers to the situation of a multiple failure caused by a common cause. For example, failure of station battery may be the reason of failure of both circuit breaker failure and local CBF. In addition, if all primary relays fail to operate and no tripping signals are initiated, which is highly unlikely of course, then the timer of CBF would not be initiated, which would then require remote backup protection to clear the fault with a relatively longer time delay [IEE16]. The high expense of CBF has also been viewed as a major disadvantage in the past, but more recent developments involving integrated CBF instead of standalone systems, and the reducing costs of modern microprocessor-based protective relays, mean that CBF functionality can be made available with no additional equipment required in some cases, although this may not align with policy for some power system operators [ATM07]. Poor flexibility of CBF in the past (when the tripping outputs were "hard-wired" to specific breakers) when the primary power system configuration was modified was sometimes a problem. However, this not such an issue now with more modern systems.

2.4.3.5 Possible impact of future power system developments on protection

2.4.3.5.1 Future energy scenarios (FES)

In order to determine the risks and develop solutions to mitigate any hazards that lie ahead, different scenarios are analysed in the Future Energy Scenarios (FES) [Nat15a], which is authored by National Grid, to provide different assumptions about future energy situations as shown in Figure 7.20. Four scenarios are considered, which take into account varying levels of future prosperity, political considerations and the presumed levels of "green ambition": The our scenarios are "Consumer power", "Gone Green", "No Progression" and "Slow Progression", although these names are sometimes modified – refer to Future Energy Scenarios (FES) [Nat15a] for full definitions of the latest scenarios. These scenarios are based on changes in future power systems which include anticipated growth of embedded generation, changes to the type of generation, increased interconnection with other countries' power systems, developments at the demand side and anticipated changes in loads (e.g. widespread proliferation of electric vehicles, the electrification of previously gas-fired heating, etc.). A common aspect across all scenarios is that increasing installed capacity of non-synchronous generation, and the performance of power systems will change significantly as a result of the different performance characteristics synchronous generation and non-synchronous generation. One of the major changes that this change to non-synchronous, inverter-connected, generation will be a major reduction in fault levels.

Figure 2.14: The future energy scenarios [Nat15a]

Such significant reductions and increased variability in fault levels arising from the increasing penetration of renewables (non-synchronous and inverter-interfaced) introduce challenges to the backup zones of distance and overcurrent protection, either rendering them prone to unwanted or non-operation, or requiring complex evaluation and possibly adaption of settings based.

2.4.3.5.2 Power system scenario – system strength and resilience

System strength is the ability of power systems to stay within a normal state or to recover from an emergency to normal state following a disturbance and is a primary indicator of the "robustness" of any system [Nat15a]. Fault level is one of the most important contributor to power system strength. As mentioned in the previous section, fault infeed or fault level will decrease significantly, which will consequently act to reduce system strength. The reduction of short circuit level will exacerbate fault-induced voltage depressions (in terms of their severity and the distance that they will propagate throughout the system from the fault

location) and may also impact existing low-voltage protection schemes and low voltage ride through capability of generators [Nat15a].

System resilience is a measure of the system to alleviate the influence of an unstable state (e.g. a major imbalance between supply and demand following an incident) using strategies such as load shedding. It is an indicator of the operability of the system under stressful situations.

2.4.3.5.2.1 Declining short circuit levels (SCL)

Since the research project to which this dissertation relates focuses on backup protection of transmission networks, the worst case of reduced short circuit levels (SCL) is considered in order to understand the risks to existing protection systems in the future. According to the 2015 SOF [Nat15a], four scenarios showing the average minimum SCL decline at different regions in GB for 2025/2026 are shown in Figure 2.15. The "gone green" scenario is the worst case for the majority of regions except SW England and North Scotland (probably because their fault levels are relatively low due to an already limited amount of large scale synchronous generation in these areas – they are already low at the 2015/16 time of publication of the SOF). The maximum decrease of average minimum SCL in Gone green 2025 is up to 68% in Northern England which could be a challenge for detection and clearance of fault (especially overcurrent protection) and fault ride through (FRT) capability of generation across wide areas of the system due to more pronounced voltage depression across larger areas of the system – if protection does not operate quickly there may be a real risk to the ability of remote generation to "ride-through" for faults at other locations of the system and potentially for failures in main and/or existing backup protection operations [Nat15a], which is one of the cause of the UK event in 2008 [Pri08] and the blackout in South Australia [Bad17].

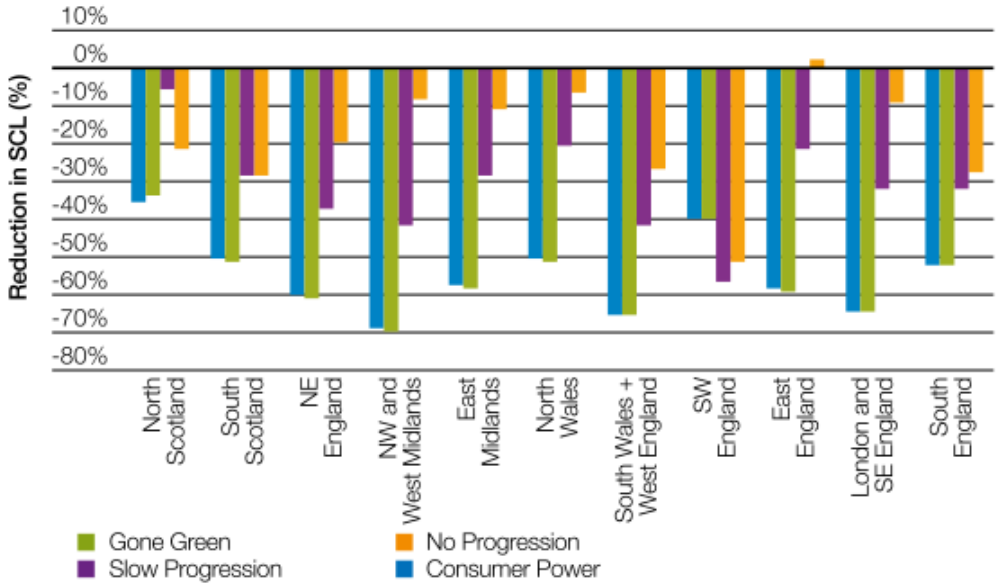

Figure 2.15: SCL decline 2025/2026 vs 2015/2016 levels [Nat15a]

The impact of low short circuit level in transmission level protection schemes is shown in Figure 2.16. According to the principles of differential, distance and over-current protection, overcurrent protection will be most severely influenced by reduction in SCL. Settings may need to be adjusted for distance and differential protection to maintain the reliability and security of the system. There remains much work to be done in analysing the performance of protection systems in the future. Fault level is of course very important, but the delay and shape of the AC waveforms output by converters in the future may also present challenges to protection system and individual relay operation [LBD+16].

Protection Scheme	Operating Principle	Impact of Low Short Circuit Level
Differential Protection	Compares the current infeed and output from the equipment; if the difference between the two is greater than bias current, the relay is set to trip.	If the difference between the currents is very small, it may not be detected by the relay. The bias may need to be set comparatively high at times of low short circuit level to avoid mal-operation.
Distance Protection	Calculates the impedance at the relay point and compares it with the reach impedance; if the measured impedance is lower than the reach impedance, the relay is set to trip.	Not affected if the ratio of voltage to current decreases following the short circuit. This ratio however will be affected by the significantly different volumes of synchronous generation at peak and minimum demand and may drive additional settings.
Over-Current Protection	The operating time of the relay is inversely proportional to the magnitude of the short circuit current.	This type of protection is the most likely to be affected by low short circuit levels, however these schemes are mainly used for back-up protection and therefore the consequences may not be severe, provided that main protection schemes are not compromised.

Figure 2.16: Impact of low SCL on operability [Nat15a]

In addition, with reduction of synchronous generation, the ratio between reactance and resistance (X/R ratio) of the power systems due to the limitation of reactive power support from converter-based sources will be lower which will result in a faster attenuation of fault current – this would still mostly affect over-current protection – distance and differential may not be so affected. Existing backup protection may not be fast enough to detect faults because of attenuation. If the setting is adjusted to be more sensitive to operate for these faults, the chance of mal-operation will increase. In order to adapt potential scenarios with lower fault level in the future to maintain system stability, a backup protection which is not affected by fault level variation or reduction, and has the potential to operate fast enough may be needed [HYH+16, GHCT06]. In 2007 Broad River Event, due to the 0.5 s delay of fault clearance by remote backup protection, four 230 kV transmission lines and three Broad River Energy Center Units were lost from the power system [Nor11].

2.4.3.5.2.2 Voltage dips during fault

Voltage dips can be caused by many events, such as the starting of a large machine or connection of a large power transformer to the system, however, short circuits are typically the most serious challenge to voltage stability and the major cause of any temporary or longer-term severe voltage depressions. As the depth and severity of propagation of a voltage dip throughout a power system is related

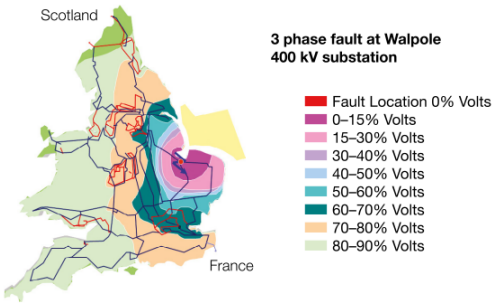

(a) Effect three-phase earth fault at Walpole 400 kV in 2015

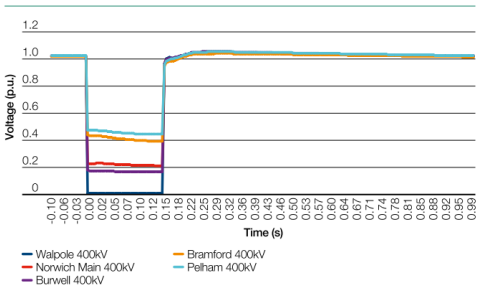

(b) Graph of 3-phase earth fault at Walpole 400 kV in 2015

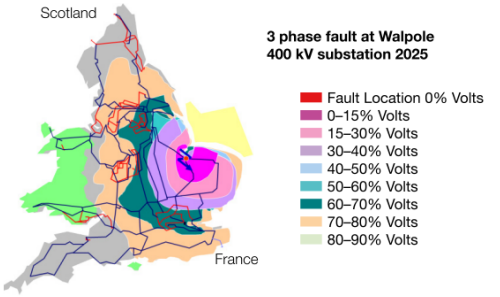

(c) Effect three-phase earth fault at Walpole 400 kV in 2025

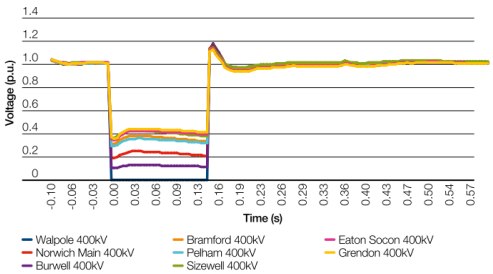

(d) Graph of 3-phase earth fault at Walpole 400 kV in 2025

Figure 2.17: Three-phase earth fault at Walpole 400 kV on voltage dip in 2015 vs 2025 [Nat15a]

to the strength of the system, then with the aforementioned increasing number of non-synchronous generations, voltage depressions will be generally more "severe" when short circuits occur in the future, as shown below in Figure 2.17.

Documents produced by National Grid, the transmission system operator for Great Britain (GB) [Nat15a], have indicated how in the future fault levels may decrease and vary over a very wide range, and how voltage depressions during faults may increase in magnitude and geographic extent. Figure 2.17 shows how, less than 10 years in the future, the impact of a three-phase fault (cleared in 140 ms – the maximum permissible time according to the grid code [Nat15d]) will have further-reaching severe voltage depressions compared to the present day, and how these depressions also propagate to sub-transmission (and indeed distribution) voltages. The fault shown in Figure 2.17 is at 400 kV Walpole which is a region with high levels of interconnection and will see a growth in NSG and a moderate increase in synchronous generation in the future, according to [Nat15a]. The further spread of voltage depression indicates that more transient support

for voltage is needed (such as the improvement of fault ride through capabilities of both synchronous machines and NSG) or faster protection may be required to contain the further propagation of voltage depression in time, as there is risk that other generators (or loads) could be affected by the voltage depression if it is not addressed quickly. Although no studied now shown in the voltage traces, it is anticipated that the recovery from such events may not be as fast in the future following fault clearance, and this may be worthy of further investigations in the future.

2.4.3.5.2.3 Fault ride through (FRT) capability of existing synchronous generation

Fault ride through (FRT) capability is the ability of the generations to remain connected to the power systems during low voltage situations (such as those caused by short circuit faults) to avoid further loss of generation during or immediately following a short circuit fault. In the European context, ENTSO-E (the European Network of Transmission System Operators for Electricity), has recently been very active in producing codes and recommendations for generators and HVDC interfaces, outlining how such systems should behave during faults and in terms of their "ride through" capability. According to ENTSO –E [ENT16], the general fault ride through profile is shown in Figure 1.3 and the parameters for transmission level synchronous machine is shown in Table 2.2. Both t_{clear} and U_{clear} are within a range rather than a fixed number. t_{rec1} and U_{rec1} are the upper boundary of the range of t_{clear} and U_{clear}.

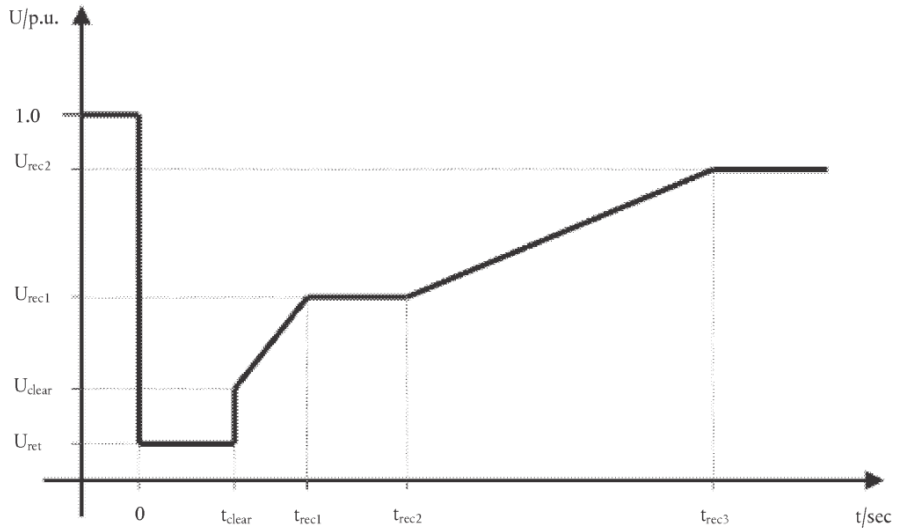

Figure 2.18: Fault ride through profile of generation [ENT16]

In the future, with decline of fault level and further propagation of voltage dip, if the primary protection failed, synchronous generations maybe do not have the ability to ride through faults and may cause blackout of a large region of the power system (although it is known that Low Frequency Demand Disconnection – based on frequency – is used as a "last resort" in GB, but has only once operated in the past as far as the author can ascertain [Ene15]). For the example of fault at 400 kV Walpole in 2025 shown in Figure 2.17, the voltage of 400 kV Burwell will be less than 20% during fault. If primary protection failed, even circuit breaker failure protection (CBF) operate normally which needs 300ms [Nat15d], the synchronous generation connected to Burwell would probably still disconnect from the system (according to the minimum ride-through curves in [ENT16])and this may cause cascading outage of the system. Therefore, in such cases, faster backup protection may be desirable. Furthermore, if the entire protection system were to fail (i.e. circuit breaker fail was not operational) then power system protection backup operation time is at least 500 ms, so the impact on other generators in the vicinity could be even more severe.

Voltage parameters (p.u.)		Time parameters (seconds)	
U_{ret}:	0.05-0.3	t_{clear}:	0.14-0.15 (or 0.14-0.25 if system protection and secure operation so require)
U_{clear}:	0.7-0.9	t_{rec1}:	t_{clear}
U_{rec1}:	U_{clear}	t_{rec2}:	$t_{rec1-0.7}$
U_{rec2}:	0.85-0.9 and $\geqslant U_{clear}$	t_{rec3}:	$t_{rec2-1.5}$

Table 2.2: Parameters for fault ride through capability of synchronous generation

2.5 Summary

This chapter has conducted a review of the fundamentals of power system protection, especially backup protection, as well as the challenge of the future power systems in the view of power system protection. Occurrence of electrical faults can never be eliminated, which can lead to damage of equipment, power system outages and even blackout if appropriate protection and other response systems are not in place or configured correctly. Power system protection can detect and isolate the faults in a very short period of time to minimise the impact of any faults. Thus, providing protection for all system elements, and in particular transmission lines (which are often overhead in nature, exposed to the environment and the components of the power system that generally experiences most faults) [ENT09]. Ideally, primary protection can operate near-instantaneously to clear the fault from the system. However, in reality, primary protection scheme can fail to operate, which lead to the demand of backup protection to remedy the failure of primary protection with a time delay. The principles and GB requirements for transmission lines have been presented in this chapter. The benefits and drawbacks of the different schemes were also discussed in this chapter, which provides a benchmark for the backup protection functionality of the proposed scheme in this dissertation.

One of the main drivers for the proposed scheme is the challenges brought about by future power systems. Changes such as declining fault levels and reduced system inertia due to increasing numbers of converter-based sources could

cause ride-through problems for generators and failure or mal-operation of existing backup protection schemes. With development of communication technologies and potential popularity of PMUs, the scheme proposed in this dissertation could potentially be an extra layer of protection to maintain stability and resilience of power systems of the future.

Chapter 3

Wide-area PMU-based monitoring and protection schemes

3.1 Introduction

This chapter reviews the basic principles and applications of PMU-based wide-area measurements and review wide-area monitoring and protection applications proposed and applied by others, with relevance and reference to the contributions of this dissertation. Section 3.2 describes the fundamental principles, categories and standards of PMUs, which underpin wide-area applications, including the algorithm developed and used within the scheme proposed in this dissertation. Sections 3.3 and 3.4 review selected wide-area monitoring, control and backup protection schemes proposed by other researchers, with specific commentary on any identified "gaps" or perceived shortcomings of other researchers' work that are addressed by the contributions made in the research reported in this dissertation.

3.2 Phasor measurement units (PMUs)

3.2.1 Principles and standards

PMUs provide real-time measurements of magnitude and phase of voltage and/or current. PMU data (or derived data from PMUs) may include positive sequence voltages and currents, individual phase voltage and currents, local frequency and ROCOF (rate of change of frequency) and many other quantities, which can be used in wide-area monitoring, control and protection schemes. Quantities from geographically-separate substations are synchronised and can be compared and analysed accurately via measurements from PMUs and wide-area communication networks, which have accurate time stamps. The accuracy is 1 µs [HP08] and is derived using the Global Positioning System (GPS), with time traceable to Universal Time Coordination (UTC) [US15]. PMUs can communicate with several clients via various communications protocols, typically via Transmission Control Protocol/Internet Protocol (TCP/IP) and User Datagram Protocol (UDP). IEEE C37.118 (synchrophasor protocol) is applied to ensure the validation of measurement and communication [KHL04b].

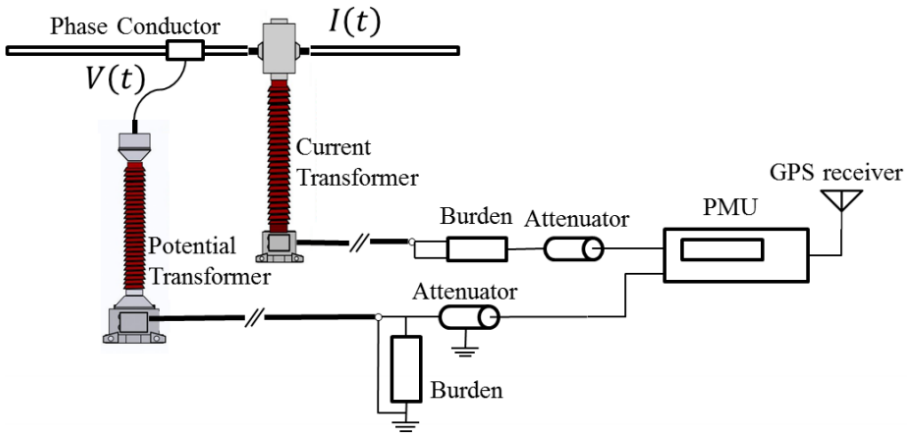

Figure 3.1: PMU power system connection diagram [LYY+17]

In order to filter and output the quantities such as individual phase voltages and currents, each PMU requires a three-phase measurement connection to the power system. Figure 3.1 illustrates the typical single-phase connection of a PMU

System frequency	50 Hz			60 Hz					
Reporting rates (Fs-frames per second)	10	25	50	10	12	15	20	30	60

Table 3.1: Required reporting rates [STD11]

at a substation. Inputs to PMUs are the scaled down analogue voltage and current waveforms from the power systems provided by current transformers (CT) and voltage transformers (VT). The voltages and currents are scaled down to fit the range of analogue-to-digital converters (A/D converters). The burdens are used to output the desire voltage. The attenuators are passive bidirectional devices also used to adjust voltage by lowering or attenuating the voltage or power level without distortion of the signal waveform [HBM02].

The input signals from transformers are isolated, filtered and sampled at a desired rate which is depends on user requirements and PMU algorithm design. The time domain data collected from an A/D converter is transferred into phasor representations by the microprocessor via Discrete Fourier Transform (DFT) for further comparison and calculation [LYY+17].

According to the IEEE standard for power system synchrophasor measurements, the output data reporting rate shall be supported at sub-multiples of the nominal power-line (system) frequency, which are listed in Table 3.1.

The reporting rated implemented in reality should be selected by users and other reporting rates, which could either be higher or lower, such as 100 Hz for 50 Hz system or 10 Hz for systems with both frequencies, are also permitted [STD11].

According to [STD11], PMUs have two performance classes based on applications, which are P class and M class. The use of either class based on the requirements of individual requirements.

- P class represents protection class, which is aimed at for systems that require fast response and no dedicated filters such us anti-aliasing filters are required. While P class is used to denote protection, implementation of PMUs for primary protection is rarely considered, as previously the phasors essentially require at least one cycle (20ms) to produce a stable output,

while main protection is often required to operate in less than one cycle. With higher reporting rate (can be up to 200 Hz for 50 Hz networks) and the installation of more efficient communication infrastructures, PMUs can be potentially implemented for primary protection. Nevertheless, in P class devices, relatively shorter measurement window lengths are used for phasor estimation. However, the length of measurement window has a trade off with accuracy, particularly during transients, and incorrect measurement window length could have a negative impact on functions that involve near real-time monitoring and decision making.

- M class is used for systems that do not require fast response but require very high accuracy, and their accuracy during short-term transients is not critical. M represents measurement applications. Relatively longer window lengths are required for phasor estimation and therefore the phasor estimation is generally more accurate than P class, but accuracy in capturing transients is limited as the transient is filtered or "averaged" over the measurement window.

More standards and requirements for PMUs are shown in [STD11]. However, for brevity, this section only presents in detail the most relevant aspects of the standards that are relevant to the work reported in this dissertation, which are reporting rate and performance class.

3.2.2 Global deployment of PMUs

Currently, the major application area for PMUs has been at the transmission level. According to the report of U.S. department of energy, the average overall cost per PMU (cost for procurement, installation, and commissioning) is ranged from $40,000 to $180,000 in 2014 (could be cheaper at present due to the lower price of the hardware - PMU units)[U.S14]; this presumably includes equipment costs, commissioning cost, the cost of the associated communications network, etc. This figure should be taken into consideration for projects and schemes

which aim to provide monitoring, control and protection based on information from PMUs [QUA17].

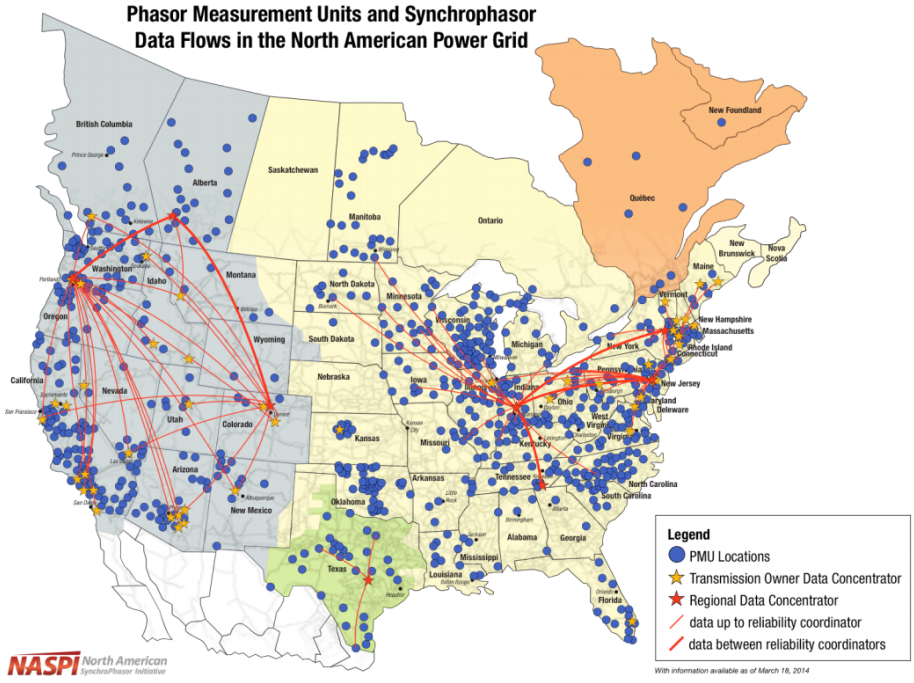

Figure 3.2: Phasor measurement units and synchrophasor data flows in the North American Power Grid [Nor14]

PMUs have already be installed in many countries to improve security and enhance stability of power systems around the world. In the US, there are over 1,000 substations equipped with over 1,700 PMUs and the number is growing continually [U.S14]. A map of PMUs deployment in the US is shown in Figure 3.2. China had installed approximately 2,400 PMUs in over 1,700 substations by 2013, which covers all 500 kV substations, a number of important power plants and several 220/110-kV substations [LSWS15]. 62 PMUs has been deployed in India in 2014 and over 1,700 PMUs will be installed across India based under the Unified Real-Time Dynamic State Measurement (URDSM) scheme, which approved an investment of 6.550 billion Rupees (around 71 million dollars) and 11,000 km of optical fibre [Muk14]. In the UK, 50 Hz PMUs and 200 Hz waveform measurement units (WMUs) are deployed across more than 100 sites in Scotland, England and Wales for visualisation of real time system dynamics [Sco17]. The deployment map is shown in Figure 3.3. As a tool with compelling benefits, PMUs have been deployed all around the world, in the context of unprecedented requirements for

real time monitoring and control of the power systems, particularly in the future, to maintain the reliability of the power systems [KHL04a] due to the following facts.

- Unexpected and unpredictable changes in the system's operational condition are happening now and more in the future due to the proliferation of DGs, renewable energy sources, HVDC links, electric vehicles, etc. New, and potentially unanticipated, load flow patterns may be experienced more frequently by the system operator in the future [KHL04a].

- Reliability of electricity supply is continually becoming more and more crucial for society as electricity is relied upon for financial, internet, transport and other uses in addition to the traditional uses for heating and lighting. Blackouts are becoming more and more costly and disruptive (e.g. the outage for data centres cost $740,357 per incident on average) [NGR17].

- Wide-area disturbances during the last decade, have forced/encouraged power companies to design system protection schemes to counteract voltage instability, angular instability, frequency instability, to improve damping properties or for other specific purposes [KHL04a].

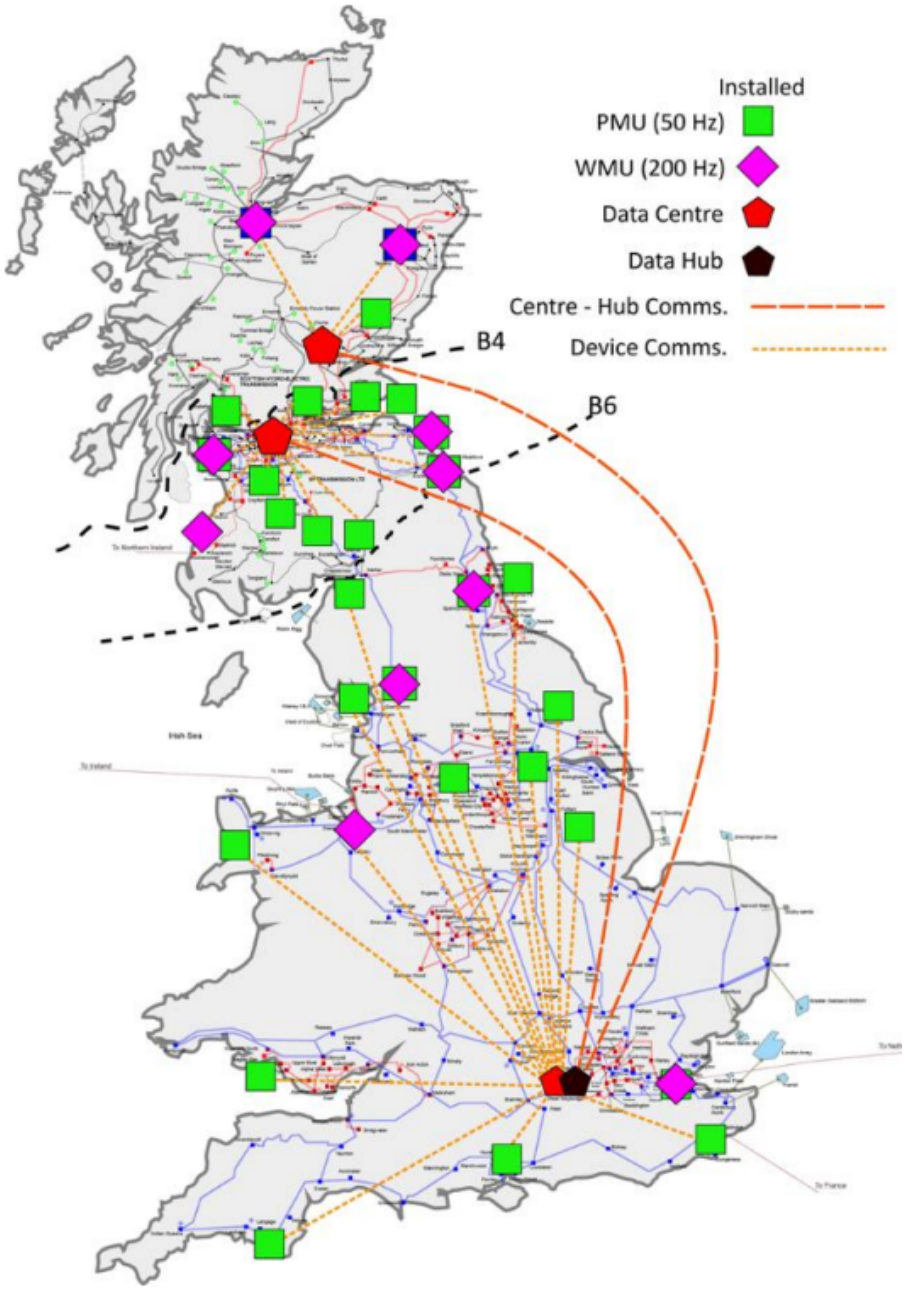

Figure 3.3: WAM deployment of VISOR [Sco17]

In addition to the aforementioned counties, Japan, Russia, Brazil, Australia and many European countries such as Sweden and France have all deployed PMUs for various purposes [Nag16].

3.3 Wide-area monitoring and control schemes

3.3.1 Conventional (non-PMU) measurement & monitoring infrastructure (using Supervisory control and data acquisition - SCADA)

SCADA is an industrial computer-based system for real-time monitoring and control, which is capable of tracking and analysing data and information from remote field devices such as sensors through microprocessor based controllers - either Remote Terminal Units (RTUs) or Programmable Logic Controller (PLCs), which gather data from a range of devices and can transfer control signals to field devices. The functionalities of RTUs and PLCs are presented later in this section.

For implementation in power systems, as opposed to manual inspection, measurement logging and control, the SCADA system can remotely monitor the system and automatically send control signals to the remote site, which highly improves the efficiency of power systems by conducting functionality such as substation control, feeder voltage (VAR) control and load control [Ele15].

Figure 3.4 shows the basic architecture of SCADA systems. In power systems, a range of sensors and controllers are clustered at substations, which are distributed throughout the power system. Data from substations are transmitted from RTUs or PLCs via communication infrastructures to a supervisory system which acquires and analyses the process data [Tec]. The data then is displayed via a Human-machine Interface (HMI), which is in a human readable format and enable operators to make decisions and apply operational commands as required; with some systems having applications that can issues control signals automatically, and provide users with summarised information from a large amount of data [T.A]. The functionality of each element of SCADA systems is discussed below - from field monitoring and sensor devices up to the central control system. SCADA systems have been in use to monitor and control power systems for several decades.

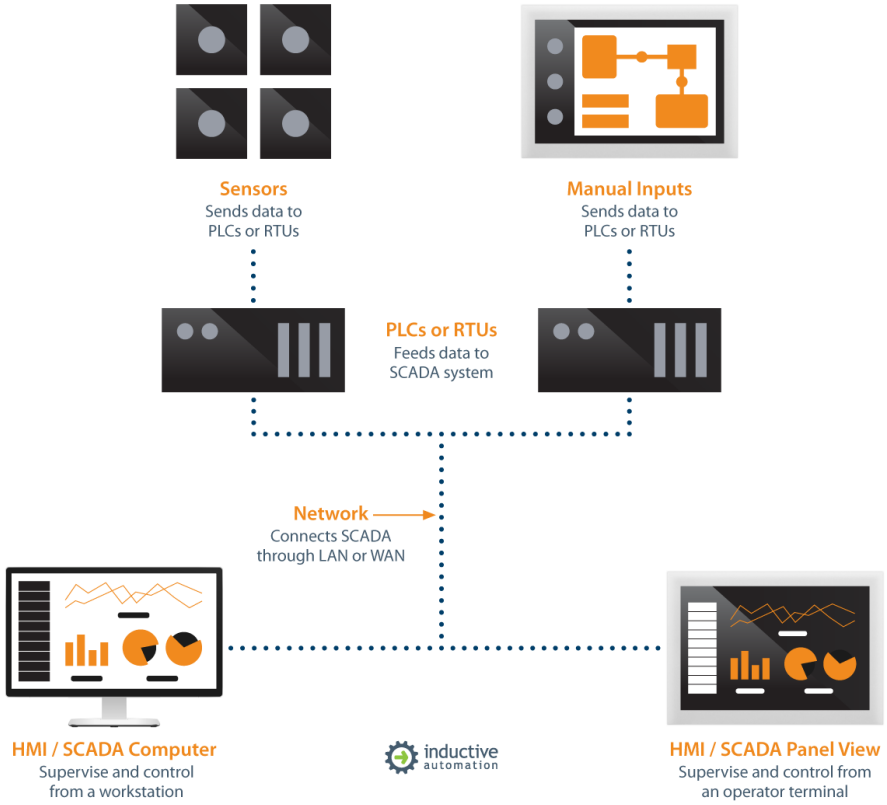

Figure 3.4: Architecture of a SCADA system [Ind]

Field devices and control elements: sensors and direct control elements such as CTs and VTs (field devices) and circuit breakers (control elements).

RTUs and PLCs: units that gather and transmit inputs from field devices and control elements to the supervisory system through a communications infrastructure and may automatically control the system by initiating direct control actions (in some cases the control software is distributed within the RTUs, in other cases the RTUs merely relay commands on from the central system which carries out the monitoring and control process).

Communication infrastructures: the component that transfer data between the central supervisory system and RTUs and PLCs, via various media such as optic fibre, microwave, Ethernet or a combination of media. The quality and availability of the communications infrastructure has a critical impact on SCADA system. Some typical communication protocols that are used for various SCADA applications are shown in Figure 3.5.

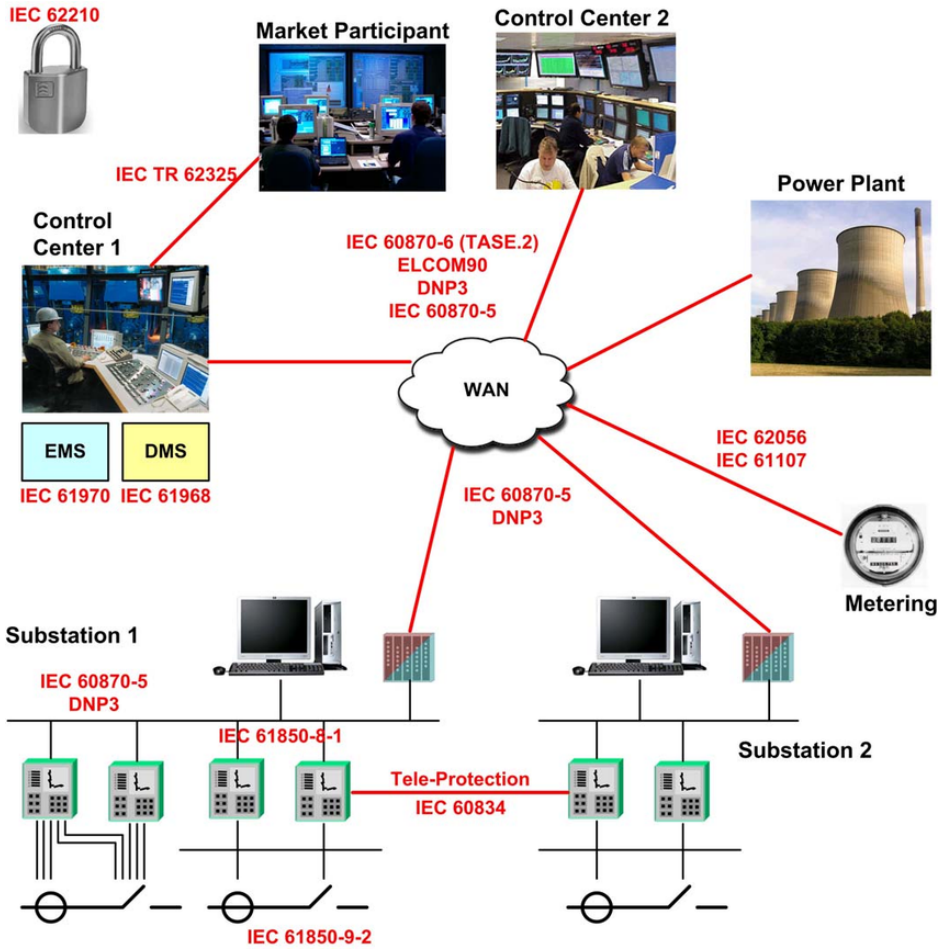

Figure 3.5: Typical communication protocol in power systems [MSW09]

A supervisory system: a centralised computerised system that acquires data from the RTUs and PLCs, performs analysis and issues control commands when necessary. Functions typically include trend analyses, centralised processing and summarisation for alarms and indications, and reporting. The application areas are listed in Table 7. Although RTUs and PLCs may in some occasions automatically control the system by a feedback control loop, the supervisory system monitors the overall performance of the loop. For example, the PLCs can automatically send command to controller to operate if the processed quantity is outside of the threshold and the supervisory system can adjust the threshold based on performance of the whole system [KDS10].

Human-Machine Interface (HMI): the user-friendly interface for a human operator of the system, via which the operator can easily monitor and control the behaviour of the system [Kra15].

SCADA systems are still widely used in the industry, but can only provide indications relating to events (e.g. protection operation, status of circuit breakers, etc.) and relatively low resolution non-synchronised measurement data (e.g. power flows, indications of voltage/current levels, alarms when levels go outside of normal limits etc.). They typically do not have the full capability to provide high-resolution data (e.g. their refresh rate may be 0.5 Hz [Roy]) that could be used for online monitoring, control or protection purposes.

3.3.2 PMU-based wide-area monitoring and control schemes

Since SCADA systems are generally not capable of carrying out real-time fast-acting functions, due to relatively slow data collection and refresh frequency, PMU-based WAMC schemes have emerged in response to the requirement for faster-acting monitoring and control functions that can operate over a wide area [LTY12]. The aim of WAMC systems is to monitor and evaluate the status of power systems and take appropriate actions within the timescales required to maintain the integrity of power systems; typically through analysing data acquired from various locations [ZLK+05]. According to Section 3.2 and 3.3.1, the comparison between SCADA systems and synchrophasor technology is shown in Table 7.12. It can be observed that synchrophasor technology possesses high data acquisition resolution and accurate time synchronisation characteristics, which enables the accurate and relatively fast analysis of dynamic situations as they evolve within power systems and therefore provide the possibility of conducting either preventive or remedial actions to maintain security and integrity of the power system [GK15].

Based on data flow between the acquisition analysis (decision making) locations, the architecture of PMU-based wide-area monitoring and control (WAMC) systems can be defined within three categories – centralised, decentralised and distributed systems [GK15].

Figure 3.6 shows the centralised architecture, where visualisation, analysis and

SCADA Technology	Synchrophasor (PMU) technology
Limited or no universal time synchronisation	Universal time synchronisation
No global angle reference	Global angle reference
Refresh rate 2-5 second	Refresh rate 30-60 sample/sec
Communications – latency, jitter and skew	Time tagged data, minimal latency
"Older" legacy communications and often use proprietary (non-open) protocols and standards	Compatible with modern communication technology
Responds to quasi-static behaviour	Responds to system dynamic behaviour

Table 3.2: Comparison between SCADA and synchrophasor technology

action decisions are all made by the central phasor data concentrator (PDC), typically situated in a control room and using data collected directly from distributed PMUs [KWK10].

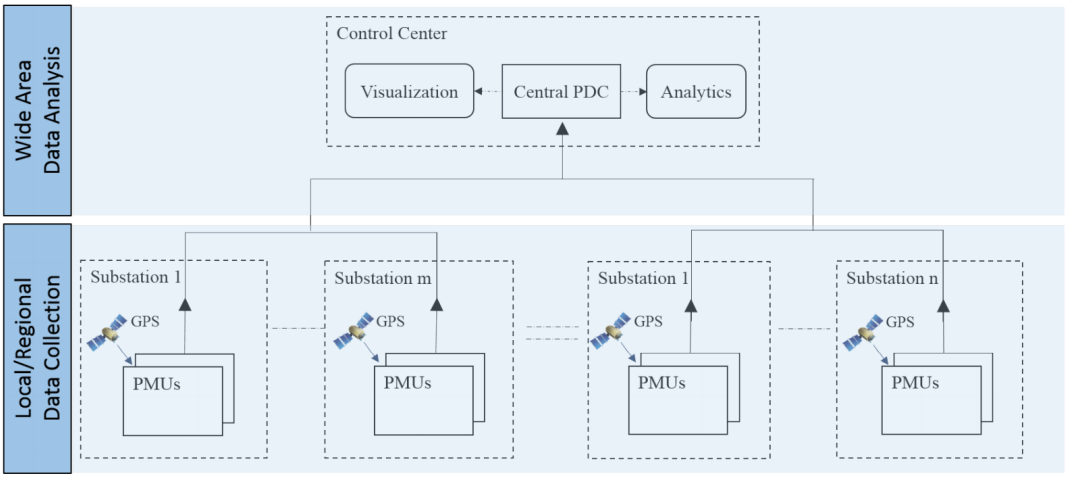

Figure 3.6: Centralised structure of WAMC systems [GK15]

Figure 3.7 shows the decentralised architecture, where the overall monitored and controlled area is divided into multiple relatively small regions. PDCs are sited locally at each region for data processing and analysis take actions locally to control the system to maintain integrity. Local PDCs can share information with each other to monitor and control a larger area. This architecture is normally used for regional monitoring, control and protection with an overlap between

Architecture type	Strengths	Weaknesses
Centralised	Relatively lower communication latency due to elimination of PDC	Requirement of high data storage capacity of PDCs
	Easy data access	Vulnerability to single node failure
	Coordinated alarming an remedial actions	
Decentralised	Low requirements for data storage capacity	Overlap cells are required
	Reliability	
	Relatively lower communication latency compared to distributed architecture	
Distributed	Low requirements for data storage capacity	Relatively higher communication latency
	Reliability	
	Regional coordinating functions	

Table 3.3: Comparison between architectures of (wide-area monitoring and control) WAMC systems [GT18] [KWK10]

regions as presented in [SGNP].

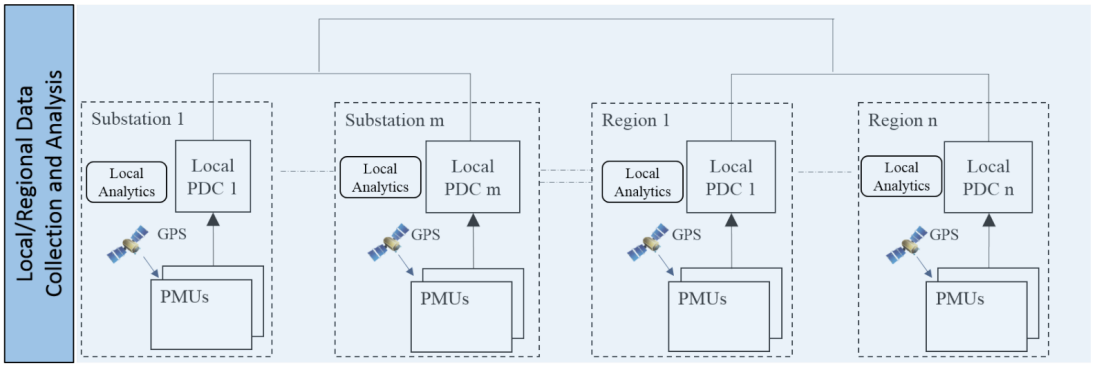

Figure 3.7: Distributed structure of WAMC systems [GK15]

Figure 3.8 shows the distributed architecture, where a master PDC is added at the top of the hierarchy, which has access to all distributed PDCs and supervises and controls the system based on analysed information from local PDCs.

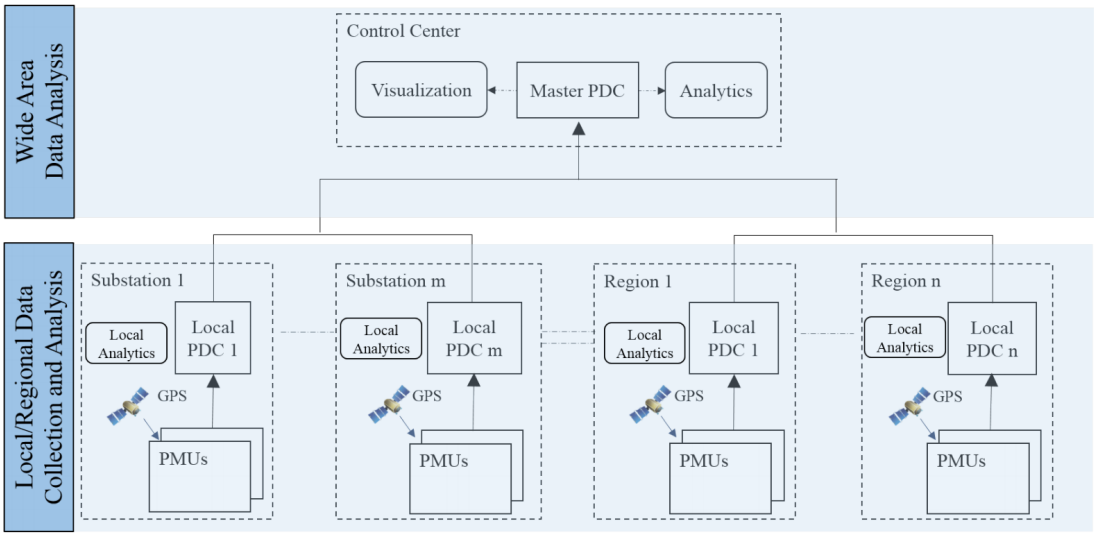

Figure 3.8: Decentralised structure of WAMC systems [GK15]

Table 3.3 compares the strengths and weaknesses of centralised and distributed and decentralised architectures.

There are a multitude of applications spanning monitoring and control using PMU data. Table 3.9 provides a brief summary of a range of monitoring and control schemes using PMU data, along with a brief comment on their strengths and possible weaknesses. There is no real need for a detailed analysis of these applications in this dissertation; the focus of the research reported in this document is on wide-area protection reporting and backup protection functionality, so a more detailed review of applications in this domain will be presented in the next section.

Application area	Strengths	Weaknesses	Institute/company implementation
Voltage control monitoring and control	• Increase level of transmissible power levels [12] • Reduce active power loss and take full advantage of reactive power [13] • Allow adequate reactive power to maintain voltage for emergency [14] • Provide real time power-voltage curve (stability situation of voltage) • Allow operators to make decisions fast • Allow rapid computation of real-time transfer capability applied to paths	• Data security • Communication reliability • Available communication infrastructure and speed • Relatively high expense	• Institut de recherche d'Hydro-Québec (IREQ) [15] • Bonneville Power Administration [16] • Western Electricity Coordinating Council (WECC)[17] • Consortium for Electric Reliability Technology Solutions (CERTS), Lawrence Berkeley National Lab (LBL) and Department of Energy (DOE) [21]
State estimation	• Improve network observability measurement redundancy level • Improve efficiency of bad data detection and elimination – voltage could be calculated by current phasors		• Georgia Institute of Technology [18] • Duke Energy [19] • Virginia Tech and Pacific Gas and Electric Company [20].
Frequency monitoring and stability control	• Allow relatively fast operation • Provide large scale of coordination [9]		• Department of Energy (DOE) and North American Electric Reliability Corporation (NREC) [22] • National grid [23] • Scottish power [24]
Calibration of instrument transformers	• Provide accurate measurement of CT and VT under various loading condition [14]		• Dominion Virginia Power (DVP)[25]
Line thermal monitoring and control	• Allow fast operation for emergency scenarios • Allow individual warning and alarm to be set [8]		• Italian Transmission System Operator (TSO) [26] • ABB Group [27] • Atel Transmission Ltd and in cooperation with ETRANS [28]
Power system oscillation monitoring and control	• Provide improved power system visibility [11] • Allow individual warning and alarm to be set • Differentiate local and inter-area power swing [8]		• Thailand with installation of PSGuard [29] • Scottish Power [24] • Norwegian Transmission Network [30] • The French transmission system operator (RTE) [31] • The North American Synchrophasor Initiative (NASPI) [32]

Figure 3.9: Applications of wide-area monitoring and control[San11] [ZLK+05] [LBI+17] [Cor09] [XTEK14] [HD16] [TVC00] [U.S09] [Geo13] [ZCM+17] [CZMK16] [CGLW15] [Con08] [Nat18] [Sco18] [PVV16] [ABBb] [WSR+06] [UVd+12] [VPXP17] [NAS17] [WTS+12] [ABB15]

3.4 Review of wide-area backup protection schemes proposed by other researchers

3.4.1 Overview

The application of wide-area measurements from PMUs for backup protection is considered to be an effective extra layer of protection that can work alongside and in addition to conventional backup protection [HZC+11]. Currently, PMU protection applications mostly focus on backup (often requiring current measurements, whereas the schemed developed through this research requires only voltage), adaptation of protection settings and/or protection blocking in certain cases to enhance security [LH14, Ter07, PWDV16, LZV16]. Communication system delays associated with wide-area measurements, in most cases, are too long for primary short-circuit protection applications [HZC+11, PWDV16]. However, such measurements are adequate for wide-area monitoring and backup protection schemes [Udr14a].

A wide range of wide-area backup protection (WABP) schemes have been proposed and reported by researchers and they can be categorised in many ways (e.g. presented in [SGNP]). In the dissertation, they are classified into four categories: current-based, impedance-based, voltage-based and status of protective devices based, which are reviewed in detail in the following sections.

3.4.2 Current-based methods

A current-differential based method is proposed in [UDR14b]. With a thorough analysis of Synchrophasor Standard and the impact of communication systems (e.g. latency, data stream availability), the scheme can provide relatively backup protection compared with existing back protection at transmission level (zone 2 distance protection). The scheme can remove faults from power systems as precisely selective and as fast as possible with consideration of communication latency, measurement times and breaker inter-tripping times. It is also immune

from loads and power swings. However, the scheme requires the installation of PMUs to be at both terminal of the lines and corresponding communication infrastructure and auxiliary cyber security measure, which lead to relatively high extra cost. An approach is described in [ZAS15] which is based around faulted feeder detection through comparing the terminal currents of transmission lines. This is effectively current differential based scheme and does not therefore identify the faulted feeder through voltage measurements from PMUs. With the help of network topology analysis, the system can accomplish the its function in the absence of data from specific PMUs. For practical purposes, the paper also provides a way of optimising the required PMUs, in terms of the minimum number of PMUs required and their corresponding locations, and it proposes a method to "regionalise" the protected area to minimise communication latency. Since the quantities used for protection purpose are the terminal currents, installation of PMUs at both terminals of the line is required, which may be expensive and not practical – in most of the reported applications, single PMUs are typically installed only at substations (measuring phasors from the node/busbars) rather than at terminals of lines [NAP17]. The cost of PMUs has been considered in the paper, and it has been stated that data from a number of locations can be absent and the system will remain functional. However, this may still not be practical, as PMUs are typically only installed at substations rather than at the individual line terminals. Even though the scheme can deal with missing data, it is still implied that there would be a large number of PMUs in the vicinity at all other line terminal locations. The approach has been tested using a range of IEEE benchmark systems using Simulink, however no real-time validation is carried out. In [NR15], an adaptive scheme based on current measurements is proposed. In this work, the protection decision-making process is conducted following two initial steps – backup protection zone identification and faulted line determination. The scheme limits cost by only stipulating that PMUs be installed at substations with generators(impacts of loads are neglected during short circuit faults). The scheme utilises the measurement data together with a bus impedance matrix to represent and estimate the system performance at various nodes. Since

currents at substations without generators can be calculated using current measurements from the lines importing/exporting from the substation based on KCL, only substations with generators are required to be equipped with PMUs. The protected zones are bounded by PMUs and if the sum of zero or/and positive sequence current entering the zone is over the threshold (threshold is the larger value between the defined minimum threshold value – constant and the average of the last minute theshold), a fault is indicated occurred in the corresponding zone (the defined minimum threshold value is not clearly defined though). The faulted line is then identified using a linear least square method, and the faulted feeder is also identified at the same time. The scheme can be applied to detect various types of faults with different fault locations, and has been tested using both the WSCC 9-bus and IEEE 118-bus networks using Simulink in Matlab. However, fault resistance is not considered in the scheme, which would have a significant impact on performance in reality, and real-time validation is not conducted. Furthermore, the impact of load connections (which would result in a differential current from the PMUs at generator) is not considered, which is a shortcoming of the paper, and the fact that phase-phase faults (that may require the involvement of the negative sequence components) are not considered, indicate that this method may not be ready for practical implementation. [EME10] presents a method for unit backup protection based on positive sequence voltage and current angle measurements at the terminals of transmission lines. By comparing the voltage magnitudes of all buses, the area of voltage collapse/short circuit fault can be identified as the area including the feeders directly connected to the bus with the lowest magnitude. The absolute value of angle difference of current contributed from each terminal of the line (within the identified area) is then calculated and recorded. By comparison, the feeder with the maximum absolute value of angle difference (between the connected faulted line and the busbar with the minimum voltage value) is identified as the faulted line, which shares the same principle as differential protection which is discussed in Section 2.4.2.2. The scheme is tested using a 5 bus, 6 line system via simulation. The scheme can accurately identify the fault location to the feeder level relatively

quickly. However, since current measurements at both terminals (or more in a multi-terminal arrangement) of the feeders are required, the expense and the need for data synchronisation would be high and the large volumes of data required would perhaps cause issues with the performance capabilities of the existing communications infrastructure (in common with many of the reviewed schemes). In [KP15], an approach involving comparing positive sequence voltage magnitudes at substations and positive current and voltage angle deviation at line terminals is described. The faulted region is identified as the feeders connected to the bus with the lowest positive sequence voltage magnitude. The specific faulted line is subsequently identified as the one with the largest deviation of angle between voltage and current within the faulted region. By monitoring the status of protection devices from their trip output signals, the scheme compares the operating status of protection devices and the identified faulted feeder to identify errors in protection operation. However, since multiple inputs are required for decision-making, the number of PMUs required for deployment of such a scheme is higher than schemes proposed by other researchers. A method suitable for application to transmission networks incorporating series compensation is presented in [NPB14]. Balanced and unbalanced faults are identified from analyses of positive sequence and negative sequence components respectively, using two main steps. For balanced faults, the first step is to identify the bus with the lowest positive sequence voltage magnitude as being the bus closest to the fault. Subsequently, for all lines connected to that bus, the cosines of the angles between the positive sequence currents and voltages at each terminal of the lines is calculated (and at the "other side" of any series compensators if series compensation is used on the lines). The line with positive cosine values (if no compensation, only at both terminals; if with compensation, at both terminals and on the remote side of the series compensators) is deemed to be the faulted circuit. This is the second step of the operation of the system. For unbalanced faults, the first step involves identifying the bus with the relatively highest value of negative sequence voltage magnitude as the bus located closest to the fault. The second step is the same as that for balanced faults, apart from the fact that all quantities used for comparison are

negative sequence components. The method is tested in a 9-bus, 3-source network simulated using EMTDC/PSCAD. The scheme has the potential to be fast and accurate. However, voltage and current phasors are required to be measured at both ends of a feeder, especially for a feeder with series compensations, which could lead to extra expense for measurement equipment and for installation. A current differential based approach is proposed in [SMK+98], which describes the concept both functionally and structurally. Thanks to the unit protection principle of differential protection, the scheme can accurately identify the fault location and selectivity is greatly improved compared to conventional backup protection schemes, which are typically non-unit in nature. Subsequently, the area isolated by protection devices can potentially be minimised (and the speed of operation of backup protection could be potentially improved). Utilising an Asynchronous Transfer Mode (ATM) network (ATM is a switching technique used by telecommunication networks that uses asynchronous time-division multiplexing to encode data into small, fixed-sized cells). This is different from Ethernet or internet, which use variable packet sizes for data or frames [KINO98], a specific system configuration and application details are also proposed. A method based on predictions of current direction is proposed in [QWHL11] to cater for embedded generation (DG) injections of power within distributed networks. By sharing such current information from multiple locations, the scheme is able to detect the faulted component in the network (bus, transformer or line). The optimal protective operation is subsequently initiated based on fault information. Since the requirement for communication infrastructure and synchronisation of data is high, it is proposed that this scheme would be practical to implement.

3.4.3 Impedance-based methods

A method based on measurements of both currents and voltages from a wide area is proposed in [ZLZ+12]. The faulted region is ascertained by comparing the measured voltage value, directly measured at the bus, with the theoretical value, which is calculated using currents, line impedance and voltages measured from the remote line terminal. For a line under normal operating condition, and for

the buses connected to the line, the actual value should be equal or very close to the theoretical value. Therefore, for relatively larger deviations between these values, there is a higher probability that there is a fault is on the line connected to the corresponding bus, and subsequently, a faulted region is identified based on deviations between actual and theoretical values. Two steps are involved in identifying the faulted line. The first step is to calculate the ratio between the measured value and the calculated values and rank them in the descending order (in terms of differences between expected and actual values) and selecting the top three as the potential faulted lines. The ratio would be equal to one when an external fault occurs, and greater than 1 when an internal fault occurs. Then, the variance (based on measured values and calculated values) for each of the identified potentially faulted lines is calculated and the faulted line is identified as the one with the largest variance. The scheme is tested on a 4-bus, 6-line network with different types of faults. The scheme requires both current and voltage measurement from PMUs (and per-line measurements of current), which is not practical or commercially applicable at present. In addition, configuration is not considered and many practical factors (e.g. fault resistance) are not considered. The approach described [HZC+11] is accomplished using two main steps: faulted area detection, followed by identification of the specific faulted line. The first step is based on the method proposed in [EME10]. It "regionalises" the faulted area by comparing thresholds (95% of nominal voltage magnitude in the paper) against actual values for positive sequence voltage magnitudes (no justification of voltage threshold settings). The faulted line is subsequently identified by comparing the ratios (the ratio of measured voltage magnitudes to calculated voltage magnitudes) of substations within the faulted area. The calculated voltage magnitudes are based on KVL (impedance-based) with the assumption that the system is under normal operation status. The calculated values are estimated using currents, line impedance and voltages measured from the remote line terminal. The two buses with highest ratios are the buses connected to the faulted feeder. Since both current and voltage are utilised in this scheme, PMUs (and possibly extra measurement transformers/cores) are required to be deployed at feeder terminals,

which may be prohibitively expensive. Only positive sequence is considered during the first step – fault region identification – and this may limit the capability for detecting unbalanced faults, especially resistive unbalanced faults. In addition, fault resistance is not considered as a factor in this research, which can be a significant aspect in a practical application. An impedance angle based method is proposed in [JSP17], and is applied to series-compensated transmission systems through measuring voltages at each substation and currents at the terminals of the feeders. The phase angle of positive-sequence integrated impedance (PAPSII) is the quantity used to identify the faulted feeder. The value of PAPSII is calculated through dividing the sum of the sending and receiving end positive sequence voltage phasors by the sum of the sending and receiving end positive sequence current phasors. Generally, a positive PAPSII value indicates an internal fault and vice versa. The scheme is validated using a system with 3 sources and 9 feeders on a real-time simulation platform, which indicates sensitivity of the scheme to various faults and the stability of the scheme for various scenarios, such as during power swings and load encroachment. Similar to the other aforementioned schemes, currents at both terminals of the feeders are required to be measured, which calls for large amount of extra PMU installations (and possibly measurement transformers), high processing ability of PDCs and relatively high performance communication infrastructures. [JSP16] proposes a data-mining algorithm based on the PAPSII variable introduced in [JSP17]. The scheme aims to prevent Zone 3 distance protection from tripping during "stressful" scenarios by adding another condition (PAPSII) for tripping. The tripping operation of Zone 3 distance protection will only be triggered if a Zone 3 fault is detected and the PAPSII values indicates a fault, therefore increasing the confidence in Zone 3 and prohibiting it from operating unnecessarily (although the amount of cases when a Zone 3 operation would ever be required is very small, and a number of network operators no long use Zone 3 as some data has shown that it maloperates more often than it operates correctly – e.g. the 2003 US blackout [AK18]). Using a data-mining/decision tree (DT) method (Data mining is defined as the process of discovering patterns in data) first introduced in [BTC12], the minimum number

of PMUs and their optimal can be determined offline according to the authors. The source data that is mined consists of fault records that are assumed to be available. However, due to the relatively low possibility of fault occurrence in power systems and potentially limited access to comprehensive fault record data, the training data may not be a large enough set /reliable enough to permit real time on-line application. The methodology flow chart is shown in Figure 3.10. The methodology aims to reduce the likelihood of hidden failures and potential cascading events by adjusting the security/dependability balance of protective relays to suit prevailing system conditions, through modifying the settings of relays. When the power system is in a "safe" state, a bias toward dependability is desired. Under these conditions, not clearing a fault with primary protection has a greater impact on the system than a relay misoperation due to a lack of security. However, when the power system is in a "stressed" state, unnecessary line trips can greatly exacerbate the severity of the outage, contribute to the geographical propagation of the disturbance, and may even lead to a cascading event and subsequent blackout. Under these states, it is desirable to alter the reliability balance in favor of security. It should be emphasized that the classification of the system state into "safe" and "stressed" is done with respect to the selected critical location (i.e., it is not a general statement regarding the system state. The estimation of the states are based on the off-line training data. The algorithm is validated on the Western System Coordination Council's (WSCC) 9-bus system in the real time digital simulator platform. Since the algorithm is based on [JSP17], it requires both current and voltage phasor magnitudes, which, as with many of the systems proposed by other researchers, would require large number of PMUs deployment in an actual application. In addition, the data-mining method would involve analysing large amounts of data, which may be relatively difficult to achieve in the power systems due to the low possibility of faults, as well as concerns over modifying settings and ensuring that they remain valid and in accordance with policies, which is very important.

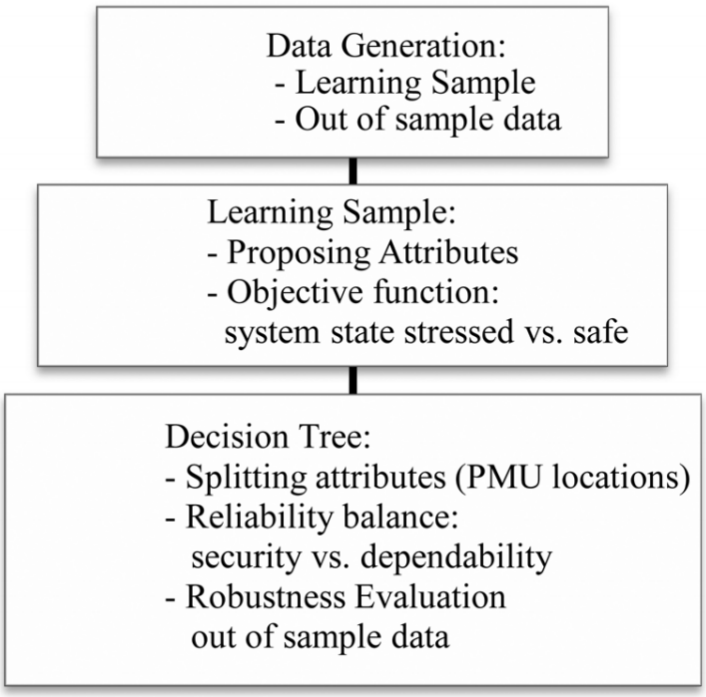

Figure 3.10: DT methodology flowchart [BTC12]

3.4.4 Voltage-based schemes

In [WZZ+17], an adaptive scheme for both primary and backup protection has been proposed by comparing settings and the magnitudes of line voltages. Three phase faults and double phase faults are considered by the authors. Under normal operation state, the voltage magnitudes of the line terminals are assumed to be equal (which, in the author's opinion, is not convincing) and the phase angle difference between them is within 90°. Therefore the magnitude of the phase voltage difference (using vector calculation) between the two line terminals (e.g.the difference between phase A voltages of two terminals using vector calculation) is no more than $\sqrt{2}$ times either of the line terminal's phase voltage magnitude. The measured value is the line voltage magnitude of the local terminal. The primary setting is 0.9 times (protective range is assumed to be 90% of the line) the voltage magnitude across the line (voltage difference between the line terminals). Under normal state, the magnitude of terminal voltage difference is less than the setting and the primary protection would require to operate if the magnitude of local ter-

minal voltage is larger than the setting. For backup protection, the protective line and the backward (upstream) line are both considered and measurements from both local and backward looking busbars are required for analysis and comparison. Only local information is needed for primary protection, which will not be delayed by any requirement for communication, and backup protection is based on both local and remote information. The scheme is tested using a 10.5 kV radial distribution network with one DG unit connected, and the results indicate that the scheme can be adaptive and cater for various ranges of DG output and fault types. However, the principle can only be applied to three-phase faults and phase-to-phase faults. Since single-phase-to-earth fault is the most common type of faults, the scheme could potentially have issues regarding to ability to operate for single-phase-to-earth faults. In [ZAS15], a relatively fast wide-area unit backup protection is developed by comparing calculated and measured values of positive sequence terminal voltages. For no fault and external fault scenarios, the local voltage phasor can be calculated using the remote voltage and the current phasors measured at remote end of the feeder. However, for an internal fault, the local voltage phasor cannot be calculated correctly based on the remote end voltage, the current infeed from the remote end and the impedance of the feeder, since a conducting path (the fault current path) is formed between the fault and the substations and current infeed from both remote end and the local substation towards the fault. Therefore, whether the evaluated value is equal to the actual value of the bus voltage is the criteria of internal fault determination. The method is tested in IEEE 57-bus system by linking DIgSILENT and Matlab, including a range of scenarios that could potentially destabilise the protection function, such as load encroachment, generator outages and power swing. However, since terminal currents are the required input to the scheme, installation locations of PMUs are terminals of the feeders rather than substations which is the current situation. Thus, extra expense is needed for implementation of the scheme and its functionality can really be carried out by standard differential protection, so the benefits are not completely clear. [GRM15] proposes a voltage angle-based method to accomplish the detection of fault occurrence and faulted

line identification. The scheme can also provide fault location analysis based on current angles using a machine intelligence approach. Since the focus of the dissertation is mainly on protection, only the fault occurrence detection and faulted line identification functions are analysed here. Using the Fast Fourier Transform (FFT) technique in the frequency domain, harmonic components of the Equivalent Voltage Phasor Angle (EVPA) at the generator bus, which is the inverse tangent of the ratio between the direct and quadrature axes components of the three-phase voltage phasors, is analysed. Under normal conditions, the EVPAs at all generators at all harmonics (apart from the zero - DC - harmonic) are zero. Therefore a non-zero value of any non-zero harmonic indicates the occurrence of a fault. Subsequently, the faulted region is identified by determining one of the two buses, which is connected to the faulted line, which is then denoted as the parent bus. By analysis the of EPVA deviations of all buses with reference to any of the generators, the bus with highest deviation of EVPA for the 2nd harmonic is identified as the parent bus (observed and concluded from spectrum in the FFT). All lines directly connected to the parent bus are therefore within the faulted region. The boundary of the faulted region constitutes the other buses (not the parent bus) directly connected to the lines within the faulted region. The other bus directly connected to the faulted line is determined by comparing the deviation of EVPA of the boundary buses for the 2nd harmonic with reference to the parent bus. The bus with the smallest deviation is the required bus. This is because EVPA of parent bus and the connected bus that share faulty branch will have similar EVPA variation. Hence, when both get subtracted (for finding the deviation in EVPA), the 2nd harmonic results in low value. The faulted line is subsequently identified as the line connecting the parent bus and the bus with the smallest 2nd harmonic deviation of EVPA. The method is tested in Matlab using IEEE 14-bus system considering the factor of fault type. However, the requirements for PDC processing, synchronisation and communication capability is very high, since the angle comparisons of all buses is required, and this may be problematic. A voltage measurement based method is presented in [JZLZ13] to implement online setting of over current protection. Based on real time volt-

age measurement from PMUs, topology and system parameters of the system, the scheme provides onsite overcurrent setting determination process to improve selectivity of overcurrent protection. Based on the real-time operation mode, the fault current is calculated before any fault occurs. Settings of the protection devices are then adjusted in real time to optimise protection coverage and shorten the operating times. Fault levels are not evaluated appropriate in the proposed scheme with assumptions of access to source voltage "before" internal impedance. The scheme is functionally demonstrated (2-bus system), but no comprehensive case studies are conducted. Also, fault resistance is not considered in the scheme which could potentially lead to non-operation of overcurrent protection during high fault resistance scenario, so this scheme may not be practical.

3.4.5 Methods with Requirements to gather the status of protective devices

A distance relay-based approach is introduced in [CWSH17]. By collecting information from local and remote relays (i.e. those operating with zone 1 and perhaps those indicating that they would operate in zone 2 or 3 if required), the scheme can identify fault location and the status of protection devices on local and adjacent lines, and subsequently coordinates well with conventional protective relays. The signals acquired from the distance protection (potentially operating in backup mode) relate to fault detection (i.e. the outputs of the zone comparators) rather than tripping signals sent to circuit breakers (which would be too late for decision-making relating to backup protection). The scheme identifies the faulted feeder based on relay information and determines appropriate time delay and operating sequence using wide-area information rather than local information based on various scenarios rather than fixed settings, which can provide relatively fast and secure backup protection. The scheme is validated using the IEEE RTS-96 system at a voltage level of 230 kV, considering various factors, encompassing communication failure and high resistance faults. The scheme is fully based on the decision making status of Zone 2 and Zone 3 elements to

accelerate the backup protection. However, under the scenario of maloperation (e.g. 2003 blackout caused by Zone 3 maloperation), the scheme would have difficulties in hard to distinguishing between correct operation and maploperation. An adaptive wide-area current differential based protection system is proposed in [CWSH17]. The statuses of several protection devices are collected by the scheme and subsequently the protection zone including primary and backup protection zones are rationalised. Components within each zone can share information with each other by communication. Faults within a zone are detected and isolated based on current differential protection principles. The protection zones are adaptive to the system status rather than fixed, unlike conventional protection zones, and the coverage of differential protection can be extended to cover more than one line and larger areas of the system. The scheme is tested using a 5 bus, 4 line, system using simulation. As with any current differential based schemes, this method requires high resolution and synchronisation of measurement data, as well as PMUs installed at both terminals of a line, and would require a very high speed of data transfer to operate in the required timescales. [LYZH13] proposes a method with based on fusion of multiple sources of data, which including the operation status (decision making signal) from conventional both primary and backup protection without delay. Although the decision making signal might be theoretically accessible, the actual application and realisation of this functionality involves many factors, such as the compatibility between relays and measuring/outputting devices (e.g. PMUs), in addition to the availability of a high-performance, low-latency communications infrastructure. Based on selectivity, each protection scheme has a unique weight coefficient, which is used for a "fitness value" calculation. The selectivity of protection schemes can be divided into three categories: 1) if the relay has clear a very high degree of selectivity, and its weight coefficient is set to 1 (e.g. zone-1 of distance protection); 2) the relay has fuzzy selectivity but it could protect the entire transmission line with long a delay, and its weight coefficient is set to 0.5 (e.g. zone 2 distance protection); and 3) the relay has fuzzy selectivity but it could protect the entire transmission line and the adjacent line with longer delay, then its weight

coefficient is set to 0.33 (e.g. zone 3 distance protection). The approach seems somewhat arbitrary in nature and the selection of these coefficients is not fully justified. The redundancy and independent operation information, including primary protection, fast backup protection, zone 2 and 3 of distance protection, and negative- and zero-sequence directional protection are used. Taking advantage of multisource information from local relays and disturbances, such as "information error" (term used by the authors to signify when received information is not complete or even opposite to the actual status), could be eliminated to realise high fault tolerance. The fitness value of each component in the system is based on the combination of weight coefficients and the difference between actual status and expected status of protective elements. The fitness value of a fault element is the sum of the difference between actual status and expected status of all types of aforementioned protection schemes with a coefficient of weight coefficient. The fault element can be identified when the fitness value meets the setting value. The fitness value of the faulted element has the highest fitness value compared to other elements. The scheme is tested using an IEEE 10 generator, 39 bus system, which shows the ability of the system to withstand the impact of information error scenarios (when received information is not complete or even opposite to the actual status). The scheme has the advantages of withstanding loss of faulted data due to the use of multiple independent data sources. However, the practicality of the access to relay decision-making signals is limited, especially for older devices, and it could be difficult to ensure that communications is achieved with a range of devices of different vintages, possibly without standard protocols, and it may also require a high performance communication infrastructure. Another method, based on fitness values, is proposed in [MLT16]. The inputs to the scheme are the tripping output data of distance protection (both primary and backup distance protection, if it has operated). With the assumption of equal possibility of fault occurrence on all locations of feeders, the protection fitness function of a specific line, which is based on actual distance protection operation information and probability of the fault being on each protective zone (defined by distance protection scheme), and protection fitness expectation function of

the line, which is based on the theoretical operating status of the distance protection when a fault occurs on specific sections of the line and the probability of the fault being properly protected by each protective zone, can be calculated. The "fitting factor" is also described, and this is the ratio between the protection fitness function to protection fitness expectation function, which is between 0 and 1. The closer the fitting factor is to 1, the higher possibility the fault is on the evaluated line. Therefore, among all lines, the one with the highest fitting factor is the faulted feeder. The scheme is tested on IEEE 10-Machine 39-Bus system and Guizhou Duyun RTDS with consideration of information loss and error. Although probability of the fault being on each protective zone and the protection fitness expectation function are both evaluated offline, the burden of calculation of protection fitness function for all lines is relatively heavy, and the benefits and practicality of the scheme are not very clear. Responding to the issues of communication congestion, a novel algorithm focusing on protection priority, of which data is sent to the central processor with a high priority when the condition of communication is good, otherwise sending high priority information only, is introduced in [MGSX16]. Components are categorised into different priorities with evaluation indices, which take account of failure rate of the line (which in practice may not be readily available), loading level and the historical local protection "mis-operation" (the authors' terminology) rate (which again may not be high – in properly designed protection systems for transmission application, protection maloperation (or "mis-operation") should never happen, so again, this paper may not be realistic). The system analyses the system status based on data from all protection devices and system components. With the status analysis and priority sequence, the protection decision is sent to the central processing centre by priority if the communication channels have enough capacity, otherwise only the highest priority information is sent, which reduces risks of protection failure caused by communication congestion. The system is tested on a 6-bus network using OPNET simulation software. The scheme can solve the problem of communication congestion; however, the process of fault location identification is presented with a sufficient level of detail and due to the

low possibility of line faults and device failure, the statistics used for deciding priority may not be sensible.

3.5 Summary

This section has presented a review of several wide-area backup protection schemes using PMUs proposed by other researchers over the last 20 years or so. The direction of research can be generally divided into four types according to principles and requirements of measurement: current-based, impedance-based, voltage-based and methods with requirements for data relating to protective device status. A table summaries the characteristics and weakness of the reviewed schemes is predestine in Figure 3.11. Although the pros and cons of each individually reviewed method has been discussed in the foregoing sections, the strengths and weakness of each type is presented below for summary purposes. Current-based schemes, especially current differential based schemes, can accurately detect faults and are immune to non-fault transients such as load swings and temporary overloads. However, current-based methods often require a relatively high number of measurements and related data at both terminals of the lines, which can be both expensive and complex when considering a wide-area application, and is likely to require relatively high processing power, high resolution of data (e.g. sample-by-sample current measurements), as well as adequate communication bandwidth and infrastructure. For other current-based (and often requiring voltage too) methods, they are generally based on existing distance protection principles. However, they require both voltage and current measurement, may be difficult to coordinate and could be prone to issues associated with decreasing and variable system strength (e.g. affecting remote infeed levels). Accordingly, the reach/accuracy of distance protection, especially when applied to backup mode in future power systems, could be compromised, especially when increasing amounts of renewable generation are connected. Solely voltage-based methods (as with the scheme developed in this research) have the advantages of requiring less measurements compared to others scheme requiring current. However, for

the schemes proposed by other researchers, some crucial factors are often not considered, such as fault resistance and ensuring that the scheme would operate for all fault types. For methods which require information relating to the status of protection relay devices, there are typically purported advantages in terms of simplicity, security and dependability. However, they often require both current and voltage measurements, in addition to circuit breaker status data, potentially rendering them impractical and costly.

Characteristics	Weakness	Schemes (references)
Current-based	1. High cost - PMUs installation at both terminal of the lines 2. High requirements for communication infrastructure	[UDREN14] [ZAS15] [NAP17] [EME10] [KP15] [NPB14] [SMK+98] [KINO98] [QWHL11]
Impedance-based	1. High cost - PMUs installation at both terminal of the lines 2. Limited availability of practical fault data for data analysis methods	[ZLZ+12] [JSP16] [JSP17] [HZC+11] [BTC12]
Voltage-based	1. Incomplete consideration of a variety factors e.g. fault types, fault resistance 2. High cost - the schemes with requirements of current measurements	[WZZ+17] [ZAS15] [GRM15] [JZLZ13]
Requirements of protection device status	1. Incompatibility between relays and PMUs	[CWSH17] [LYZH13] [MLT16] [MGSX16]

Figure 3.11: Review of wide-area backup protection schemes proposed by other researchers

Based on the analysis of the relevant literature in this section, a voltage-based scheme with consideration of crucial factors such as fault types and fault resistance is clearly a direction of novel research, and can address some of the shortcomings and "gaps" in the related work reviewed. The scheme proposed in this paper only requires measurements of voltage magnitudes and is capable

of providing a relatively fast and accurate fault location to the circuit/feeder level, followed by the analysis of protection and circuit breaker performance from observed voltage magnitudes and the ability to provide backup protection for the network.

Chapter 4

Wide-area backup protection and protection Performance Analysis Scheme

4.1 Introduction

This chapter describes the function and methodology of the proposed wide-area backup protection and protection performance analysis scheme.

In power systems, short circuit faults will typically lead to phase voltage depressions measured at substations in the vicinity of the fault. High fault resistance can lead to relatively small voltage depression compared with solid (or bolted) short circuits. Furthermore, weakened systems (with reduced fault currents) can also act to change the magnitudes of voltage depressions at various locations in the vicinity of faults and this will be more of an issue in the future. In order to increase tolerance to fault resistance (i.e. increase the highest fault resistance that can be detected for a short circuit fault), sequence components of voltage magnitudes are used as indicators of faults (in addition to solely basing fault detection on voltage magnitudes) for the various different fault types as explained in Section 4.2. Based on voltage measurement data supplied from remote PMUs, the scheme detects the presence of a fault, identifies any subsequent status changes

of circuit breakers solely from analysis of the measured voltage profiles (sequence components) and identifies the faulted feeder and any failure of protection or circuit breaker(s). Since only voltage magnitudes are analysed by the scheme, phase shifts introduced by different transformer connection types would not have significant impact on the operation of the scheme and if there's any (when PMUs are installed at the primary side of the generator transformers), compensation would be made before implementation of the scheme. The analysed information can be reported to the system operator for better understanding of the network status and to support further decisions after the occurrence of a fault. Since the time required for analysis is short, backup protection can be provided based on the analysed information.

The proposed scheme consists of three main stages of operation for each type of fault: fault occurrence identification; faulted feeder identification and backup protection based on the analysis of circuit breaker status. The detailed operational principles and process of the three main stages for different types of faults and the method of fault type identification are presented in Section 4.2. The applicability of the scheme to large scale systems is discussed in Section 4.3 to show the practical potential in actual applications.

4.2 Principle of scheme operation

4.2.1 Overview

This section presents the principle of the scheme operation in detail. The aim of the scheme is to provide backup protection and report information relating to the faulted circuit, the fault types and the circuit breaker(s) status. Due to the different quantities utilised to identify different types of faults, this section is structured according to operation for different fault types to explain the principles of the scheme as clearly as possible.

The flow chart shown in Figure 4.1 demonstrates the mechanism of the scheme and presents clearly how the various elements of the scheme work together realise

the full functionality of the scheme.

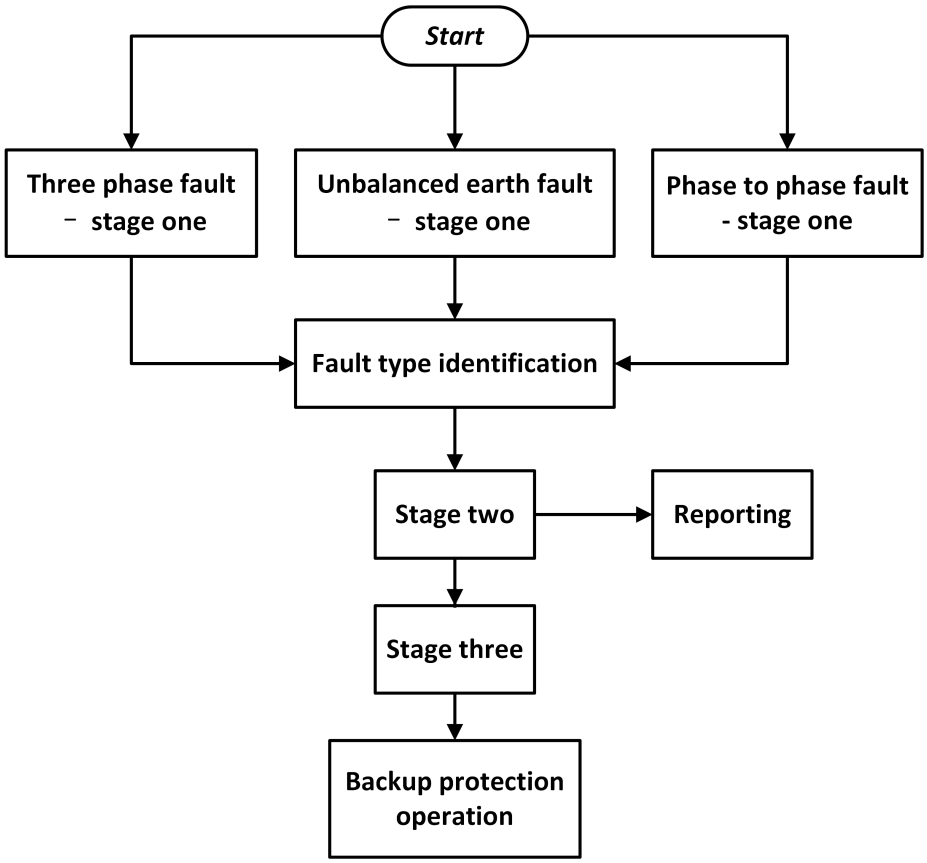

Figure 4.1: Flow chart of scheme process

The first stage of operation for all disturbances is to identify if any faults have occurred corresponding to one of the three fault categories (three-phase fault, unbalanced phase-earth fault and phase-phase fault) based on voltage magnitudes measured from PMUs, which is presented in Section 4.2.2.2.1 (three-phase faults), Section 4.2.3.2.1 (unbalanced earth faults) and Section 4.2.4.2.1 (phase-phase fault). The fault type and the occurrence of a fault can be identified simultaneously, which is presented in detail in Section 4.2.5. After identification of the fault type, stage two of the corresponding fault type is initiated, which is explained in Section 4.2.2.2.2 (three-phase faults), Section 4.2.3.2.2 (unbalanced earth faults) and Section 4.2.4.2.2 (phase-phase faults). The second stage of the scheme identifies the faulted circuits and circuit breaker status based on analysing the performance of voltage magnitude performances and can report the information to the system operator for further action determination. If all both

line-end primary protection operate correctly, this stage will indicate the correct operation of the system. Likewise, if all primary protection failed to operate, the scheme will indicate the fault region and the failure of all main protection. The aforementioned information reported from the scheme can provide system operator with simplified and synthesised information of the system status to help with faster decision-making process. With analysis from stage two, tripping signals will be sent in stage three and backup protection will be provided. This process is presented in Section 4.2.8.

4.2.2 Operation of the system for three-phase faults (balanced faults)

4.2.2.1 Overview

According to the theory of sequence components, as discussed in Section 2.3, sequence networks would only consist of positive sequence components under either normal operating status or during a three-phase faults scenario. During three-phase faults, positive sequence voltage magnitudes would depress from nominal values (dependent on fault level, impedance of the line to the fault location from where measurements are taken, and any fault path resistance). The scheme can identify and analyse three-phase faults based solely on behaviours of positive sequence voltage magnitudes.

The operation of the scheme for three-phase faults identification consists of the aforementioned three stages: stage one - fault region identification; stage two - fault location to feeder level (faulted feeder identification) and stage three - backup protection operation. The first stage is initiated if at least one individual voltage measurement from any of the PMU measurements drops below a certain threshold (determination of thresholds is explained in Chapter 6), and this will be used to form a bounded network region with multiple candidate faulted lines and nodes, within which the fault has occurred. A block for fault type identification is applied between stage one and stage two, which is explained in detail in Section 4.2.7. Since the process of fault type identification is based on stage one for all

fault types, the detail of this process is presented following the description of the operation principles for each type of fault. For any fault type, the outputs of the fault type identification block are align with the outputs of stage one of the specific type of fault, as described in Section 4.2.7. The second stage is based on the analysis of stage one (fault type identification block) outputs and the behaviours of node voltage magnitudes to further locate the faulted line. In parallel with this, the performance of the primary protection and the status of the associated circuit breakers can be analysed and reported in the second stage. In the third stage, tripping signals are sent to execute the backup protection function, as discussed in Section 4.2.8.

With voltages measured from PMUs at each node and the analysis approach based on the aforementioned three stages, the scheme can provide fast backup protection with affiliated information describing the faulted region, faulted line and circuit breaker status for reporting and decision support purposes.

4.2.2.2 Detailed scheme operation

4.2.2.2.1 Stage one – fault region identification

An example 5-node radial system is used to explain the scheme as shown in Figure 4.2. A three-phase solid fault is applied close to node C, on the line connecting C and E.

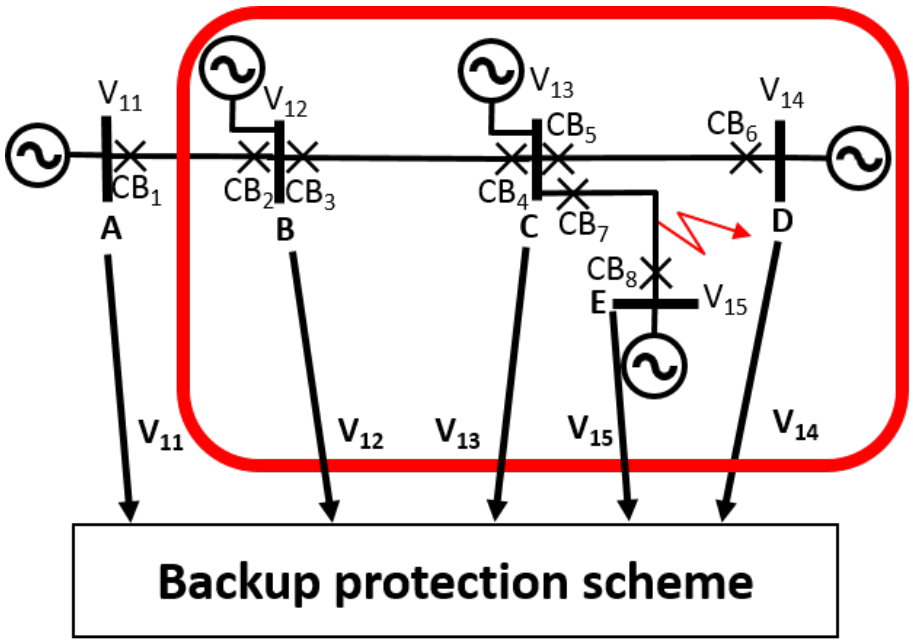

Figure 4.2: Single line diagram of 5-node system

The flow chart of stage one is shown in Figure 4.3. In stage one, the positive sequence voltage magnitudes at all nodes, as measured by the PMUs at each node, are monitored and recorded. The positive sequence voltage magnitudes of node i is denoted as V_{1i}, which belongs to a voltage set $\boldsymbol{V_1}$. V_{1i} is a time sensitive value, which means it may change with time depending on system situation. The pre-fault positive sequence voltage magnitude of node i is denoted as $V_{10}{}^{\mathrm{i}}$, which belongs to a voltage set $\boldsymbol{V_{10}}$ that contains pre-fault positive sequence voltage magnitudes from all nodes. $V_{10}{}^{\mathrm{i}}$ varies with time but is fixed before occurrence of a fault. The process of pre-fault voltages identification is explained further in Section 4.2.5.2. The occurrence of a three-phase fault would cause a depression of positive voltage magnitudes at several locations around the vicinity of the fault and the operation of the scheme is then initiated by a pre-defined voltage threshold k_{1Th} (the threshold is a relative value to $V_{10}{}^{\mathrm{i}}$ and is further explained in Section 9.2). Decisions within the scheme are made based on the ratio of monitored positive sequence voltage magnitudes of all nodes to their pre-fault values $V_{10}{}^{\mathrm{i}}$, which are denoted as k_{1i}, i.e. $k_{1i} = V_{1i}/V_{10}{}^{\mathrm{i}}$, and the set containing k_{1i} from all nodes is denoted as $\boldsymbol{K_1}$. Set $\boldsymbol{K_1}$ is introduced to compare the ratio of voltage depression rather than absolute value, which would be more flexible

when pre-fault voltages varies for different nodes (for example as a result of overall system loading, operation of the network controllers to set different operational voltage levels, etc.). Before occurrence of a three-phase fault, k_{1i} is always very close to 1. With occurrence of a three-phase fault, k_{1i} of node i around the fault, will depress. If k_{1i} of at least one node is lower than the threshold, the node with the smallest k_{1i} (i.e. k_{1min}), defined as N_{1min}, and is identified as a node that is definitely connected to the faulted feeder. The voltage magnitude of N_{1min} is denoted as V_{1min}. Based on topology of the network, a subset of nodes is then formed, which includes N_{1min} and all neighbouring nodes. This subset of nodes, N_{1reg}, defines the region of the network where the fault is located. The corresponding subset of $\boldsymbol{K_1}$, denoted as K_{1reg}, contains the k_{1i} of all nodes within N_{1reg}. The corresponding subset of V1, denoted as V1reg, contains the V_{1i} of all nodes within N_{1reg}. All voltages (V_{1i}) are relative values to nominal voltages and expressed in p.u., for example, for a 132 kV system, if positive sequence of node 1 is 132 kV, V_{11} is 1 p.u.

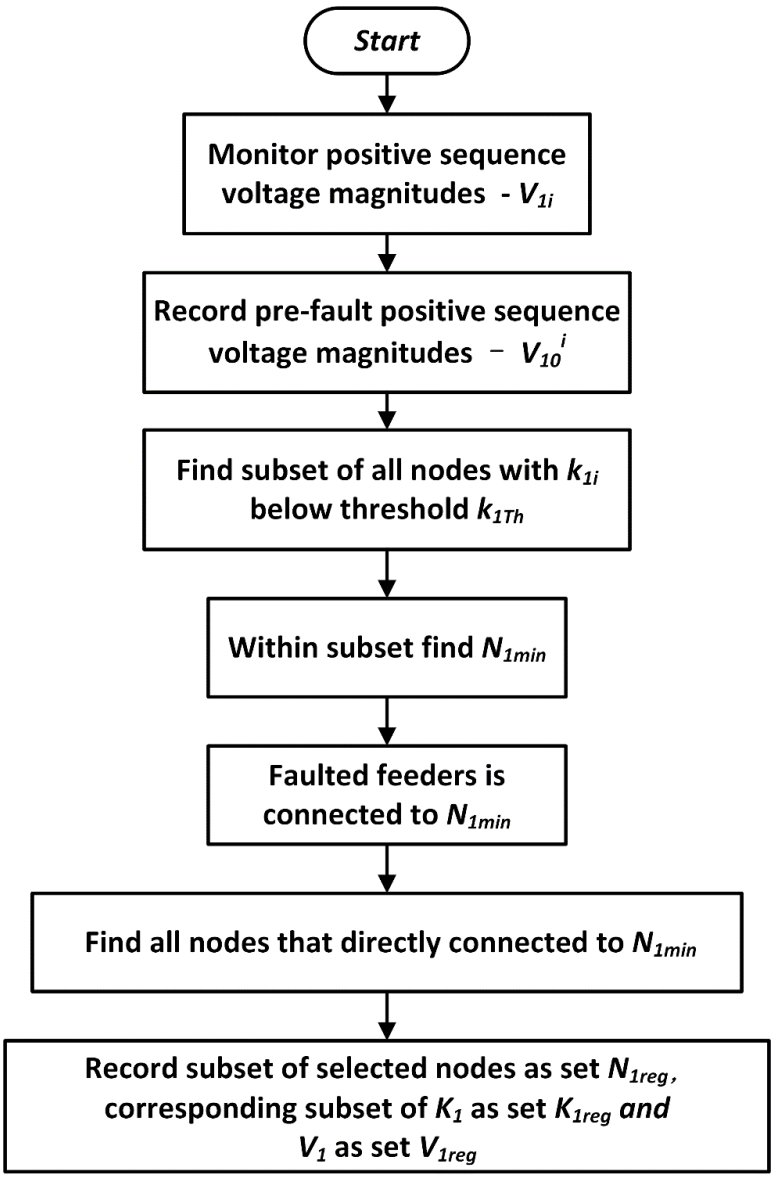

Figure 4.3: Stage one for three-phase fault

Under the scenario shown in Figure 4.2, V_{1i} of all nodes is 1 p.u. and with application of a solid three phase fault, k_{13} (V_{13}) would have the largest depression. k_{1i} (as well as the voltage magnitudes) of the neighbouring nodes (B, D and E) will depend on line lengths, the fault levels within the system, the topology of the system and the fault resistance. The impact of these factors is described further in Chapter 6. The fault region can be identified as the area bounded by nodes B, C, D and E. It is known that C is definitely connected to the faulted feeders, and that the other node of the faulted feeder must be within N_{1reg}. That is, one of nodes B, D or E.

4.2.2.2.2 Stage two – faulted line identification

At this stage, it is presumed that the primary protection has operated correctly at least at one end of the faulted feeder. Since two sets of main protection (differential and distance protection) are normally applied to transmission lines and it was common practice that communication channels are redundant for each of the main protection schemes, the probability of failure of both primary protections at all terminals of the line is assumed to be negligible. In addition, it's presumed that for double-circuit scenarios, both circuits are installed with PMUs at the substations.

The flow chart of stage two is illustrated in Figure 4.4, where after fault type is identified as a three-phase one, the node set N_{1reg}, the corresponding K_{1reg} set and V_{1reg} set established in stage one are used as the main inputs to stage two. If there is at least one node in V_{1reg}, then identification of the faulted circuit requires operation of one of the line-end primary protection and the change of consequent observable positive sequence voltages at a number of PMUs. The time period t, shown in Figure 4.4, is pre-defined and can be configured based upon the anticipated maximum primary protection fault clearance time (e.g. 140 ms in Great Britain [Nat11]). The measured positive sequence voltage magnitudes V_{1i} are examined to identify any instances of voltage recovery, i.e. either partial recovery due to the opening of one of the circuit breakers only, or full recovery (restoration of the voltage to the pre-fault voltage level), following the successful fault clearance at all terminals of the faulted feeder. If all voltages are fully recovered during time t, then all protections/breakers have operated correctly and no further analysis is required. Conversely, if there is no voltage recovery observed within time t, then all primary protections would have failed at all line terminals (which is highly unlikely) and the scheme can only report upon the fault region (potentially containing several feeders).

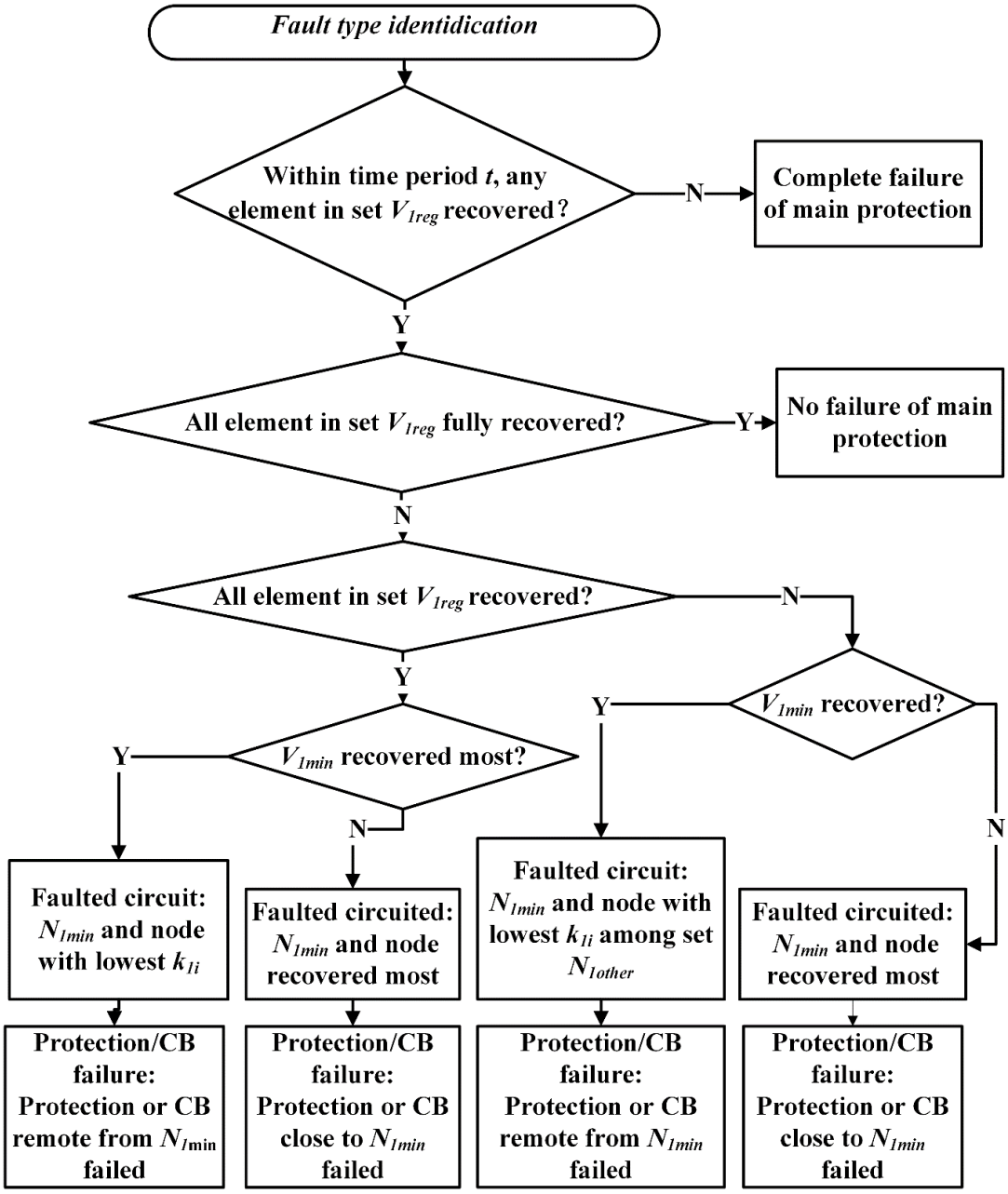

Figure 4.4: Flow chart of stage two – faulted feeder identification for three-phase fault

With operation of primary line-terminal protection schemes and their controlled circuit breakers, there are four possible behaviour patterns of the elements within set V_{1reg} that may be observed. 1) it could remain unchanged 2) it could further reduce 3) it could partially recover, or 4) fully recover (e.g. to greater than 90% of the total voltage dip magnitude). The choice of the value of 90% to signify full recovery is deemed acceptable. These values have been proposed based on the results of extensive simulations and can be modified if necessary.

Figure 4.5 shows the voltage behaviours for the fault scenario depicted in Figure 4.2. The variable x_1 indicates the maximum magnitude of the voltage dips and y_1 indicates any increase in voltages after the voltages have reached their minimum values. A dedicated functional block has been developed for capturing the values of x_1 and y_1 during simulation. The fault is applied at 0.5 s in the simulation and it is assumed that CB8 at node C operates correctly and opens 80 ms later at 0.58 s. A positive value of the ratio of y_1 to x_1 is used to identify voltage recovery (which could be indicative of either partial or full recovery). A ratio of y_1 to x_1 of greater than 0.9 indicates full recovery – e.g. in V_{15} in Figure 4.5. A negative value for $y_1$to x_1 indicates a further depression after the initial depression (e.g. V_{11}, V_{12}, V_{13} and V_{14}).

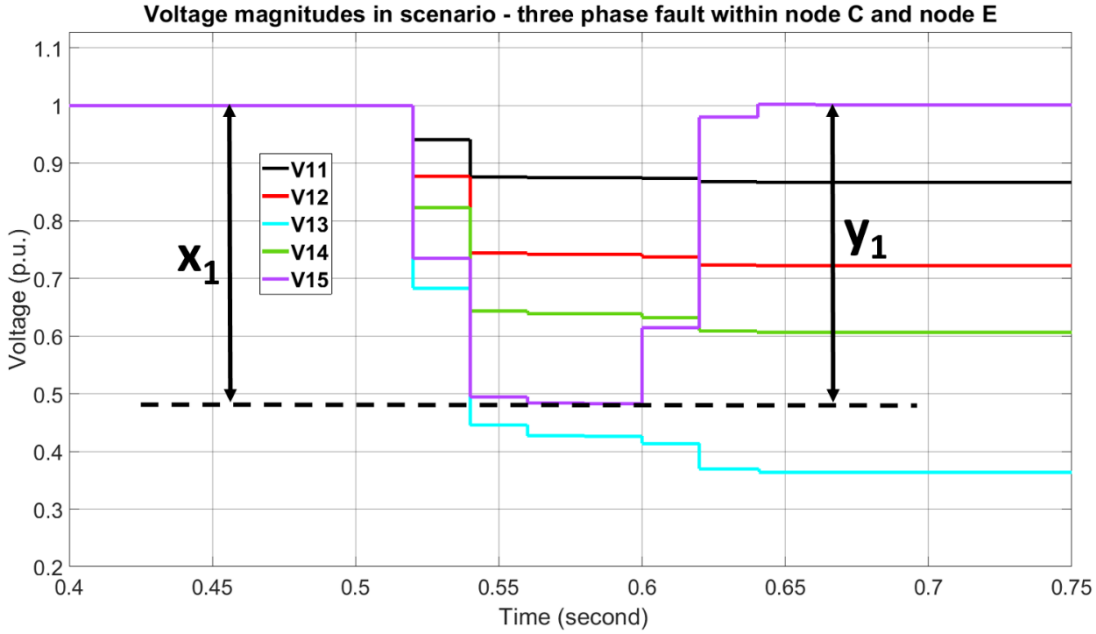

Figure 4.5: Positive sequence voltage magnitudes of 5-bus system with a three-phase fault

It is very important to identify when a voltage has partially or fully recovered (which can be assumed with confidence to indicate that a circuit breaker has opened and therefore protection has operated). If any voltage remains unchanged after it has dropped to a steady state value, then it can be assumed that the fault is persisting on the system. If it is reduced further then that may be due to the operation of a circuit breaker remote from the measured voltage location

(e.g. if the voltage at a closed breaker on a faulted line reduces after the initial reduction it could mean that the breaker at the other end of the line has opened, and therefore the elimination of the fault infeed from the other end of the line may result in a further voltage depression at the point of fault (particularly for resistive faults). These behaviour patterns provide indication for further analysis of circuit breaker status and faulted lines.

During and following fault events that are not properly responded to correctly (e.g. if a line terminal protection system or its controlled breaker does not operate), then, realistically, only two scenarios can be observed. Scenario 1 is where all elements in set $\boldsymbol{V_{1reg}}$ exhibit some recovery (but do all fully recover); while scenario 2 is where some elements do not recover at all, but a subset of $\boldsymbol{V_{1reg}}$ exhibits recovery. A new set of elements within set $\boldsymbol{V_{1reg}}$, from stage 1, containing all voltages that subsequently exhibit partial or full recovery behaviour, is denoted as set $\boldsymbol{N_{1up}}$. The remaining elements within the set $\boldsymbol{V_{1reg}}$, which have not partially or fully recovered, form the set $\boldsymbol{N_{1other}}$.

In scenario 1, if V_{1min} has not recovered most significantly within set $\boldsymbol{V_{1reg}}$, then the faulted line is identified as the line connecting N_{1min} and the node with the most significant voltage recovery within set $\boldsymbol{N_{1reg}}$. Operational failure of the protection/circuit breaker on this line at N_{1min} can be reported. Otherwise, if V_{1min} has recovered most significantly within the set $\boldsymbol{V_{1reg}}$, then the faulted line is identified as the line connecting N_{1min} and the node with the lowest k_{1i} within set $\boldsymbol{N_{1reg}}$. Operational failure of the protection/circuit breaker on this line remote from N_{1min} can be reported.

In scenario 2, if V_{1min} has recovered, the faulted line is identified as the line connected between N_{1min} and the node with the lowest k_{1i} within $\boldsymbol{V_{1other}}$. Operational failure of the protection/circuit breaker at the node on this line remote from N_{1min} can be reported. Otherwise, the faulted line is identified as the line within N_{1min} and the node with the most significant voltage recovery within set $\boldsymbol{N_{1up}}$. Operational failure of the protection/circuit breaker on this line at N_{1min} can be reported.

Under the scenario depicted in Figure 4.2, the resulting voltage profiles are

presented in Figure 4.5. C is N_{1min} and, at the initial stage, it can be deduced that the other node connected to the faulted line is one of either nodes B, D or E. From around 0.6 s, there is no recovery behaviour for V_{1min} (V_{13}), but V_{15} has the most significant recovery (fully recovering to the pre-fault voltage level from 0.64 s). In the future, voltage recovery following faults may be different (depending on the nature of generation and loads, and this may represent an area for future study). Accordingly, the faulted line is then identified as the line connected between C and E. However, the protection or circuit breaker at C (CB7) can be deemed as having failed to operate, as the voltage remains depressed after the opening of the circuit breaker at E - note that all other voltages also remain depressed and do not recover - in this case backup protection would be required to operate. The system would report on the failure of the protection/circuit breaker at C.

The output of stage two includes reporting of summary information from analysis of the various voltage profiles during the event. If one line-end primary protection fails to operate (the most realistic scenario for any faults that do not have the correct protection system – including breaker - response), the operation of the wide-area system will proceed to stage three to provide the required backup protection function (which could be in addition to, or as an alternative to, existing backup schemes). For this scenario, the faulted line, the failed protection/circuit breaker and the identified fault type can be reported and corresponding protection action will be initiated in stage three. A case study demonstrating this process is presented in Section 7.2.3.

A scenario where all elements in set $\boldsymbol{V_{1reg}}$ fully recover within the appropriate timescales (maximum operation time of main protection plus a small margin) indicates that no failure of primary protection systems or circuit breakers has occurred, therefore no backup protection operation is required. Using the analysis from stage two, the faulted region and the information that all protection has operated correctly are reported to the system operator for monitoring purposes. Stage three is not proceeded to or used in this scenario, since there is no need for backup protection.

For the extreme unlikely situation where none of the primary protection sys-

tems operate correctly (i.e. circuit breakers at all line terminals do not trip), the no elements in set $\boldsymbol{V_{1reg}}$ would recover and the faulted region, and information that total failure of primary protection has occurred, would be reported to the system operator. It is re-iterated that this is a highly unlikely event in practice, as there are two (or three) main protections for each line, each using different principles of operation and different means of communications, along with various other redundancy methods. There appears to be no literature or information on the internet showing where such an event has ever occurred in practice. Protection failures seems to involve only one line end, but this can of course lead to cascade tripping and blackouts if backup protection does not operate correctly, or quickly enough, and the risk of this in future could be exacerbated under future scenarios where power systems are weakened.

4.2.3 Operation of the system for earth faults (unbalanced)

4.2.3.1 Overview

According to the theory of sequence components, as explained in Section 2.3, in addition to positive sequence components, unbalanced earth faults will introduce both negative and zero sequence components to the circuit, which is different to the three-phase fault case. Either negative or zero sequence voltages can be used as better and more sensitive indicators of unbalanced earth faults compared to positive sequence voltages. Pre-fault values for both negative and zero sequence voltages would be minimal (ideally zero) for balanced operation prior to any unbalanced earth faults, and will increase markedly during unbalanced earth faults. Furthermore, even for scenarios where pre-fault values are non-zero due to a degree of unbalance or voltage transformer errors, relative values rather than absolute can be used as indicators and this enhances greatly the ability to identify faults, as explained in Section 4.2.5. Since unbalanced earth faults are the only fault type that introduce zero sequence components, zero sequence components are utilised as the indicators for unbalanced earth fault detection,

which, in conjunction with analyses of negative sequence components, allows the system to have the beneficial feature of being able to distinguish between unbalanced earth faults and phase-phase faults (not involving earth). In this section, it is presumed that PMUs measures the voltages on the same voltage level, therefore the transformer connections (transformers between networks of voltage levels) will not affect the zero sequence voltage magnitudes (where one side of a transformer is connected grounded-wye, and the other side is delta, circulating zero sequence currents can be induced in the delta winding [Sor17]). At transmission level, generators are normally connected to the grid by delta/star connection transformers (delta/star connection transformers are normally used as step-up transformers) [Par12]. Due to the measurements from the PMUs are at the secondary side (grid side), zero sequence currents and voltage will not be affected by the connection.

As with three-phase faults, the detection of unbalanced earth faults also consists of three stages. For stage one, if at least one zero sequence voltage measurement from any of the PMU measurements increases above a certain threshold (threshold determination process is be explained in Section 6.3), the faulted region will be identified. A block for fault type identification is applied between stage one and stage two, which is explained in detail in Section 4.2.7. After identification of fault types, stage two will be triggered to further locate the faulted line and analyse circuit breaker status. After all information gathering from the scheme is integrated (information regarding to fault type which is discussed in Section 4.2.7, faulted line and protection/circuit breaker status), backup protection decision is made and tripping signals are sent in stage three, which is discussed in Section 4.2.8.

4.2.3.2 Detailed scheme operation

4.2.3.2.1 Stage one – fault region identification

As shown in Figure 4.2, the 5-node radial system, the same as that used to demonstrate operation for three-phase faults, is used to demonstrate the scheme operation for unbalanced earth faults. A single-phase to earth fault is applied

close to node C, on the line connecting C and E.

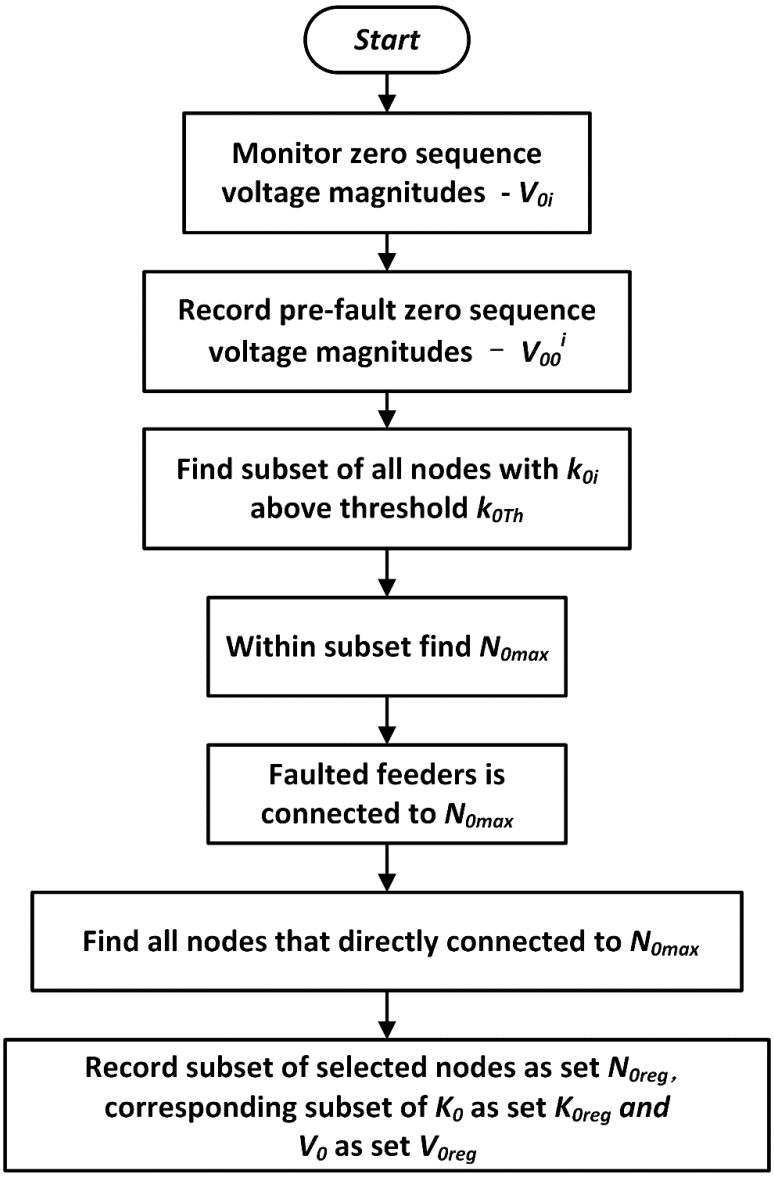

Figure 4.6: Stage one for unbalanced earth faults

The process of stage one is shown in Figure 4.6. Zero sequence voltage magnitudes are monitored and recorded at all nodes in stage one. The meanings and characteristics of variables in this scenario are similar to three-phase fault scenarios but have different denotations for distinction. The zero sequence voltage magnitudes of node i is denoted as V_{0i}, which belongs to a voltage set V_0. The pre-fault positive sequence voltage magnitude of node i is denoted as $V_{00}{}^{\mathrm{i}}$, which belongs to a voltage set $\boldsymbol{V_{00}}$ that contains pre-fault zero sequence volt-

age magnitudes from all nodes. $V_{00}{}^{\mathrm{i}}$ varies with time but is stored as a fixed value immediately before the occurrence of a fault (a "moving window" is used to continually monitor the present and stored the short-term past values of all variables – a measurement window of two cycles is used and all measurements are buffered for at least 3 cycles to enable ratios to be calculated). The process of pre-fault detection is presented in Section 4.2.5.3. A rise of zero sequence voltage magnitudes will be observed at several locations around the vicinity of a fault when it occurs and the operation of the scheme is initiated by a pre-defined zero sequence voltage threshold k_{0Th} (the threshold is a relative value to $V_{00}{}^{\mathrm{i}}$). This is explained further in Section 6.3. The decisions of the scheme are made based on the difference between monitored zero sequence voltage magnitudes of all nodes to their pre-fault values $V_{00}{}^{\mathrm{i}}$), which are denoted as k_{0i}, i.e. $k_{0i} = V_{0i}$ - $V_{00}{}^{\mathrm{i}}$), and the set containing k_{0i} from all nodes is denoted as $\boldsymbol{K_o}$. Set $\boldsymbol{K_o}$ is introduced to easily compare the ratio/rise of voltage rather than the absolute value of zero sequence voltage, which would be more flexible when pre-fault voltages are non-zero values. Before occurrence of an unbalanced earth fault, k_{0i} is always close to 0. With the occurrence of an unbalanced earth fault, the value of k0i in the area of the fault will increase. If k_{0i} of at least one node is above the threshold, the node with the largest k_{0i} (i.e. k_{0max}), defined as N_{0max}, is identified as a node that is definitely connected to the faulted line. The voltage magnitude of N_{0max} is denoted as V_{0max}. Using the topology of the network, a subset of nodes is then formed, which includes N_{0max} and all neighbouring nodes. This subset of nodes, $\boldsymbol{N_{oreg}}$, defines the region of the network where the fault is located. The corresponding subset of $\boldsymbol{K_o}$, denoted as $\boldsymbol{K_{oreg}}$, contains the k_{0i} of all nodes within $\boldsymbol{N_{oreg}}$. The corresponding subset of $\boldsymbol{V_o}$, denoted as $\boldsymbol{V_{oreg}}$, contains the V_{0i} of all nodes within $\boldsymbol{N_{oreg}}$. As with the three-phase fault scenario, all voltages (V_{0i}) are relative values to line nominal voltages and expressed in p.u.

For the scenario shown in Figure 4.2, V_{0i} of all nodes is 0 p.u. before fault occurrence and with a single-phase to earth solid fault, k_{03} (V_{03}) would have the largest rise. K_{0i} (as well as the voltage magnitudes) of the neighbouring nodes (B, D and E) will depend on line lengths, the fault levels within the system, the

topology of the system and the fault resistance. The impact of these factors is described further in Chapter 6. The fault region can be identified as the area bounded by nodes B, C, D and E. It is known that C is definitely connected to the faulted lines, and that the other node of the faulted line must be within $\boldsymbol{N_{oreg}}$. That is, one of nodes B, D or E.

4.2.3.2.2 Stage two – faulted line identification

In this stage, as with all other examples, it is presumed that the primary protection has operated correctly at least at one end of the faulted line. In addition, it's presumed that for double-circuit scenarios, both circuits are installed with PMUs at the substations.

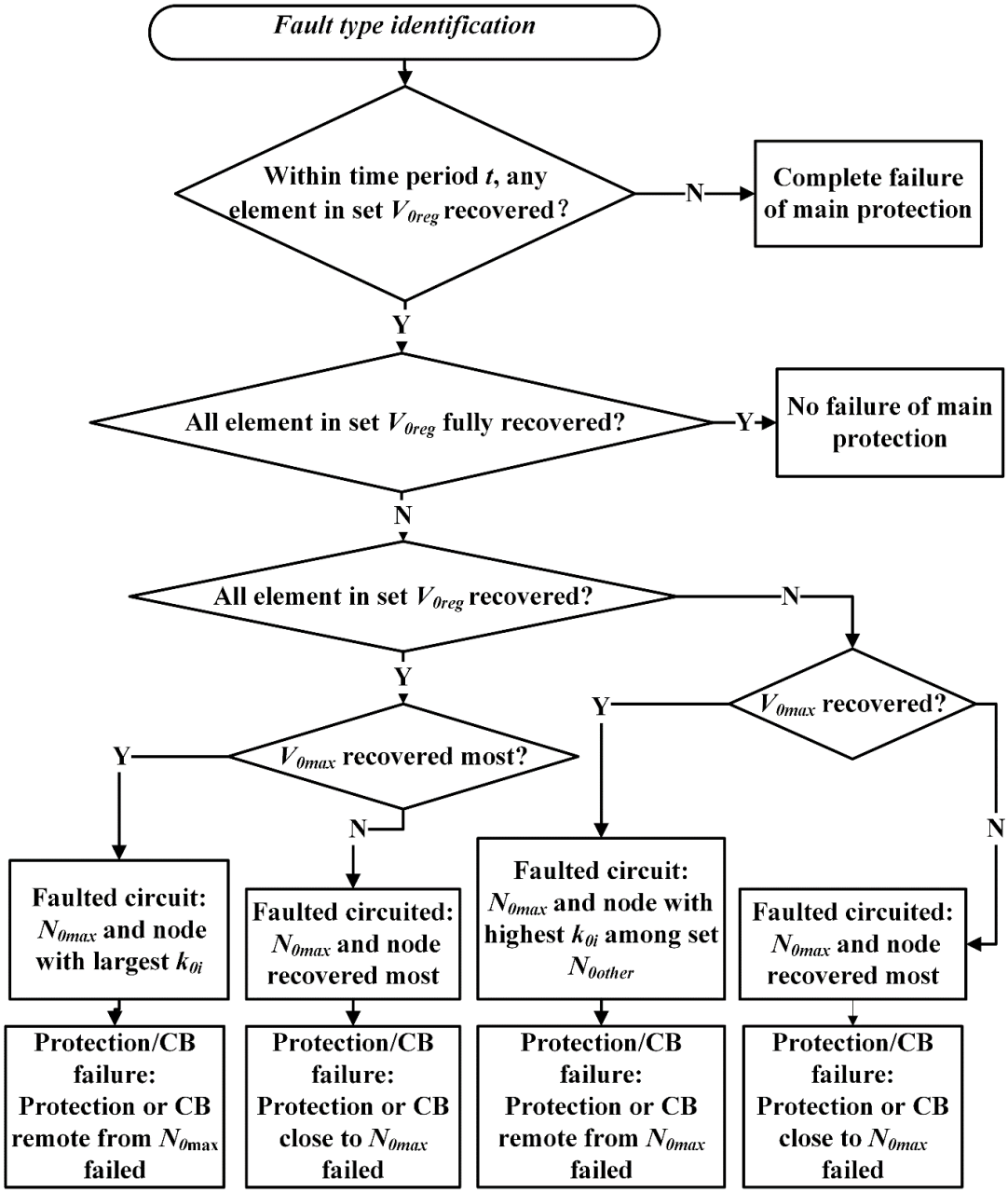

Figure 4.7: Flow chart of stage two – faulted line identification for unbalanced earth faults

The process of stage two is illustrated in Figure 4.7, where after fault type is identified as an unbalanced earth one, the node set $\boldsymbol{N_{oreg}}$, the corresponding $\boldsymbol{K_{oreg}}$ set and $\boldsymbol{V_{oreg}}$ set established in stage one are used as the main inputs to stage two. If there is at least one node in $\boldsymbol{V_{oreg}}$, then identification of the faulted line requires operation of one of the circuit breakers and a consequent observable zero sequence voltage magnitude V_{0i} change at a number of PMUs.

The time period t, shown in Figure 4.7, is the same as that defined for three-phase fault identification, as discussed in Section 4.2.2.2.2. Zero sequence voltage magnitudes of each node - V_{0i} - are examined to identify any instances of zero sequence voltage recovery, i.e. either partial recovery due to the opening of one of the circuit breakers only, or full recovery (returning to the pre-fault voltage level), following successful fault clearance at all terminals of the faulted line. If all voltages are fully recovered during time t, then all protections/breakers have operated correctly and no further analysis is required. Conversely, if there is no voltage recovery observed within time t, then all primary protections would have failed at all line terminals (which is highly unlikely) and the scheme would report the fault region (potentially containing several lines).

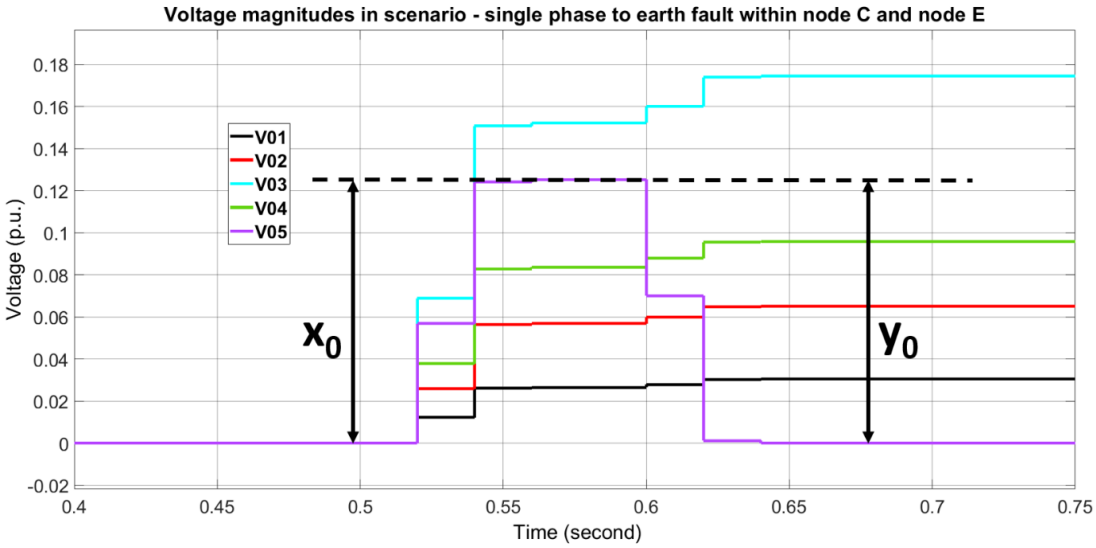

Figure 4.8: Zero sequence voltage magnitudes of 5-bus system for single-phase to earth fault

With operation of line-terminal protection schemes and their controlled circuit breakers, there are four possible behaviour patterns for the elements within set $\boldsymbol{V_{oreg}}$ that may be observed. 1) values could remain unchanged; 2) values could increase further 3) values could partially recover, or 4) fully recover (e.g. returning to greater than 90% of the total voltage rise magnitude). The value of 90% to signify full recovery is deemed acceptable, and is proposed based on the results of extensive simulations; it can be modified if necessary. Figure 4.8 shows the voltage behaviours for the fault scenario depicted in Figure 4.2. The variable x_0

indicates the maximum magnitude of the voltage rise, while y_0 indicates any drop in voltages after the voltages have reached their maximum values. A dedicated functional block has been developed for capturing the values of x_0 and y_0 during simulation. The fault is applied at 0.5 s in the simulation and it is assumed that CB8 at node C operates correctly and opens 80 ms later at 0.58 s. A positive value of the ratio of y_0 to x_0 is used to identify voltage recovery (which could be indicative of either partial or full recovery). A ratio of y_0 to x_0 of greater than 0.9 indicates full recovery – e.g. in V_{05} in Figure 4.8. A negative value for y_0 indicates a further rise after the initial rise (e.g. V_{01}, V_{02}, V_{03} and V_{04}).

It is crucial to identify when a voltage has partially or fully recovered (indicating that a circuit breaker has opened and therefore protection has operated), and when it has gone up further due to the operation of a circuit breaker remote from the measured voltage location. These behaviour patterns provide the input data required for further analysis of circuit breaker status and faulted lines.

During and following fault events that are not properly responded to, the only two scenarios that can be observed are similar to those for three-phase fault scenarios. Scenario 1 is where all elements in set $\boldsymbol{V_{oreg}}$ exhibit some recovery (but do all fully recover); while scenario 2 is where some elements do not recover at all, but a subset of $\boldsymbol{V_{oreg}}$ exhibits recovery. A new set of elements within set $\boldsymbol{N_{oreg}}$, from stage 1 containing all voltages that subsequently exhibit partial recovery or full recovery behaviour, is denoted as set $\boldsymbol{V_{odown}}$. The remaining elements within the set $\boldsymbol{N_{oreg}}$, which have not partially recovered or fully recovered, form the set $\boldsymbol{N_{oother}}$.

In scenario 1, if V_{0max} has not recovered most significantly within set $\boldsymbol{V_{oreg}}$, then the faulted line is identified as the line connected between N_{0max} and the node with the most significant voltage recovery within set $\boldsymbol{N_{oreg}}$. Operational failure of the protection/circuit breaker on this line at N_{0max} can be reported. Otherwise, if V_{0max} has recovered most significantly within the set $\boldsymbol{V_{oreg}}$, then the faulted line is identified as the line connecting N_{0max} and the node with the largest k_{0i} within set $\boldsymbol{N_{oreg}}$. Operational failure of the protection/circuit breaker on this line remote from N_{0max} can be reported.

In scenario 2, if V_{0max} has recovered, the faulted line is identified as the line connected between N_{0max} and the node with the highest k_{0i} within $\boldsymbol{V_{oother}}$. Operational failure of the protection/circuit breaker at the node on this line remote from N_{0max} can be reported. Otherwise, the faulted line is identified as the line within N_{0max} and the node with the most significant voltage recovery within set $\boldsymbol{V_{odown}}$. Operational failure of the protection/circuit breaker on this line at N_{0max} can be reported.

For the scenario depicted in Figure 4.2, the resulting voltage profiles are presented in Figure 4.8. C is N_{0max} and, at the initial stage, it can be deduced that the other node connected to the faulted line is one of either nodes B, D or E. From around 0.6 s, there is no "falling back" (i.e. reducing towards pre-fault values) behaviour for V_{0max} (V_{03}), but V_{05} has the most significant recovery (fully recovering to the pre-fault value from 0.64 s). Accordingly, the faulted line is then identified as the line connected between C and E. However, the protection or circuit breaker at C (CB7) has failed, as the voltage remains in excess of the pre-fault value (after the opening of the circuit breaker at E - note that all other voltages also remain elevated and do not fall back - in this case backup protection would be required to operate. The system would quickly report on the failure of the protection/circuit breaker at C.

The output of stage two consists of information from the analysis that can be reported to operators. The information for the system operator is the same as that provided from stage two for three-phase fault, which is presented in Section 4.2.2.2.2. A case study illustrating full operation of the scheme, including reporting of information, is demonstrated in Section 7.2.3.

4.2.4 Operation of the system for phase-phase faults (unbalanced)

4.2.4.1 Overview

Phase-phase faults will introduce both positive and negative sequence components as outlined in Section 2.3. Since pre-fault values for negative sequence voltages

are typically zero and will increase during unbalanced earth faults, and are more indicative of the presence of phase-phase compared to positive sequence values, negative sequence voltages are used as indicators to identify phase-phase faults and distinguish such fault types within the scheme. As with unbalanced earth faults, three stages are involved in identification of phase-phase faults. For stage one, if at least one negative sequence voltage measurement from any of the PMUs measurements increases above a certain threshold, the fault region is identified. After identification of the fault type (presented in Section 4.2.7), faulted lines and circuit breaker status are identified based on analysis from stage two. Based on the identified faulted elements at the second stage, the performance of the primary protection and the operation of the associated circuit breakers are analysed in the third stage, which then enables the backup protection action if required.

4.2.4.2 Detailed scheme operation

4.2.4.2.1 Stage one – fault region identification

The 5-node radial system shown in Figure 4.2 with a phase-phase fault close to node C, on the line connecting C and E, is again used to demonstrate the concept of operation.

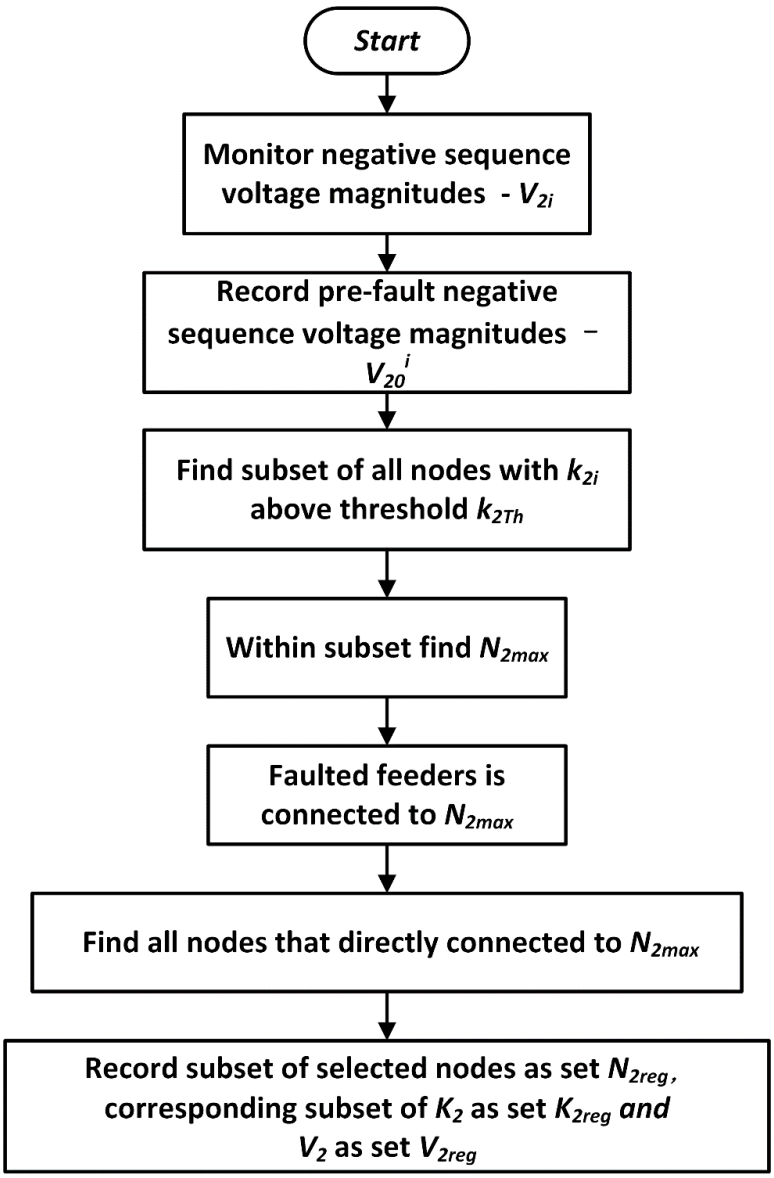

Figure 4.9: Stage one for phase-phase fault

The process of stage one is shown in Figure 4.9. The principle of stage one for phase-phase fault is the same as that for unbalanced earth faults, except that the monitored voltages and calculated variables are all negative sequence rather than zero sequence in this scenario. The aim of this stage is to find the node which has the maximum negative sequence voltage rise and subsequently identify the fault region by monitoring negative sequence voltages at all node via the PMUs. The negative sequence voltage magnitudes of node i is denoted as V_{2i}, which belongs to a voltage set $\boldsymbol{V_2}$. The pre-fault negative sequence voltage magnitude of node i is denoted as $V_{20}{}^{\mathrm{i}}$, which belongs to a voltage set $\boldsymbol{V_{20}}$ that contains pre-fault

negative sequence voltage magnitudes from all nodes. The program to identify $V_{20}{}^{i}$ is explained further in Section 4.2.5.3. For the scheme, decisions are made based on the difference between V_{2i} and their pre-fault values $V_{20}{}^{i}$, which are denoted as k_{2i}, i.e. $k_{2i} = V_{2i}$ - $V_{20}{}^{i}$, and the set containing k_{2i} from all nodes is denoted as $\boldsymbol{K_2}$. If k_{2i} of at least one node is above the threshold k_{2Th}, the node with the largest k_{2i} (i.e. k_{2max}), defined as N_{2max}, is identified as a node that is definitely connected to the faulted line. The voltage magnitude of N_{2max} is denoted as V_{2max}. Based on topology of the network, a subset of nodes is then formed, which includes N_{2max} and all neighbouring nodes. This subset of nodes, $\boldsymbol{N_{2reg}}$, defines the region of the network where the fault is located. The corresponding subset of $\boldsymbol{K_2}$, denoted as $\boldsymbol{K_{2reg}}$, contains the k_{2i} of all nodes within $\boldsymbol{N_{2reg}}$. The corresponding subset of $\boldsymbol{V_2}$, denoted as $\boldsymbol{V_{2reg}}$, contains the V_{2i} of all nodes within $\boldsymbol{N_{2reg}}$. All voltages (V_{2i}) are relative values to nominal voltages and expressed in p.u.

For the demonstrated scenario shown in Figure 4.2, V_{2i} of all nodes is 0 p.u. and for this fault, k_{23} (V_{23}) would have the largest voltage depression. k_{2i} (as well as the voltage magnitudes) of the neighbouring nodes (B, D and E) will depend on line lengths, the fault levels within the system, the topology of the system and the fault resistance, which is described further in Section 6.4. The fault region can be identified as the area bounded by nodes B, C, D and E. It is known that C is definitely connected to the faulted lines, and that the other node of the faulted line must be within $\boldsymbol{N_{2reg}}$. That is, one of nodes B, D or E.

4.2.4.2.2 Stage two – faulted line identification

At the second stage, for faulted line identification, the assumption is made that at least one line-end primary protection operates correctly (the probability of failure of both primary protection at both terminals of the line is extremely low) to identify the faulted line. In addition, it's presumed that for double-circuit scenarios, both circuits are installed with PMUs at the substations.

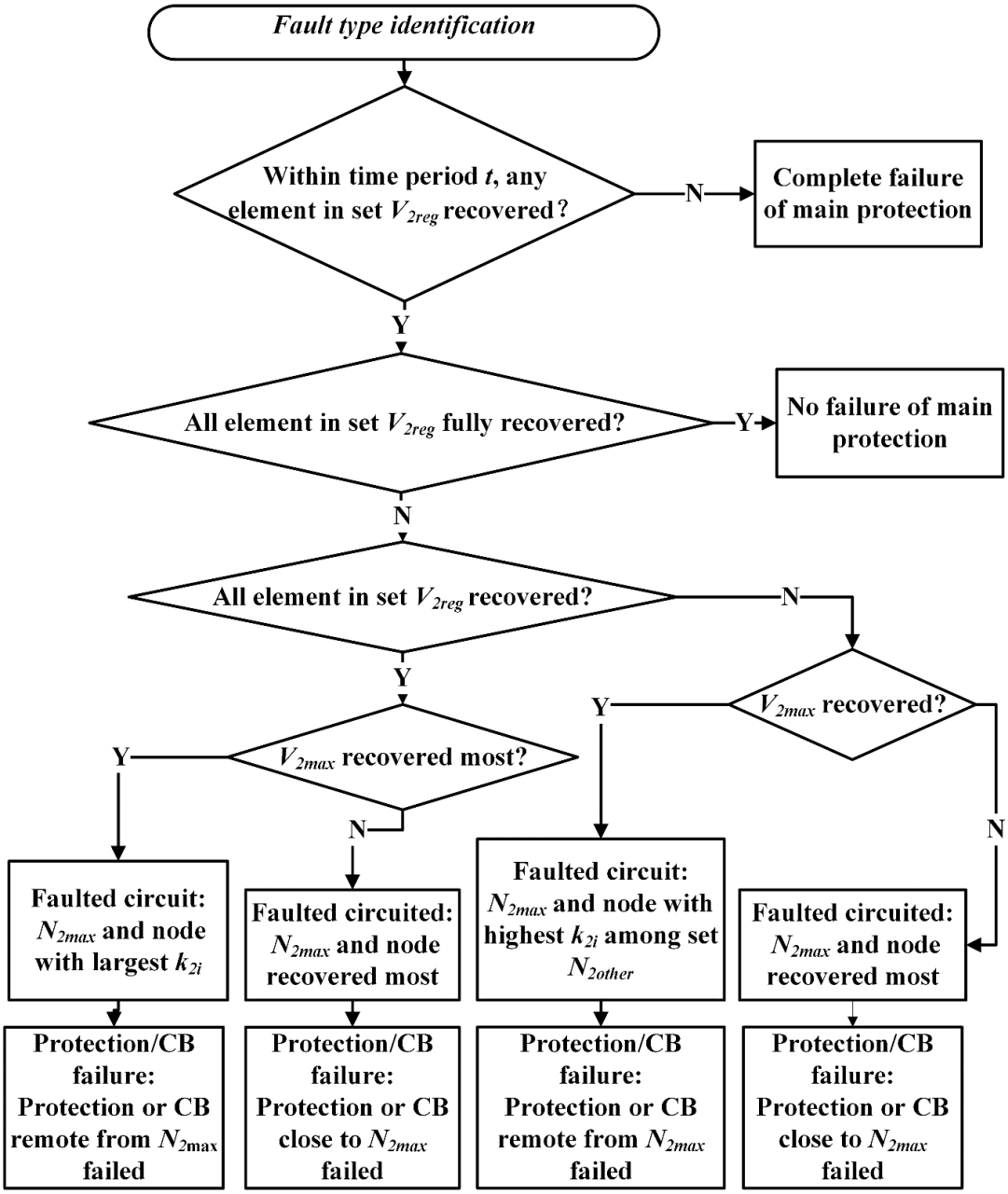

Figure 4.10: Flow chart of stage two – faulted line identification

Under the situation that both line-end primary protection systems operate correctly, the faulted line does not need to be identified for backup protection purposes and the occurrence of the fault and the fault region have already be identified in step one. This stage for phase-phase faults, as illustrated in Figure 4.10, shares the same principle for identification of unbalanced earth faults but utilising negative sequence variables as indicators for analysis. With set $\boldsymbol{N_{2reg}}$, $\boldsymbol{K_{2reg}}$ and $\boldsymbol{V_{2reg}}$ as inputs, after identification of a phase-phase fault, stage two

can identify the faulted line with operation of one line-end circuit breaker based on the analysis of subsequent observable change of elements within $\boldsymbol{V_{2reg}}$ at a number of PMUs. The negative sequence voltage magnitudes of the measured node V_{2i} are examined to identify any instances of negative sequence voltage recovery, i.e. either partial recovery due to the opening of one of the circuit breakers only, or full recovery (returning to the pre-fault voltage level), following the successful fault clearance at all terminals of the faulted line. If all voltages fully recover during time t, then all protection/circuit breakers have operated correctly and no further analysis is required. Conversely, if there is no voltage recovery observed within time t, then all primary protections would have failed at all line terminals (which is highly unlikely) and the scheme can report upon the fault region (potentially containing several lines).

With operation of line-terminal protection schemes and their controlled circuit breakers, there are four possible behaviour patterns of the elements within set $\boldsymbol{V_{2reg}}$ that may be observed. 1) values could remain unchanged; 2) values could increase further 3) values could partially recover, or 4) fully recover (e.g. falling back with a magnitude of greater than 90% of the total initial voltage rise magnitude). These values have been proposed based on the results of extensive simulations and can be modified if necessary. Figure 4.11 shows the voltage behaviours for the fault scenario depicted in Figure 4.2. The variable x_2 indicates the maximum value of the voltage rise and y_2 indicates any reduction in voltages after the voltages have reached their maximum values. A dedicated functional block has been developed for capturing the values of x_2 and y_2 during simulation. The fault is applied at 0.5 s in the simulation and it is assumed that CB8 at node C operates correctly and opens 80 ms later at 0.58 s. A positive value of the ratio of y_2 to x_2 is used to identify voltage recovery (which could be indicative of either partial or full recovery). A ratio of y_2 to x_2 of greater than 0.9 indicates full recovery e.g. V_{25} in Figure 4.11. A negative value for y_2 indicates a further depression after the initial depression (e.g. V_{21}, V_{22}, V_{23} and V_{24}).

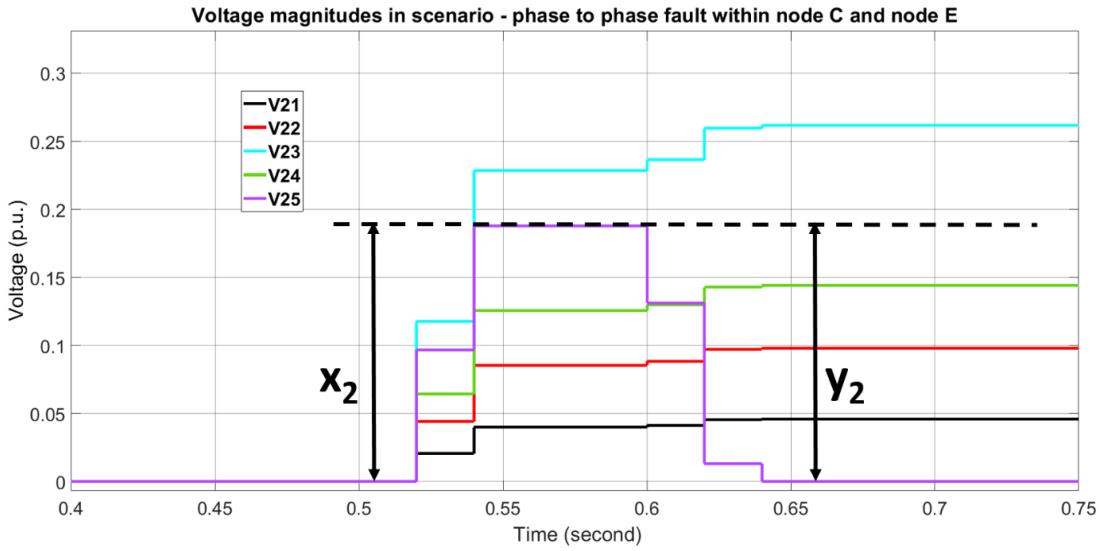

Figure 4.11: Voltage magnitudes of 5-bus system

It is very important to identify when a voltage has partially or fully recovered (indicating that a circuit breaker has opened and therefore protection has operated), and when it has further increased due to the operation of a circuit breaker remote from the measured voltage location (e.g. V_{23} in Figure 4.11). These behaviour patterns provide indication for further analysis of circuit breaker status and faulted lines.

During and following fault events that are not properly responded to correctly (i.e. a line terminal protection system or its controlled breaker does not operate), realistically, only two scenarios can be observed (as is also the case unbalanced earth faults). Scenario 1 is where all elements in set $\boldsymbol{V_{2reg}}$ exhibit some recovery (but do all fully recover); while scenario 2 is where some elements do not recover at all, but a subset of $\boldsymbol{V_{2reg}}$ exhibits recovery. A new set of elements within set $\boldsymbol{N_{2reg}}$, from stage one containing all voltages that subsequently exhibit partial or full recovery behaviour is denoted as set $\boldsymbol{N_{2down}}$. The remaining elements within the set $\boldsymbol{V_{2down}}$, which have not partially recovered or fully recovered, form the set $\boldsymbol{V_{2other}}$. In scenario 1, if V_{2max} has not recovered most significantly within set $\boldsymbol{V_{2reg}}$, then the faulted line is identified as the line connected between N_{2max} and the node with the most significant voltage recovery within set $\boldsymbol{N_{2reg}}$. Operational failure of the protection/circuit breaker on this line at N_{2max} can be reported. Otherwise, if V_{2max} has recovered most significantly within the set $\boldsymbol{V_{2reg}}$, then

the faulted line is identified as the line connecting N_{2max} and the node with the highest k_{2i} within set $\boldsymbol{N_{2reg}}$. Operational failure of the protection/circuit breaker on this line remote from N_{2max} can be reported.

In scenario 2, if V_{2max} has recovered, the faulted line is identified as the line connected between N_{2max} and the node with the highest k_{2i} within $\boldsymbol{V_{2other}}$. Operational failure of the protection/circuit breaker at the node on this line remote from N_{2max} can be reported. Otherwise, the faulted line is identified as the line within N2max and the node with the most significant voltage recovery within set $\boldsymbol{V_{2down}}$. Operational failure of the protection/circuit breaker on this line at N_{2max} can be reported.

For the scenario depicted in Figure 4.2, the resulting voltage profiles are presented in Figure 4.11. C is N_{2max} and, at the initial stage, it can be deduced that the other node connected to the faulted line is one of either nodes B, D or E. From around 0.6 s, there is no recovery behaviour for V_{2max} (V_{23}), but V_{25} has the most significant recovery (fully recovering to pre-fault from 0.64 s). Accordingly, the faulted line is then identified as the line connected between C and E. However, the protection or circuit breaker at C (CB7) has failed as the voltage (V23) continues to increase after the opening of the circuit breaker at E - note that all other voltages also remain depressed and do not recover - in this case backup protection would be required to operate. The system would quickly report on the failure of the protection/circuit breaker at C.

The output of stage two includes reporting of summary information from analyses of the various voltage profiles during the event. The information reported to the system operator is same as that for stage two for three-phase fault scenarios, as presented in Section 4.2.2.2.2. A case study to demonstrate the operation of the scheme is presented in Section 7.2.3.

4.2.5 Pre-fault voltage identification for threshold determination

4.2.5.1 Overview

This Section introduces the method used to identify pre-fault voltage magnitudes for different types of faults. The reason for this stage of the process is to set the threshold for detection of fault occurrence as accurately as possible, using relative indicators rather than absolute values, and to prepare for the automatic calculation of x and y values for determination of voltage recovery as discussed in Section 4.2.2.2.2, Section 4.2.3.2.2 and Section 4.2.4.2.2. This method is inspired by the calculation of superimposed components in numerical relays (superimposed components are the differences of voltage or current between the pre-fault and fault scenarios) [ATR04] and can identify the pre-fault voltages in a timely manner, and can be adapted to cater for scenarios where the voltage profile is dynamic due to variations in load and generation and/or routine voltage control activity such as reactive power compensation, transformer tap changing, etc. Both superimposed components and the method proposed in this section requires a buffer to hold the sample of a couple of samples. However, superimposed components are implemented to phase sinusoidal waveforms and the method proposed in this section is implemented to PMU outputs (lower reporting rate than numerical relays).

4.2.5.2 Pre-fault voltage magnitudes for three-phase faults

For three-phase faults, although positive sequence voltage will drop immediately after occurrence of the fault, the reported voltage magnitudes from PMUs may take up to three cycles to stabilise (due to the measurement techniques used within PMUs). This is demonstrated in Figure 4.13 with a three-phase fault applied at 0.211 s. It can be observed from Figure 4.13(b) that the phase voltage magnitudes drops immediately after the fault occurs. Since the assumption is made that the PMU utilised in the scheme is of the most common P class, which

has two-cycle measuring windows and 50 Hz report rates for 50 Hz networks (UK standard), the minimum voltage magnitude during fault would not be reported until the "completion" of the red measuring window - shown in Figure 4.13(b), which is at 0.26 s. The analysis is conducted by combining graph (a) and (b) of Figure 4.13. For Figure 4.13(b), the measuring window in black from 0.16 s to 0.2 s corresponds to the magnitude measured at 0.2 s in Figure 4.13(a), in which case, the system is operating under normal operating condition (pre-fault values). The measuring window in green with measurements from 0.18 s to 0.22 s in Figure 4.13(b), which is the first measuring window impacted by the fault occurrence, corresponds to the magnitude at 0.22 s in Figure 4.13(a). In this measuring window, since the pre-fault voltage occupies the majority of the window (about 75% of this window is during the pre-fault period), then only a small voltage drop is recorded by the PMU at 0.22 s as shown in Figure 4.13(a). For the next measuring window, which is highlighted in yellow in Figure 4.13(b), part of the window is still occupied by pre-fault voltage, but less than before. Thus, positive sequence voltage magnitude reported from PMU further reduces at 0.24 s as shown in Figure 4.13(a). It will decline further towards the actual correct value once the measuring window does not include pre-fault voltage (assuming that the during-fault voltage remains constant and does not change), which is the red window shown in Figure 4.13(b). The final step down, which leads to the actual minimum voltage magnitude during the fault, is reported at 0.26 s by the PMU as shown Figure 4.13(a). For Figure 4.13(a), the "step down" at 0.22 s is denoted as D1, the step down at 0.24 s as D2 and the step down at 0.26 s as D3.

Since the relative value of the minimum /steady state positive voltage magnitude during fault to the pre-fault voltage magnitude $V_{10}{}^{\mathrm{i}}$ are used to compare with the threshold for identification of fault occurrence, $V_{10}{}^{\mathrm{i}}$ should be the positive voltage magnitude before D1 for threshold determination. Since it can take up to 3 cycles for the PMU to report the minimum/steady state value of voltage during the fault as described above, $V_{10}{}^{\mathrm{i}}$ is set to be the voltage magnitude three cycles before the present measurement output until the time at which fault occurrence is identified. The time when the scheme identifies the fault occurrence

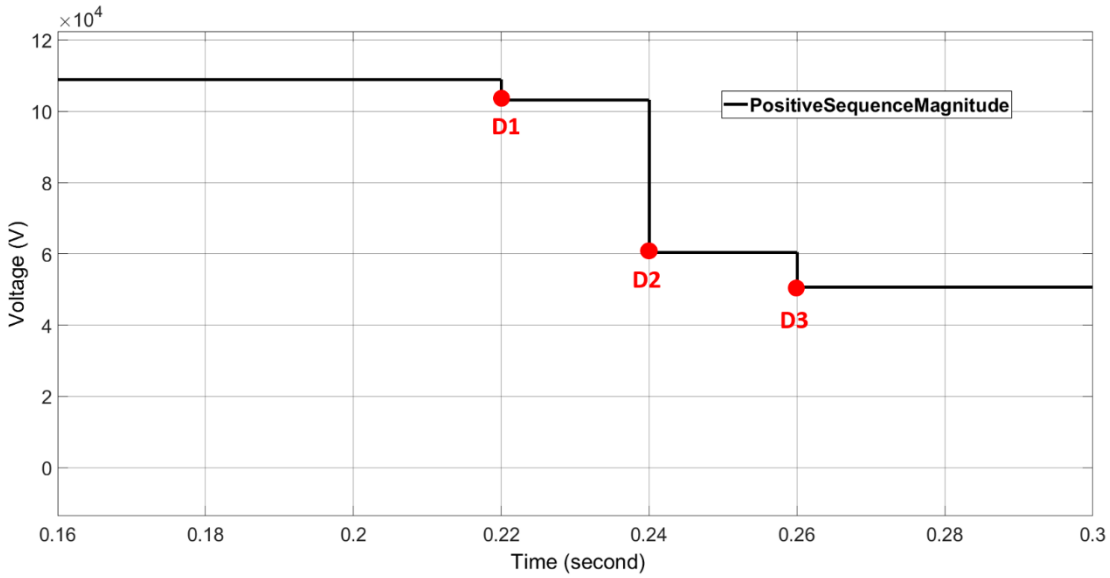

(a) Positive sequence voltage magnitudes from PMU

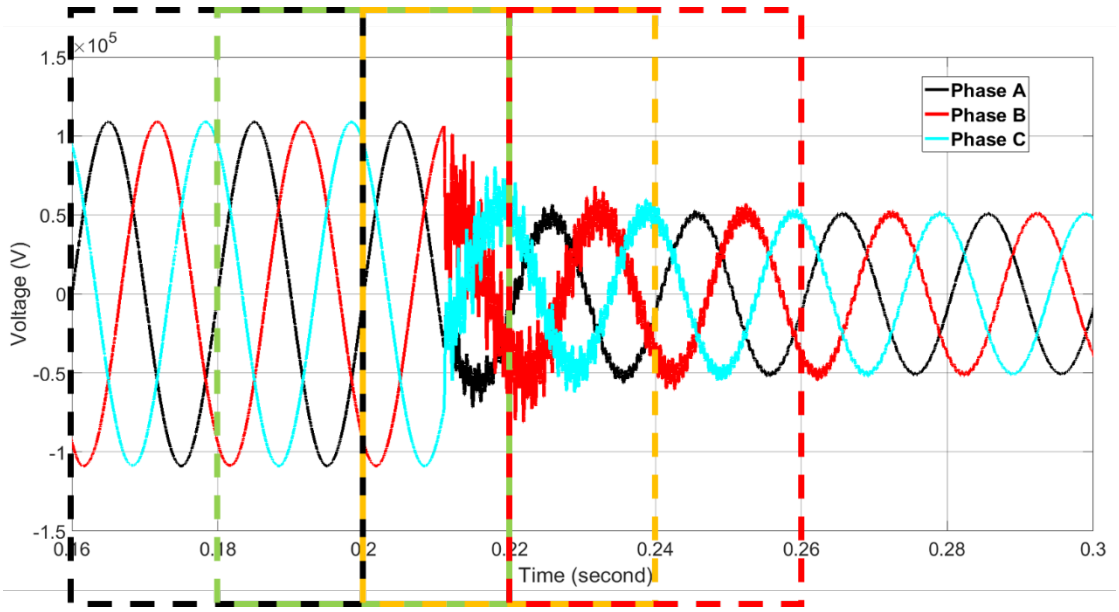

(b) Waveform of phase voltages

Figure 4.12: Measurements for three-phase faults

is denoted as t_f; one cycle before t_f is denoted t_{f1}; two cycles before t_f as t_{f2} and three cycles before t_f as t_{f3}. After identification of fault occurrence, comparison between positive sequence voltage magnitudes at t_{f1} and t_{f2} is conducted and if the value at t_{f2} is larger than that of t_{f1}, then the positive sequence voltage magnitude at t_{f2} is is compared with that at t_{f3}. The larger value of t_{f2} and t_{f3} is assigned to ${V_{10}}^{\mathrm{i}}$ for further use in the analysis conducted in stage two, which is further explained in Section 4.2.2.2.2. Otherwise the positive sequence voltage magnitude at t_{f1} is assigned to ${V_{10}}^{\mathrm{i}}$.

For the example demonstrated in Figure 4.13(a), if the threshold is set such that the fault occurrence cannot be identified until the time 0.26 s, ${V_{10}}^{\mathrm{i}}$ is set to be the voltage magnitude at 0.20 s at the time 0.26 s (similarly, at 0.22 s, ${V_{10}}^{\mathrm{i}}$ is the positive sequence voltage magnitude at 0.16 s; at 0.24 s, ${V_{10}}^{\mathrm{i}}$ is the positive sequence voltage magnitude at 0.18 s and at 0.26 s, ${V_{10}}^{\mathrm{i}}$ is the positive sequence voltage magnitude at 0.20 s.). In this case, t_f is 0.26 s; t_{f1} is 0.24 s; t_{f2} is 0.22 s and t_{f3} is 0.20 s. A comparison between positive sequence voltage magnitudes at t_{f1} and t_{f2} is conducted. Since the positive sequence voltage magnitude at t_{f2} is larger than t_{f1}, the positive sequence voltage magnitude at t_{f2} is compared to that at t_{f3}. The larger value of these, which is the positive sequence voltage magnitude at t_{f3} (0.2 s) is selected as the pre-fault voltage ${V_{10}}^{\mathrm{i}}$ for further analysis in stage two.

If fault occurrence is identified at 0.22 s, ${V_{10}}^{\mathrm{i}}$ is set to be the voltage magnitude at 0.16 s at the time of 0.22 s. In this case t_f is 0.22 s; t_{f1} is 0.20 s; t_{f2} is 0.18 s and t_{f3} is 0.16 s. A comparison between positive sequence voltage magnitude at t_{f1} and t_{f2} is conducted. Since the positive sequence voltage magnitude at t_{f2} is not larger than t_{f1}, the positive sequence voltage magnitude at t_{f1} (0.2 s) is assigned to ${V_{10}}^{\mathrm{i}}$ for further analysis in stage two.

When a fault occurs at a specific point on a network, all voltages will change simultaneously in the vicinity of the fault and the corresponding time of ${V_{10}}^{\mathrm{i}}$ is the same for all nodes in the network. Therefore, when ${V_{10}}^{\mathrm{i}}$ of one node is identified, the ${V_{10}}^{\mathrm{i}}$ at all other nodes can be identified as the corresponding voltage magnitudes at the time of identification of ${V_{10}}^{\mathrm{i}}$. To demonstrate, under

the scenario shown in Figure 4.13, the time corresponding to pre-fault voltage magnitude is 0.2 s. Thus, the voltage magnitudes at 0.2 s for all nodes in the power system are the identified pre-fault voltage values.

4.2.5.3 Pre-fault voltages for unbalanced faults

The method used to identify $V_{20}{}^{\mathrm{i}}$ for phase-phase fault scenarios and to identify $V_{00}{}^{\mathrm{i}}$ for unbalanced earth fault scenarios share the same principle to that used for three-phase faults. Thus $V_{20}{}^{\mathrm{i}}$ ($V_{00}{}^{\mathrm{i}}$) is also set to be the voltage magnitude three cycles before the present measurement until identification of fault occurrence. t_f, t_{f1}, t_{f2} and t_{f3} have the meaning as for the scenario analysed for $V_{10}{}^{\mathrm{i}}$ identification. After identification of fault occurrence, comparison between the negative (or zero) sequence voltage magnitudes at t_{f1}, t_{f2} and t_{f3} are compared, and the smallest of these values is assigned to $V_{20}{}^{\mathrm{i}}$ ($V_{00}{}^{\mathrm{i}}$) for further analysis in stage two.

To explain the method, examples of phase-phase fault and unbalanced earth fault scenarios (use single-phase to earth fault as an example) are demonstrated in Figure 4.13. If the threshold is set such that the fault occurrence cannot be identified until 0.26 s, $V_{20}{}^{\mathrm{i}}$ ($V_{00}{}^{\mathrm{i}}$) is set to the value of the voltage magnitude at 0.20 s at the time 0.26 s. In this case, t_f is 0.26 s; t_{f1} is 0.24 s; t_{f2} is 0.22 s and t_{f3} is 0.20 s. A comparison between negative (zero) sequence voltage magnitude at t_{f1} and t_{f2} is conducted. Since the negative (zero) voltage magnitude at t_{f2} is smaller than t_{f1}, the negative (zero) sequence voltage magnitude at t_{f2} is compared to that at t_{f3}. The smallest of the values is chosen, which is the negative (zero) sequence voltage magnitude at t_{f3} (0.2 s), and set to $V_{20}{}^{\mathrm{i}}$ ($V_{00}{}^{\mathrm{i}}$) for further analysis in stage two.

If fault occurrence is identified at 0.22 s, $V_{20}{}^{\mathrm{i}}$ ($V_{00}{}^{\mathrm{i}}$) is set to be the voltage magnitude at 0.16 s at 0.22 s. In this case, t_f is 0.22 s; t_{f1} is 0.20 s; t_{f2} is 0.18 s and t_{f3} is 0.16 s. A comparison between negative (zero) voltage magnitude at t_{f1} and t_{f2} is conducted. Since the negative (zero) voltage magnitude at t_{f2} is not less than t_{f2}, the negative (zero) voltage magnitude at t_{f1} (0.2 s) is assigned to $V_{20}{}^{\mathrm{i}}$ ($V_{00}{}^{\mathrm{i}}$) for further analysis in stage two.

As with the pre-fault voltage identification process for positive sequence com-

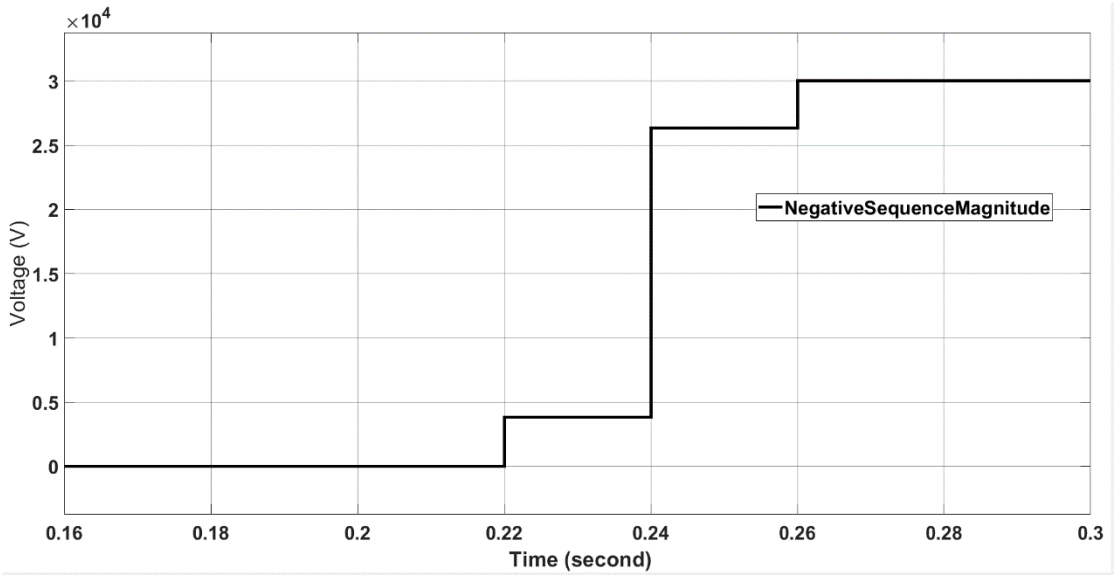

(a) Negative sequence for phase-phase fault

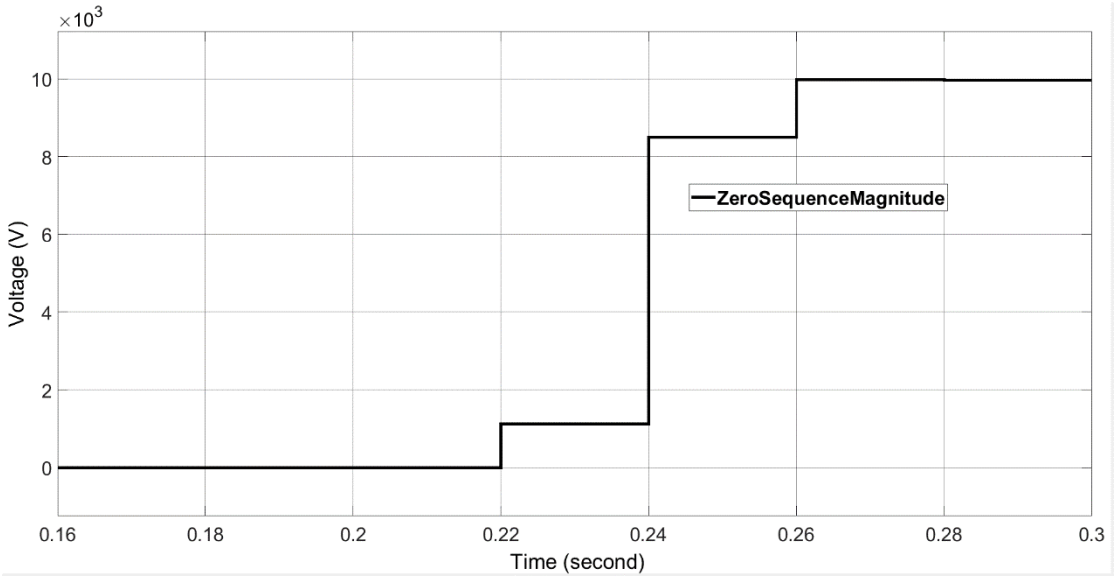

(b) Zero sequence fault for single-phase to earth fault

Figure 4.13: Sequence voltage magnitude from PMU

ponents, for negative (zero) sequence components, once $V_{20}{}^{\mathrm{i}}$ ($V_{00}{}^{\mathrm{i}}$) of one node is identified, then $V_{20}{}^{\mathrm{i}}$ ($V_{00}{}^{\mathrm{i}}$) of other nodes can be identified as the voltage magnitude at the time of $V_{20}{}^{\mathrm{i}}$ ($V_{00}{}^{\mathrm{i}}$) identification. To demonstrate, for the scenario shown in Figure 4.13, the time corresponding to pre-fault voltage magnitude is 0.2 s. Thus, the voltage magnitudes of 0.2 s for all nodes in the power system are the identified pre-fault voltage values.

4.2.6 Mitigation against interference and signal distortion during transient behaviour

Since the principle of the scheme is based upon analysis of sequence components, it is very important to choose the correct sequence component to analyse and use within decision-making processes, as there may be temporary "pulses" in sequence components due to transients, and it is important to "wait and see" until it can be established that a particular sequence component(s) has definitely changed as a result of a fault.

As discussed in Section 4.2.5, the priority of the sequence of fault type identification is unbalanced earth faults (identified by zero sequence components), phase-phase faults (identified by negative sequence components) and three-phase faults (identified by positive sequence components), to reflect the likelihood of occurrence. It is crucial to avoid mal-operation caused by the temporary impact of three-phase faults on negative/zero sequence voltages (hence the "wait and see" approach described above). The waveforms of phase voltages and sequence voltages for a three-phase fault scenario are shown in Figure 4.14. The fault occurs at 0.2 s. It can be seen from Figure 4.14(a) that the phase voltages have "transient unbalance" (due to phase shift) at the instance of fault occurrence and revert to a balanced situation soon afterwards. This situation will result in negative sequence components being present. As explained Section 4.2.5, it requires at least 3 cycles for PMUs to output steady state during fault voltage magnitudes after the initial occurrence of the fault. Therefore, the negative sequence voltages have two cycle "pulses" corresponding to the "transient unbalance" introduced

by the three-phase fault. Similarly, due to the operation of one line-end protection/circuit breaker, a two cycle "pulse" can also be introduced to the negative sequence components, as demonstrated in Figure 4.14(c). For zero sequence components, the transients associated with non-earth faults and breaker operations can also introduce temporary "pulses". However, the magnitudes are very small. Finally, phase-phase fault can also introduce two cycle "pulses" in zero sequence voltages.

In order to identify the fault type accurately and to subsequently analyse the network status accurately, the scheme must avoid mal-identification caused by two cycle pulses as described previously. Therefore, for all fault types, the voltage must violate any threshold for at least 3 cycles before the occurrence of the fault can be identified with certainty. For the pulses caused by operation of primary protection/circuit breaker, no action is required. As the fault type has been correctly identified before operation of primary protection/circuit breaker, only the corresponding stage two (corresponding to the fault type identified previously) will be used for further analysis. For the example demonstrated in Figure 4.14, negative sequence voltages have pulses for two cycles from 0.22 s and cease to exist from the subsequent cycle. V_{1_2} is below the threshold from 0.22 s for 3 cycles until 0.28 s. Therefore, the fault is identified as a three-phase fault. Then, stage two (for three-phase faults) is triggered to analyse the voltages for the next stage of operation.

4.2.7 Identification of fault type

Since sequence components are utilised for fault detection, positive sequence, negative sequence and zero sequence voltages are used to distinguish between three-phase (to earth) faults, phase-phase faults and unbalanced earth faults.

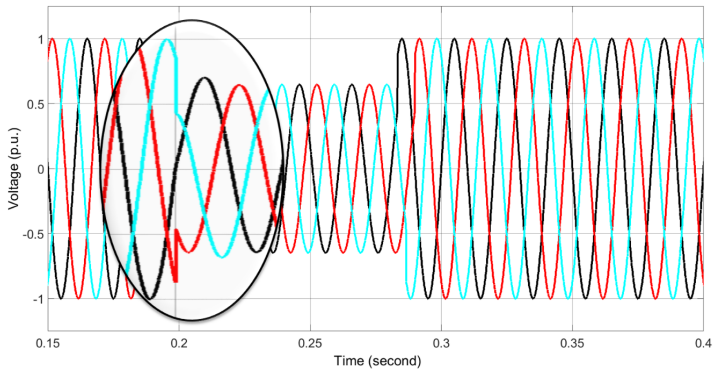

(a) Phase voltages

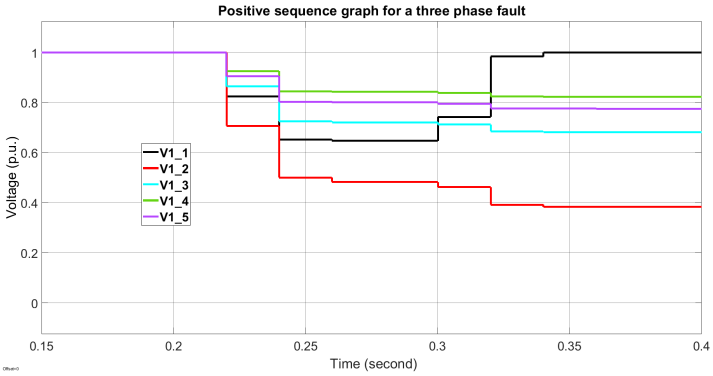

(b) Positive sequence

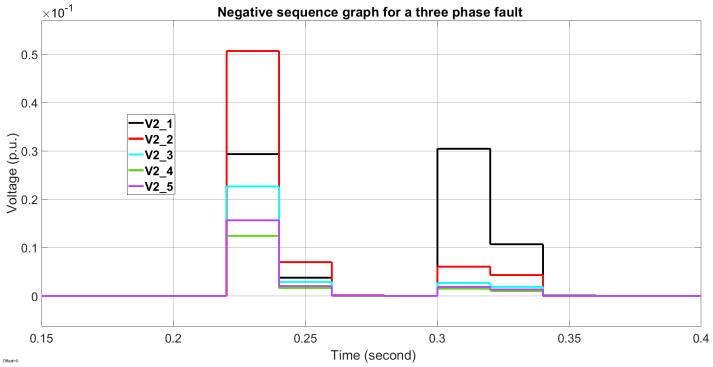

(c) Negative sequence

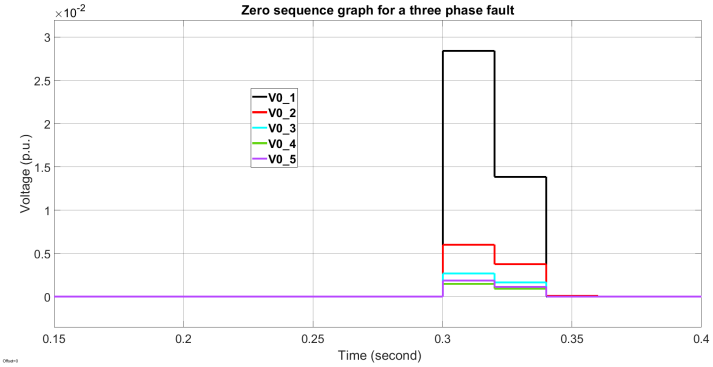

(d) Zero sequence

Figure 4.14: Voltage waveforms for a three-phase fault

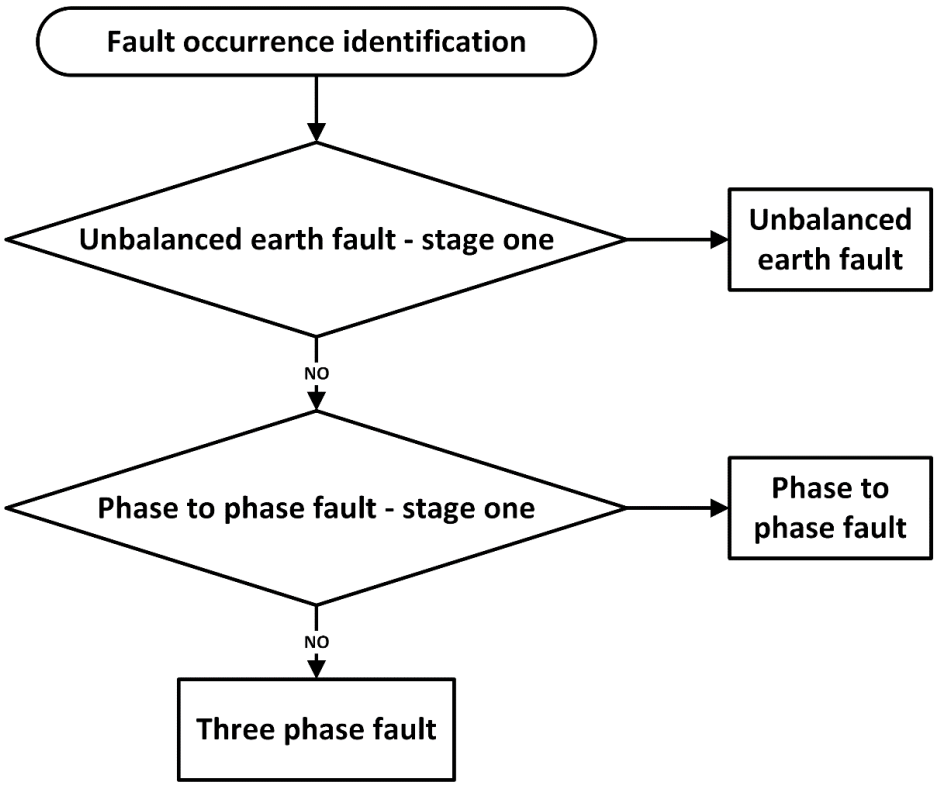

Figure 4.15: Fault type identification

As described in Section 2.3, only positive sequence components are involved during balanced faults; both negative and positive sequence components are used during phase-phase faults and all sequence components are utilised during unbalanced earth faults. The flow chart for the fault type identification process is demonstrated in Figure 4.15.

4.2.8 Stage three - backup protection

Based on the analysis results from stage two - faulted line identification and primary protection performance analysis - backup protection actions can be initiated if required. The scheme will send tripping signals to all neighbouring (directly connect to the same node or busbar section, taking into account that the busbar may be segregated) circuit breakers around the failed circuit breaker to provide backup protection. For the 5-node case study shown in Figure 4.2, whichever type of fault is applied to the network, the faulted line is identified as the line connecting nodes C and E and the protection/circuit breaker at C is identified

as having failed to operate from stage two of the scheme operation. A tripping signal will be sent to CB4, CB5 and CB7 to disconnect the faulted line from the system and provide backup protection. Results of case studies are demonstrated using both Matlab simulations in Section 7.2 and using a hardware in the loop arrangement with an RTDS in Section 8.2.

4.3 Applicability to large-scale systems

In order to apply the scheme to an actual power system with potentially large number of nodes, a distributed wide-area hierarchy is proposed as shown in Figure 4.16. Each area consists of several substations equipped with PMUs. The distributed processors handle the PMU data from their corresponding areas only. In the first instance, the distributed processor identifies whether the area includes a node with a voltage below the pre-set threshold using stage one for three-phase faults and/or negative/zero sequence voltages above the pre-set threshold in stage one for unbalanced earth faults or phase-phase faults. Subsequently, the node with the lowest voltage, if identified by stage one of three-phase faults, or the highest sequence voltage if identified by stage one of the unbalanced earth or phase-phase faults analyses within the area is identified and noted.

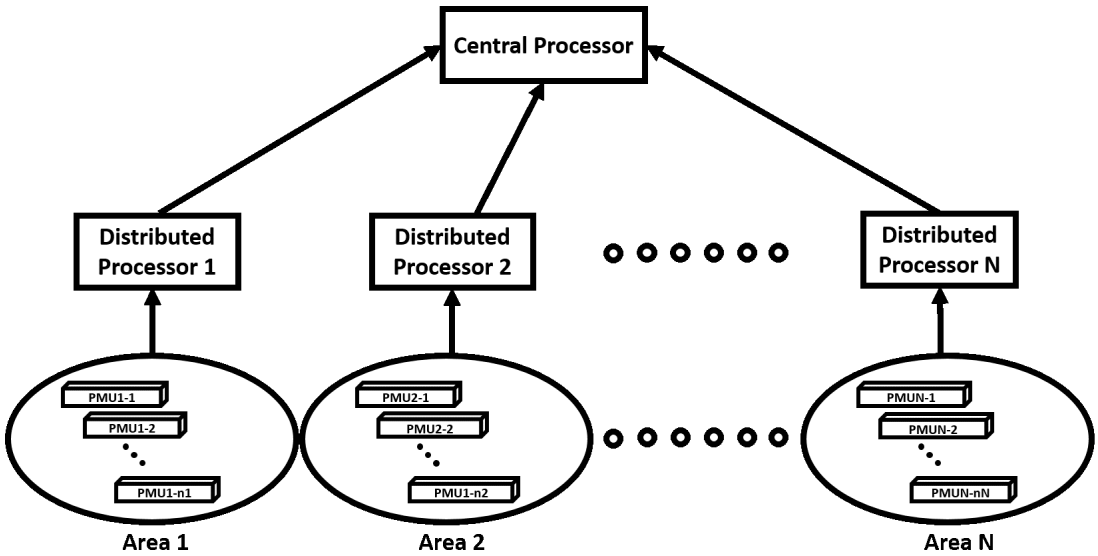

Figure 4.16: Scheme structure for application in real networks

The nodes in the vicinity of this node are identified as the fault region. If fault occurrence is identified by stage one as being of potentially more than one type of faults, the fault type identification block then identifies the correct fault type from the different categories and selects the corresponding variables (such as fault region and minimum/maximum voltage magnitudes, sequence components etc.) for further analysis. Stage one operation for different fault types is presented in Section 4.2.2.2.1 (three-phase faults), Section 4.2.3.2.1 (unbalanced earth faults) and Section 4.2.4.2.1 (phase-phase faults). The fault type identification block is explained in Section 4.2.7.

For a scenario where the fault is identified as a three-phase fault, if more than one area indicates the presence of a fault, the central processor is then initiated to determine, through comparison, the smallest k_{1i} from the areas where voltages have fallen below the threshold. The node with the lowest relative voltage magnitude among these areas is assigned as N_{1min} - the node with lowest k_{1i} in the network. If N_{1min} is not a boundary node, the faulted line is identified within the corresponding area, which includes N_{1min}. The faulted region in this case includes N_{1min} and all neighbouring nodes. Only the distributed processor corresponding to this area is required for further analysis, as only one area is involved and no information from other areas is required. The process follows the stages as outlined in Section 4.2.2.2.2 (faulted line identification) and 4.2.8 (backup protection). However, when N_{1min} is a boundary node, the faulted line can be within either of the neighbouring areas as the faulted region includes N_{1min} and all neighbouring nodes. In this case, multiple areas are involved, so the central processor is needed to analyse the information from all associated areas. With inputs from stage one applied to those areas, a combined faulted region is formed, which is then analysed by the central processor to identify the faulted line and protection failure (stage two), followed by the backup protection if required (stage three).

For a scenario where the fault is identified as a phase-phase or an unbalanced earth fault, if more than one area indicates the presence of a fault, the central processor is then initiated to determine, through comparison, the largest k_{2i} (k_{0i})

from the areas where voltages have fallen below the threshold. The node with the highest relative voltage magnitude among these areas is assigned as N_{2min} (N_{0max}) - the node with highest k_{2i} (k_{0i}) in the network. If N_{2min} (N_{0max}) is not a boundary node, the faulted line is identified within the corresponding area which includes N_{2min} (N_{0max}). The faulted region in this case includes N_{2min} (N_{0max}) and all neighbouring nodes. Only the distributed processor corresponding to this area is required for further analysis, as only one area is involved and no information from other areas is required. The process follows the stages as outlined in Section 4.2.3.2.2 (Section 4.2.4.2.2) and Section 4.2.8. However, when N_{2min} (N_{0max}) is a boundary node, the faulted line can be within either of the neighbouring areas as the faulted region includes N_{2min} (N_{0max}) and all neighbouring nodes. In this case, multiple areas are involved, so the central processor is needed to analyse the information from all associated areas. With inputs from stage one applied to those areas, a combined faulted region is formed, which is then analysed by the central processor to identify the faulted line and protection failure (stage two), followed by the backup protection if required (stage three).

4.4 Conclusions

The focus of this chapter has been to thoroughly present the principles of operation of the proposed scheme, to highlight the applicability of the scheme to practical power systems. With voltage measurements from PMUs, the scheme has two main functions: reporting network and circuit breaker/protection status; and providing backup protection if required. The reporting function simplifies and summarises information received by system operators during system events, while the wide-area backup protection function can provide fast backup protection to maintain the security of the networks. The chapter focussed on how the scheme can identify fault region and fault type through analysis of the behaviour of the various voltages and their corresponding sequence components.

Chapter 5

Method of network simplification

5.1 Chapter overview

To determine the general applicability of the proposed scheme to a range of different network topologies and fault levels, it is important to quantify factors such as the highest detectable fault resistance and the thresholds that can be used to detect the presence of faults. For practical purpose, a simplified system model (a 2-bus equivalent model, that is representative of the entire power system around the specific line being analysed) as demonstrated in Figure 5.1 is used to determine the highest detectable fault resistance and the associated threshold that would be applicable at nodes for a fault with the aforementioned resistance value. This information could then be used to "set" the system and establish the limits of its applicability by a developed software. Based on the simplified 2-bus model, Chapter 6 can automatically evaluate the capability of the scheme and set threshold of the scheme based on requirements for different networks.

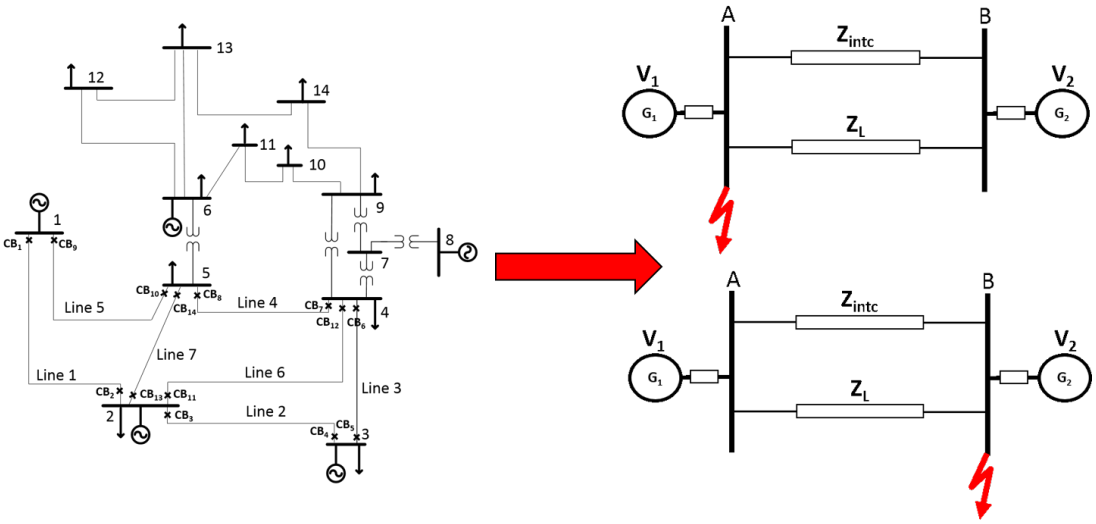

Figure 5.1: simplification from full model to 2-bus model

5.2 Simplified equivalent system model – single-phase to earth fault

In order to ascertain the highest detectable fault resistance for different scenarios and/or to determine the appropriate setting of voltage thresholds for fault identification, a 2-bus simplified equivalent model derived from the system under study has been developed, as shown in Figure 5.2.

The 2-bus equivalent model has been developed to simplify the process of ascertaining the highest detectable fault resistance. Rather than running hundreds of simulations using a full power system model, the 2-bus equivalent model, in conjunction with the configuration identification software, can directly calculate the limits of applicability of the system, via a much faster and simpler process.

Since the structure of transmission networks is typically meshed, the equivalent model adds an "interconnected" line (with impedance of Z_{intc}) to represent the many paths that will be connected in parallel (in an actual interconnected system) using the line L (with impedance of Z_L) that is directly connected between the nodes. line L is the actual line in the network, and its impedance and sequence components are assumed to be known in practice.

For any specific line within a network, the parameters of the equivalent 2-bus

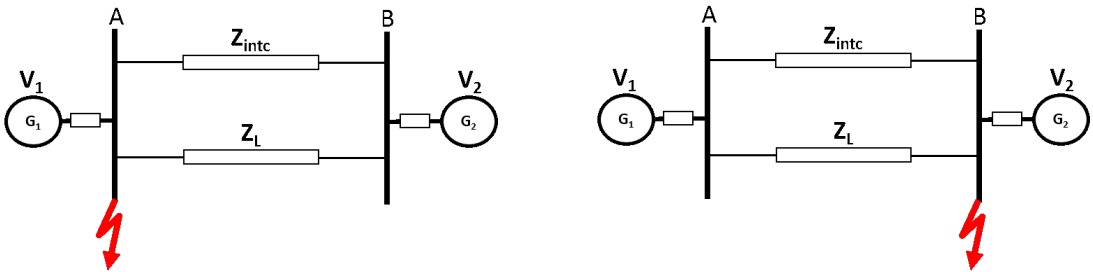

(a) Fault occurs at A

(b) Fault occurs at B

Figure 5.2: Single line diagram of simplified equivalent 2-bus model for system

model can be calculated using data from fault level studies (by simulating solid faults at each terminal of the line respectively, using the full model). Figure 5.2 shows this, but for the reduced model, where the "interconnected" line represents the impedance between the two paths via the alternative parallel routes through the interconnected network.

Solid single-phase to earth faults at each terminal of the line are applied to the full model respectively to calculate parameters of the 2-bus equivalent circuits, because in this situation all positive, negative and zero sequence components are included as shown in Figure 5.3. (a) and (b) in Figure 5.3 are corresponding to situations of (a) and (b) in Figure 5.2. As the parameters of the system will not change with variation of fault types, all positive, negative and zero sequence parameters of the system can be calculated.

5.2.1 Parameter introduction

For both (a) and (b) of Figure 5.3, from top to bottom, the circuits are positive, negative and zero sequence respectively. N0, N1, N2 are the neutral points of zero sequence, positive sequence and negative sequence circuits (the voltage magnitudes at neutral points are zero).

The following are the parameters that do not change with variation of fault locations on line L:

- V_1 and V_2 are the source voltage without source impedances.
- Z_{s1_1} and Z_{s1_2} are the positive sequence source impedances of G_1 and G_2

respectively. Similarly, Z_{s2_1} and Z_{s2_2} are the negative sequence source impedances and Z_{s0_1} and Z_{s0_2} are the zero sequence source impedances of G_1 and G_2 respectively.

- Z_{L1}, Z_{L2} and Z_{L0} are the positive sequence, negative sequence and zero sequence impedance of line L.
- R_f is the fault resistance. As for both scenarios, solid fault is applied, R_f is 0 when calculating equivalent circuit parameters.

For a scenario where a fault occurs at node A (as shown in (a) of Figure 5.3) – scenario 1:

- V_{1_1} and V_{2_1} are the calculated internal source voltages without impact of source impedance.
- V_{A1_1} and V_{B1_1} are the positive sequence source voltage including source impedances of node A and B (Z_{s1_1} and Z_{s1_2}) respectively, which can be measured directly from system full model. Similarly, V_{A2_1} and V_{B2_1} are the negative sequence source voltage and V_{A0_1} and V_{B0_1} are the zero sequence source voltage of node A and B respectively.
- Z_{intc1_1}, Z_{intc2_1} and Z_{intc0_1} are the positive sequence, negative sequence and zero sequence impedance of the "interconnected line" which is an equivalent of the interconnection between node A and B.
- V_{L1_1}, V_{L2_1} and V_{L0_1} are the positive sequence, negative sequence and zero sequence voltage drop of line L or the "interconnected line" as shown in Figure 5.3.
- I_{f1_1}, I_{f2_1} and I_{f0_1} are the positive sequence, negative sequence and zero sequence total fault current at the fault location (node A in this scenario).
- I_{L1_1}, I_{L2_1} and I_{L0_1} are the positive sequence, negative sequence and zero sequence current flowing through line L towards fault.
- I_{2f_1} is the positive sequence current flow from G_2 towards fault.

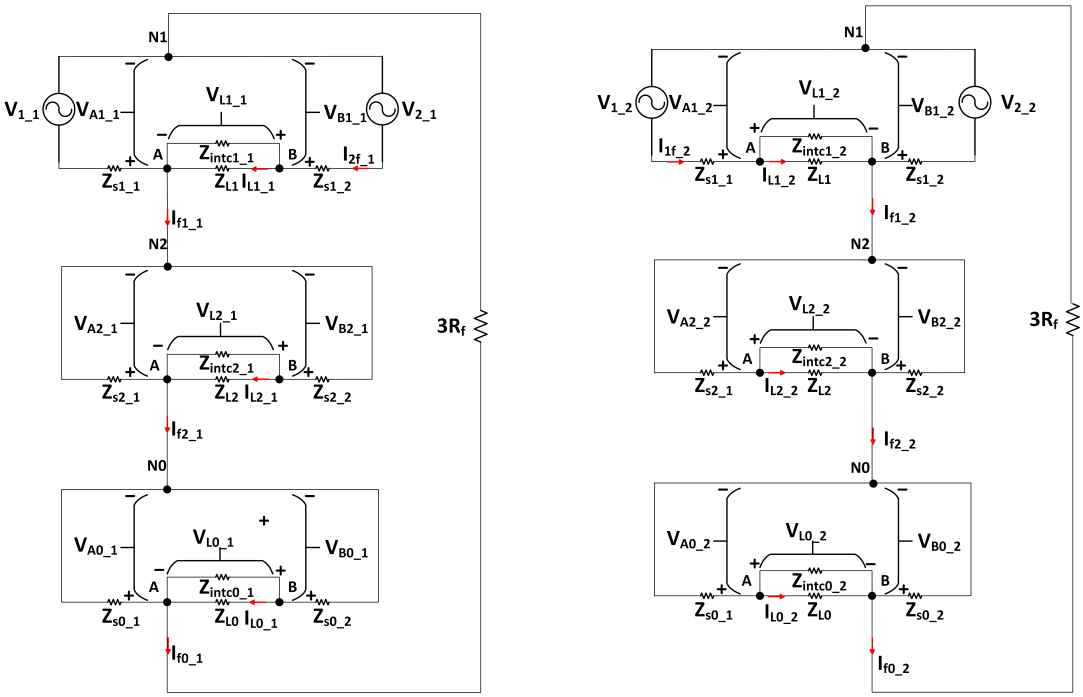

(a) Fault occurs at A (b) Fault occurs at B

Figure 5.3: Sequence components of single-phase to earth fault

Similarly, for the scenario that fault happens at node B (as shown in (b) of Figure 5.3) – scenario 2:

- V_{1_1} and V_{2_1} are the calculated internal source voltages without impact of source impedance.
- V_{A1_2} and V_{B1_2} are the positive sequence source voltage including source impedances of node A and B (Z_{s1_1} and Z_{s1_2}) respectively, which can be measured directly from system full model. Similarly, V_{A2_2} and V_{B2_2} are the negative sequence source voltage and V_{A0_2} and V_{B0_2} are the zero sequence source voltage of node A and B respectively.
- Z_{intc1_2}, Z_{intc2_2} and Z_{intc0_2} are the positive sequence, negative sequence and zero sequence impedance of the "interconnected line" which is an equivalent of the interconnection between node A and B.
- V_{L1_2}, V_{L2_2} and V_{L0_2} are the positive sequence, negative sequence and zero sequence voltage drop of line L or the "interconnected line" as shown in Figure 5.3.

- I_{f1_2}, I_{f2_2} and I_{f0_2} are the positive sequence, negative sequence and zero sequence total fault current at the fault location (node A in this scenario).
- I_{L1_2}, I_{L2_2} and I_{L0_2} are the positive sequence, negative sequence and zero sequence current flowing through line L towards fault.
- I_{1f_2} is the positive sequence current flow from G_1 towards fault.

5.2.2 Calculation of equivalent model parameters

As the sequence component circuits are connected in series when a single-phase to earth fault is applied (for both scenarios), the total fault current for sequence components are the same ($I_{f1\_1} = I_{f2\_1} = I_{f0\_1}$; $I_{f1\_2} = I_{f2\_2} = I_{f0\_2}$).

In order to calculate the parameters of the 2-bus equivalent model, the following parameters are needed to be measured/calculated in the full model:

1. Fault current flowing through line L towards the fault: I_{L1_1}, I_{L2_1} and I_{L0_1} for scenario 1 and I_{L1_2}, I_{L2_2} and I_{L0_2} for scenario 2.
2. Voltage magnitudes at node A and node B (source magnitudes with consideration of source impedance): V_{A1_1}, V_{B1_1}, V_{A2_1}, V_{B2_1}, V_{A0_1} and V_{B0_1} for scenario 1. V_{A1_2}, V_{B1_2}, V_{A2_2}, V_{B2_2}, V_{A0_2} and V_{B0_2} for scenario 2.
3. Total fault current at fault location: I_{f1_1}, I_{f2_1} and I_{f0_1} for scenario 1 and I_{f1_2}, I_{f2_2} and I_{f0_2} for scenario 2.

If sequence components can be directly measured from the system, then no extra steps are required. Otherwise, phase values can be measured from the system and sequence components can be calculated based on phase values, which is explained in Section 2.3 in detail.

With the values measured/ calculated above, the followings are the target parameters that require to be identified for the 2-bus equivalent model:

1. Voltage source internal impedance: Z_{s1_1}, Z_{s1_2}, Z_{s2_1}, Z_{s2_2}, Z_{s0_1} and Z_{s0_2}.

2. Impedance of the "interconnected line": Z_{intc1_1}, Z_{intc2_1}, Z_{intc0_1}, Z_{intc1_2}, Z_{intc2_2} and Z_{intc0_2}.

3. Source voltage magnitudes without internal source impedance: V_1 and V_2.

There are a number of intermediate parameters are used in the process of calculation, but they do not need to be output to the user or used in the final calculations of the system. Intermediate parameters include the voltage drop of line L or the "interconnected line" (as shown in Figure 5.3); the current flow from G_2 to fault (I_{2f_1}) in scenario 1 and the current flow from G_1 to fault (I_{1f_2}) in scenario 2.

All parameters in the system (both measured and calculated) are phasors, which include both magnitudes and angles.

5.2.2.1 Negative sequence parameter calculation

To calculate negative sequence parameters of the 2-bus equivalent circuit, Equation (5.1) is created based on Kirchhoff's Voltage Law (KVL); Equation (5.2) is created based on Kirchhoff's Current Law and (KCL) and Equation (5.3) is based on KCL and Ohm's law. Equation (5.1) is to represent intermediate quantity V_{L2_1} and V_{L2_2} by other quantities (either are the known ones or the ones remain to be solved). Z_{s2_1} and Z_{s2_2} can be calculated by Equation (5.1) and Equation (5.2). Z_{intc2_1} and Z_{intc2_2} can be calculated by equation Equation (5.1) and Equation (5.3).

$$\begin{cases} V_{L2\_1} = I_{L2\_1} \times Z_{L2} \\ V_{L2\_2} = I_{L2\_2} \times Z_{L2} \end{cases} \tag{5.1}$$

$$\begin{cases} -I_{f2\_1} = V_{A2\_1}/Z_{s2\_1} + (V_{A2\_1} + V_{L2\_1})/Z_{s2\_2} \\ -I_{f2\_2} = V_{B2\_2}/Z_{s2\_2} + (V_{B2\_2} + V_{L2\_2})/Z_{s2\_1} \end{cases} \tag{5.2}$$

$$\begin{cases} Z_{intc2\_1} = V_{L2\_1}/(-(V_{A2\_1} + V_{L2_1})/Z_{s2\_2} - I_{L2\_1}) \\ Z_{intc2\_2} = V_{L2\_2}/(-(V_{B2\_2} + V_{L2_2})/Z_{s2\_1} - I_{L2\_2}) \end{cases} \tag{5.3}$$

5.2.2.2 Zero sequence network parameter calculation

As with the process for negative sequence, to calculate zero sequence parameters of the 2-bus equivalent circuit, Equation (5.4) is created based on Kirchhoff's Voltage Law (KVL); Equation (5.5) is created based on Kirchhoff's Current Law (KCL) and Equation (5.6) is based on KCL and Ohm's law.

Equation (5.4) is to represent intermediate quantity V_{L0_1} and V_{L0_2} by other quantities (either are the known ones or the ones remain to be solved). Z_{s0_1} and Z_{s0_2} can be calculated by Equation (5.4) and Equation (5.5). Z_{intc0_1} and Z_{intc0_2} can be calculated by Equation (5.4) and Equation (5.6).

$$\begin{cases} V_{L0\_1} = I_{L0\_1} \times Z_{L0} \\ V_{L0\_2} = I_{L0\_2} \times Z_{L0} \end{cases} \tag{5.4}$$

$$\begin{cases} -I_{f0\_1} = V_{A0\_1}/Z_{s0\_1} + (V_{A0\_1} + V_{L0\_1})/Z_{s0\_2} \\ -I_{f0\_2} = V_{B0\_2}/Z_{s0\_2} + (V_{B0\_2} + V_{L0\_2})/Z_{s0\_1} \end{cases} \tag{5.5}$$

$$\begin{cases} Z_{intc0\_1} = V_{L0\_1}/(-(V_{A0\_1} + V_{L0\_1})/Z_{s0\_2} - I_{L0\_1}) \\ Z_{intc0\_2} = V_{L0\_2}/(-(V_{B0\_2} + V_{L0\_2})/Z_{s0\_1} - I_{L0\_2}) \end{cases} \tag{5.6}$$

As the assumed equivalent circuit ignores shunt elements such as line capacitances (line capacitances are relatively small and the impact of capacitance on the scheme is minimal and can be neglected), the calculated impedance of the "interconnected line" based on scenario 1 and scenario 2 (Z_{intc2_1} and Z_{intc2_2} for negative sequence; Z_{intc0_1} and Z_{intc0_2} for zero sequence) may have slightly different values compared to the actual situation based on a full network model. However, it has been determined that the difference in practical situations is not significant (less than 0.18% for IEEE 14-bus system), and therefore, will not impact on the overall capability and performance of the scheme. This will be highlighted in the case studies presented later in Section 7.2.2.

For the validation of the scheme, Z_{intc2} (negative sequence impedance of the "interconnected line") and Z_{intc0} (zero sequence impedance of the "interconnected

line") are therefore taken as an average of the value calculated in scenario 1 and scenario 2 to minimise the error introduced by any limitations of the assumed equivalent circuit, as demonstrated in Equation (5.7).

$$\begin{cases} Z_{intc2} = (Z_{intc2\_1} + Z_{intc2\_2})/2 \\ Z_{intc0} = (Z_{intc0\_1} + Z_{intc0\_2})/2 \end{cases} \tag{5.7}$$

5.2.2.3 Positive sequence parameters calculation

For the calculation of positive sequence parameters, line impedances and source impedances are the same as the negative sequence values as outlined in Section 2.3 and they are presented in Equation (5.8).

$$\begin{cases} Z_{s1\_1} = Z_{s2\_1} \\ Z_{s1\_2} = Z_{s2\_2} \\ Z_{intc1} = Z_{intc2} \\ Z_{L1} = Z_{L2} \end{cases} \tag{5.8}$$

The internal source voltage (without source impedance) can be calculated for the positive sequence circuit. As with the calculation of the impedance of the "interconnected line", shunt and neglecting elements such as line capacitances in the equivalent circuit, the calculated internal source voltages without source impedance - based on scenario 1 and scenario 2 (V_{1_1} and V_{2_1} under scenario 1 and V_{1_2} and V_{2_2} under scenario 2) - may have slightly different values compared to the actual situation using a full network model. However, it has been determined that the difference in practical situations is not significant (less than 0.18% for IEEE 14-bus system), and therefore, will not have a significant impact on the overall capability and performance of the scheme. This will be highlighted in the case studies presented later in Section 7.2.2. To minimise the error introduced by any limitations of the assumed equivalent circuit, V_1 and V_2 are taken as an average of the value calculated in scenario 1 and scenario 2, as shown in Equation (5.13).

For scenario 1, as shown in Equation (5.9), intermediate quantity I_{2f_1} is represented using the known quantity I_{L1_1} and calculated quantities Z_{intc1} and Z_{L1} based on Kirchhoff's Current Law (KCL).

$$I_{2f\_1} = I_{L1\_1}/Z_{intc1} \times (Z_{L1} + Z_{intc1}) \tag{5.9}$$

Internal source voltages without source impedance (V_{1_1} and V_{2_1}) can be calculated using Equation (5.10), which is created based on Kirchhoff's Voltage Law (KVL) and Ohm's law.

$$\begin{cases} V_{2\_1} = V_{A1\_1} + I_{2f\_1} \times Z_{s1\_2} + I_{L1\_1} \times Z_{L1} \\ V_{1\_1} = V_{A1\_1} + Z_{s1\_1} \times (I_{f1\_1} - I_{2f\_1}) \end{cases} \tag{5.10}$$

For scenario 2, as shown in Equation (5.11), the intermediate quantity I_{1f_2} is represented using the known quantity I_{L1_2} and calculated quantities Z_{intc1} and Z_{L1} based on Kirchhoff's Current Law (KCL).

$$I_{1f\_2} = I_{L1\_2}/Z_{intc1} \times (Z_{L1} + Z_{intc1}) \tag{5.11}$$

Internal source voltages without source impedance (V_{1_1} and V_{2_1}) can be calculated using Equation (5.12), which is created based on Kirchhoff's Voltage Law (KVL) and Ohm's law.

$$\begin{cases} V_{1\_2} = V_{B1\_2} + I_{1f\_2} \times Z_{s1\_1} + I_{L1\_2} \times Z_{L1} \\ V_{2\_2} = V_{B1\_2} + Z_{s1\_2} \times (I_{f1\_2} - I_{1f\_2}) \end{cases} \tag{5.12}$$

$$\begin{cases} V_1 = (V_{1\_1} + V_{1\_2})/2 \\ V_2 = (V_{1\_2} + V_{2\_2})/2 \end{cases} \tag{5.13}$$

5.2.3 Method demonstration

As the example shown in Figure 5.1, the IEEE 14-bus network is simplified to the equivalent 2-bus network in order to evaluate the capability of the scheme.

Positive (and negative) sequence (Ω) Angles are in radians			
Line	Z_{s1_1}	Z_{s1_2}	Z_{intc1}
1	11.01 ∠1.47	28.38 ∠1.44	70.27 ∠1.27
Zero sequence (Ω) Angles are in radians			
Line	Z_{s0_1}	Z_{s0_2}	Z_{intc0}
1	6.95 ∠1.47	30.44 ∠1.44	182.61 ∠1.30

Table 5.1: Calculated parameters for 2-bus equivalent circuits

To demonstrate, the equivalent circuit parameters of Line 1 is presented in Table 5.1. The simplification method is proposed to automatically calculate the system parameters (pure mathematical calculation rather than simulations) with minimum effort.

5.3 Summary

This chapter has presented a methodology for simplifying a full model network model down to a 2-bus equivalent model and explained the methods used to calculate parameters of the equivalent model. The focus of this chapter has been to thoroughly analyse the sequence component circuits of the 2-bus equivalent model with fault level information and measured voltages of nodes directly connected to the protected line by applying a solid single-phase to earth fault at each line terminal in the system full model. It has been shown that positive, negative and zero sequence impedances of all elements and the voltages that the two ideal voltage sources provide to the 2-bus equivalent circuit can be identified using only one scenario. These parameters are fixed with variation of fault locations and resistance. Therefore, they are very important both in evaluation of the capability of the scheme and in determination of the configuration of the scheme. The calculations within the methodology are performed automatically in the system, enhancing the practicality of the developed system.

Chapter 6

Detailed evaluation and quantification of scheme capabilities

6.1 Overview

A method of evaluating the capabilities of the scheme is proposed in this chapter to show how the settings of the scheme may be determined. Since the scheme consists of three main parts which can be used to identify different types of fault (three-phase fault, unbalanced earth fault and phase-phase fault) using sequence components, the developed package for configuration setting is composed of three corresponding parts (settings determination for positive sequence, negative sequence and zero voltage magnitudes).

The proposed method aims to automatically evaluate the scheme capability and determine the setting of the scheme (by mathematical calculation rather than simulations) with minimum effort based on the simplified equivalent network.

The worst-case scenario with respect to fault detection is when a fault is at a location on a line which results in the lowest terminal voltage depression for a fixed fault resistance (i.e. the highest magnitude of "retained voltage" at a terminal). In order to find the highest detectable fault resistance for a

predetermined voltage threshold, the worst-case fault position on the line must be identified, which results in the minimum sequence component voltage change at the line end (different sequence components for different type of fault). If, under the worst-case scenario, the voltage caused by a fault resistance results in the voltage magnitude (of at least one of the nodes directly connected to the faulted line) falling below/above threshold (below for three-phase fault and above for other types of fault which are explained in Section 4.2), then the corresponding fault resistance is considered detectable.

For the proposed scheme, a fault is deemed to exist if the voltage of at least one of the two nodes connected to the faulted line is below/above a threshold (below a threshold for three-phase fault and above a threshold for other types of fault as discussed in Section 4.2). In order to find the highest detectable resistive fault for a given network, a method for automatically identifying this worst case and highest detectable fault resistance has been developed. This information can be used to specify the voltage thresholds for a given maximum fault resistance, or conversely to specify the maximum fault resistance that could be detected for a predetermined voltage threshold. For all scenario calculations, known values for various system parameters are used as discussed in Chapter 5 and operation is demonstrated using case studies in Section 7.2.2. The unknown variables are the sequence voltages – positive sequence for three-phase faults; negative sequence for phase-phase faults and zero sequence for unbalanced earth faults. All other variables are intermediate variables which can be calculated from known quantities and used to evaluate unknown variables.

6.2 Three-phase faults

6.2.1 Circuit transformation

As discussed in Section 4.2, the voltage magnitude of at least one end of a faulted line needs must be below a predetermined threshold. To find the fault location that results in the smallest voltage depression (i.e. highest retained voltage) for

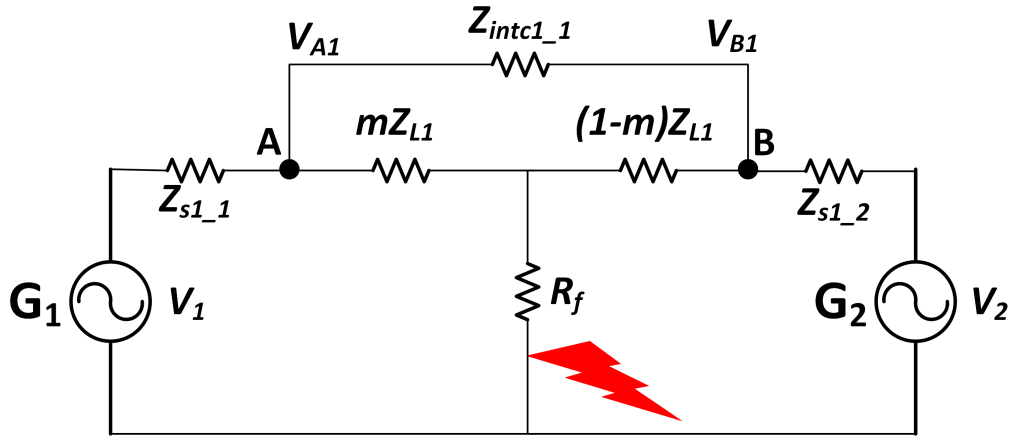

(a) Original circuit

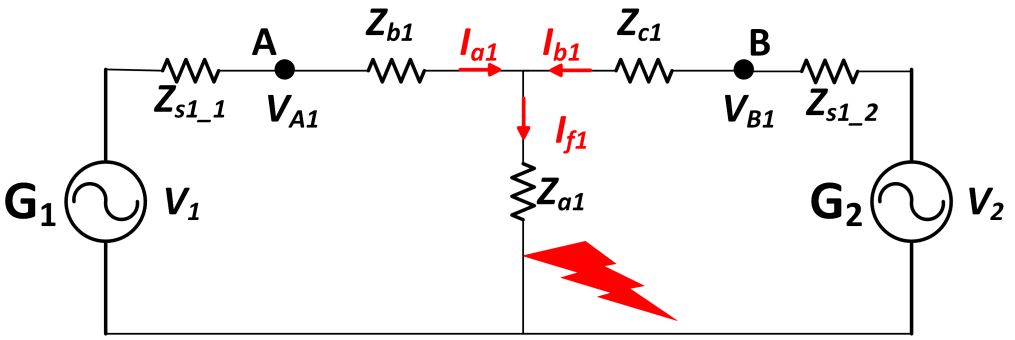

(b) After transformation

Figure 6.1: Equivalent circuit with variable fault location and fault impedance on the specific line

a specific line "during fault" is crucial, as this is one of the most important steps in the process, and the information can be used to determine the setting for the scheme and to identify the practical limitations of the scheme in terms of identifying faults (with high resistance).

A delta star transformation is applied to the simplified model as shown in Figure 6.1 to enable simple calculation of V_{A1} and V_{B1} as a function of the relative fault position along the line, m, which has a value of between 0 and 1. The impedances of the equivalent system were derived from simulation as described in Section 5.2.

According to the delta-star transformation, Z_{a1}, Z_{b1} and Z_{c1} are represented by m, Z_{L1} and Z_{intc1} as shown in Equation 6.1.

$$\begin{cases} Z_{a1} = (1-m)m{Z_{L1}}^2/(Z_{intc1}+Z_{L1}) + R_f \\ Z_{b1} = mZ_{intc1}Z_{L1}/(Z_{intc1}+Z_{L1}) \\ Z_{c1} = (1-m)Z_{intc1}Z_{L1}/(Z_{intc1}+Z_{L1}) \end{cases} \tag{6.1}$$

6.2.2 Variable calculation

$$\begin{cases} I_{a1\_v1} = V_1/((Z_{s1\_1}+Z_{b1})+Z_{a1}//(Z_{c1}+Z_{s1\_2})) \\ I_{b1\_v1} = I_{a1\_v1} \times Z_{a1}/(Z_{a1}+Z_{c1}+Z_{s1\_2}) \\ I_{b2\_v2} = V_2/((Z_{s1\_2}+Z_{c1})+Z_{a1}//(Z_{b1}+Z_{s1\_1})) \\ I_{a1\_v2} = I_{b1\_v2} \times (Z_{a1}/(Z_{a1}+Z_{b1}+Z_{s1\_1})) \\ I_{a1} = I_{a1\_v1} - I_{a1\_v2} \\ I_{b1} = I_{b1\_v2} - I_{b1\_v1} \\ V_{A1} = V_1 - I_{a1} \times Z_{s1\_1} \\ V_{B1} = V_2 - I_{b1} \times Z_{s1\_2} \end{cases} \tag{6.2}$$

Using superposition theory, as depicted in Figure 6.2, the calculations shown in Equation 6.2 can be derived using KCL, KVL and Ohm's Law. Z_{s1_1} and Z_{s1_2} are the internal impedances of the equivalent sources. V_1 and V_2 are the phase voltages of the equivalent sources (without internal impedances) at the line ends. V_{A1_v1} (V_{B1_v1}) and V_{A2_v2} (V_{B2_v2}) represent the voltages with incorporation of the equivalent sources close to nodes A and B respectively. V_{A1} and V_{B1} represent voltages at A and B respectively when both sources are connected, in accordance with superposition theory. I_{a1_v1} (I_{b1_v1}) and I_{a2_v1} (I_{b2_v1}) represent the currents with incorporation of the equivalent sources close to nodes A and B respectively. I_{a1} and I_{b1} represent the total fault currents contributed from nodes A and B respectively. Z_{a1}, Z_{b1} and Z_{c1} are the impedances calculated from Equation 6.1.

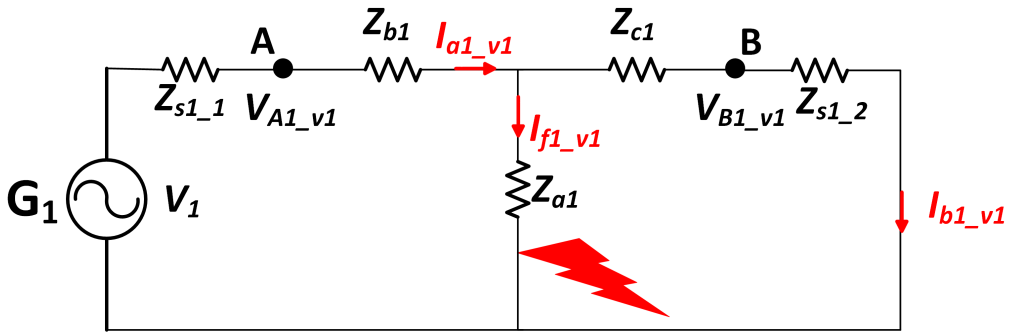

(a) With source close to A only

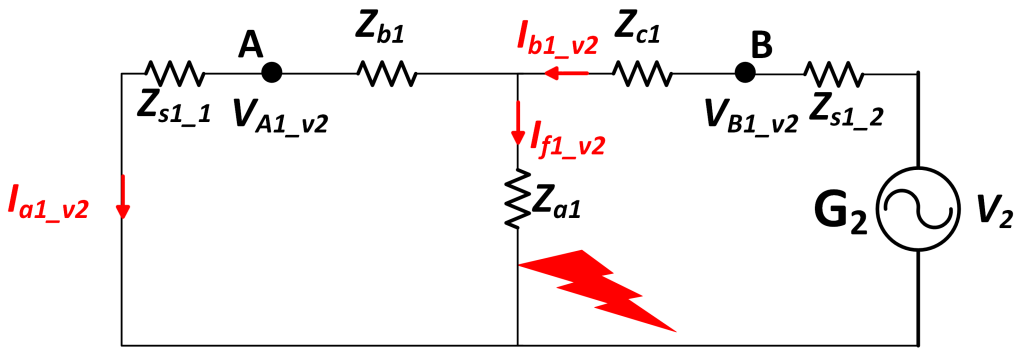

(b) With source close to B only

Figure 6.2: Application of Superposition theory of electric circuit

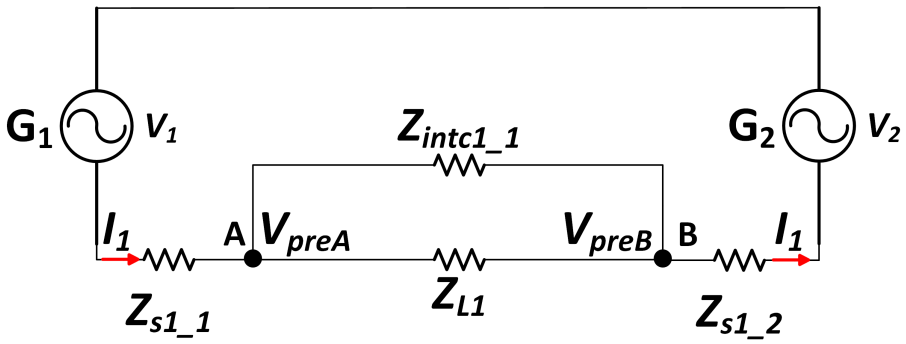

Figure 6.3: Line diagram to determine pre-fault positive node voltages

The method for determining pre-fault positive sequence voltage magnitudes at nodes A and B for the 2-bus equivalent circuit is presented via Equation 6.3 and uses KVL (the line diagram is shown in Figure 6.3), and is used to calculate k_1 as discussed in Section 4.2. I_1 is the pre-fault current from G_1 to G_2.

$$\begin{cases} I_1 = (V_1 - V_2)/(Z_{s1\_1} + Z_{L1}//Z_{intc1\_1} + Z_{s1\_2}) \\ V_{preA} = V_1 - I_1 \times Z_{s1\_1} \\ V_{preB} = V_2 + I_1 \times Z_{s1\_2} \end{cases} \tag{6.3}$$

6.2.3 Establishing threshold settings and capabilities of the scheme

The voltage thresholds (e.g. depressions in positive sequence voltages, increases in negative and/or zero sequence voltages) that are used within the scheme to detect the occurrence of a fault (and initiate operation of the scheme) can be established through one of the following methods:

- Based on engineering judgement/historical experience, voltage thresholds that are deemed to be indicative of faults, could be selected (e.g. later in this dissertation, thresholds of 85% and 2% for sequence voltages are described);
- Alternatively, a target maximum fault resistance could be selected (e.g. 50 Ω) and the associated voltage thresholds calculated that would ensure that

the system would identify all faults with a resistance up to this level.

The location of the fault and the line and source impedances are also factors that can act to influence the threshold setting.

The process of establishing the highest detectable fault resistance that the system can detect can therefore be driven with a "target" voltage threshold from the outset, or the maximum fault resistance to be detected can be fixed as a "target" and the associated voltage thresholds calculated

In order to find the worst-case fault location (worst case meaning the fault location on a line which would result in the minimum voltage depression being measured at one end of the line) as well as the highest detectable fault resistance/voltage thresholds for a given maximum fault resistance, four steps are included. As the calculations are based on the simple 2-bus equivalent circuit solved analytically in Section 5.2, the overall process is much simpler and faster compared to a simulation-based solution using a full power network model.

- Step 1: For a fixed line with a solid fault and m=0 (fault location on the line end at node A), V_{A1} and V_{B1} are calculated based on Equation 6.2 and the smaller value of k_{1A} and k_{1B} is chosen (k_{1A} and k_{1B} represent the ratios of "during fault" positive sequence voltage magnitudes to pre-fault positive sequence voltage magnitudes at nodes A and B respectively and are demonstrated in Equation 6.4, denoted as k_{1min}. The value of k_{1min} is recorded.

- Step 2: The value of m is increased from 0 to 1 incrementally in steps of 0.01 (i.e. the assumed fault location on the line moves from node A to node B) and step 1 is repeated. The maximum value of k_{1min} and the corresponding value of m are ascertained and these are recorded as the worst-case values.

- Step 2 is repeated with fault resistance increasing from 0 to a suitably high fault resistance value.

- Step 4a: If the target is to find the highest detectable fault resistance (R_{1max}) for a predetermined voltage threshold k_{1pre}, then the value of fault

Line	$R_{1fmax}(\Omega)$	m	Terminal at threshold
1	16.6	0	node A

Table 6.1: Highest three-phase fault resistance for Line 1

resistance corresponding to the scenario when k_{1min} is equal to the predetermined voltage threshold is determined, based on the results of step 3.

- Step 4b: If the target is to calculate the voltage thresholds for a given maximum fault resistance (R_{1pre}), then based on the results of step 3, the value of k_{1min} corresponding to the scenario when fault resistance is equal to the given maximum fault resistance must be determined. This voltage magnitude, denoted as k_{1Th}, represents the threshold which can be used to detect any fault with a resistance less than the specified maximum.

$$\begin{cases} k_{1A} = V_{A1}/V_{preA} \\ k_{1B} = V_{B1}/V_{preB} \end{cases} \tag{6.4}$$

To demonstrate, the capability (the highest detectable fault resistance with a 85% threshold) of the scheme for Line 1 in the IEEE 14-bus network as shown in Table 6.1. The highest detectable fault resistance on Line 1 is 16.6 Ω. The results of the case studies are explained in detail in Section 7.2.

6.3 Earth faults (unbalanced)

6.3.1 Single-phase to earth fault – scenario A

As discussed in Section 4.2.3, in order to detect unbalanced earth faults (single-phase to earth fault and phase-phase to earth fault), the zero sequence voltage magnitude measured at one end of the faulted line must be above the predetermined threshold – as demonstrated in Section 4.2.3. For a specific fault resistance, the fault location which results in the smallest "during fault" zero sequence voltage increase for a specific line must be established to inform the threshold setting.

6.3.1.1 Circuit transformation

Similarly, but slightly differently, for three-phase fault scenarios (the same method is used, but since the fault resistance has a different location in the circuit, the equations used are slightly different), a delta star transformation is applied to the equivalent model as shown in Figure 6.4 to enable simple calculation of V_{A0} and V_{B0} as a function of the relative fault position along the line, m, which has a value of between 0 and 1. According to the delta-star transformation, Z_{a1}, Z_{b1} and Z_{c1} are represented by m, Z_{L1} and Z_{intc1} as shown in Equation 6.5. Similarly, the transformation of negative sequence and zero sequence circuits are shown in Equation 6.6 and 6.6.

$$\begin{cases} Z_{a1} = (1-m)m{Z_{L1}}^2/(Z_{intc1}+Z_{L1}) \\ Z_{b1} = mZ_{intc1}Z_{L1}/(Z_{intc1}+Z_{L1}) \\ Z_{c1} = (1-m)Z_{intc1}Z_{L1}/(Z_{intc1}+Z_{L1}) \end{cases} \tag{6.5}$$

$$\begin{cases} Z_{a2} = (1-m)m{Z_{L2}}^2/(Z_{intc2}+Z_{L2}) \\ Z_{b2} = mZ_{intc2}Z_{L2}/(Z_{intc2}+Z_{L2}) \\ Z_{c2} = (1-m)Z_{intc2}Z_{L2}/(Z_{intc2}+Z_{L2}) \end{cases} \tag{6.6}$$

$$\begin{cases} Z_{a0} = (1-m)m{Z_{L0}}^2/(Z_{intc0}+Z_{L0}) \\ Z_{b0} = mZ_{intc0}Z_{L0}/(Z_{intc0}+Z_{L0}) \\ Z_{c0} = (1-m)Z_{intc0}Z_{L0}/(Z_{intc0}+Z_{L0}) \end{cases} \tag{6.7}$$

The impedances of the equivalent system were derived from simulation as described in Section 5.2.

6.3.1.2 Variable calculation

As shown in Figure 6.4 (b), in order to calculate V_{A0} and V_{B0} based on known system parameters (discussed in Section 5.2 and demonstrated by case studies in Section 7.2.2), since N0 is the neutral point (with a voltage of zero) I_{a0} and I_{b0}

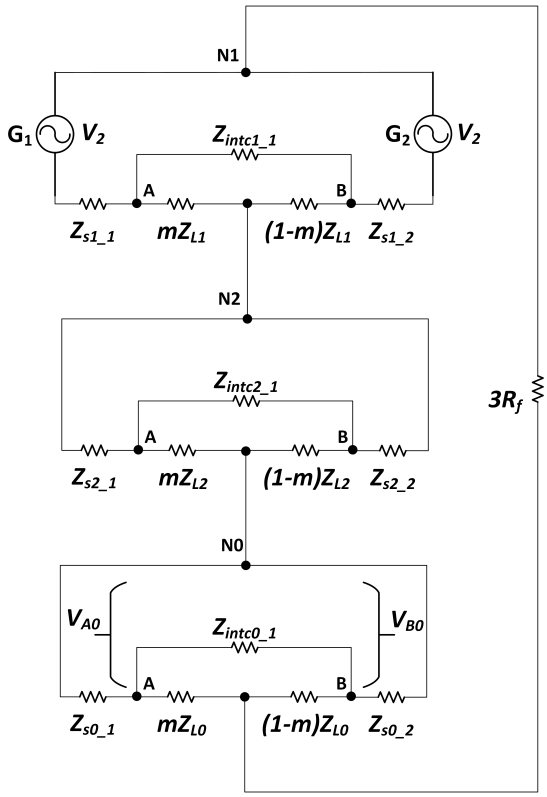

(a) Original circuit

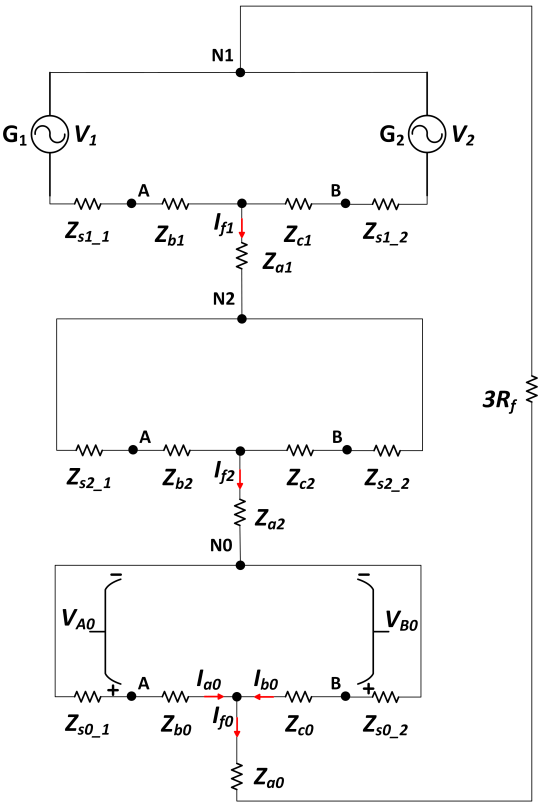

(b) Circuit after the delta-star transformation has been applied

Figure 6.4: Equivalent circuit for single-phase to earth fault with variable fault location and fault impedance on the specific line

must be calculated as shown in Equation 6.8 by KVL.

$$\begin{cases} V_{A0} = I_{a0} \times Z_{s0\_1} \\ V_{B0} = I_{b0} \times Z_{s0\_2} \end{cases} \tag{6.8}$$

To calculate I_{a0} and I_{b0}, I_{f0} (as sequence component circuits are in series, I_{f0} $= I_{f1} = I_{f2}$) needs to be calculated using Equation 6.9.

$$\begin{cases} I_{a0} = I_{f0} \times ((Z_{c0} + Z_{s0\_2})/(Z_{s0\_1} + Z_{c0} + Z_{b0} + Z_{s0\_2})) \\ I_{b0} = I_{f0} \times ((Z_{b0} + Z_{s0\_1})/(Z_{s0\_1} + Z_{c0} + Z_{b0} + Z_{s0\_2})) \end{cases} \tag{6.9}$$

To calculate I_{f0}, the circuit is simplified again as shown in Figure 6.5. Z_{v1} and Z_{v2} are the equivalent positive sequence impedances between the fault location and ideal sources G_1 and G_2 respectively. Z_2 and Z_0 are the equivalent impedances of the negative and zero sequence circuits. The equations used to calculate these quantities are shown in Equation 6.10.

$$\begin{cases} Z_{v1} = Z_{s1\_1} + Z_{b1} \\ Z_{v2} = Z_{s1\_2} + Z_{c1} \\ Z_2 = (Z_{s2\_1} + Z_{b2})//(Z_{s2\_2} + Z_{c2}) + Z_{a2} \\ Z_0 = (Z_{s0\_1} + Z_{b0})//(Z_{s0\_2} + Z_{c0}) + Z_{a0} \end{cases} \tag{6.10}$$

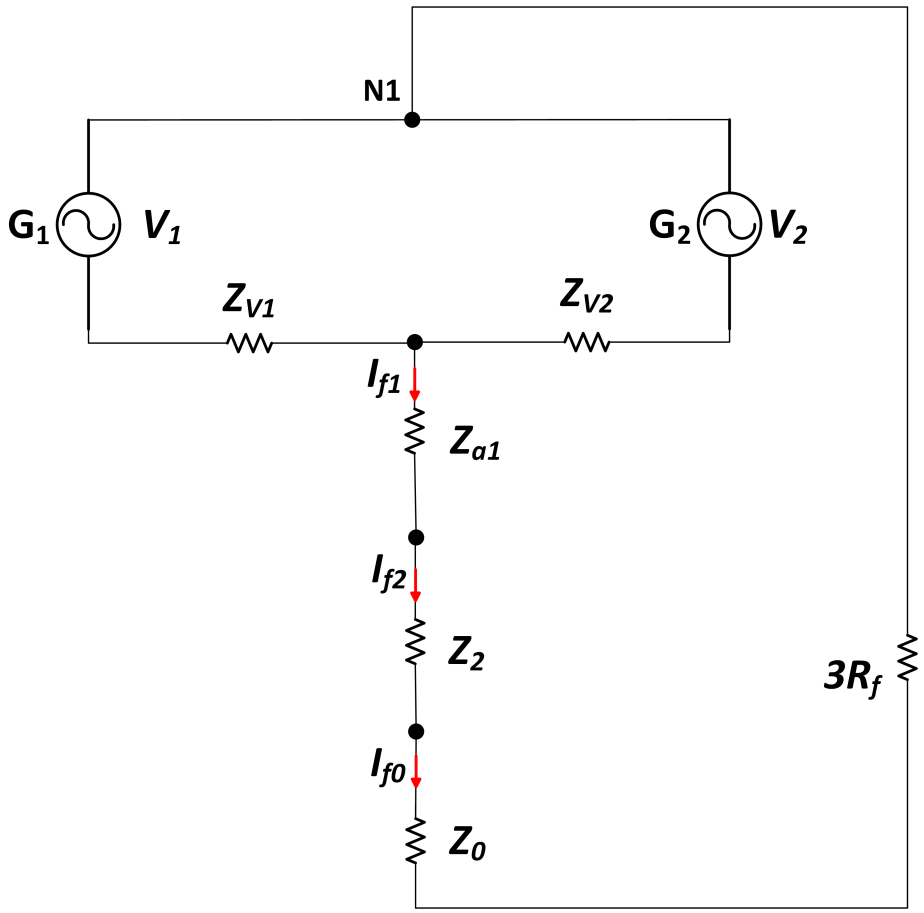

Figure 6.5: Further simplification of the circuit

Since V_1 and V_2 can be different, superposition theory is applied to calculate I_{f0}, as depicted in Figure 6.6. For scenario 1 ((a) of Figure 6.6), Z_{v2} is in parallel with (Z_{a1}+Z_2+Z_0+$3R_f$) and the total impedance of them is in series with Z_{v1}. For scenario 2 ((b) of Figure 6.6), Z_{v1} is in parallel with (Z_{a1}+Z_2+Z_0+$3R_f$) and the total impedance of them is in series with Z_{v2}. Based on the analysis of the circuit, Equation 6.11 can be derived by KCL, KVL and Ohm's Law to calculate I_{f0}.

V_1 and V_2 are the phase voltages of the equivalent sources (without internal impedances) at the line ends. I_{f0_v1} (I_{f0_v1} = I_{f1_v1}= I_{f2_v1}) and I_{f0_v2} (I_{f0_v2} = I_{f1_v2}= I_{f2_v2}) represent the zero/positive/negative sequence fault currents as supplied by the equivalent source G_1 and G_2 respectively.

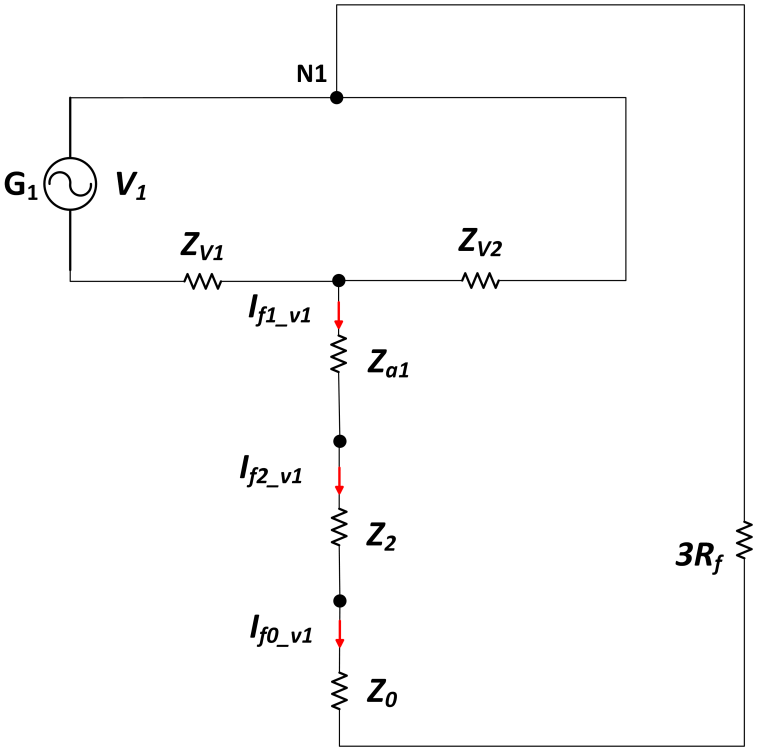

(a) With source G1 only

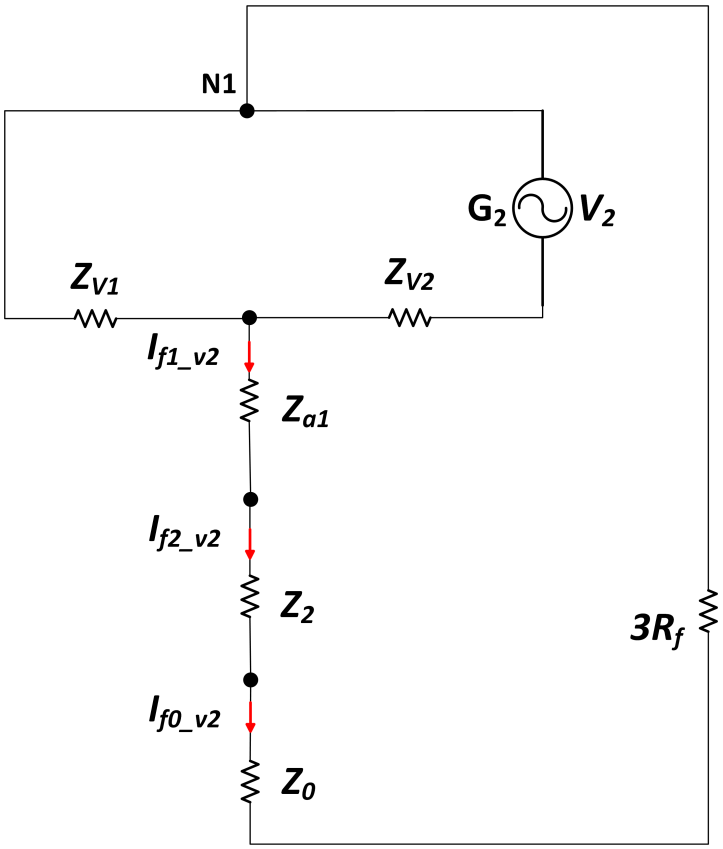

(b) With source G2 only

Figure 6.6: Application of Superposition theory of electric circuit

$$\begin{cases} a_{01} = Z_{v2}/(Z_{a1} + Z_2 + Z_0 + 3R_f + Z_{v2}) \\ b_{01} = Z_{v1}/(Z_{a1} + Z_2 + Z_0 + 3R_f + Z_{v1}) \\ I_{f0\_v1} = V_1/(Z_{v1} + Z_{v2}//(Z_{a1} + Z_2 + Z_0 + 3R_f)) \times a_{01} \\ I_{f0\_v2} = V_2/(Z_{v2} + Z_{v1}//(Z_{a1} + Z_2 + Z_0 + 3R_f)) \times b_{01} \\ I_{f0} = I_{f0\_v1} + I_{f0\_v2} \end{cases} \tag{6.11}$$

Using the calculated I_{f0} in conjunction with Equation 6.8 and Equation 6.9, V_{a0} and V_{b0} can be calculated using system parameters.

6.3.2 Phase-phase to earth fault – scenario B

6.3.2.1 Circuit transformation

As with single-phase to earth fault scenarios, a delta star transformation is applied to the equivalent model as shown in Figure 6.7 to enable simple calculation of V_{A0} and V_{B0} as a function of m (the relative fault position along the line), which has a value between 0 and 1 (from node A to node B).

According to the delta-star transformation, Z_{a1}, Z_{b1} and Z_{c1} are represented by m, Z_{L1} and Z_{intc1} as shown in Equation 6.12. Similarly, the transformations of the negative sequence and zero sequence circuits are shown in Equation 6.13 and Equation 6.14.

The impedances of the equivalent system were derived from simulation as described in Section 5.2.

$$\begin{cases} Z_{a1} = (1-m)m{Z_{L1}}^2/(Z_{intc1} + Z_{L1}) + R_f \\ Z_{b1} = mZ_{intc1}Z_{L1}/(Z_{intc1} + Z_{L1}) \\ Z_{c1} = (1-m)Z_{intc1}Z_{L1}/(Z_{intc1} + Z_{L1}) \end{cases} \tag{6.12}$$

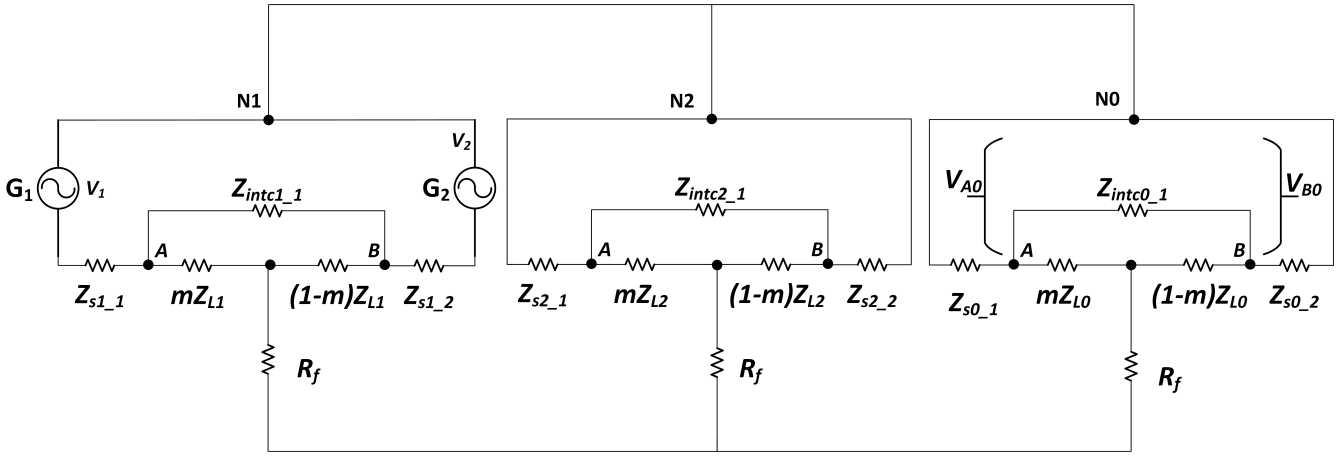

(a) Original circuit

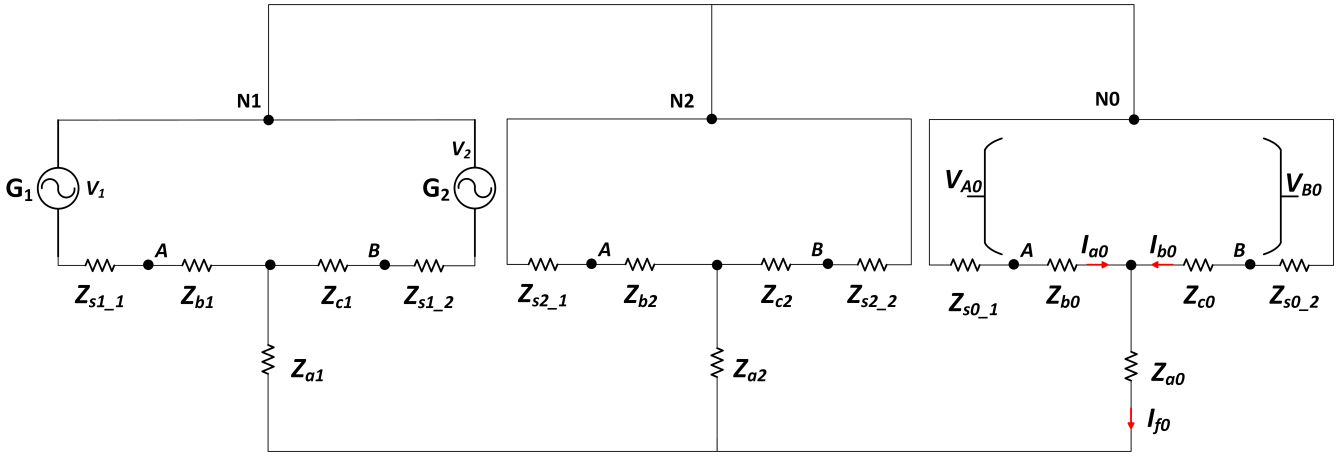

(b) After delta-star transformation

Figure 6.7: Equivalent circuit of phase-phase to earth fault with variable fault location and fault impedance on the specific line

$$\begin{cases} Z_{a2} = (1-m)m{Z_{L2}}^2/(Z_{intc2}+Z_{L2}) + R_f \\ Z_{b2} = mZ_{intc2}Z_{L2}/(Z_{intc2}+Z_{L2}) \\ Z_{c2} = (1-m)Z_{intc2}Z_{L2}/(Z_{intc2}+Z_{L2}) \end{cases} \tag{6.13}$$

$$\begin{cases} Z_{a0} = (1-m)m{Z_{L0}}^2/(Z_{intc0}+Z_{L0}) + R_f \\ Z_{b0} = mZ_{intc0}Z_{L0}/(Z_{intc0}+Z_{L0}) \\ Z_{c0} = (1-m)Z_{intc0}Z_{L0}/(Z_{intc0}+Z_{L0}) \end{cases} \tag{6.14}$$

6.3.2.2 Variable calculation

As shown in Figure 6.7 (b), and as for the single-phase to earth fault scenario, in order to calculate V_{A0} and V_{B0} based on known system parameters (discussed in Section 5.2 and demonstrated by case studies in Section 7.2), I_{a0} and I_{b0} must be calculated as shown in Equation 6.8 by KVL as discussed in Section 6.3.1.2. To calculate I_{a0} and I_{b0}, I_{f0} needs to be calculated because of equation 6.9 as discussed in 6.3.1.2.

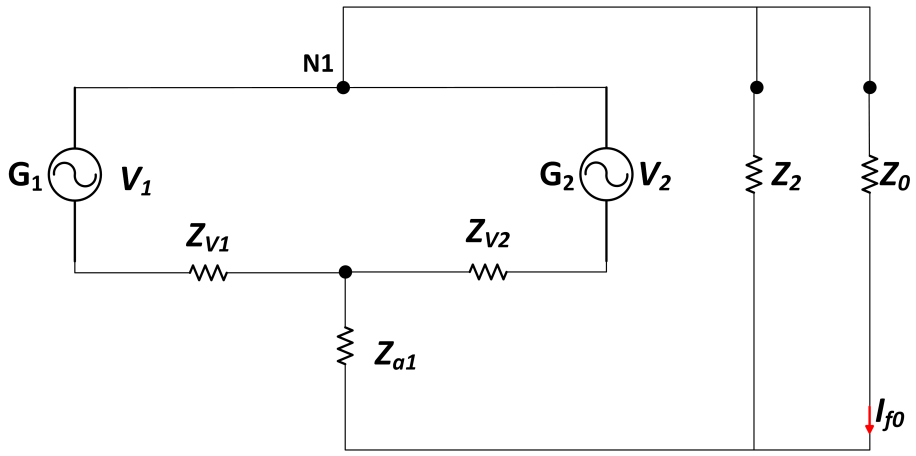

Figure 6.8: Further simplification of the circuit

To calculate I_{f0}, the circuit is simplified again as shown in Figure 6.9. Z_{v1} and Z_{v2} are the equivalent positive sequence impedances between fault location and sources G_1 and G_2 respectively. Z_2 and Z_0 are the equivalent impedances of the negative and zero sequence circuits. The equations used to calculate these quantities are presented in scenario A shown in Equation 6.10.

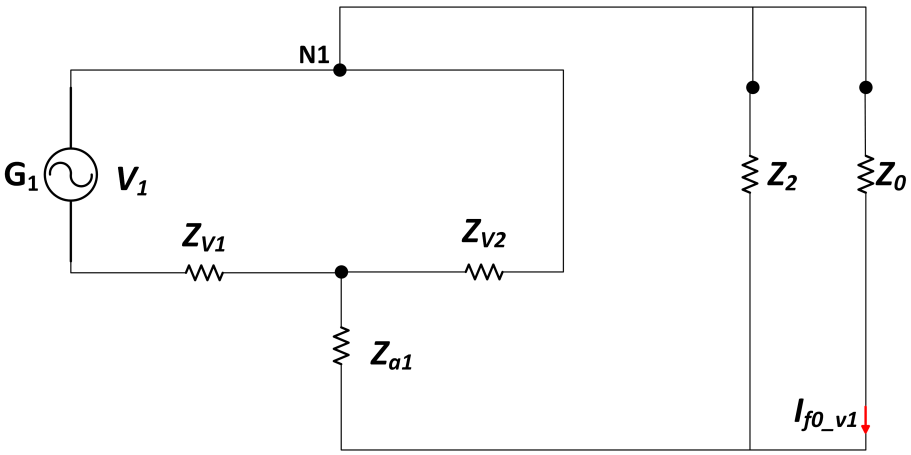

(a) With source G1 only

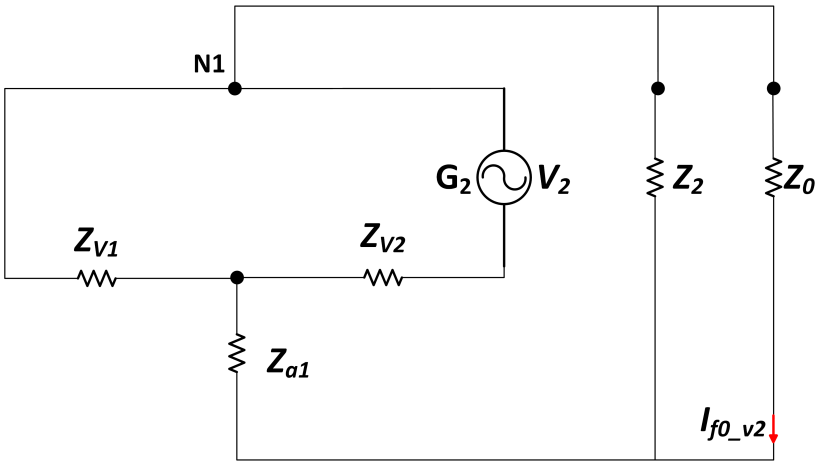

(b) With source G2 only

Figure 6.9: Application of Superposition theory of electric circuit

Superposition theory is applied to calculate I_{f0}, as depicted in Figure 6.9. For scenario 1 ((a) of Figure 6.9, Z_2 and Z_0 are in parallel and connected in series with Z_{a1}, of which Z_{v2} is in parallel with. The total impedance of them then is in series of Z_{v1}. the For scenario 2 ((b) of Figure 6.9), Z_2 and Z_0 are in parallel and in series with Z_{a1}, which Z_{v1} is in parallel with. The total impedance of them is connected serially with Z_{v2}. Based on the analysis of the circuit, Equation 6.15 can be derived by KCL, KVL and Ohm's Law to calculate I_{f0}.

$$\begin{cases} a_{02} = Z_{v2}/(Z_{v2} + Z_{a1} + Z_2//Z_0) \\ b_{02} = Z_{v1}/(Z_{v1} + Z_{a1} + Z_2//Z_0) \\ I_{f0\_v1} = V_1/(Z_{v1} + Z_{v2}//(Z_{a1} + Z_2//Z_0) \times a_{02} \times (Z_2/(Z_0 + Z_2)) \\ I_{f0\_v2} = V_2/(Z_{v2} + Z_{v1}//(Z_{a1} + Z_2//Z_0) \times b_{02} \times (Z_2/(Z_0 + Z_2)) \\ I_{f0} = I_{f0\_v1} + I_{f0\_v2} \end{cases} \tag{6.15}$$

V_1 and V_2 are the phase voltages of the equivalent sources (without internal impedances) at the line ends. I_{f0_v1} and I_{f0_v2} represent the zero sequence fault current supplied by sources G_1 and G_2 respectively.

Using the calculated I_{f0} in conjunction with Equation 6.8 and 6.9, V_{a0} and V_{b0} can be represented (calculated) with system parameters for this scenario.

6.3.3 Establishing threshold settings and capabilities of the scheme

For both single-phase to earth fault and phase-phase to earth fault scenarios (scenarios A and B), the formulas used to calculate zero sequence node voltages (V_{A0} and V_{B0}) using the system parameters (sequence impedances and ideal source voltage values) as calculated in Section 6.3.1.2 (for scenario A) or Section 6.3.2.2 (for scenario B), can be used to determine the worst-case scenario fault location as well as the highest detectable fault resistance/voltage thresholds for a given maximum fault resistance. This is identified using a six step process, similar to

that adopted for the three-phase fault scenario.

As two scenarios are included in this Section, to clarify the process, if a solid single-phase to earth fault is applied then all of the variables mentioned in the following four steps are from scenario A, e.g., VA_{01} and V_{B01} are the ones calculated from Section 6.3.1.

- Step 1: A single-phase to earth fault is applied (scenario A) on a fixed line (line L) at node A (m=0). V_{A01} and V_{B01} are calculated using the process outlined in Section 6.3.1 (for scenario A) and the larger value of k_{0A1} and k_{0B1} is selected (k_{0A1} and k_{0B1} represent for the difference between "during fault" and pre-fault zero sequence voltage magnitudes at node A and B respectively), denoted as k_{0max1}, and its value is recorded. In this case, the magnitude of V_{A01} (V_{B01}) is the same as the magnitude of k_{0A1} (k_{0B1}), as ideally (for calculation and analysis), when no fault is applied to the circuit, the pre-fault zero sequence voltage magnitudes at nodes A and B should both be zero. If the pre-fault zero sequence voltage magnitudes were not zero, since k_{0A1} and k_{0B1} are relative values, they would still be the same as in this ideal calculation, which means the calculated value of V_{A01} and V_{B01} in this scenario can always be used as k_{0A1} and k_{0B1}.

- Step 2: The value of m is increased from 0 to 1 incrementally in steps of 0.01 (i.e. the assumed fault location on the line moves from node A to node B) and step 1 is repeated. The minimum value of k_{0max1} and the corresponding value of m are ascertained and these are recorded as the worst-case values.

- Step 3: As for three-phase faults, step 2 is repeated with fault resistance increasing from 0 to a suitably high fault resistance value.

- Step 4a: Again, as with three-phase faults, the value of fault resistance corresponding to the scenario when k_{0max1} is equal to the predetermined voltage threshold (k_{0pre}) is determined to find the highest detectable k_{0pre}, based on the results of step 3, and is denoted as R_{0max1}.

- Step 4b: As with three-phase faults, based on results of step 3, the value

of k_{0max1} corresponding to the scenario when fault resistance is equal to the given maximum fault resistance (R_{0pre}) must be determined to specify the voltage thresholds for R_{0pre}. This voltage magnitude, denoted as k_{0Th1}, represents the threshold which can be used to detect any fault with a resistance less than the specified maximum.

- Step 5: A phase-phase to earth fault (scenario B) is applied on a fixed line (line L) at node A (m=0). V_{A02} and V_{B02} are calculated based on Section 6.3.2 (for scenario B) and steps 1 to 4 are repeated for scenario B.

- Step 6a: If the target is to find the highest detectable fault resistance (R_{0max}) for a predetermined voltage threshold (k_{0pre}), the smaller of the calculated fault resistance values for scenario A (R_{0max1}) and scenario B is selected as the highest detectable fault resistance (R_{0max2}).

- Step 6b: If the target is to specify the voltage thresholds (k_{0Th}) for a given maximum fault resistance (R_{0pre}), the smaller of the calculated voltage thresholds for scenario A (k_{0Th1}) and scenario B (k_{0Th2}) is chosen as the threshold (k_{0Th}).

  To clarify, even though the process of establishing threshold settings and capabilities of the scheme relates to both scenarios A and B, there is only one overall setting for the process. Therefore, if the target is to find the highest detectable fault resistance, k_{0pre} is used as the predetermined voltage threshold for calculation in both scenarios A and B. Similarly, if the target is to specify the voltage thresholds, R_{0pre} is used as the given maximum fault resistance for calculation in both scenarios A and B.

  To demonstrate, the capability (the highest detectable fault resistance with a 2% threshold) of the scheme for Line 1 in the IEEE 14-bus network as shown in Table 6.2. The highest detectable unbalanced earth fault resistance on Line 1 is 92.3 Ω. The results of the case studies are explaine in details in Section 7.2.

Line	$R_{0fmax}(\Omega)$	m	Terminal at threshold
1	92.3	0	node A

Table 6.2: Highest unbalanced earth fault resistance for Line 1

6.4 Phase-phase faults

6.4.1 Circuit transformation

As presented in Section 4.2.4, the negative sequence voltage magnitude of at least one end of the faulted line needs to be above the predetermined threshold to detect phase-phase faults. It is very important to find the fault location for a specific fault resistance, which results in the smallest negative sequence voltage increase for a specific line "during fault", as this is one of the steps for configuration setting.

Again, a delta star transformation is applied to the equivalent model as shown in Figure 6.10 to enable simple calculation of V_{A2} and V_{B2} as a function of the relative fault position along the line, m. The impedances of the equivalent system were derived from simulation as described in Section 5.2.

After transformation, it can be observed from Figure 6.10 that both positive and negative sequence impedance values (Z_{a1}, Z_{b1} and Z_{c1}) and (Z_{a2}, Z_{b2} and Z_{c2}) can be represented using the same way as outlined in scenario A for unbalanced earth faults and shown in Equation 6.5 and Equation 6.6.

6.4.2 Variable calculation

Since V_{A2} and V_{B2} are the quantities to be calculated for configuration determination based on known system parameters (discussed in Section 5.2 and demonstrated via case studies in Section 7.2), I_{a2} and I_{b2} must be calculated as shown in Equation 6.16 using KVL. The direction (relative direction with respect to some reference value) and value represented by I_{a2} and I_{b2} are shown in Figure 6.10.

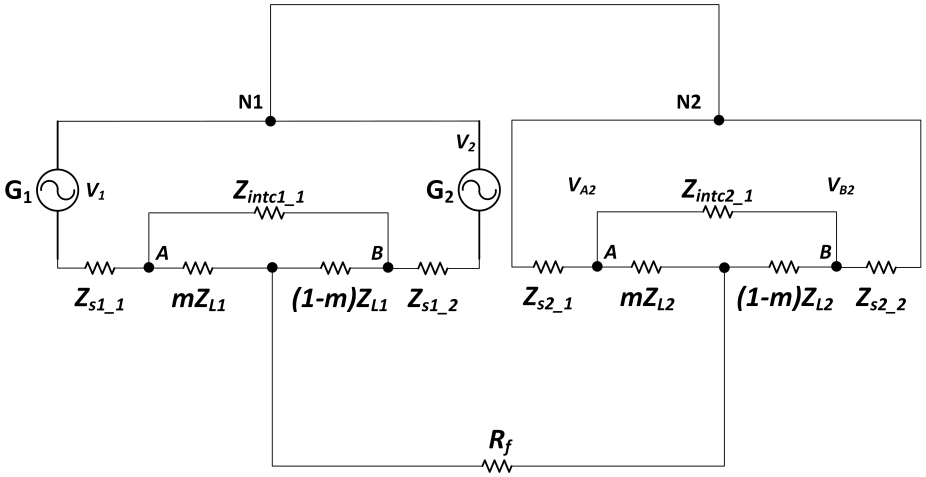

(a) Original circuit

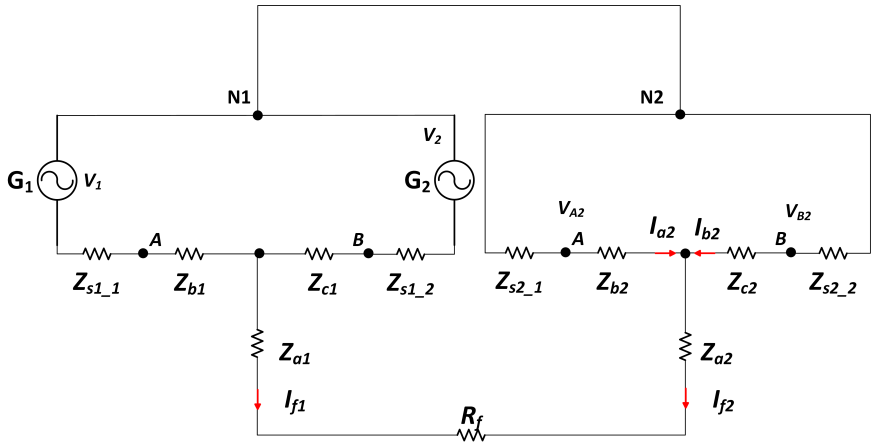

(b) After delta-star transformation

Figure 6.10: Equivalent circuit of phase-phase fault with variable fault location and fault impedance on the specific line

$$\begin{cases} V_{A2} = I_{a2} \times Z_{s2\_1} \\ V_{B2} = I_{b2} \times Z_{s2\_2} \end{cases} \tag{6.16}$$

To calculate I_{a2} and I_{b2}, I_{f2} must be calculated using Equation 6.17.

$$\begin{cases} I_{a2} = I_{f2} \times ((Z_{c2} + Z_{s2\_2})/(Z_{s2\_1} + Z_{c2} + Z_{b2} + Z_{s2\_2})) \\ I_{b2} = I_{f2} \times ((Z_{b2} + Z_{s2\_1})/(Z_{s2\_1} + Z_{c2} + Z_{b2} + Z_{s2\_2})) \end{cases} \tag{6.17}$$

To calculate I_{f2}, the circuit is simplified again as shown in Fig. 58. Z_{v1} and Z_{v2} are the equivalent positive sequence impedances between the fault locations and sources G_1 and G_2 respectively. Z_2 is the equivalent impedance of the negative sequence circuit. The equations used to calculate these quantities are the same as used in scenario A for the unbalanced earth fault condition which are shown in Equation 6.10.

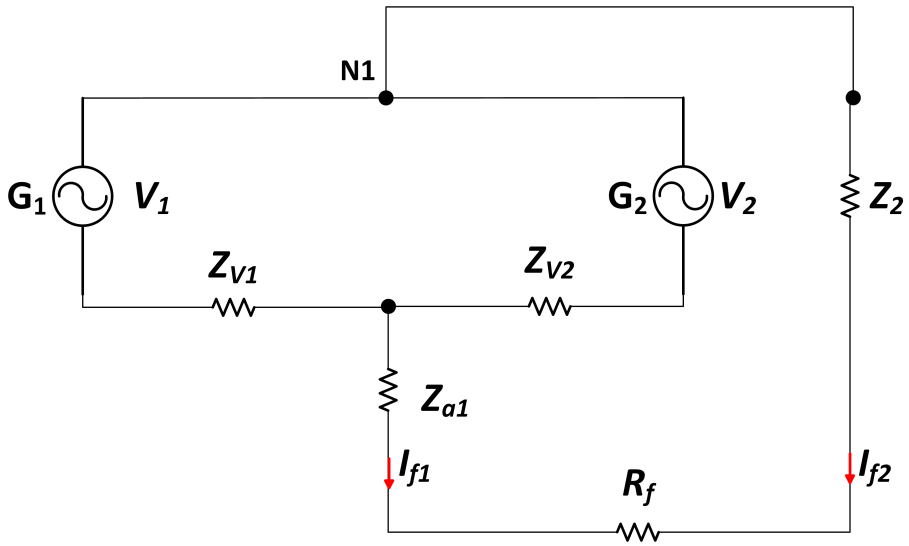

Figure 6.11: Further simplification of the circuit

Since V_1 and V_2 can be different, superposition theory is applied to calculate I_{f2}, as depicted in Figure 6.12. For scenario 1 ((a) of Figure 6.12), Z_{v2} is in parallel with (R_f +Z_{a1}+Z_2) and the total impedance of them is in series with Z_{v1}. For scenario 2 ((b) of Figure 6.12), Z_{v1} is in parallel with (R_f +Z_{a1}+Z_2) and the total impedance of them is in series with Z_{v2}. Based on the analysis of the circuit, Equation 6.18 can be derived by KCL, KVL and Ohm's Law to calculate

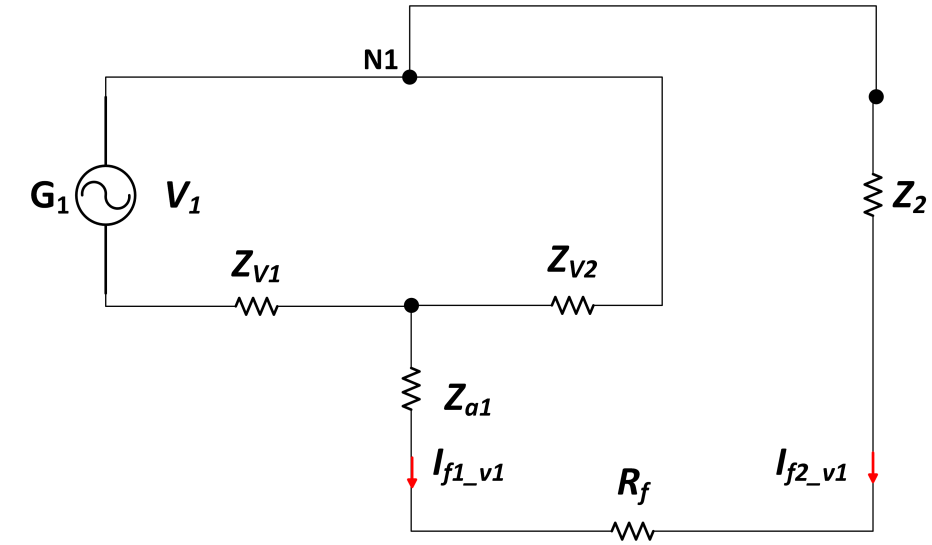

(a) With source G1 only

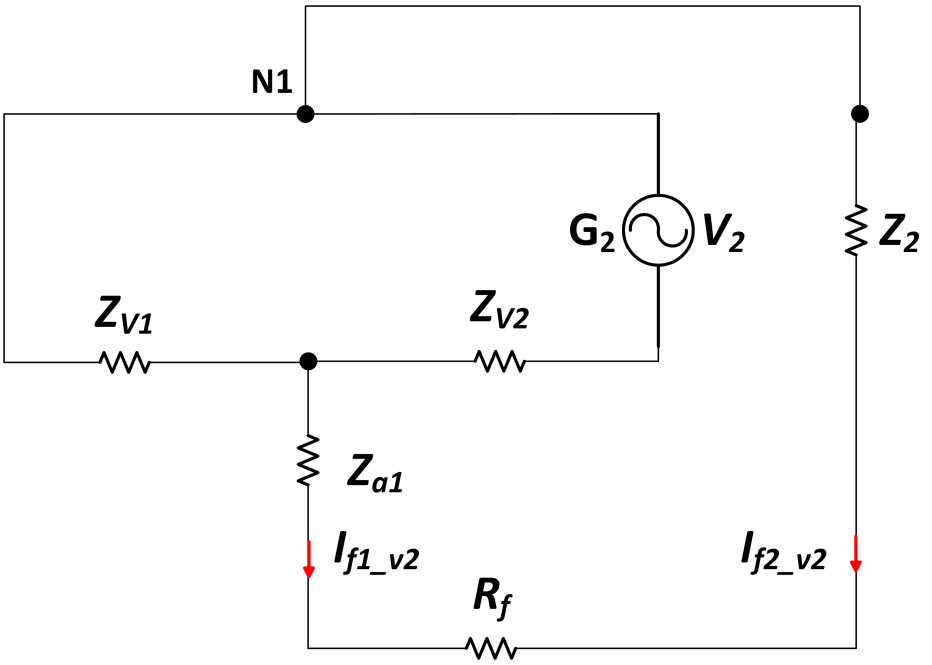

(b) With source G2 only

Figure 6.12: Application of Superposition theory of electric circuit

I_{f2}.

V_1 and V_2 are the phase voltages of the equivalent source (without internal impedance) at line end. I_{f2_v1} and I_{f2_v2} represent the negative sequence fault current with application of equivalent source G_1 and G_2 respectively.

$$\begin{cases} a_2 = Z_{v2}/(Z_{a1} + Z_2 + R_f + Z_{v2}) \\ b_2 = Z_{v1}/(Z_{a1} + Z_2 + R_f + Z_{v1}) \\ I_{f2\_v1} = V_1/(Z_{v1} + Z_{v2}//(Z_{a1} + Z_2 + R_f)) \times a_2 \\ I_{f2\_v2} = V_2/(Z_{v2} + Z_{v1}//(Z_{a1} + Z_2 + R_f)) \times b_2 \\ I_{f2} = I_{f2\_v1} + I_{f2\_v2} \end{cases} \tag{6.18}$$

With calculated I_{f2} as well as Equation 6.16 and 6.16, V_{a2} and V_{b2} can be represented (calculated) with system parameters for this scenario.

6.4.3 Establishing threshold settings and capabilities of the scheme

Similar to the process adopted for the three-phase fault and unbalanced earth-fault scenario, a 4 steps process is applied to determine the worst-case scenario fault location as well as the highest detectable fault resistance/voltage thresholds for a given maximum fault resistance.

- Step 1: A phase-phase fault is applied on a fixed line (line L) at node A (m=0). V_{A2} and V_{B2} are calculated using the process outlined in Section 5.2 and the larger value of k_{2A} and k_{2B} is selected (k_{2A} and k_{2B} represent for the difference between "during fault" and pre-fault negative sequence voltage magnitudes at node A and B respectively), denoted as k_{2max}, and its value is recorded. In this case, the magnitude of V_{A2} (V_{B2}) is the same as the magnitude of k_{2A} (k_{2B}), as ideally (for calculation and analysis), when no fault is applied to the circuit, the pre-fault negative sequence voltage magnitudes at nodes A and B should both be zero. If the pre-fault negative sequence voltage magnitudes were not zero, since k_{2A} and k_{2B} are relative

values, they would still be the same as in this ideal calculation, which means the calculated value of V_{A2} and V_{B2} in this scenario can always be used as k_{2A} and k_{2B}.

- Step 2: The value of m is increased from 0 to 1 incrementally in steps of 0.01 (i.e. the assumed fault location on the line moves from node A to node B) and step 1 is repeated. The minimum value of k_{2max} and the corresponding value of m are recorded as the worst-case values.

- Step 3: As for three-phase faults (and unbalanced earth faults), step 2 is repeated with fault resistance increasing from 0 to a suitably high fault resistance value.

- Step 4a: Again, as with three-phase faults (and unbalanced earth faults), the value of fault resistance corresponding to the scenario when k_{2max} is equal to the predetermined voltage threshold (k_{2pre}) is determined to find the highest detectable k_{2pre}, based on the results of step 3, and is denoted as R_{2max}.

- Step 4b: As with three-phase faults (and unbalanced earth faults), based on results of step 3, the value of k_{2max} corresponding to the scenario when fault resistance is equal to the given maximum fault resistance (R_{2pre}) must be determined to specify the voltage thresholds for R_{2pre}. This voltage magnitude, denoted as k_{2Th}, represents the threshold which can be used to detect any fault with a resistance less than the specified maximum.

  To demonstrate, the capability (the highest detectable fault resistance with a 2% threshold) of the scheme for Line 1 in the IEEE 14-bus network as shown in Table 6.3. The highest detectable phase-phase fault on Line 1 is 196.5 Ω. The results of the case studies are explained in details in Section 7.2.

Line	$R_{2fmax}(\Omega)$	m	Terminal at threshold
1	196.5	0.28	node A

Table 6.3: Highest phase-phase fault resistance for Line 1

6.5 Summary

A simple and effective process for evaluating the capabilities of the scheme (and establishing the associated threshold settings) has been developed to automatically provide settings (thresholds) and establish the limitations of the system in terms of maximum fault resistance for a fault at a specific location (the "worst case").

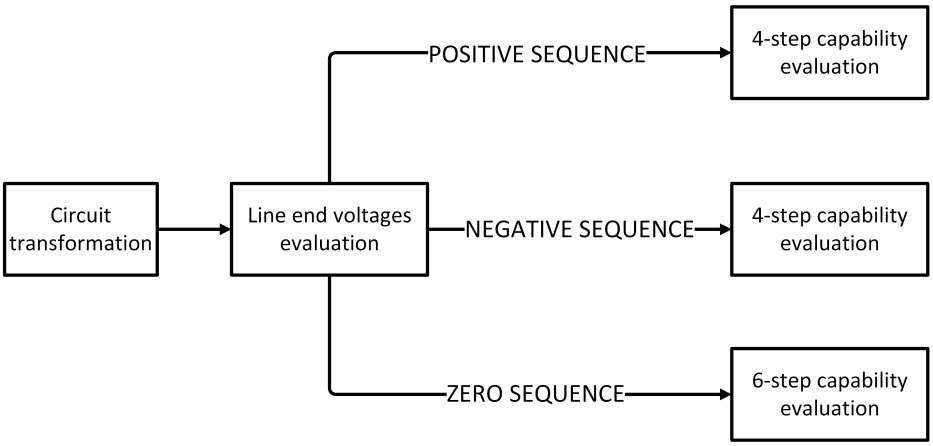

Figure 6.13: Flow chart of system capability evaluation

The process of evaluation of the system capabilities and determining threshold is presented in Figure 6.13. A delta-star circuit transformation and superposition theory are applied to the circuit to evaluate sequence components of line-end voltages in terms of fault locations (m), since the worst-case with respect to fault detection is one of the key factors in establishing the capabilities and threshold settings of the scheme.

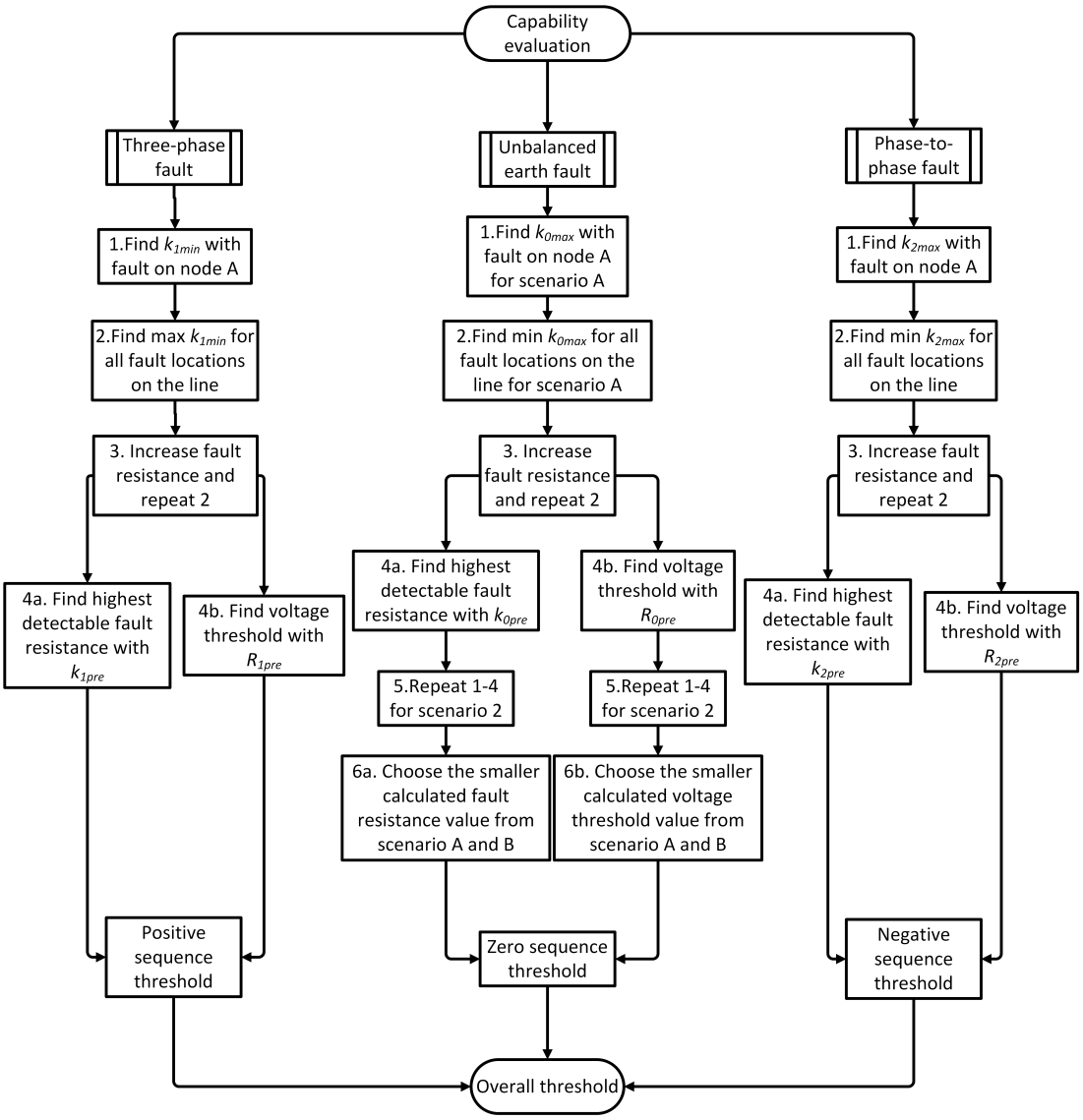

Figure 6.14: Detailed process of scheme capability evaluation

For three-phase faults, positive sequence voltage magnitudes are used as they key indicator and input quantity to trigger scheme operation, and a 4-step process is used to determine the positive sequence threshold settings/highest detectable fault resistance with for a the predetermined threshold setting, or the threshold for a predetermined maximum detectable fault resistance. For phase-phase faults, negative sequence voltage magnitudes and a 4-step process are used. For unbalanced earth faults (either single-phase to earth or phase-phase to earth), the process consists of 6 steps. The details of these processes is shown graphically in Figure 6.14.

With this automatic evaluation process, the settings and the capability of the scheme can be evaluated efficiently. These settings can also cater for fault level variations, as demonstrated in Chapter 7. Any reductions in fault level from the fault levels used in the calculation of scheme capabilities will actually be beneficial to the scheme in terms of its capabilities, as reductions in fault level will result in increased voltage depressions (or increases in negative or zero sequence components) for faults with the same characteristics (location and resistance), so the sensitivity of the scheme would not be compromised (indeed, it would be enhanced). It is anticipated that changes in network topology will not have a great influence on the thresholds/maximum detectable fault resistance, and this could be investigated as future work. In practice, a number of iterations of establishing thresholds/maximum detectable fault resistances could be conducted, and average values could be selected such that the system will be fit for purpose over a wide range of network configurations.

Chapter 7

Case studies and tests

7.1 Introduction

The operation of the scheme presented in Chapter 4 and the evaluation of scheme capabilities/thresholds introduced in Chapter 5 and 6 have been validated using case studies that have been created using the IEEE 14-bus system as shown in Figure 7.1 and modelling this within the Simscape Electrical simulation package supplied with Matlab [Mata]. The studies only consider the 132 kV system elements.

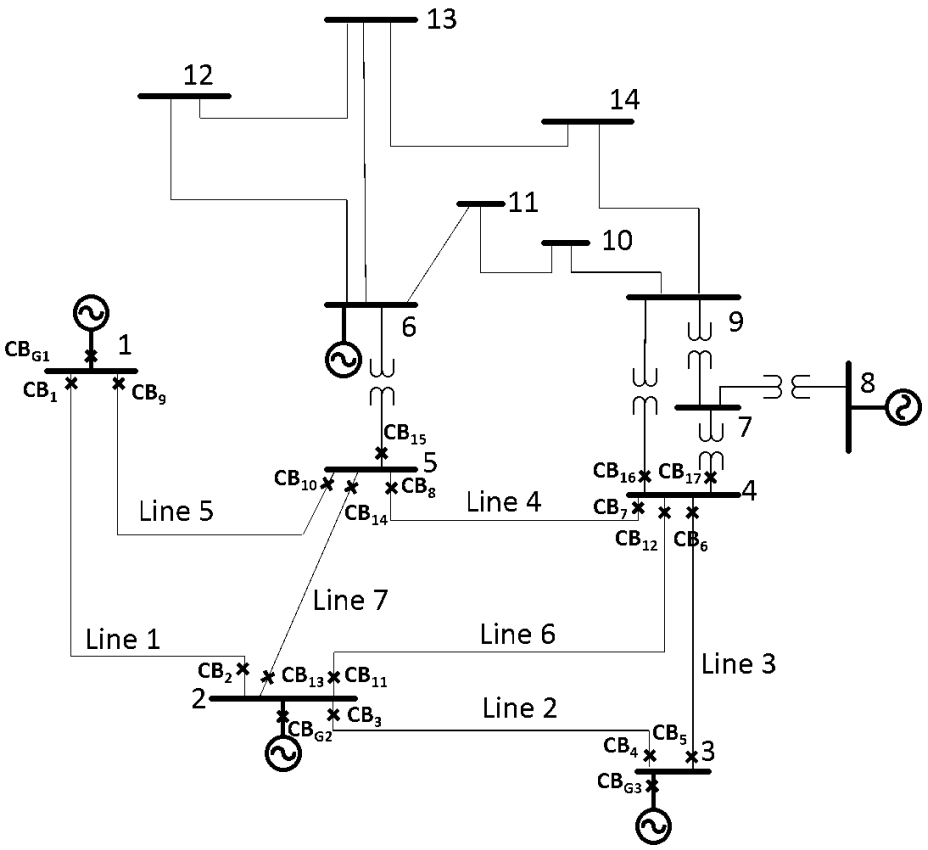

Figure 7.1: Single line diagram of IEEE 14 bus network

The Simscape package is useful for testing and validation of the scheme under a number of different scenarios and the Matlab environment is used to facilitate analyses of results via its programming function [Matb]. In addition, Simscape Electrical supports C-code generation which enables conversion of the model to another simulation environment, and in particular to hardware-in-the-loop environments, which has been used in this research to deploy the system within an RTDS, providing further validation and credibility for the operation of the scheme and assisting in proving the practicality of the scheme. This is demonstrated in detail in Chapter 8.

The IEEE standard 14-bus systems represents a simple but comprehensive approximation of an area of the electric power system in the United States of America as of February 1962 [Uni], and has been used extensively by many researchers to demonstrate and benchmark novel ideas and concepts over the years. The system is comprised of 14 buses, with 5 generating units connected to the

system.

In order to investigate the factors that may affect the operation of the scheme, case studies of system operation, where the fault (and return path) resistances, and fault levels, are varied, are described in the remainder of chapter.

7.2 Case studies for scheme validation

7.2.1 Overview

This section aims to demonstrate the setting determination method and the operation of the scheme through conducting various fault scenarios using the IEEE 14-bus network. Section 7.2.2 presents the calculated results of the 2-bus equivalent circuits (which are used in preparation for setting and capability determination) and the capability of the scheme with pre-defined operational thresholds (e.g. when measured positive sequence voltage magnitudes decrease to less than 85% of the pre-fault positive sequence voltage magnitude for three-phase faults, when zero or negative sequence voltage magnitudes increase to more than 2% of the pre-fault positive sequence voltage magnitude for unbalanced faults). The justification for the use of these thresholds is presented in Section 7.2.2.2.4. Section 7.2.3 demonstrates and validates the functionality of the scheme according to the methodology explained in Chapter 4 for a range of scenarios, including correct operation of both line-end main protections, failure of both line-end main protection systems and failure of one line-end main protection system by presenting time-domain diagrams of voltages and scheme outputs.

7.2.2 Establishing threshold settings and capabilities of the scheme

7.2.2.1 Simplified equivalent model

A set of 2-bus equivalent models are used to simplify the IEEE 14-bus as preparation for configuration determination (as described in Chapter 6). The calculated

2-bus equivalent circuit parameters for each of the 132 kV lines (7 in total) within the 14-bus model are shown in Table 7.1.

Slight differences exist between Z_{intc1_1} and Z_{intc1_2}, between Z_{intc2_1} and Z_{intc2_2} and between Z_{intc0_1} and Z_{intc0_2}, which are due to capacitance in the system and rounding errors. These can be quantified using Equation 7.1 and demonstrated in Table 7.1. As can be seen from Table 7.1 the difference is less than 0.18% for all lines, which is considered acceptable and can be neglected. Z_{intc1}, Z_{intc2} and Z_{intc0} are then defined as an average value of the two individually calculated values to minimise any error introduced by this equivalent circuit approach, which is shown in Equation 7.1.

$$\begin{cases} \Delta Z_{intc1} = |Z_{intc1\_1} - Z_{intc1\_2}|/min(|Z_{intc1\_1}|, |Z_{intc1\_2}|) \\ \Delta Z_{intc2} = |Z_{intc2\_1} - Z_{intc2\_2}|/min(|Z_{intc2\_1}|, |Z_{intc2\_2}|) \\ \Delta Z_{intc0} = |Z_{intc0\_1} - Z_{intc0\_2}|/min(|Z_{intc0\_1}|, |Z_{intc0\_2}|) \end{cases} \tag{7.1}$$

$$\begin{cases} Z_{intc1} = (Z_{intc1\_1} + Z_{intc1\_2})/2 \\ Z_{intc2} = (Z_{intc2\_1} + Z_{intc2\_2})/2 \\ Z_{intc0} = (Z_{intc0\_1} + Z_{intc0\_2})/2 \end{cases} \tag{7.2}$$

7.2.2.2 Detailed evaluation and quantification of scheme capabilities

7.2.2.2.1 Three-phase faults

According to the calculated 2-bus equivalent parameters presented in Table 7.1 and the method of capability evaluation explained in Section 6.2, the highest detectable resistance for a three-phase fault corresponding to a predetermined voltage threshold can be established. For a specific line, the first step is to define a voltage threshold that can be used to identify the presence of faults. The second step is to calculate the "worst-case" scenario for all scenarios with resistance from 0 Ω to a relatively high resistance (e.g. 50 Ω for three-phase faults on the IEEE 14-bus system) for reference. The final step is to identify the highest detectable resistance using the results from the second step as demonstrated in Section 6.2.

Positive (and negative) sequence (Ω) Angles are in radians						
Line	Z_{s1_1}	Z_{s1_2}	Z_{int1_1}	Z_{int1_2}	Z_{intc1}	ΔZ_{intc1}
1	11.01 ∠1.47	28.38 ∠1.44	70.21 ∠1.27	70.33 ∠1.27	70.27 ∠1.27	0.18%
2	14.21 ∠1.40	48.75 ∠1.44	60.47 ∠1.17	60.46 ∠1.17	60.47 ∠1.17	0.02%
3	39.24 ∠1.45	21.38 ∠1.38	86.04 ∠1.25	86.01 ∠1.26	86.03 ∠1.25	0.03%
4	34.08 ∠1.37	23.68 ∠1.41	32.45 ∠1.16	32.44 ∠1.16	32.44 ∠1.16	0
5	15.69 ∠1.41	34.58 ∠1.43	24.13 ∠1.23	24.12 ∠1.23	24.13 ∠1.23	0.03%
6	10.29 ∠1.47	32.50 ∠1.44	30.56 ∠1.22	30.56 ∠1.22	30.56 ∠1.22	0
7	16.31 ∠1.41	29.87 ∠1.45	23.38 ∠1.24	23.37 ∠1.24	23.38 ∠1.24	0.03%
Zero sequence (Ω) Angles are in radians						
Line	Z_{s0_1}	Z_{s0_2}	Z_{int0_1}	Z_{int0_2}	Z_{intc0}	ΔZ_{intc0}
1	6.95 ∠1.47	30.44 ∠1.44	182.56 ∠1.30	182.66 ∠1.31	182.61 ∠1.30	0.06%
2	18.80 ∠1.38	39.56 ∠1.46	161.12 ∠1.20	161.11 ∠1.19	161.11 ∠1.20	0
3	33.24 ∠1.45	57.41 ∠1.31	398.91 ∠1.24	398.60 ∠1.24	398.75 ∠1.24	0.08%
4	66.28 ∠1.29	64.25 ∠1.33	465.02 ∠1.14	465.09 ∠1.14	465.06 ∠1.14	0.02%
5	17.91 ∠1.39	92.66 ∠1.33	87.03 ∠1.22	86.99 ∠1.22	87.01 ∠1.22	0.05%
6	6.47 ∠1.46	85.50 ∠1.35	122.48 ∠1.18	122.34 ∠1.17	122.41 ∠1.18	0.11%
7	17.95 ∠1.38	90.08 ∠1.35	89.81 ∠1.23	89.78 ∠1.23	89.79 ∠1.23	0.04%

Table 7.1: Calculated parameters for 2-bus equivalent circuits

In order to test and validate the method, a threshold of 85% of pre-fault voltage is specified, which is applied in step one. In other work, 90% has been used, and 85% has been chosen to build in a further margin to mitigate the risk of incorrect operation for non-fault transients. However, other thresholds could be used in practice (e.g. if a higher maximum fault resistance was desired) – as with all protection settings, the balance between sensitivity and stability is subject to various factors and different network operators may choose to adopt different settings policies.

As the threshold is a proportional value of pre-fault voltage, variations in the prevailing pre-disturbance voltage will not impact the scheme. For the second step, all "worst-case" scenarios for fault resistance from 0 Ω to 50 Ω are automatically calculated as reference for the final step. The results for faults on all lines are shown in Figure 7.2 and 7.3. In the diagrams of relationship between k_1 and R_{f1}, the red line is the relationship between k_1 and R_{f1} and the black line is the threshold, which is 85% is this case. The terminal of the line with the subscript that has the lower numerical value of the line terminals is denoted as node A and the other is denoted as node B. The voltages of node A and node B are denoted as V_A and V_B respectively. m=0 indicates that fault location is at node A and m=1 indicates that fault location is at node B. The value of m, when increasing from 0 to 1, indicates that the fault location is moving away from node A to node B. For example, line 3, when analysed for a voltage threshold of 85%, the fault resistance for scenarios when terminal voltage (k_1) is just at the threshold is approximately 35 Ω. The fault resistance calculated in the scenario when V_B (node 4) is equal to the threshold is identified as the highest detectable fault resistance for line 3 (with m=0.62 as shown in Figure 7.2 (f) - the final step. k_1 is the minimum voltage magnitude at one of the line terminals when a fault with a fixed resistance occurs on the line, as explained in detail in Section 6.2. With the predetermined threshold (85% of pre-fault voltage magnitude), the maximum fault resistances that can be detected are shown in Table 7.2. The value for m indicates the fault location for the highest detectable fault resistance that results in the smallest voltage depression ("worst-case" scenario). For example, for line

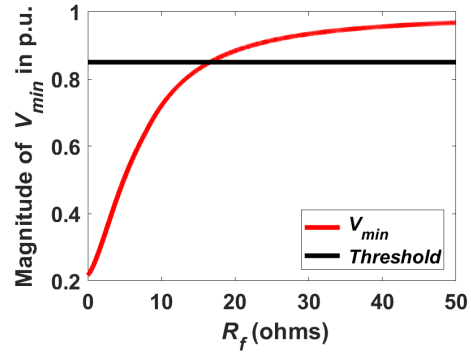

(a) line 1 - k_1 vs R_{f1}

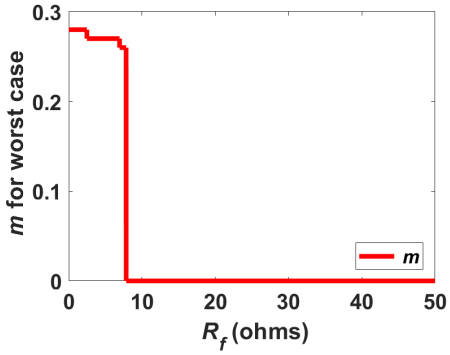

(b) line 1 - m vs R_{f1}

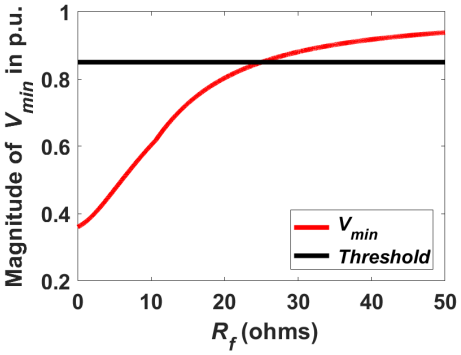

(c) line 2 - k_1 vs R_{f1}

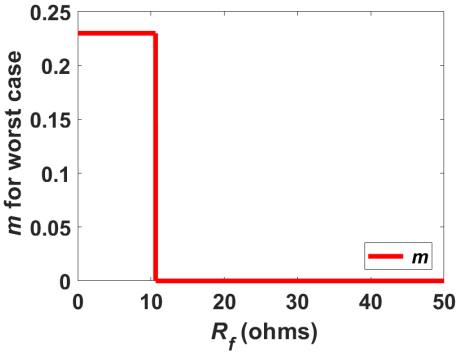

(d) line 2 - m vs R_{f1}

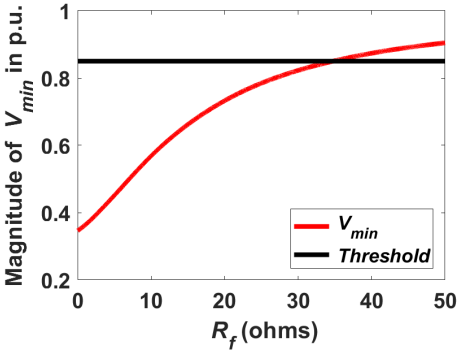

(e) line 3 - k_1 vs R_{f1}

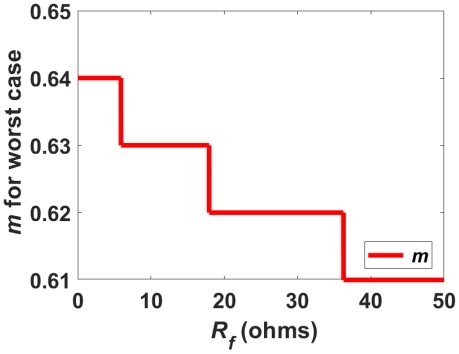

(f) line 3 - m vs R_{f1}

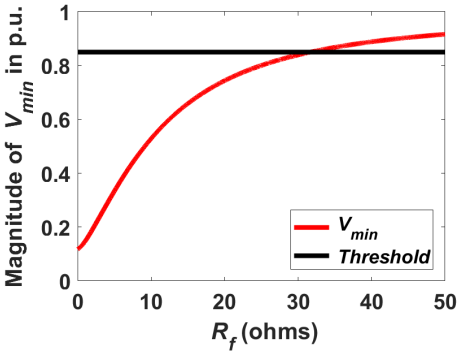

(g) line 4 - k_1 vs R_{f1}

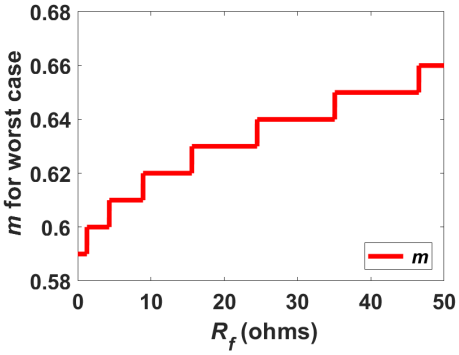

(h) line 4 - m vs R_{f1}

Figure 7.2: Highest detectable fault resistance identification of three-phase faults

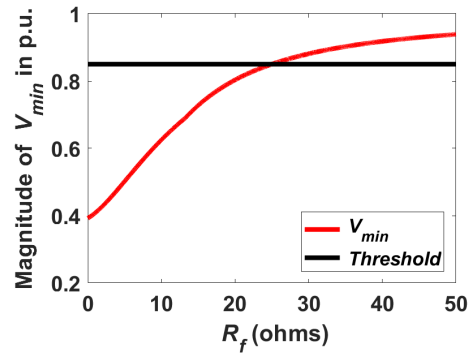

(a) line 5 - k_1 vs R_{f1}

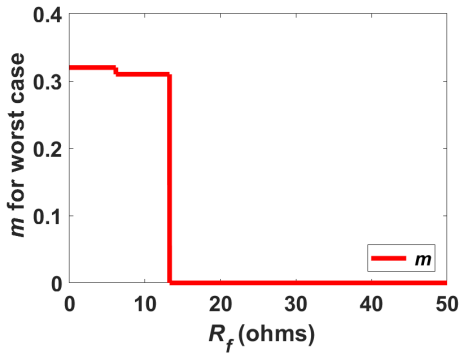

(b) line 5 - m vs R_{f1}

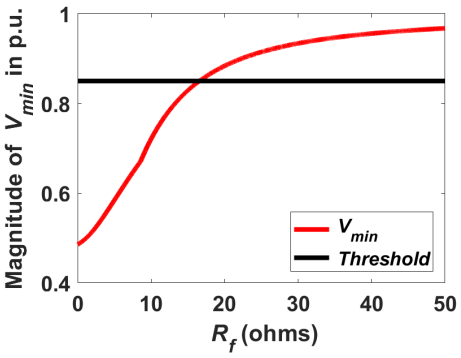

(c) line 6 - k_1 vs R_{f1}

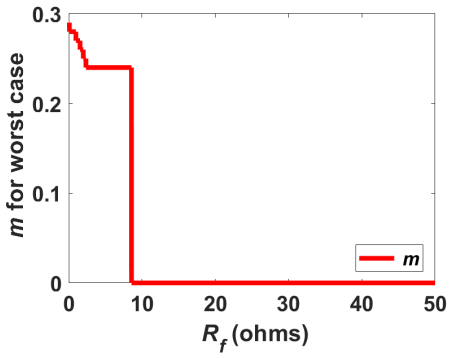

(d) line 6 - m vs R_{f1}

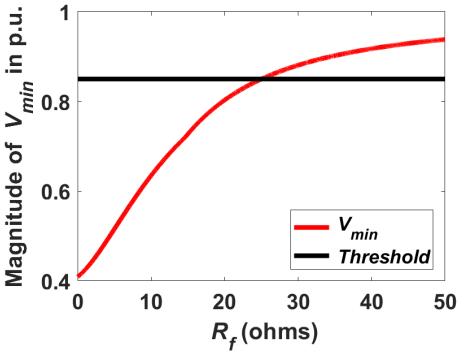

(e) line 7 - k_1 vs R_{f1}

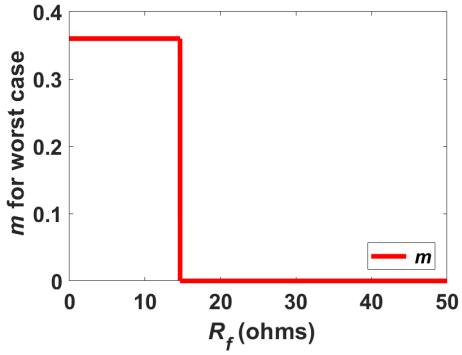

(f) line 7 - m vs R_{f1}

Figure 7.3: Highest detectable fault resistance identification of three-phase faults

line	$R_{1fmax}(\Omega)$	m	Terminal at threshold	Case
1	16.6	0	node A	1_1
2	25.0	0	node A	2_1
3	34.7	0.62	node B	3_1
4	31.7	0.64	node B	4_1
5	16.6	0	node A	5_1
6	25.0	0	node A	6_1
7	25.0	0	node A	7_1

Table 7.2: Highest three-phase fault resistance for different lines

3, R_{1fmax} is selected for the scenario where node B (node 4 in Figure 7.1) is 85% of the initial (pre-fault) voltage. The "worst case" fault location corresponds to m=0.62 (i.e. a fault at a location 62% of the line length away from node 3 in Figure 7.1).

Table 7.2 indicates that the proposed scheme can be used to analyse the protection performance anywhere within the test system for fault resistances up to 34.73 Ω, although using higher voltage thresholds would increase the maximum detectable fault resistance, at the potential expense of triggering system operation for non-fault transients - the "strength" or prevailing fault levels in the system could be used to configure the voltage thresholds and corresponding maximum detectable fault resistances in an actual application. According to the principle of the scheme, the fault will be detected if one terminal voltage moves below the threshold. To establish the boundary or limits of operation, the scenario where the voltage of only one terminal of the line is just below threshold is regarded as the worst case scenario and the node with the voltage just below the threshold is denoted as "terminal at threshold" in Table 7.2.

The column "case" indicates the boundary scenario for different lines, where the fault location and resistance are shown in the corresponding rows for reference purposes within the case study in Section 7.2.2.2.4.

7.2.2.2.2 Unbalanced earth faults

Unbalanced earth faults are identified based on changes in zero sequence voltage magnitudes. On the basis of the 2-bus equivalent parameters presented in Table 7.1 and the method explained in Section 6.3, the highest detectable re-

sistance for an unbalanced earth fault corresponding to predetermined voltage threshold settings can be established. In order to test and validate the method, a threshold of 2% of pre-fault positive sequence voltage, that is, when at least one zero sequence voltage (k_0) measurement of one terminal of the line increases by more than 2% of the pre-fault positive sequence voltage magnitude, is specified. Again, as mentioned in three-phase fault scenario, variations in the prevailing pre-disturbance voltage will not impact the scheme as the threshold is a relative proportional value, as opposed to an absolute value, of pre-fault voltage.

7.2.2.2.2.1 Single-phase to earth faults

To determine the configuration for single-phase to earth faults, it is crucial to identify the relationship between terminal voltage (k_0) and fault resistance and between worst-case scenario fault location and fault resistance, which are shown in Table 7.3. It can be observed that for Line 3 with a zero sequence voltage threshold of 2% of pre-fault positive sequence voltage (justification of 2% threshold is explained later in Section 7.2.2.2.4), the fault resistances for scenarios when terminal zero sequence voltage (k_0) is just at the threshold are between 300 and 400 Ω. The ability to detect single-phase faults with relatively high fault resistance is beneficial – while the scheme may be able to detect resistive three-phase faults, in practice these are not very common, but resistive single-phase to earth faults are more common, so this ability enhances the effectiveness of the scheme. The fault resistance calculated in scenario when V_B (node 4) is equal to the threshold is identified as the highest detectable fault resistance for line 3 (with m=0.37 as shown in Figure 7.4 (f)). Using this threshold, the maximum fault resistances that will be detected as faults are shown in Table 7.3. The value for m indicates the fault location for the highest detectable fault resistance which results in the smallest zero sequence voltage increase. For example, for line 3, R_{01fmax} is selected for the scenario where zero sequence voltage of node B (node 4 in Figure 7.1) is more than 2% of the pre-fault positive sequence voltage magnitude. The worst case corresponds to m=0.37 (i.e. a fault at a location 37% of the line length away from node 3 in Figure 7.1).

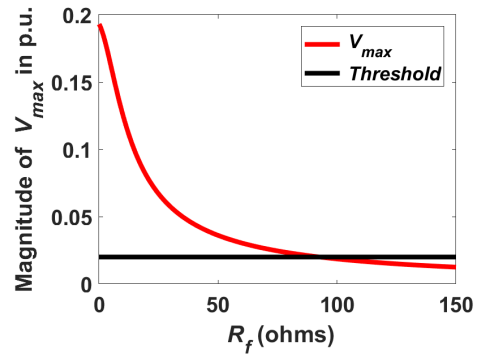

(a) line 1 - k_0 vs R_{f01}

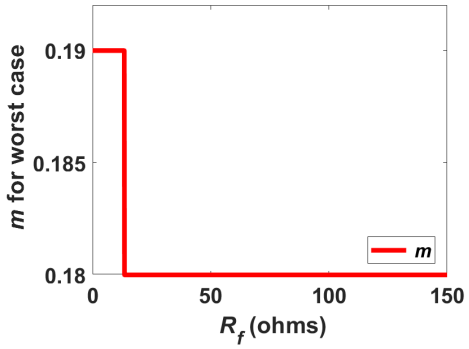

(b) line 1 - m vs R_{f01}

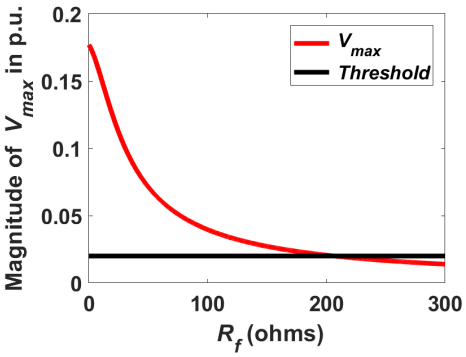

(c) line 2 - k_0 vs R_{f01}

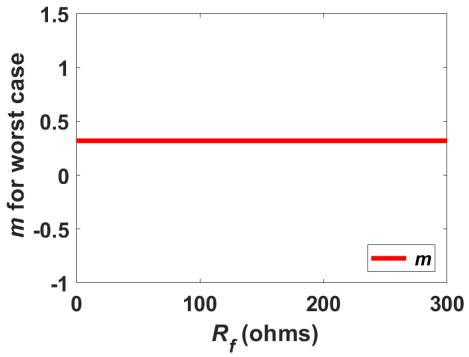

(d) line 2 - m vs R_{f01}

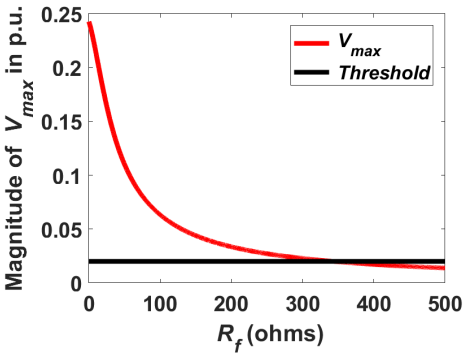

(e) line 3 - k_0 vs R_{f01}

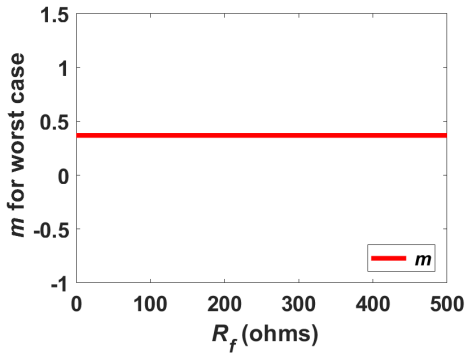

(f) line 3 - m vs R_{f01}

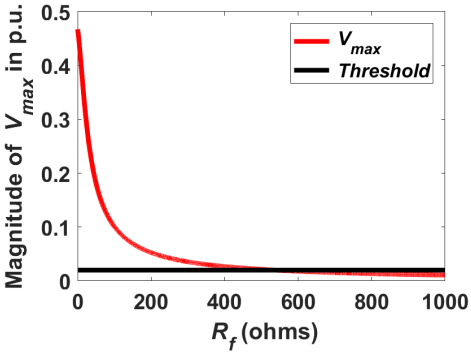

(g) line 4 - k_0 vs R_{f01}

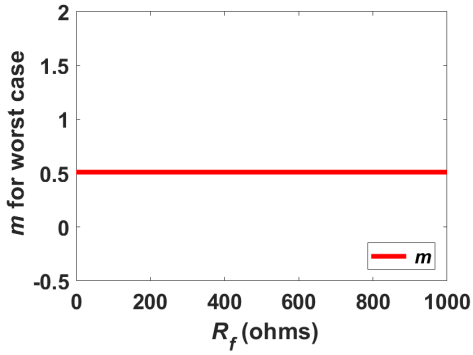

(h) line 4 - m vs R_{f01}

Figure 7.4: Highest single-phase to earth fault resistance for different lines

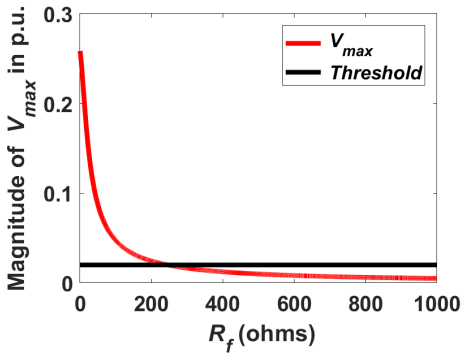

(a) line 5 - k_0 vs R_{f01}

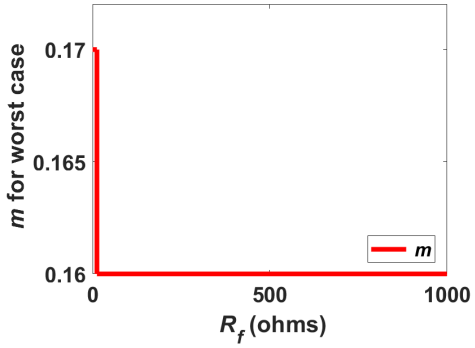

(b) line 5 - m vs R_{f01}

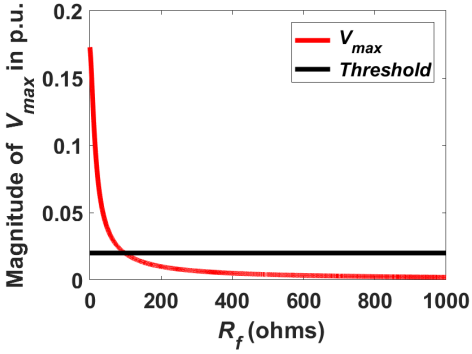

(c) line 6 - k_0 vs R_{f01}

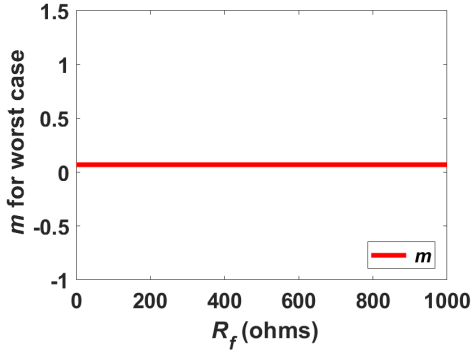

(d) line 6 - m vs R_{f01}

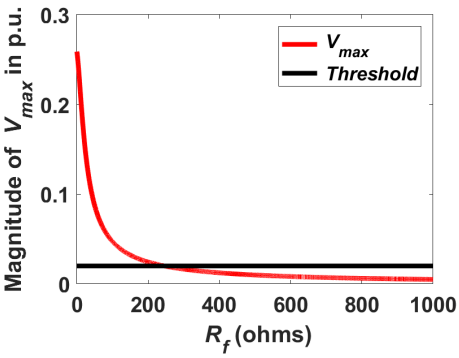

(e) line 7 - k_0 vs R_{f01}

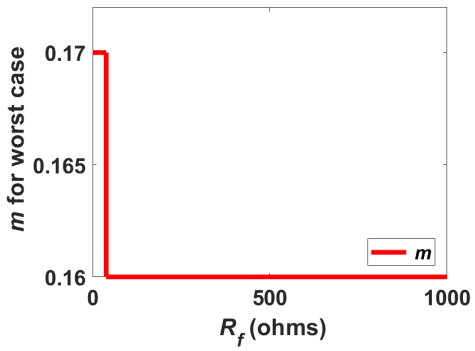

(f) line 7 - m vs R_{f01}

Figure 7.5: Highest single-phase to earth fault resistance for different lines

line	R_{01fmax} (Ω)	m	Terminal at threshold	Case
1	92.5	0.18	node A	1_01
2	206.4	0.32	node A	2_01
3	342.4	0.37	node B	3_01
4	537.8	0.51	node B	4_01
5	97.7	0.16	node A	5_01
6	245.2	0.07	node A	6_01
7	245	0.16	node A	7_01

Table 7.3: Highest single-phase to earth fault resistance for different lines

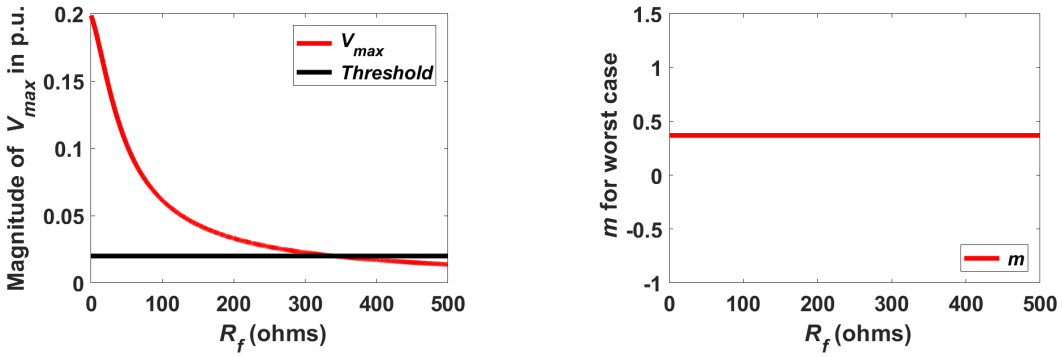

(a) line 3 - k_0 vs R_{f02}

(b) line 3 - m vs R_{f02}

Figure 7.6: Highest detectable phase-phase to earth fault resistance identification for line 3

The highest detectable single phase to earth fault resistance and the corresponding worst-case fault location is presented in Table 7.3, which indicates that the proposed scheme can be used to analyse protection performance within the test system for single-phase to earth fault resistances of up to 537.8 Ω. As shown later, this ability to detect faults with a very high "loop impedance" is beneficial, particularly when fault levels reduce, as they are expected to do in GB in the future due to increasing connection of converter-interfaced energy sources. Detection of faults require at least one of the terminal zero sequence voltages to rise above the threshold. The scenario where the zero sequence voltage of only one terminal of the line is just above the threshold is considered as the worst-case scenario and the node with the voltage just above the threshold is denoted as "terminal at threshold" in Table 7.3.

7.2.2.2.2.2 Phase-phase to earth faults

line	R_{02fmax} (Ω)	m	Terminal at threshold	Case
1	92.3	0.18	node A	1_02
2	204.6	0.0	node A	2_02
3	339.9	0.37	node B	3_02
4	535.1	0.51	node B	4_02
5	97.3	0.16	node A	5_02
6	243.7	0.07	node A	6_02
7	243.6	0.16	node A	7_02

Table 7.4: Highest phase-phase to earth fault resistance for different lines

The process of determining the maximum detectable fault resistances (for predetermined voltage thresholds) or the required voltage thresholds (for predetermined maximum fault resistance) for phase-phase to earth faults is the same as for single-phase to earth faults. For illustration, the graphs for the results for faults on line 3 are shown in Figure 7.6. With the same zero sequence voltage threshold as single-phase to earth faults (2% of pre-fault value of the positive sequence voltage magnitude), the highest detectable fault resistance is in the region of 330 Ω and the fault location for the worst-case scenario is when m is equal to 0.18 (a fault at a location 18% of the line length away from node 3 in Figure 7.1).

The scheme can analyse the protection performance and detect phase-phase to earth faults with resistances of up to 535.1 Ω and the highest detectable resistance and worst-case scenario fault location for each individual line is shown in Table 7.4. Considering line 3 as an example, for a phase-phase to earth fault, for any fault resistance of less than 339.9 Ω at any location on line 3, the scheme can detect it using a zero sequence voltage threshold of 2% of pre-fault positive sequence voltage magnitude.

7.2.2.2.2.3 Summary

As presented in detail in Section 6.3, the highest detectable fault resistance (R_{0max}) is the smaller of the calculated fault resistance value for scenario A (single-phase to earth fault) and scenario B (phase-phase to earth fault). Using the results shown in Table 7.3 and Table 7.4, the capability of the scheme for unbalanced earth faults, based on measured values of zero sequence voltages, is shown in Table 7.5. It can be observed that unbalanced earth faults can be

line	1	2	3	4	5	6	7
$R_{02fmax}(\Omega)$	92.3	204.6	339.9	535.1	97.3	243.7	243.6
Case	1_0	2_0	3_0	4_0	5_0	6_0	7_0
Fault type	II	II	II	II	II	II	II
m	0.18	0	0.37	0.51	0.16	0.07	0.16

Table 7.5: Highest detectable unbalanced earth fault resistance for all lines

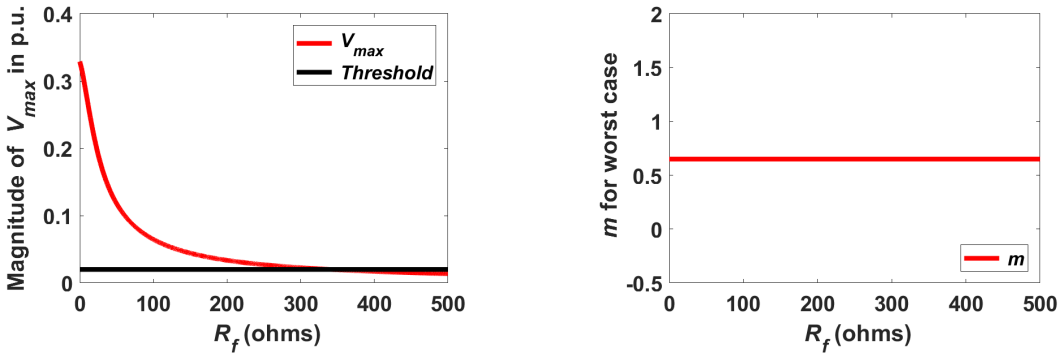

(a) line 3 - k_2 vs R_{f2}

(b) line 3 - m vs R_{f2}

Figure 7.7: Highest detectable phase-phase fault resistance identification for line 3

detected by the scheme anywhere on any 132 kV lines for fault resistances of up to 92.3 Ω. The row "case" indicates the boundary scenario for different lines, where the fault resistance are shown in the corresponding rows for the case study described in Section 7.2.2. "I" represents single-phase to earth faults and "II" represents phase-phase to earth faults in the row labelled "fault type ".

7.2.2.2.3 Unbalanced faults

Apart from utilising negative sequence voltages as indicators, the process of establishing threshold settings and capabilities of the scheme for unbalanced faults is the same as unbalanced earth faults. In order to test and validate the method, a negative sequence voltage threshold of 2% of the pre-fault positive sequence voltage (the justification of 2% is explained in Section 7.2.2.2.4), which indicates unbalanced faults will be detected when at least one negative sequence voltage (k_2) of one terminal of the line is more than 2% of pre-fault positive sequence voltage, is specified. For illustration, the graphs for the results of line 3 are shown in Figure 7.7. With the threshold set as mentioned above, the highest detectable fault resistance is between 300 and 400 Ω and the fault location for the worst-case

scenario is when m is equal to 0.65 (a fault at a location 65% of the line length away from node 3 in Figure 7.1).

line	R_{2fmax} (Ω)	m	Terminal at threshold	Case
1	196.5	0.28	node A	1_2
2	271.7	0.22	node A	2_2
3	340.2	0.65	node B	3_2
4	345.7	0.59	node B	4_2
5	192.1	0.31	node A	5_2
6	265.3	0.24	node A	6_2
7	259.3	0.35	node A	7_2

Table 7.6: Highest phase-phase faults resistance for different lines

The scheme can analyse the protection performance and detect phase-phase faults with resistances of up to 340.2 Ω and the highest detectable resistance and worst-case scenario fault location for individual line is shown in Table 7.6. Considering line 3 as an example, for a phase-phase fault with a fault resistance of less than 340.2 Ω at any location of line 3, then the scheme can detect it with using the aforementioned 2% negative sequence voltage threshold. The worst case scenario for each line is numbered in the last column and is referred to in Section 7.2.2.2.4. The scheme can analyse the protection performance and detect phase-phase faults with resistances of up to 340.2 Ω and the highest detectable resistance and worst-case scenario fault location for individual line is shown in Table 7.6. Considering line 3 as an example, for a phase-phase fault with a fault resistance of less than 340.2 Ω at any location of line 3, then the scheme can detect it with using the aforementioned 2% negative sequence voltage threshold. The worst case scenario for each line is numbered in the last column and is referred to in Section 7.2.2.2.4.

7.2.2.2.4 Threshold justification

The zero sequence threshold is used as an indicator for unbalanced earth fault identification. A value of 2% (of pre-fault positive sequence voltage magnitude) has been chosen and is deemed to be a reasonable threshold, since the typical accuracy classes for voltage transformers are 0.3%, 0.6% and 1.2% for voltages within range of $\pm$ 10% of nominal range [RAB13]. For the boundary

scenario (the minimal change of voltages – most difficult to detect) where the zero sequence voltage is equal to 2% of the pre-fault positive sequence voltage magnitude, the phase magnitude of the faulted phase(s) is/are 94% of the nominal voltage (which would be correspond to a high impedance fault scenario), which is within the normal operational voltage range of ± 10% of nominal. Using any voltage transformer (e.g. with the previously stated accuracy class of 0.3%, 0.6% and 1.2%) will mean that the 2% increase/threshold will definitely be evident on the output of the transformer [ABBa]. Since the phase voltage drop in this scenario is 6%, much higher than the maximum acceptable errors for any voltage transformer, then the 2% sequence voltage threshold can be proposed as reasonable when considering the accuracy of voltage transformers. Although accuracy of the transformer declines as the voltage collapses, for faults with lower resistance, the phase voltage(s) would have a larger depression (and it is highly likely that the zero sequence voltage would be much higher than the 2% threshold) and it would be relatively easier for transformers to detect the depression.

For phase-phase faults, the boundary scenario where negative sequence voltage equals to 2% of the initial voltage magnitude, the phase magnitude of the faulted phase are 94% of the nominal voltage magnitude(equating to a high impedance fault), which is within the range of ± 10% of the nominal voltage range. As before, the maximum errors of voltage transformers are far less than the 6% phase voltage drop, therefore the threshold is practical when taking the accuracy of voltage transformers into account.

7.2.3 Scheme operation

Figure 7.8, Figure 7.9 and Figure 7.10 demonstrate the time sequence of the scheme's operation, illustrating the positive, negative and zero sequence voltage magnitude profiles for scenarios where line 1 experiences a three-phase fault with fault resistance of 3 Ω, an unbalanced earth fault (single-phase to earth fault in this case) with a fault resistance of 20 Ω and double phase fault with a fault resistance of 20 Ω. Solid and dashed voltage traces represent the system without and with the backup scheme respectively. The faults all occur at 0.2 s and one

line-end main protection operates correctly at 0.28s. The circuit breaker at bus 1 on line 1 operates correctly and the circuit breaker (or protection) at bus 2 on line 1 fails to operate.

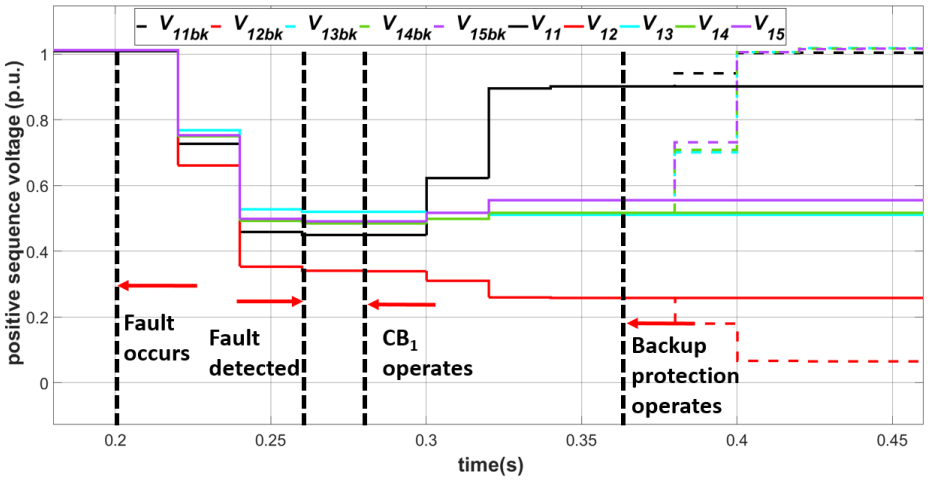

Figure 7.8: Three-phase fault on line 1

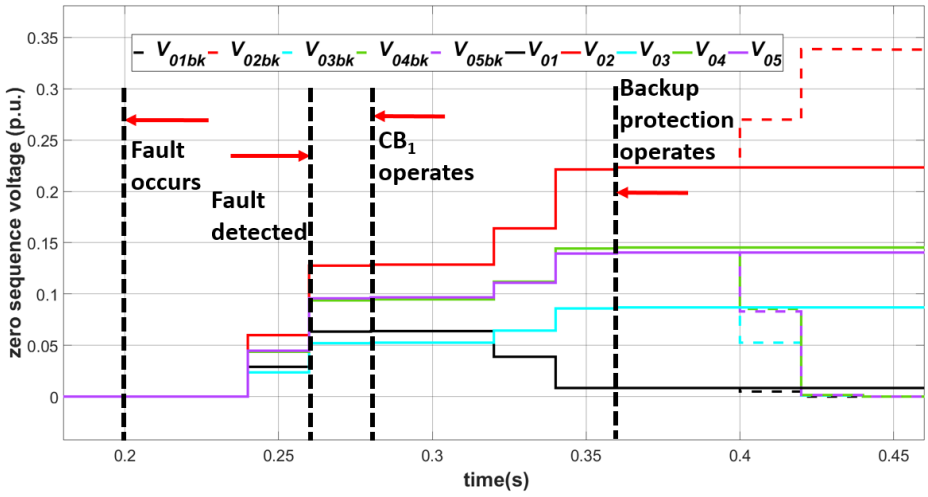

Figure 7.9: Unbalanced earth fault on line 1

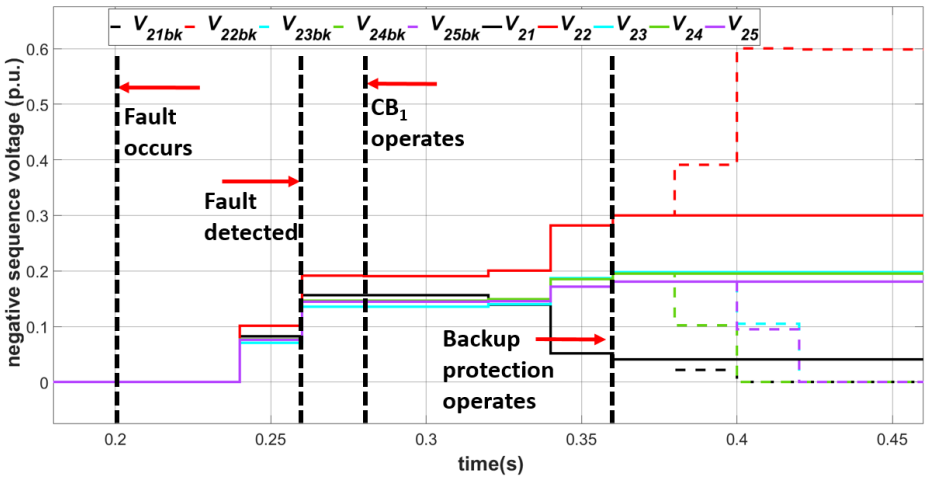

Figure 7.10: Unbalanced faults on line 1

The voltage magnitudes in each of the scenarios show how 60 ms of fault occurrence identification time with reference to the point of fault occurrence is required, and how a further 80 ms is required for faulted line identification/backup protection functionality is required (with correct operation of one line-end main protection, which is the case for all scenarios presented here). From a comparison of operation with (dashed lines) and without the proposed scheme (solid lines), it can be observed that the operation of the backup protection provided by the scheme (sending tripping signals to all circuit breakers around the bus directly connected the failed to operate circuit breaker), results in all bus voltages recovering apart from the bus directly connected to the failed circuit breaker – bus 2 in these cases. The appropriate sequence voltages of bus 2 would depress further (i.e. positive sequence voltage in the three-phase fault scenario) or increase further (i.e. zero/negative sequence voltages in unbalanced fault scenarios), since the fault at this time is now supplied only via bus 2 and not from other parts of the network.

To demonstrate the operation of the scheme for both: failure of all main protection systems/breakers (highly unlikely) and for correct operation of both line-end main protection, a 20 Ω double phase to earth fault is applied at line 1 and the results of both scenarios are shown in Figure 7.11 and Figure 7.12 respectively. The situation where all protection systems fail (i.e. the breakers at each line terminal do not operate) is extremely rare but the scheme can identify this

scenario and indicates the fault region for system operator to have an enhanced understanding of the network status through provision of concise summarised information. The fault occurs at 0.2 s and both main protections operate at 0.28 s for the scenario when correct operation of both line-end main protections is assumed.

As shown in Figure 7.11 (a) for the failure of all main protections scenario, fault occurrence is identified within 60 ms, which is the same as shown in Figure 7.10, and is not affected by the status of protection. Then, after a further 240 ms delay, the scheme identifies the failure of all main protections and output the faulted region as shown in Figure 7.11 (b) and (c). Although main protection normally operates within 140 ms, a margin is added to the scheme to cater for any delay in the operation of main protection (National Grid standards stipulate maximum operating time of 140 ms for main protection); this can be adjusted based on requirements. To simply represent the fault region, the diagram shows it in decimal. For Figure 7.11 (b), the fault region is identified as 99 in decimal at 0.5 s, which equals to 1100011 in bits. For the converted binary number, the location with "1" presents the subscript of the line as an element the identified faulted region. In this case, fault region is therefore identified as encompassing lines 1, 2, 6 and 7.

As for the other scenarios, fault occurrence is identified within 60 ms for the scenario of failure of all main protection as shown in Figure 7.12 (a). With correct operation of main protection at 0.28 s, the scheme identifies the correct operation of main protection and outputs the fault region as shown in Figure 7.12 (b) and (c) within a further 80 ms. Figure 7.12 (b) shows the identified fault region, which is presented using the same method as in Figure 7.11 (b) and Figure 7.12 (c) indicates the correction operation of main protection. Outputs relating to fault region and protection status revert to 0 to indicate the case is complete (all protection operated correctly and no further action is required).

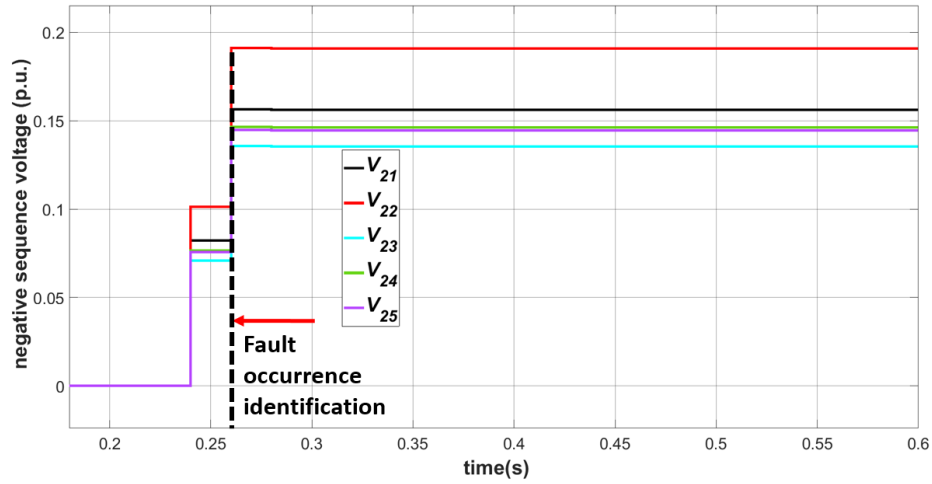

(a) Negative sequence voltage magnitudes from PMUs

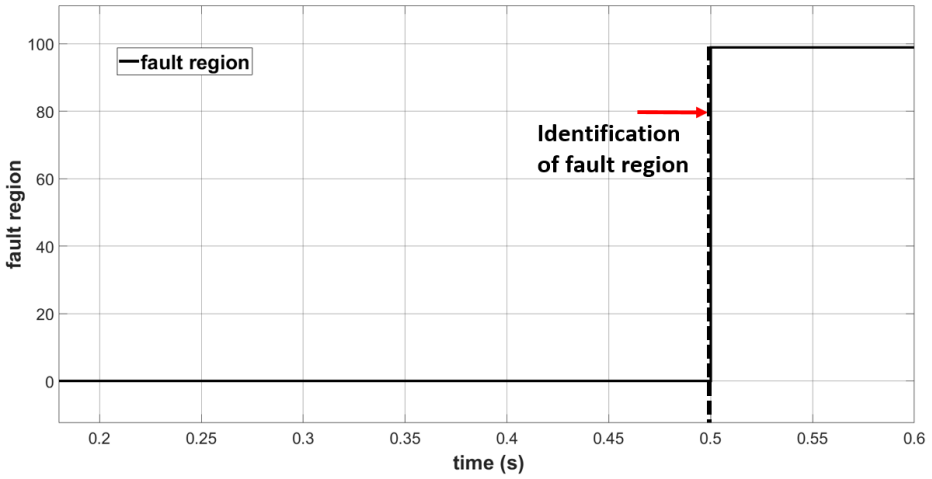

(b) Fault region identification

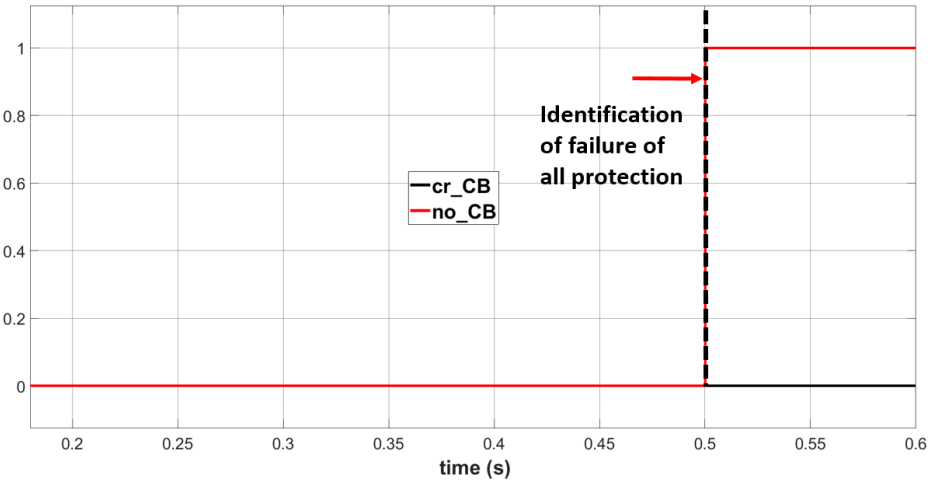

(c) Indication of protection status

Figure 7.11: Scheme output under failure of all main protection scenario

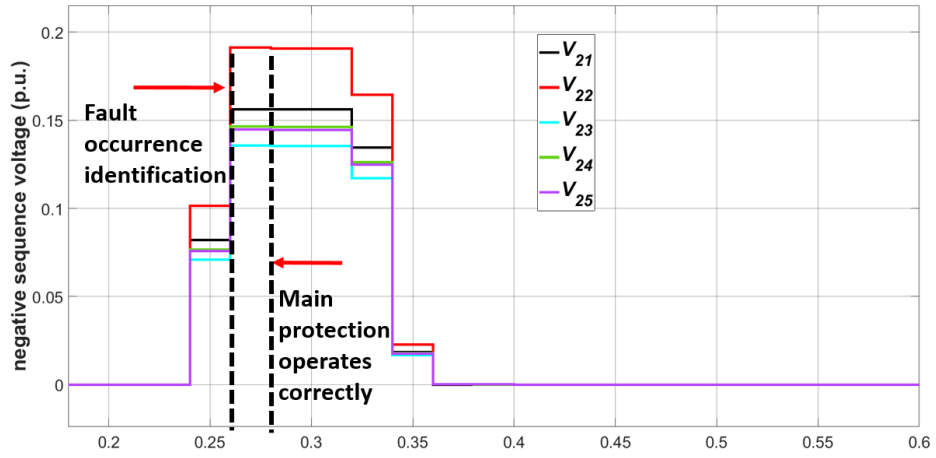

(a) (Negative sequence voltage magnitudes from PMUs

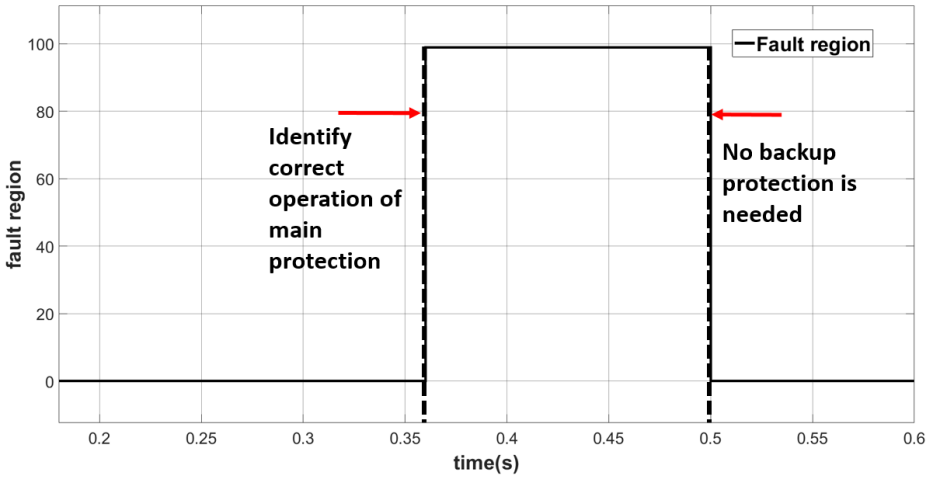

(b) Fault region identification

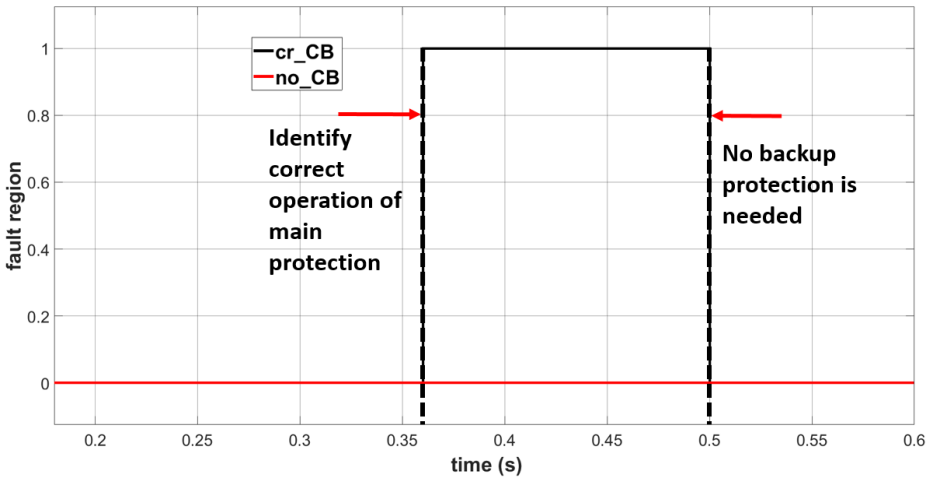

(c) Indication of protection status

Figure 7.12: Scheme output under successful operation of main protection scenario

7.3 Influence of variations in fault resistance on the scheme

Fault resistance varies on a case-by-case basis, and depends on many factors. High impedance faults are normally most challenging to the scheme, thus it is important to test the capability of the scheme when fault resistance is subject to variation. In order to validate the scheme, it is very important to ensure that the scheme can operate correctly for all fault locations for the specific value of fault resistance being tested. Fault types, the time of fault occurrence and identification, faulted line identification and circuit breaker status are also included in the case study results. Case studies illustrating correct operation of main protection and complete failure of all main protections is also presented.

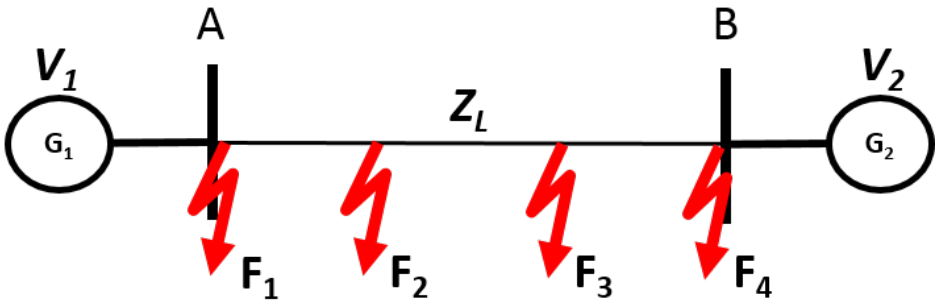

Figure 7.13: Single line diagram for fault location demonstration

As shown in Figure 7.13, four fault locations are tested for each line; at the terminals of the line and at 33% and 67% along the line from one terminal. For each fault, only one line-end main protection operates, which is the most common situation that would require backup protection operation, and each fault scenario is conducted twice to cover failure of protection at each line end individually. All faults occur at 0.2 s and the correctly operated circuit breaker opens at 0.28 s.

7.3.1 Three-phase faults

Based on the setting information discussed in Section 7.2.2, case studies using fault resistances varying from 1 Ω to 40 Ω with an increment of 3 Ω for each

of the four fault locations have been conducted in this section to investigate the impact of fault locations and fault resistance upon the operation of the scheme.

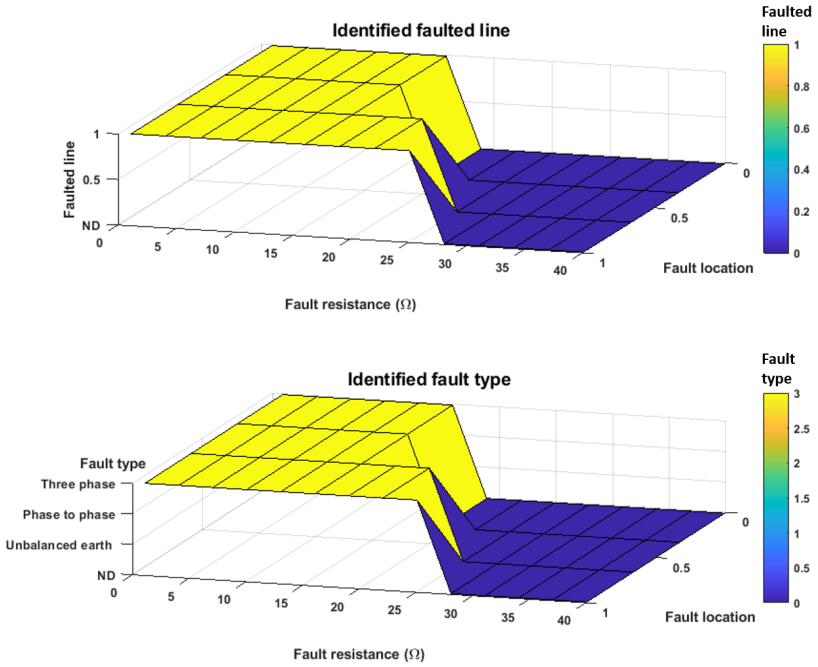

Figure 7.14: Identified fault type and faulted line vs fault resistance and fault locations for three-phase faults

A wide range of scenarios were simulated and a large number of results have been generated. Figure 7.14 presents the ability of the scheme to detect faulted lines and report fault types for line 1. It can be observed that the scheme can successfully detect the faulted line and fault type with fault resistances of up to approximately 15 Ω for all tested fault locations. For fault resistance between 15 Ω and 30 Ω, the scheme can successfully detect faults for a section of the line rather than the entire line, where the scheme tends to detect faults close to node 2 more "easily". For high resistance scenarios where the fault cannot be detected by the scheme, the output of the scheme is 0 rather than providing incorrect information, such as wrong faulted line information or wrong fault type information, which guarantees the reliability of the scheme.

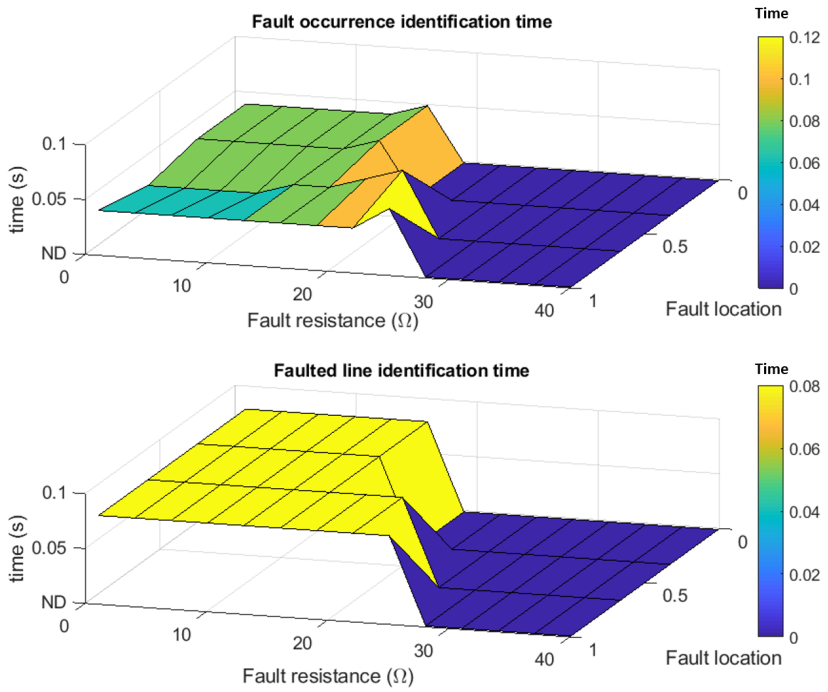

Figure 7.15: Identification time with variation of fault resistance and fault locations for three-phase faults

In order to demonstrate the impact of variation of fault resistance, a 3D figure is shown in Figure 7.15 to present the fault occurrence identification time as well as the faulted line identification time (the backup protection time) for line 1. It can be inferred that for fault resistances of less than approximately 15 Ω, the scheme can successfully identify the fault occurrence and the faulted line. The time of detecting fault occurrence ranges from 60 ms to 100 ms with variation of fault locations and resistance. The time of detecting fault occurrence increases with increasing fault resistance. With fault location moving from node 1 to node 2, the general fault occurrence identification time reduces. For the scenarios where faults can be detected by the scheme, the faulted line identification time (i.e. the backup protection time) is also 80 ms which indicates that as long as the fault resistance is within the detectable range, the backup protection can be provided after a further 80 ms has passed following operation of one line-end main protection.

The results for all lines are shown in Table 7.7. The column of correct protection operation status detection indicates the protection operation status detection

Faulted line	Highest detectable fault resistance (Ω)	Correct protection operation status detection	Fault type detection	Fault occurrence identification time (ms)	Faulted line identification time (ms)
line 1	16	✓	1	100	80
line 2	25	✓	1	100	80
line 3	34	✓	1	100	80
line 4	31	✓	1	100	80
line 5	16	✓	1	100	80
line 6	25	✓	1	100	100
line 7	25	✓	1	100	100

Table 7.7: Results of three-phase faults

under the scenarios where fault resistance is within the highest detectable fault resistance and he inclusion of a "tick" indicates the correct indication of protection operation status. The fault occurrence identification time and faulted line identification time columns present the maximum time that the scheme would require to identify fault occurrences and faulted lines respectively. The second column, highest detectable fault resistance, indicates the maximum fault resistance that can be detected at any point on all lines. The column "fault type detection" indicates the fault type identified by the scheme ("1" for three-phase faults; "2" for unbalanced earth faults and "3" for phase-phase faults). Faults are identified as three-phase faults in all scenarios demonstrated in Table 7.7

It can be inferred from the table that the scheme can correctly detect / provide backup protection for three-phase faults with resistance of up to 16 Ω fault at any location of the transmission line in the IEEE 14-bus 132 kV network within a maximum time of 100 ms following operation of one line-end main protection.

7.3.2 Unbalanced earth faults

Based on the setting information discussed in Section 7.2.2, case studies using fault resistances varying from 1 Ω to 241 Ω with an increment of 20 Ω for each of the four fault locations have been conducted in this section to investigate the impact of fault locations and fault resistance upon the operation of the scheme.

7.3.2.1 Single-phase to earth faults

Figure 7.16 presents the ability of the scheme to detect high resistive single-phase to earth faults for line 1. Based on the test results, the scheme can successfully detect the faulted line and fault type with fault resistance up to around 100 Ω for all tested fault locations (both of the busbars and 33% and 67% of the line).

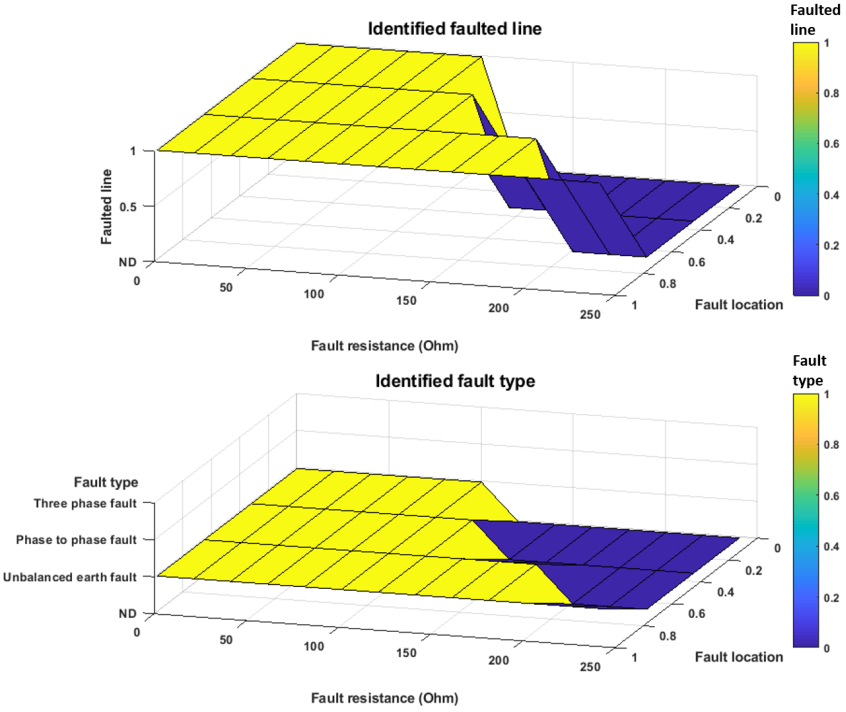

Figure 7.16: Identified fault type and faulted line vs fault resistance and fault locations for single-phase to earth faults

In order to demonstrate the impact of variation of fault resistance, a 3D figure is shown in Figure 7.17 to present the fault occurrence identification time as well as the faulted line identification time (the backup protection time) for line 1. It can be inferred that for fault resistances of less than approximately 100 Ω, the scheme can successfully identify the fault occurrence and the faulted line. The time of detecting fault occurrence ranges from 60 ms to 100 ms with variation of fault locations and resistance. The time of detecting fault occurrence increases with increasing fault resistance. With fault location moving from node 1 to node 2, the general fault occurrence identification time reduces. For the scenarios where faults can be detected by the scheme, the faulted line identification time

Faulted line	Highest detectable fault resistance (Ω)	Correct protection operation status detection	Fault type detection	Fault occurrence identification time (ms)	Faulted line identification time (ms)
line 1	101	✓	2	100	80
line 2	201	✓	2	100	80
line 3	241	✓	2	100	100
line 4	241	✓	2	80	80
line 5	101	✓	2	100	100
line 6	241	✓	2	100	100
line 7	241	✓	2	100	100

Table 7.8: Results of single-phase to earth faults

(i.e. the backup protection time) is also 80 ms which indicates that as long as the fault resistance is within the detectable range, the backup protection can be provided after a further 80 ms has passed following operation of one line-end main protection.

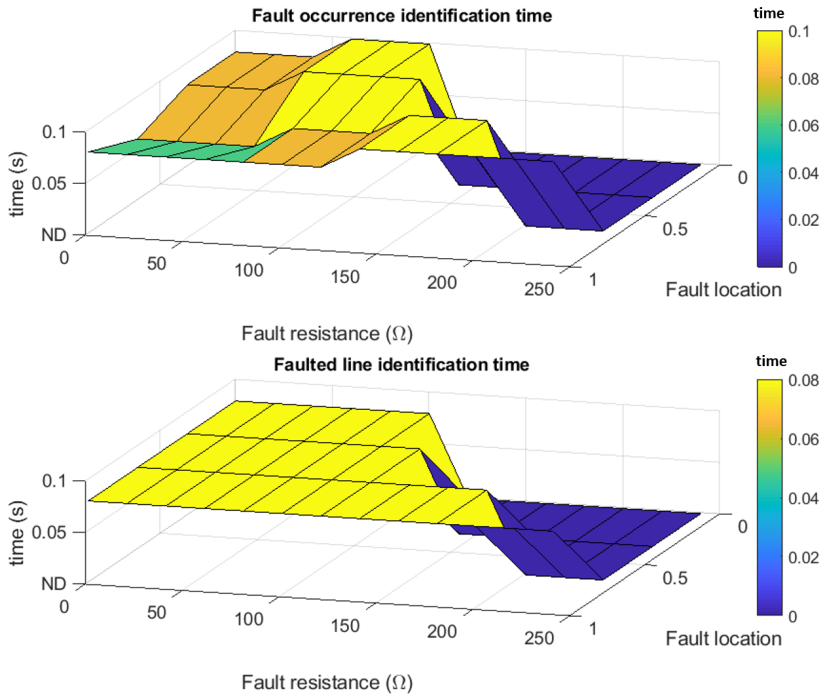

Figure 7.17: Identification time with variation of fault resistance and fault locations for single-phase to earth faults

The results for all lines are shown in Table 7.8. The column of correct protec-

tion operation status detection indicates the protection operation status detection under the scenarios where fault resistance is within the highest detectable fault resistance and he inclusion of a "tick" indicates the correct indication of protection operation status. The fault occurrence identification time and faulted line identification time columns present the maximum time that the scheme would require to identify fault occurrences and faulted lines respectively. The second column, highest detectable fault resistance, indicates the maximum fault resistance that can be detected at any point on all lines. The column "fault type detection" indicates the fault type identified by the scheme ("1" for three-phase faults; "2" for unbalanced earth faults and "3" for phase-phase faults). Faults are identified as unbalanced earth faults in all scenarios demonstrated in Table 7.8

It can be inferred from the table that the scheme can correctly detect / provide backup protection for single-phase to earth faults with resistance of up to 100 Ω fault at any location of the transmission line in the IEEE 14-bus 132 kV network within a maximum time of 100 ms following operation of one line-end main protection.

7.3.2.2 Phase-phase to earth faults

The results of phase-phase to earth faults with variation of fault locations and fault resistance are illustrated in Table 7.9, which indicates that the scheme can correctly detect / provide backup protection to a phase-phase fault with up to 241 Ω on any location of the transmission line in the IEEE 14-bus 132 kV level networks with maximum a further 100 ms with operation of one line-end main protection.

7.3.3 Phase-phase faults

Based on the setting information discussed in Section 7.2.2, case studies using fault resistances varying from 1 Ω to 341 Ω with an increment of 20 Ω for each of the four fault locations have been conducted in this section to investigate the impact of fault locations and fault resistance upon the operation of the scheme.

Faulted line	Highest detectable fault resistance (Ω)	Correct protection operation status detection	Fault type detection	Fault occurrence identification time (ms)	Faulted line identification time (ms)
line 1	101	✓	2	100	80
line 2	201	✓	2	100	80
line 3	241	✓	2	100	80
line 4	241	✓	2	100	80
line 5	101	✓	2	100	100
line 6	241	✓	2	100	100
line 7	241	✓	2	100	100

Table 7.9: Results of phase-phase to earth faults

Figure 7.18 presents the ability of the scheme to detect high resistive phase-phase faults for line 1. Based on the test results, the scheme can successfully detect the faulted line and fault type with fault resistance up to around 200 Ω for all tested fault locations (both of the busbars and 33% and 67% of the line).

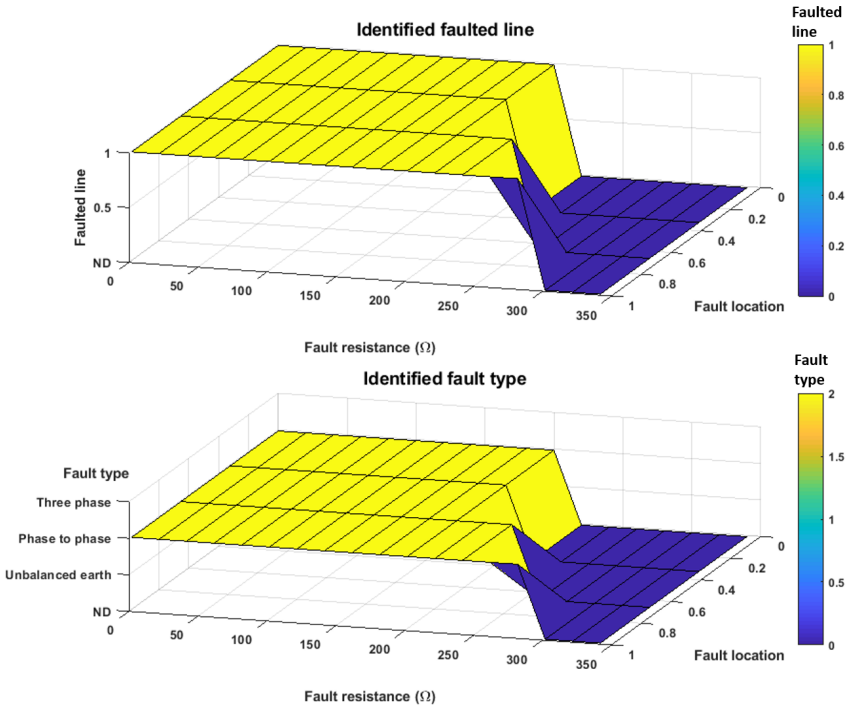

Figure 7.18: Identified fault type and faulted line vs fault resistance and fault locations for phase-phase faults

In order to demonstrate the impact of variation of fault resistance, a 3D figure

is shown in Figure 7.19 to present the fault occurrence identification time as well as the faulted line identification time (the backup protection time) for line 1. It can be inferred that for fault resistances of less than approximately 200 Ω, the scheme can successfully identify the fault occurrence and the faulted line. The time of detecting fault occurrence ranges from 60 ms to 100 ms with variation of fault locations and resistance. The time of detecting fault occurrence increases with increasing fault resistance. With fault location moving from node 1 to node 2, the general fault occurrence identification time reduces. For the scenarios where faults can be detected by the scheme, the faulted line identification time (i.e. the backup protection time) is also 80 ms which indicates that as long as the fault resistance is within the detectable range, the backup protection can be provided after a further 80 ms has passed following operation of one line-end main protection.

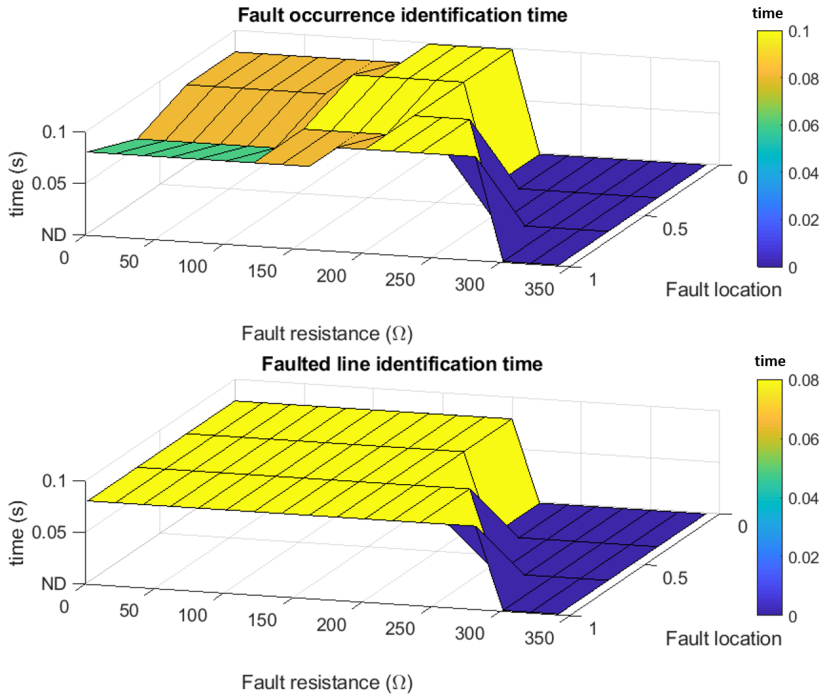

Figure 7.19: Identification time with variation of fault resistance and fault locations for phase-phase faults

The results for all lines are shown in Table 7.10. The column of correct protection operation status detection indicates the protection operation status detection

Faulted line	Highest detectable fault resistance (Ω)	Correct protection operation status detection	Fault type detection	Fault occurrence identification time (ms)	Faulted line identification time (ms)
line 1	201	✓	3	100	80
line 2	281	✓	3	100	100
line 3	341	✓	3	100	80
line 4	341	✓	3	100	80
line 5	201	✓	3	100	100
line 6	261	✓	3	100	100
line 7	261	✓	3	100	100

Table 7.10: Results of phase-phase faults

under the scenarios where fault resistance is within the highest detectable fault resistance and he inclusion of a "tick" indicates the correct indication of protection operation status. The fault occurrence identification time and faulted line identification time columns present the maximum time that the scheme would require to identify fault occurrences and faulted lines respectively. The second column, highest detectable fault resistance, indicates the maximum fault resistance that can be detected at any point on all lines.The column "fault type detection" indicates the fault type identified by the scheme ("1" for three-phase faults; "2" for unbalanced earth faults and "3" for phase-phase faults). Faults are identified as phase-phase earth faults in all scenarios demonstrated in Table 7.10

It can be inferred from the table that the scheme can correctly detect / provide backup protection for phase-phase faults with resistance of up to 200 Ω fault at any location of the transmission line in the IEEE 14-bus 132 kV network within a maximum time of 100 ms following operation of one line-end main protection.

7.3.4 Conclusions

The focus of this section has been to thoroughly analyse the impact of fault resistance (and fault location) on the operation of the scheme, through using case studies on the IEEE 14-bus 132 kV network with consideration of different fault locations (and resistances), to highlight the capability of the scheme and

illustrate the reporting functionality of the scheme.

This section has conducted simulations of different types of faults with a wide range of fault resistances at four representative locations on a transmission line - both terminals of the lines and 33% and 67% of the line, which is assumed to be enough to represent performance for fault locations across the entire line length. It has been established that the scheme has the ability to detect relatively high resistance faults and does not mal-operate or report erroneous information under very high resistance scenarios.

It has been demonstrated that, for all fault types, the occurrence of the fault can be identified within a range of 60 ms to 100 ms; the exact time is dependent on variations in fault resistance and location. The faulted line can be identified and backup protection provided within a further 80 ms to 100 ms after operation of one of the line-end main protections and opening of the circuit breaker. Since the range of main protection operation time is 80 ms to 140 ms, the backup protection provided by the scheme can operate within a maximum time of 240 ms after initial fault occurrence, which has the potential to provide a relatively fast backup protection at little or no extra cost (presuming the PMUs and communications infrastructure are already installed for other purposes) compared to conventional zone 2 backup protection. The highest detectable fault resistances for three-phase fault, unbalanced earth faults and phase-phase faults are 16 Ω, 101 Ω and 201 Ω respectively for any fault location on IEEE 14-bus 132 kV networks using the tested voltage thresholds. The threshold used were 85% retained voltage for positive sequence voltage magnitudes for detection of balanced faults and a 2% increase (with respect to pre-fault positive sequence voltage magnitude) for zero and negative sequence voltage magnitudes to detect unbalanced faults. Changing the thresholds is possible if higher fault resistances require to be detected.

The reporting and analysis function of the scheme has also been demonstrated in this section. Information including fault type, faulted line and status of circuit breaker/protection (e.g. operated correctly or failed) can be provided to the system operator for better understanding of the system status. Finally, backup protection can also be provided and this functionality has also been demonstrated.

7.4 Influence of variations in fault levels on the scheme

Considering the future evolution of power systems, there are various factors that will influence the behaviour of the system and these include economics, technology development, policies and environmental considerations. National Grid regularly consider and publish findings and opinion on the future for power systems in GB, and they normally consider four possible scenarios for the future, as shown in Figure 7.20. The scenarios can be evaluated in two dimensions – the rate of economic growth, and carbon reduction and associated targets with respect to the introduction of renewables [Nat15c]. In fact, very recently National Grid has stated that the system will be able to operate on a "no carbon" basis by 2025 [Nat19]. The "gone green" scenario is normally the most significant in terms of changes in the composition and future behaviour and performance of the power system, while the "no progression" scenario is relatively the most benign, where the least significant changes are anticipated.

Figure 7.20: Future energy scenarios [Nat15c]

As shown in Figure 7.21, it is anticipated that the fault levels in GB will decline significantly, even for the "No Progression" scenario [Nat15c]. For the "Gone Green" scenario, reductions in short circuit level range from 35% to 70% reductions from present values, largely as a result of decommissioning of synchronous machines and introduction of converter-interfaced sources and infeeds.

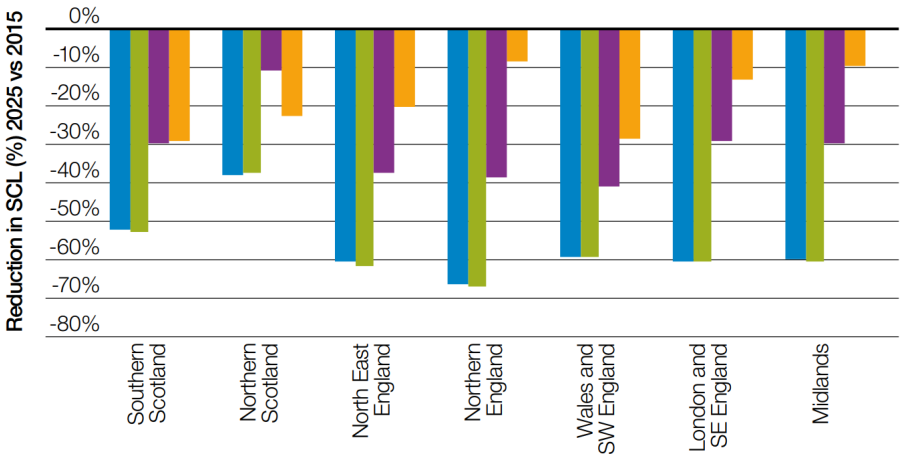

Figure 7.21: Short circuit decline 2025/26 vs 2015/16 levels [Nat15c]

In order to investigate the potential impact of reducing fault levels upon the scheme reported in this dissertation, case studies using the maximum change scenario , i.e. a 70% reduction in short circuit fault levels from prevailing values, are presented in this section.

7.4.1 Establishing threshold settings and capabilities of the scheme

According to Chapter 5, with fault levels reduced by 70% from those used in the original benchmark simulations, the sequence component parameters for the 2-bus equivalent circuits have been calculated and are presented in Table 7.11.

Based on these 2-bus equivalent model parameters and the method of evaluation and quantification of scheme capabilities (maximum fault resistances and voltage threshold for fault detection), as presented in detail in Chapter 9, a comparison of the capabilities of the scheme with the original fault levels and with reduced fault level networks is shown in Table 7.12. R_{1fmax_1} and R_{1fmax_2} rep-

Angles are in radians							
Positive (and negative) sequence (Ω)				Zero sequence (Ω)			
Line	Z_{s1_1}	Z_{s1_2}	Z_{intc1}	Line	Z_{s0_1}	Z_{s0_2}	Z_{intc0}
1	36.31 ∠1.47	84.20 ∠1.45	59.68 ∠1.29	1	23.06 ∠1.47	85.56 ∠1.45	167.52 ∠1.30
2	35.66 ∠1.40	149 ∠1.45	51.20 ∠1.20	2	37.35 ∠1.39	122.95 ∠1.46	149.43 ∠1.20
3	101.53 ∠1.47	47.54 ∠1.41	63.02 ∠1.28	3	86.36 ∠1.44	78.93 ∠1.34	260.42 ∠1.26
4	78.33 ∠1.40	54.89 ∠1.44	27.30 ∠1.18	4	100.93 ∠1.33	87.31 ∠1.36	253.26 ∠1.17
5	40.25 ∠1.44	97.61 ∠1.45	24.13 ∠1.23	5	36.51 ∠1.40	165.78 ∠1.40	69.53 ∠1.23
6	33.73 ∠1.47	100.05 ∠1.45	27.36 ∠1.24	6	20.82 ∠1.46	180.61 ∠1.40	89.68 ∠1.22
7	42.23 ∠1.44	85.45 ∠1.47	20.04 ∠1.26	7	37.00 ∠1.40	152.10 ∠1.41	69.72 ∠1.24

Table 7.11: Calculated parameters for 2-bus equivalent circuits of with reduced fault level

resent the maximum detectable three-phase fault resistance with original and reduced fault levels respectively. Similarly, R_{0fmax_1} and R_{0fmax_2} represent the maximum detectable unbalanced earth fault resistance with original and reduced fault levels. Finally, R_{2fmax_1} and R_{2fmax_2} represent the maximum detectable phase-phase fault resistance with original and reduced fault levels. In general, with the decrease in fault level, the capability of the scheme, in terms of detectable fault resistances, is higher for all types of faults. With a fault level reduction of 70%, the highest detectable fault resistance is normally 2 to 3 times of the original value and can be up to 3.25 times the value, in this case for phase-phase faults on Line 6. The highest detectable three-phase, unbalanced earth and phase-phase fault resistances can be up to 71.04 Ω, 768.4 Ω and 800 Ω respectively. For the entire network, fault resistances of 50 Ω, 196.5 Ω and 629.5 Ω for three-phase, unbalanced earth and phase-phase faults respectively could be detected at any location on any transmission line within the network.

Line	Present	Future	Present	Future	Present	Future
	R_{1fmax_1} (Ω)	R_{1fmax_2} (Ω)	R_{0fmax_1} (Ω)	R_{0fmax_2} (Ω)	R_{2fmax_1} (Ω)	R_{2fmax_2} (Ω)
1	16.6	50.1	92.3	298.1	196.5	629.5
2	25	58.78	204.6	467.6	271.7	712.6
3	34.7	71.04	339.9	672.9	340.2	800.9
4	31.7	67.37	535.1	768.4	345.7	799.6
5	16.6	50.01	97.3	305.5	192.1	624.6
6	25	58.44	243.7	488.4	265.3	704.7
7	25	58.6	243.6	486.3	259.3	698.8

Table 7.12: Comparison of scheme capability between current fault level and reduced fault level

7.4.2 Scheme operation

To demonstrate the impact of reducing fault levels on the scheme, three-phase fault scenarios are used as an example in this section. According to Table 7.12, case studies have been conducted with fault resistances varying from 1 Ω to 91 Ω with an increment of 10 Ω at four locations of each line (at each terminal and at 33% and 67% of the line length as before).

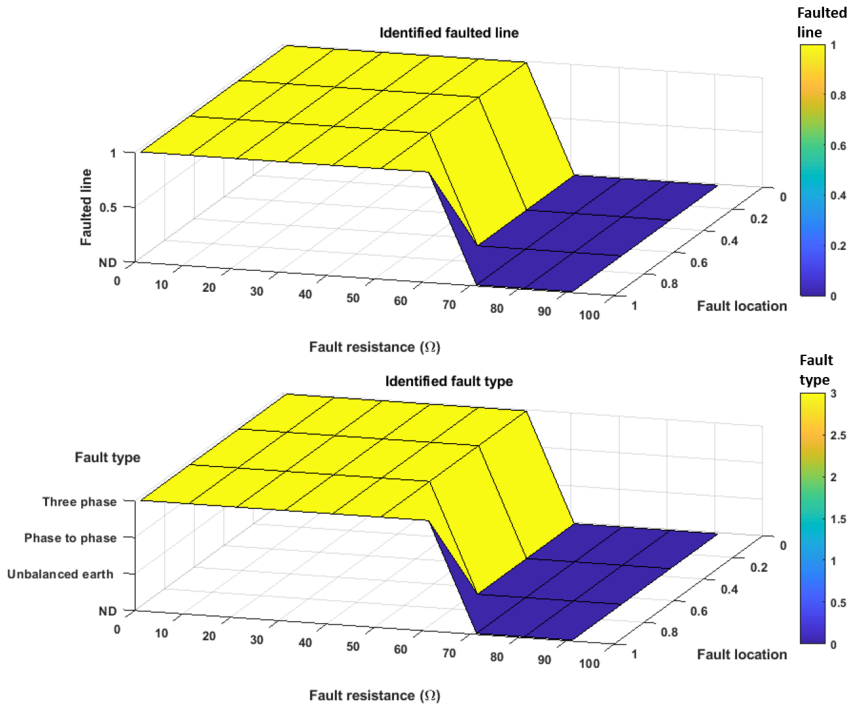

Figure 7.22: Identified fault type and faulted line vs fault resistance and fault locations for three-phase faults in reduced fault level network

Figure 7.22 presents the ability of the scheme to detect faulted lines and report fault types for line 1. It can be observed that the scheme can successfully detect the faulted line and fault type with fault resistances of up to around 50 Ω for all tested fault locations, which is much higher than the 15 Ω under the scenario where fault levels were specified with their original values. For high resistance scenarios where the fault cannot be detected by the scheme, the output of the scheme is ND which represents no detection rather than providing incorrect information, such as wrong faulted line information or wrong fault type information, which guarantees the reliability/security of the scheme for future networks with reduced fault levels.

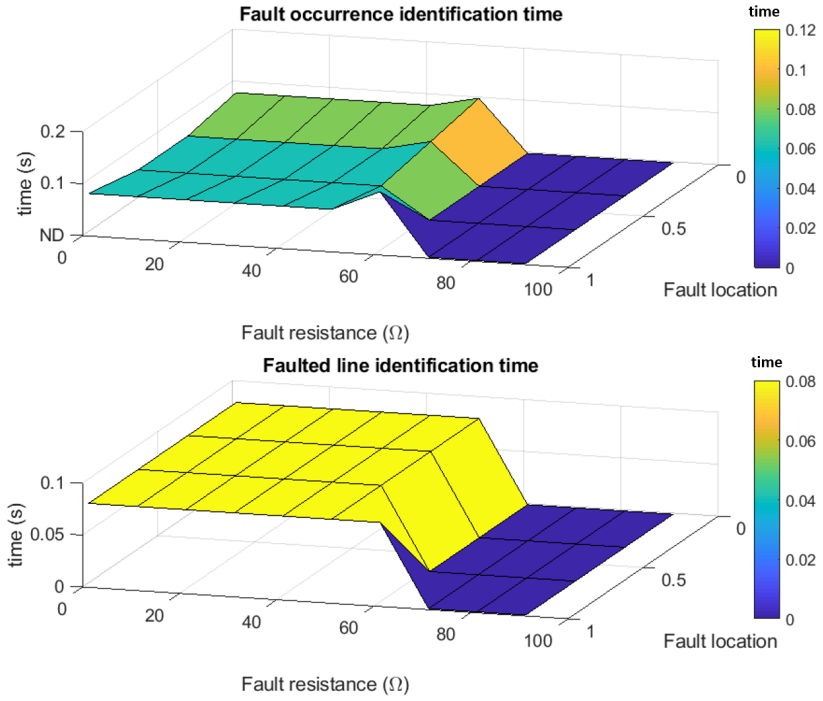

Figure 7.23: Identification time with variation of fault resistance and fault locations for three-phase faults in reduced fault level network

Figure 7.23 presents the fault occurrence and faulted line identification times (the backup protection time) for line 1. For fault resistance of less than 50 Ω, the scheme can successfully identify fault occurrence and the faulted line. The time to identify fault occurrence time ranges from 60 ms to 100 ms depending on fault locations and fault resistances. The fault occurrence identification time increases

with increasing fault resistance. As the fault location moves from node 1 to node 2, the fault occurrence identification time generally reduces. For the scenarios where faults can be detected by the scheme, the faulted line identification time (backup protection time) is always 80 ms, which indicates that as long as the fault resistance is within the detectable range, the backup protection can be provided with a delay of 80 ms following operation of one line-end main protection and opening of the circuit breaker.

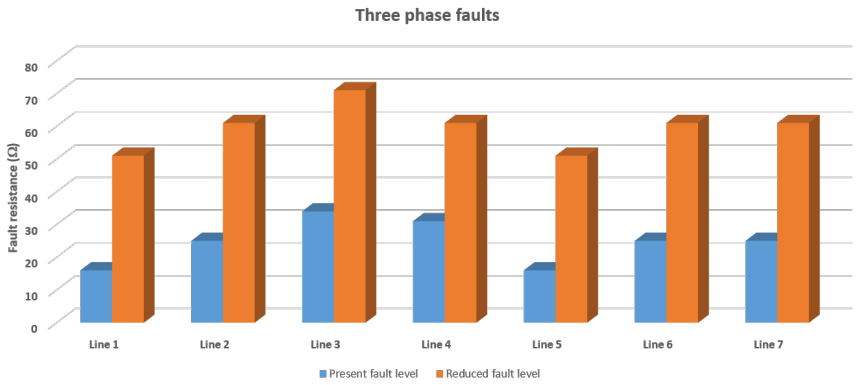

Figure 7.24: Comparison of highest detectable fault resistance between current fault level and reduced fault level

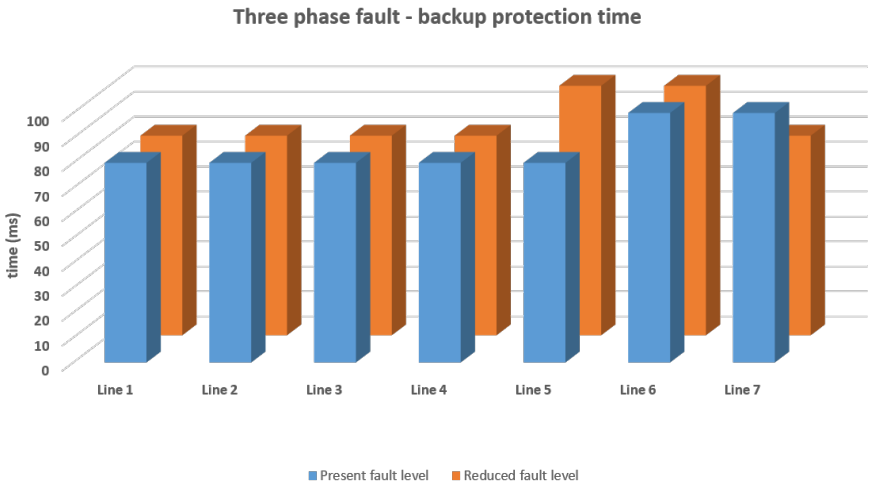

Figure 7.25: Comparison of backup protection time between current fault level and reduced fault level

Figure 7.24 and Figure 7.25 present the comparison of scheme capabilities for

the original and reduced fault level scenarios. With fault level decline by 70%, the highest detectable fault resistance increases to 2 to 3 times. The trend of the highest detectable fault resistance is consistent (e.g. the highest detectable fault resistance for line 3 is relatively the highest for both original and reduced fault level scenarios). The longest delays associated with backup protection operation (faulted line identification) for both scenarios are 100 ms, which indicates that the operation time of the scheme will not be affected by variations in fault level. Since future power systems will exhibit reduced fault levels, the case study proves the applicability of the scheme within future power networks.

7.4.3 Conclusions

This section has shown that the reduction of fault levels in future power systems will have no negative impact on the scheme. In fact, the scheme will be able to detect faults with higher resistances for future systems with reduced fault levels. The impact of reducing fault level upon the scheme has been presented through case studies on the IEEE 14-bus network as before. It has been established that the scheme is applicable to reduced fault level power systems with the ability to detect relatively high resistance faults and will not mal-operate or report wrong information under very high resistance scenarios.

Chapter 8

Hardware in the loop tests by RTDS

8.1 Introduction

The focus of this chapter is on validating the scheme, using hardware in the loop simulation (HIL)/real time simulation using RTDS facilities.

Figure 8.1 demonstrates the hardware in the loop arrangement which uses the RTDS and actual PMU hardware (created using microcontrollers and PMU algorithms developed at Strahtclyde), which can stream "real" PMU data in real time from the power system model in the RTDS – the RTDS model can also receive GOOSE messages to control circuit breakers. The real time voltage measurements from the network simulated in RSCAD are input to the PMUs interfaced to the RTDS (using a GTFPGA card) and are processed and analysed by the proposed scheme, which is implemented using a normal PC and C software (platform) and operates to read multiple PMU data streams and align the data in time. Trip signals from the algorithm are sent back to the real time simulation system and summarised information is presented via the plots in RSCAD in a real time manner using the appropriate protocols for communications (e.g. IEEE C37.118.2-2011 for PMU data and IEC 61850 GOOSE messaging for any tripping signals from the wide area backup protection scheme developed through this

research). Case studies are conducted using this simulation arrangement and the results are presented, evaluated and compared with the results from the non-real time simulation (using Matlab) results presented previously.

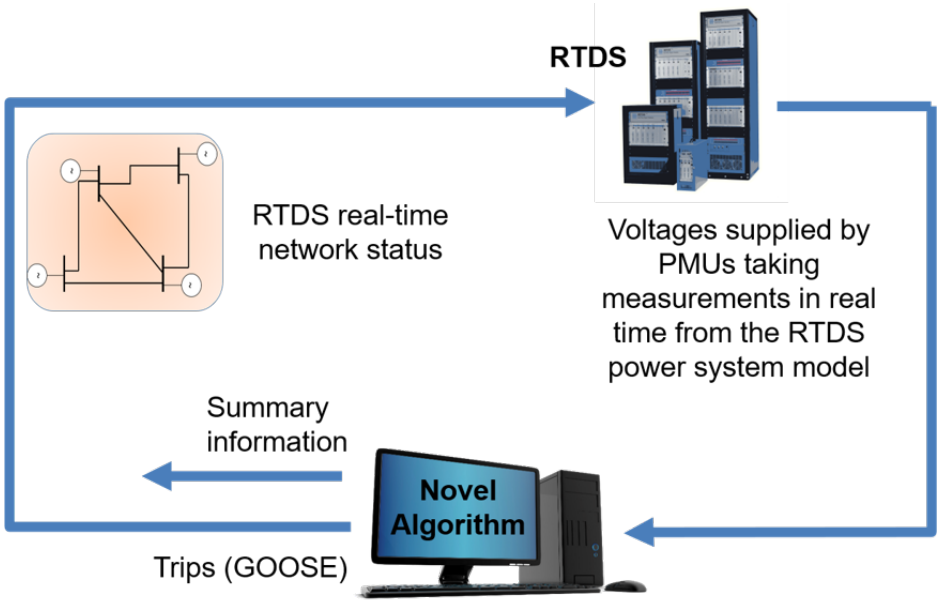

Figure 8.1: Hardware in the loop test on RTDS

The IEEE 14-bus system, identical to that used in Matlab, has been constructed using RSCAD – the power system simulation package which allows the developed models to run in real time on the RTDS. The measurement algorithms of the interfaced PMUs are based on algorithms built within University of Strathclyde [RAB13], while the software that executes the protection analysis, reporting and backup protection functions developed in this research are implemented using the RSCAD and RTDS as described earlier.

8.2 RTDS test results

8.2.1 Three-phase faults

Based on the setting information discussed in Section 7.2.2, case studies with fault resistances varying from 0.1 Ω to 50 Ω (0 Ω, 5 Ω, 10 Ω, 15 Ω, 25 Ω, 50 Ω) at four locations (terminals of the line and 33% and 67% of the line) on each line

have been conducted to validate the scheme. One of the line-end main protection operates 80 ms after fault occurrence.

Figure 8.2, 8.4 and 8.3 illustrates the response of the system for a three-phase fault on line 1 with the correct operation of main protection at the line terminal at bus 1 and the failure of the circuit breaker/protection device at the line terminal at bus 2. Figure 8.2 demonstrates the topology of the networks with generators, lines, busbars and circuit breakers. The left hand side plot of Figure 8.3 (a) indicates the tripping signal (circuit breaker status) in a digital format (1/in shadow indicates closed and 0/blank indicates open). It can be seen that after fault occurrence on line 1, BRK1 has been tripped by the main protection, and then BRK2, 3, 11, 13 and G2 are all tripped by the scheme to provide backup protection with a delay which is shown in Figure 8.3 (b). The information relating to fault type and circuit breaker status are also provided by the scheme. The right hand side plot of Figure 8.3 (a) indicates the identified faulted line (circuit) in a digital format (a fault occurrence is identified on line 1) – 0/blank indicates no fault occurrence is identified and 1/in shadow indicates the identification of the faulted line. Figure 8.3 (b) shows that the scheme can provide backup protection and trip the circuit breakers (BRK2, BRK3, BRK13, BRK11, BRKG2) connecting other lines to bus 2 within 150 ms of the original the fault occurrence and the fault is identified as a three-phase fault. Note that, while another "backup" tripping signal is also sent to BRK2 (the breaker which has not tripped, either due to failure of the breaker itself or failure of the main protection systems responsible for tripping that breaker), in a practical implementation, it is likely that the breaker has failed (rather than the both protection systems failing to trip the breaker), so the tripping signals to the other breakers (BRK3, BRK13, BRK11, BRKG2) would still be necessary. Future work could examine the possibility of "retripping" the failed breaker first, then followed by tripping the other breakers if the "retrip" was not successful.

The plot of Figure 8.4 indicates which breaker has failed (in this case it is BRK2).

The left hand side plot of Figure 8.3 (c) indicates the correct operation of main

protection – BRK1 operates correctly (i.e. has been tripped by main protection). The right hand plot of Figure 8.3 (c) indicates whether system is under the scenario of total failure of main protection or correct operation of both line-end main protection. When the output of "correct operation" (or "failure" is "1"), the system has experienced correct operation of both line-end main protections (or total failure of main protection). Otherwise, the system has not experienced a fault or there is requirement for backup (one line-end main protection has operated, but the other has failed). In the presented system, one line-end main protection (BRK1) operates correctly and one fails, so the output of both "correct operation" and "failure" are "0".

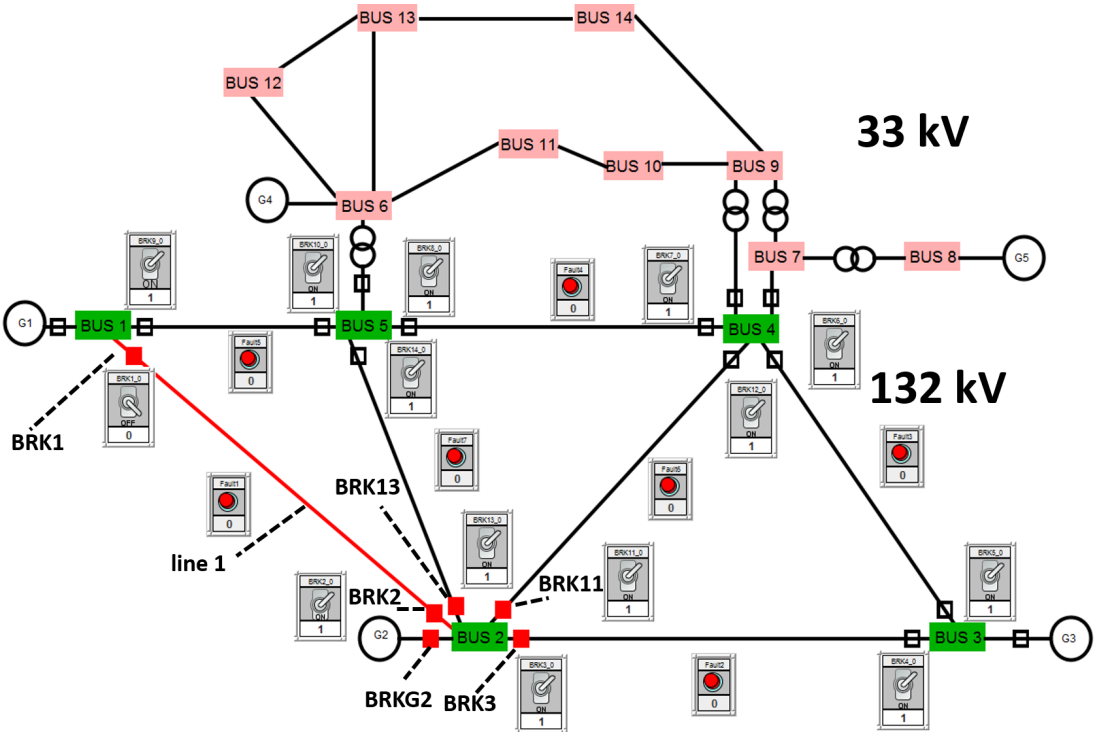

Figure 8.2: Network in RTDS

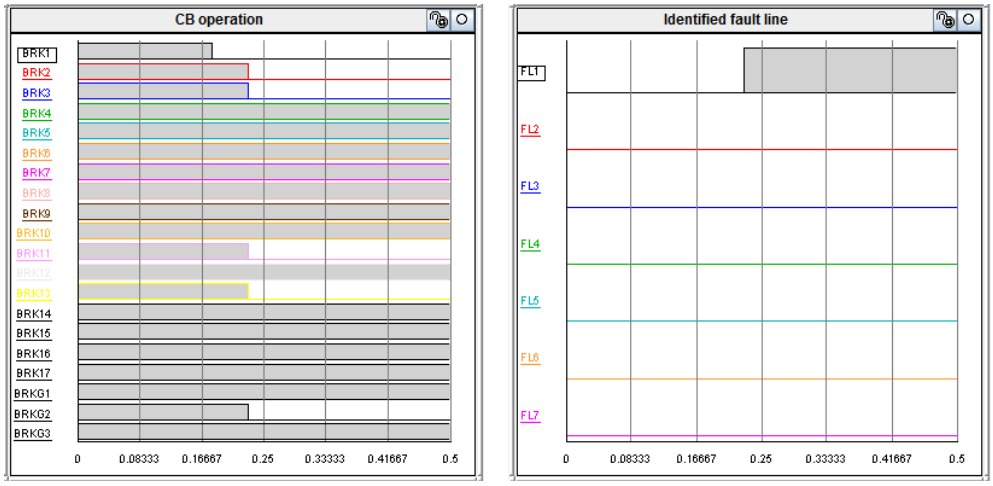

(a) Backup protection provided by the scheme and the identified faulted line

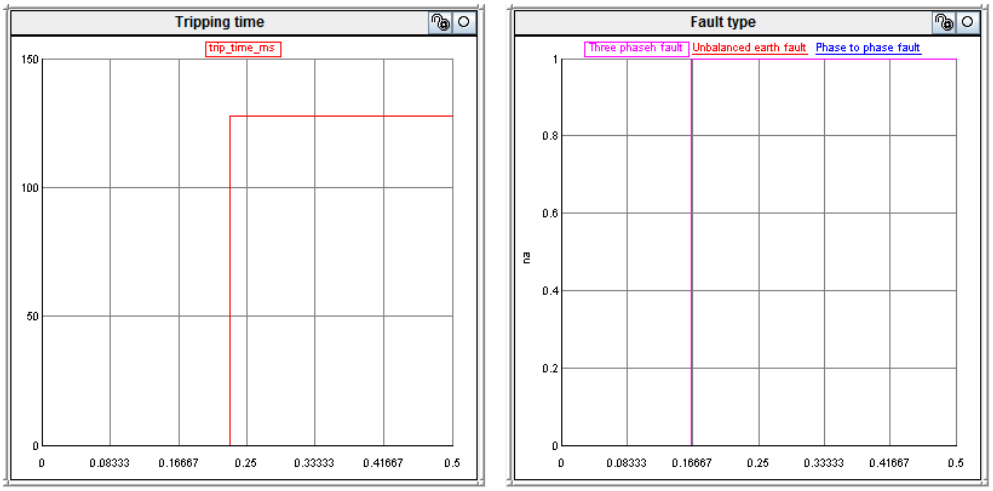

(b) Tripping time of the sche8me and the fault type of the scheme

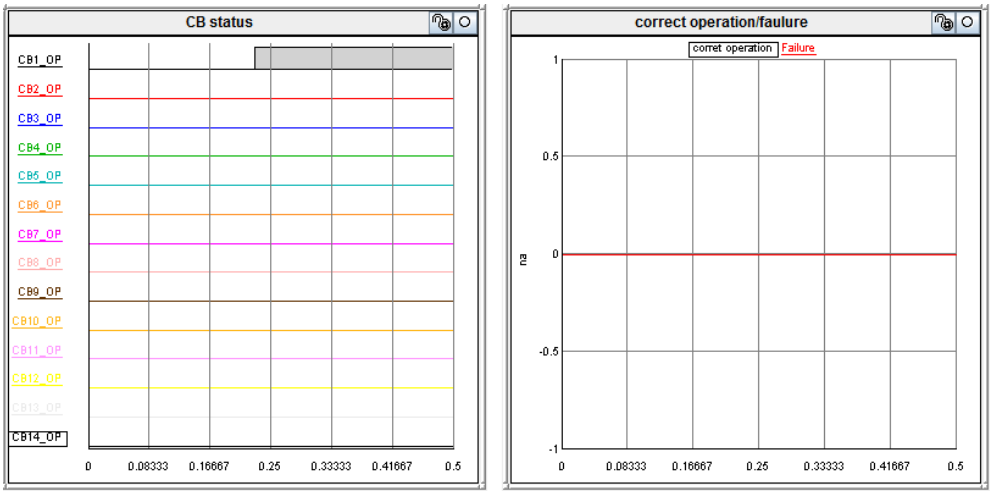

(c) Circuit breaker status

Figure 8.3: line 1 fault with operation of CB1

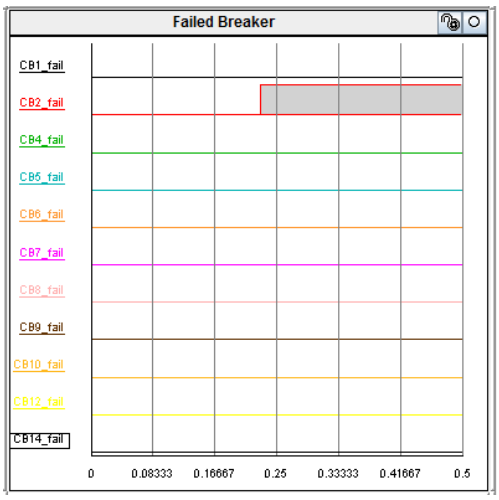

Figure 8.4: Failure of line-end main protection

In order to demonstrate the impact of variation of fault resistance, a 3D figure is shown in Figure 8.5 to present the faulted line identification time (the backup protection operation time) corresponding to variation of fault resistances and fault locations on line 1. It can be inferred that for fault resistances of less than approximately 15 Ω, the scheme can successfully provide backup protection for a fault at any location of the line. Since the tests are based on real-time operation, faulted line detection (backup protection) time is impacted by the time of occurrence (point on wave), which leads to the variation of faulted line identification time, each time conducting the test.

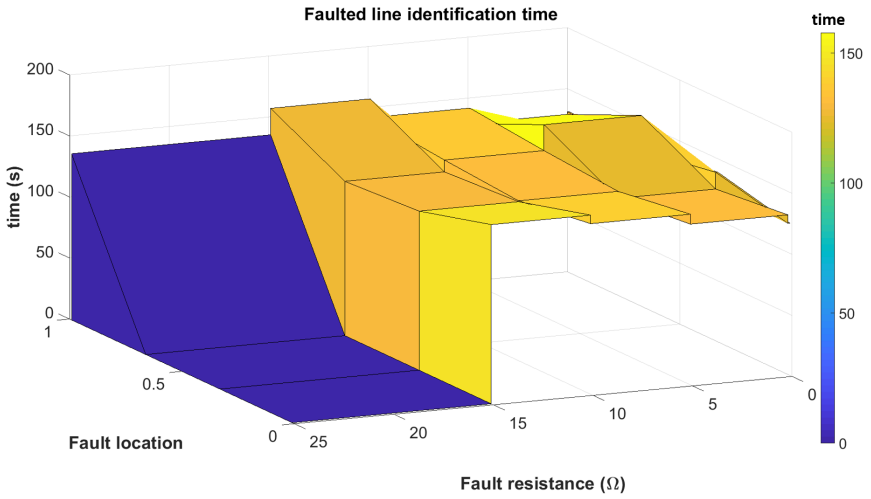

Figure 8.5: Identification time with variation of fault resistance and fault locations for three-phase faults

RTDS results							
Faulted line	Line 1	Line 2	Line 3	Line 4	Line 5	Line 6	Line 7
Highest detectable fault resistance (Ω)	15	25	25	25	15	25	25
Faulted line identification time (ms)	157.9	161.3	162.5	186.6	187.4	173.6	167.3
Matlab results							
Faulted line	Line 1	Line 2	Line 3	Line 4	Line 5	Line 6	Line 7
Highest detectable fault resistance (Ω)	16	25	34	31	16	25	25
Faulted line identification time (ms)	180	180	180	180	180	200	200

Table 8.1: Comparison between RTDS and Matlab results of three-phase to earth faults

For the scenarios where faults can be detected by the scheme, the faulted line identification time (backup protection time) is always in the range of 120 to 200 ms (after occurrence of the fault). Please note that in the figure below, and other similar figures, a time of 0 ms indicates that the faulted line has not been identified (e.g. for fault locations of 0, 33% and 67% with fault resistances of higher than 15 Ω in the figure below.

Results for all lines (both conducted by RTDS and Matlab) are shown in Table 8.1. The "faulted line identification time" row presents the maximum time the scheme requires to identify the faulted line (and execute backup protection) under the scenarios where fault resistance is less than the highest detectable fault resistance (i.e. when fault is detectable). The row, highest detectable fault resistance, is self-explanatory. Since the accuracy of tests are different between RTDS and Matlab results (50 Ω is the next tested fault resistance that higher than 25 Ω in RTDS and the tests are conducted with 1 Ω increment in Matlab), the results of highest detectable fault resistance of both Line 3 and Line 4 are different conducted in RTDS and Matlab. The faulted line identification time is generally shorter in RTDS than in Matlab due to the different sampling rate and the processing time under different environment.

8.2.2 Unbalanced earth faults

Based on the setting information discussed in Section 7.2.2, case studies with fault resistances varying from 1 Ω to 200 Ω (0.1 Ω, 5 Ω, 10 Ω, 15 Ω, 25 Ω, 30 Ω, 40 Ω, 50 Ω, 100 Ω, 200 Ω)at four locations (terminals of the line and 33% and 67% of the line) on each line have been conducted to validate the scheme. One of the line-end main protection operates 80 ms after fault occurrence.

8.2.2.1 Single-phase to earth faults

In order to demonstrate the impact of variation of fault resistance, a 3D figure is shown in Figure 8.6 to present the faulted line identification time (the backup protection time) corresponding to variation of fault resistances and fault locations on line 1. It can be inferred that for fault resistance of less than approximately 100 Ω, the scheme can successfully provide backup protection a fault at any location of the line. Since the tests are based on real-time monitoring, faulted line detection (backup protection) time would be impacted by the time of occurrence (point on wave), which again leads to the variation of faulted line identification time, each time conducting the test.

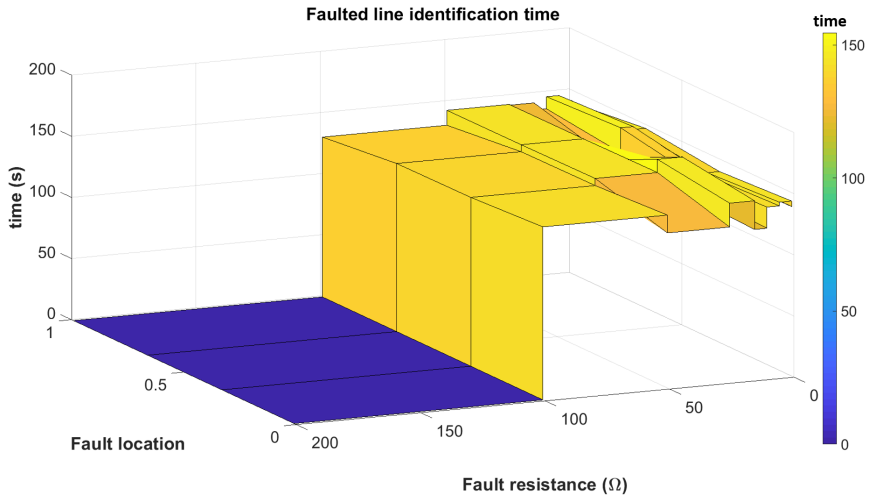

Figure 8.6: Identification time with variation of fault resistance and fault locations for single-phase to earth faults

For the scenarios that the faults can be detected by the scheme, the faulted line identification time (backup protection time) is is always in the range of 120

RTDS results							
Faulted line	Line 1	Line 2	Line 3	Line 4	Line 5	Line 6	Line 7
Highest detectable fault resistance (Ω)	100	200	200	200	100	200	200
Faulted line identification time (ms)	154.6	157.4	193.3	167.3	157.4	187.4	165.5
Matlab results							
Faulted line	Line 1	Line 2	Line 3	Line 4	Line 5	Line 6	Line 7
Highest detectable fault resistance (Ω)	101	201	241	241	101	241	241
Faulted line identification time (ms)	180	180	200	160	200	200	200

Table 8.2: Comparison between RTDS and Matlab results of single-phase to earth faults

to 200 ms (after occurrence of the fault). Again, please note that in the figure below, and other similar figures, a time of 0 ms indicates that the faulted line has not been.

Results for all lines (conducted in both RTDS and Matlab) are shown in Table 8.2. The "faulted line identification time" row presents the maximum time the scheme requires to identify the faulted line (and execute backup protection) under the scenarios where fault resistance is less than the highest detectable fault resistance (i.e. when fault is detectable). The row, highest detectable fault resistance, is self-explanatory. Since the highest fault resistance used to conduct tests in RTDS is 100 Ω and the the highest fault resistance tested in Matlab is 241 Ω with 20 Ω increment, the results of highest detectable fault resistance of Line 3, Line 4, Line 6 and Line 7 are different conducted in RTDS and Matlab. The faulted line identification time is generally shorter in RTDS than in Matlab due to the different sampling rate and the processing time under different environment.

RTDS results							
Faulted line	Line 1	Line 2	Line 3	Line 4	Line 5	Line 6	Line 7
Highest detectable fault resistance (Ω)	100	200	200	200	100	200	200
Faulted line identification time (ms)	168.5	161.5	157.8	161.2	161.2	165.5	159.9
Matlab results							
Faulted line	Line 1	Line 2	Line 3	Line 4	Line 5	Line 6	Line 7
Highest detectable fault resistance (Ω)	101	201	241	241	101	241	241
Faulted line identification time (ms)	180	180	200	180	200	200	200

Table 8.3: Comparison between RTDS and Matlab results of phase-phase to earth faults

8.2.2.2 Phase-phase to earth faults

The results of phase-phase to earth faults with variation of fault locations and fault resistance (both conducted in RTDS and Matlab) are illustrated in Table 8.3, which indicates that the scheme can correctly detect / provide backup protection to a phase-phase fault with up to 200 Ω on any location of the transmission line in the IEEE 14-bus 132 kV level networks with maximum operation time of 168.5 ms. Since the highest fault resistance used to conduct tests in RTDS is 200 Ω and the the highest fault resistance tested in Matlab is 241 Ω with 20 Ω increment, the results of highest detectable fault resistance of Line 3, Line 4, Line 6 and Line 7 are different conducted in RTDS and Matlab. The faulted line identification time is generally shorter in RTDS than in Matlab due to the different sampling rate and the processing time under different environment.

8.2.3 Phase-phase faults

Case studies with fault resistance varying from 1 Ω to 200 Ω (0.1 Ω, 5 Ω, 10 Ω, 15 Ω, 25 Ω, 30 Ω, 40 Ω, 50 Ω, 100 Ω, 200 Ω, 300 Ω) at four locations (terminals of the line and 33% and 67% of the line) on each line are conducted in this section.

RTDS results							
Faulted line	Line 1	Line 2	Line 3	Line 4	Line 5	Line 6	Line 7
Highest detectable fault resistance (Ω)	200	200	300	300	200	200	200
Faulted line identification time (ms)	157.4	167.3	162.1	163	170.9	171.3	172.6
Matlab results							
Faulted line	Line 1	Line 2	Line 3	Line 4	Line 5	Line 6	Line 7
Highest detectable fault resistance (Ω)	201	281	341	341	201	261	261
Faulted line identification time (ms)	180	200	180	180	200	200	200

Table 8.4: Comparison between RTDS and Matlab results of phase-phase faults

Results of all lines are shown in Table 8.4. The "faulted line identification time" row presents the maximum time the scheme requires to identify the faulted line (and execute backup protection) under the scenarios where fault resistance is less than the highest detectable fault resistance (i.e. when fault is detectable). The row, highest detectable fault resistance, is self-explanatory. Since the highest fault resistance used to conduct tests in RTDS is 300 Ω (with increment of 100 Ω from 200 Ω to 300 Ω) and the the highest fault resistance tested in Matlab is 341 Ω with 20 Ω increment, the results of highest detectable fault resistance of Line 3, Line 4, Line 6 and Line 7 are different conducted in RTDS and Matlab. The faulted line identification time is generally shorter in RTDS than in Matlab due to the different sampling rate and the processing time under different environment.

8.3 Conclusions

This chapter has presented a hardware implementation and validation of the scheme through conducting case studies using an RTDS with the IEEE 14-bus network and hardware in the loop, with consideration of different fault locations and resistances.

It has been shown that, for all types of faults, the scheme can provide backup protection (detect the faulted line) within 193.3 ms from fault occurrence (113.3 ms after operation of main protection). Since the range of main protection operation time is 80 ms to 140 ms (GB transmission level power systems), and in this section all case studies are conducted with 80 ms of main protection operation time, the backup protection provided by the scheme can operate within a maximum time of 253.3 ms referred to the moment of fault occurrence, which has the potential to provide a relatively fast backup protection with no extra cost compared to conventional backup protection. The chapter has demonstrated the capability of the scheme in detecting three-phase, unbalanced earth and phase-phase faults with fault resistances of up to 25 Ω, 200 Ω and 300 Ω respectively on the IEEE 14-bus network. The thresholds used are the same as in the other simulations and case studies presented earlier (85% for positive sequence voltage magnitude and 2% for zero and negative sequence voltage magnitudes).

The reporting and analysis function of the scheme has also been demonstrated in this section. Information including fault type, faulted line and status of circuit breaker/protection can be provided to the system operator for better understanding of the system status under faults .

Chapter 9

Conclusions and Further Work

9.1 Conclusions

A wide-area protection analysis and reporting scheme, with the capability to provide backup protection, has been presented and its operation demonstrated comprehensively in this dissertation. The scheme relies solely on voltage measurements from PMUs distributed throughout the power system. It can provide a cost-effective alternative (or additional layer) of backup protection and utilises measurement devices and communications infrastructure that may already be in place for other purposes, so can be viewed as a cost effective solution. It is also well-suited to address the challenges that power systems, and associated protection systems, will be facing increasingly in the future as system strength and fault levels reduce in due to the widespread integration of renewable energy sources and converter interfaces (to connected renewables and HVDC interconnectors to the AC system), the majority of which do not contribute significant inertial responses or fault current during faults.

The work has been placed in the context of related research. A comprehensive literature review has been presented, showing the merits of the developed scheme and how it compares favourably with and addresses many of the shortcomings associated with other schemes proposed by researchers working in related fields.

As already stated, the scheme is cost-effective due to the requirements for

only voltage measurements from the busbars (as opposed to measurements from the individual terminals of transmission lines, which may be prohibitively expensive and potentially impractical from the amount of measurement data and requirements for high-performance communications infrastructure).

The proposed system is capable of providing relatively fast and accurate fault location to the transmission line level, followed by analysis of protection and circuit breaker performance from observed voltage magnitudes and transients, with ability to provide backup protection for the network when it is deemed that a circuit breaker has failed to open as instructed. The methods of establishing the capabilities of the scheme (in terms of the maximum fault resistances identifiable for given voltage threshold settings, or the threshold settings required for a desired maximum fault resistance that should be identified) are presented, and settings can be readily and automatically recalculated if there is a significant change in the power system structure and/or fault levels. Accordingly the scheme can be deemed highly adaptable to system operating conditions. The operation of the scheme has been demonstrated and validated through various case studies, using both non-real time and real time platforms, namely of Matlab (Simscape) and an RTDS with hardware in the loop arrangement.

9.2 Future work

9.2.1 Demonstration and validation of the scheme in power systems incorporating converter-interfaced sources

The tests and validation exercises presented in Chapters 7 and 8 could be expanded to applications where the power system incorporates converter-based sources. One of the challenges for presently-applied protection schemes is in adapting to the future power systems where fault currents may be severely constrained converter-interfaced sources. In contrast with conventional backup protections, the scheme proposed in this dissertation depends only on voltage mea-

surements and has shown to be tolerant to the reduction of fault currents (indeed it may operate more effectively in weak systems, with the ability to identify faults with higher resistances when system fault levels decreases, as shown earlier). Further research is needed to investigate the application of the scheme to systems dominated by converter-interfaced sources, as both the voltage drops (increases of negative/zero sequence voltages) and recovery following fault clearance/circuit breaker opening, may change in the future.

9.2.2 Further testing using a range of complex networks

The scheme has been tested on the IEEE 14-bus network which is widely used by many researchers. However, before application of the scheme to actual power systems, it must to be tested and validated on a wide range of complex networks, such as IEEE 57-bus networks and IEEE 69-bus networks, and possibly, as mentioned before, on systems where the system strength has already been used (e.g. sections of the GB network with high penetrations of renewables).

The tests and case studies used in the research could be extended to include communications emulators, or even actual communications hardware/switches, along with commercially available PMUs (and computing hardware) for implementation of the scheme in a more realistic environment (either with RTDS or in a power system test/demonstration environment, such as PNDC) prior to actual installation in the field.

9.2.3 The study of voltage recovery and impact on protection

As mentioned already, the proliferation of converter-interfaced sources (HVDC links and renewable energy sources), the rate of voltage recovery following faults might be different from at present. The study of voltage recovery and the subsequent impact on the scheme could be further investigated to adapt the power systems in the future better.

9.2.4 Further development of user interface for the scheme

Before industrial application, user interfaces require to be developed. The scheme must incorporate a user-friendly intuitive and graphically-rich interface to assist system operators and provide them with analysis and summarised information for decisions support and to assist in operating the system and maintaining stability.

9.2.5 Faulted phase identification

The work in Section 4.2.7 provides the function of distinguishing fault types. Specific faulted phase could be further identified, which may potentially enhance information provided to maintenance teams through reducing the time for faulted phase identification (in the event of permanent faults) and benefits the system operator by providing extra information relating to the fault.

9.2.6 Backup protection for busbar faults

The proposed scheme aims to provide backup protection for transmission lines. Busbar faults have not been considered as a major target for application in this work to date, however, the practicality of the scheme for busbar faults (although they are very rare) could be further investigated and the scheme may be extended to provide backup protection for both line and bubar faults.

9.2.7 Implementation in distribution networks

The use of the scheme in distribution networks is of considerable interest, particular with the development of the microPMU concept [SCY$^+$17, TGCR17]. With injection of embedded generations, the conventional protection schemes for distribution networks (largely based on overcurrent protection) could prove very challenging. With wide-area information, the proposed scheme could potentially be applied in distribution level and be an alternative of traditional backup protection, or perhaps even for main protection, or to assist with fault identification

and post-fault reconfiguration. Further research is needed to investigate the suitability and applicability of the scheme within distribution networks.

9.2.8 Consideration of evolving faults

Anecdotal evidence suggests that evolving faults (e.g. a fault which begins as a single-phase to earth fault or a phase-to-phase fault but then evolves to include other phases [Cos08]) are relatively uncommon on overhead transmission systems; however they could be worthy of considering in the future to establish how the scheme developed in this research project may perform for scenarios where faults evolve from one type to another. Evolving faults may be more common on three-phase underground cable systems or GIS (Gas Insulation Substation) installations, where all three phases are contained within the same physical insulation system. In such environments, a single-phase to earth fault on a three-phase cable (or within a GIS chamber) may rapidly evolve to become a three-phase fault.

Accordingly, future work could consider evolving faults, with analysis of evolution of faults from various types to others, along with different evolution times, being investigated. Evidence for evolving faults on overhead transmission lines is scant in the literature, so the requirement for such functionality is questionable if the scheme developed through this research is applied to overhead transmission systems. Nevertheless, if appropriate statistical evidence could be gathered relating to the frequency of occurrence, typical evolution "paths" experienced in practice (i.e. how the faults might typically originate, how they evolve, and how long the process might take), then such scenarios could be simulated. The performance of the scheme could then be tested, with appropriate modifications made to the fault detection identification and location algorithms made if deemed necessary. Finally, it is anticipated that evolution times would probably be relatively short (sub-cycle), so the existing scheme is probably relatively immune to any major problems associated with rapidly-evolving faults, but this could be verified and quantified via further work.

Bibliography

[ABBa] ABB. Instrument transformers technical information and application guide. Technical report. (cited on page 184)

[ABBb] ABB. Line thermal monitoring — dynamic rating of transmission lines. Technical report. (cited on pages xi, 67)

[ABB99] ABB. Breaker failure relay REB 010. Technical report, 1999. (cited on page 40)

[ABB15] ABB. Wide-area monitoring and control. Technical report, 2015. (cited on pages xi, 67)

[ACA+12] M. Q. Ahsan, A. H. Chowdhury, S. S. Ahmed, I. H. Bhuyan, M. A. Haque, and H. Rahman. Technique to develop auto load shedding and islanding scheme to prevent power system blackout. *IEEE Transactions on Power Systems*, 27(1):198–205, Feb 2012. doi:10.1109/TPWRS.2011.2158594. (cited on page 9)

[AK18] A.M. Abdullah and K.Butler-Purry. Distance protection zone 3 misoperation during system wide cascading events: The problem and a survey of solutions. In *Electric Power Systems Research*, volume 154, pages 151–159, Jan 2018. (cited on page 74)

[Als11] Alstom Grid. *Network Protection & Automation Guide – protective relays, measurements & control.* ALSTOM GRID, 2011. (cited on pages x, 26, 28, 29, 30, 33, 34, 37)

[And99] P.M. Anderson. *Power System Protection.* IEEE Press, 1999. (cited on pages 26, 30, 35)

[ATM07] H. J. Altuve, M. J. Thompson, and J. Mooney. Advances in breaker-failure protection. In *20th Power, Industrial Applications and Industrial Exhibition Summer Meeting*, July 2007. (cited on pages 36, 41, 42)

[ATR04] A. P. Apostolov, D. Tholomier, and S. H. Richards. Superimposed components based sub-cycle protection of transmission lines. In *IEEE PES Power Systems Conference and Exposition, 2004.*, pages 592–597 vol.1, Oct 2004. doi:10.1109/PSCE.2004.1397508. (cited on page 115)

[Bad17] Babak Badrzadeh. Analysis of the South Australian blackout, 2017. (cited on page 45)

[Bla13] S. Blair. *The Analysis and Application of Resistive Superconducting Fault Current Limiters in Present and Future Power Systems.* PhD thesis, University of Strathclyde, 2013. (cited on pages x, 29)

[BTC12] E. E. Bernabeu, J. S. Thorp, and V. Centeno. Methodology for a security/dependability adaptive protection scheme based on data mining. *IEEE Transactions on Power Delivery*, 27(1):104–111, Jan 2012. doi:10.1109/TPWRD.2011.2168831. (cited on pages xi, 74, 76)

[Cas18] Castor. Symmetrical components and easy power - an introduction. Technical report, 2018. URL: https://www.easypower.com/files/Symmetrical-Components-Webinar.pdf. (cited on pages 20, 21)

[CGLW15] J. H. Chow, S. G. Ghiocel, M. Liehr, and F. Wilches-Bernal. Voltage stability applications using synchrophasor data: Final report. Technical report, 2015. (cited on pages xi, 67)

[Con08] Consortium for Electric Solutions, Electric Power Group. NERC frequency monitoring and analysis (fma) application functional specification. Technical report, 2008. (cited on pages xi, 67)

[Cor09] S. Corsi. Wide area voltage regulation amp; protection. In *2009 IEEE Bucharest PowerTech*, pages 1–7, June 2009. doi:10.1109/PTC.2009.5282180. (cited on pages xi, 67)

[Cos08] D. Costello. Lessons learned analyzing transmission faults. In *2008 61st Annual Conference for Protective Relay Engineers*, pages 410–422, April 2008. doi:10.1109/CPRE.2008.4515068. (cited on page 224)

[CWSH17] M. Chen, H. Wang, S. Shen, and B. He. Research on a distance relay-based wide-area backup protection algorithm for transmission lines. *IEEE Transactions on Power Delivery*, 32(1):97–105, Feb 2017. doi:10.1109/TPWRD.2016.2599198. (cited on pages 79, 80)

[CZMK16] H. Chen, L. Zhang, J. Mo, and K.E.Martin. Synchrophasor-based real-time state estimation and situational awareness system for power system operation. *Journal of Modern Power Systems and Clean Energy*, 4:370–382, July 2016. (cited on pages xi, 67)

[Das17] J. C. Das. *Understanding Symmetrical Components for Power System Modelling*. Wiley-IEEE Press, 2017. (cited on page 21)

[Ela17] S. Elangovan. Recent trends in sustainable development of renewable energy. In *2017 International Conference on Advances in Electrical Technology for Green Energy (ICAETGT)*, pages 148–150, Sep. 2017. doi:10.1109/ICAETGT.2017.8341469. (cited on page 2)

[Ele15] Electrical Technology. SCADA systems for electrical distribution. Technical report, 2015. (cited on page 60)

[EME10] M. M. Eissa, M. E. Masoud, and M. M. M. Elanwar. A novel back up wide area protection technique for power transmission grids using phasor measurement unit. *IEEE Transactions on Power Delivery*, 25(1):270–278, Jan 2010. doi:10.1109/TPWRD.2009.2035394. (cited on pages 70, 73)

[EME18] R. Eriksson, N. Modig, and K. Elkington. Synthetic inertia versus fast frequency response: a definition. *IET Renewable Power Generation*, 12(5):507–514, 2018. doi:10.1049/iet-rpg.2017.0370. (cited on page 4)

[Ene15] Energy & Climate. Realities behind 'blackout britain'. Technical report, 2015. (cited on page 50)

[ENT09] ENTSO-E. Grid disturbance and fault statistics. Technical report, 2009. (cited on page 51)

[ENT16] ENTSO-E. Network code on requirements for grid connection of generators. Technical report, 2016. (cited on pages xi, 8, 49, 50)

[For18] C. L. Fortescue. Method of symmetrical co-ordinates applied to the solution of polyphase networks. *Transactions of the American Institute of Electrical Engineers*, XXXVII(2):1027–1140, July 1918. doi:10.1109/T-AIEE.1918.4765570. (cited on page 18)

[GE 07] GE Grid Solutions. Transmission line protection principles. Technical report, 2007. URL: https://www.gegridsolutions.com/smartgrid/Dec07/1-transmission.pdf. (cited on page 24)

[Geo13] Georgia Institute of Technology. Distributed dynamic state estimator, generator parameter estimation and stability monitoring demonstration. Technical report, 2013. (cited on pages xi, 67)

[GHCT06] R. Giovanini, K. Hopkinson, D. V. Coury, and J. S. Thorp. A primary and backup cooperative protection system based on wide area agents. *IEEE Transactions on Power Delivery*, 21(3):1222–1230, July 2006. doi:10.1109/TPWRD.2006.876984. (cited on page 47)

[GK15] R. Gore and M. Kande. Analysis of wide area monitoring system architectures. In *2015 IEEE International Conference on Industrial Technology (ICIT)*, pages 1269–1274, March 2015. doi:10.1109/ICIT.2015.7125272. (cited on pages xi, 63, 64, 65, 66)

[GRM15] P. Gopakumar, M. J. B. Reddy, and D. K. Mohanta. Transmission line fault detection and localisation methodology using PMU measurements. *IET Generation, Transmission Distribution*, 9(11):1033–1042, 2015. doi:10.1049/iet-gtd.2014.0788. (cited on page 77)

[GSO12] J. Glover, M. Sarma, and T. Overbye. *Power System Analysis and Design*. Cengage Learning, 2012. (cited on pages x, 17, 19, 26, 29)

[GT18] F. Gonzalez-Longatt and Jose. Torres. *Advanced Smart Grid Functionalities Based on PowerFactory*. Springer International publishing AG, 2018. (cited on pages xv, 65)

[HBM02] W. Hays, BH Electronics, and M. Minn. Exploring current transformer applications. Technical report, 2002. (cited on page 55)

[HD16] T. P. Hinge and S. S. Dambhare. A novel approach for calibration of instrument transformers using synchrophasors. In *2016 National Power Systems Conference (NPSC)*, pages 1–5, Dec 2016. doi:10.1109/NPSC.2016.7858943. (cited on pages xi, 67)

[Hea98] M. Heathcote. *J & P Transformer Book*. Newnes, 1998. (cited on pages 21, 33)

[HP06] S. H. Horowitz and A. G. Phadke. Third zone revisited. *IEEE Transactions on Power Delivery*, 21(1):23–29, Jan 2006. doi:10.1109/TPWRD.2005.860244. (cited on page 9)

[HP08] S.H. Horowitz and A.G. Phadke. *Power System Relaying*. Research Studies Press Limited, 2008. (cited on pages x, 31, 32, 54)

[HTP+18] E. Hossain, M. R. Tür, S. Padmanaban, S. Ay, and I. Khan. Analysis and mitigation of power quality issues in distributed generation systems using custom power devices. *IEEE Access*, 6:16816–16833, 2018. doi:10.1109/ACCESS.2018.2814981. (cited on page 5)

[Hua15] Huawei. World's first LTE based wireless broadband network for power distribution automation. 2015. (cited on page 10)

[HYH+16] J. He, T. Yip, Y. Huang, Z. Wang, and L. Liu. Digital substation backup protection using a multi-agent system approach. In *13th International Conference on Development in Power System Protection 2016 (DPSP)*, pages 1–6, March 2016. doi:10.1049/cp.2016.0089. (cited on page 47)

[HZC+11] Z. He, Z. Zhang, W. Chen, O. P. Malik, and X. Yin. Wide-area backup protection algorithm based on fault component voltage distribu-

tion. *IEEE Transactions on Power Delivery*, 26(4):2752–2760, Oct 2011. doi:10.1109/TPWRD.2011.2165971. (cited on pages 10, 68, 73)

[IDA12] IDAHO Power. Introduction to power system. Technical report, 2012. URL: https://www.eiseverywhere.com/file_uploads/aaf42a76a5588f69c7a1348d6f77fe0f_Introduction_to_System_Protection-_Protection_Basics.pdf. (cited on page 24)

[IEE82] Summary update of practices on breaker failure protection. *IEEE Transactions on Power Apparatus and Systems*, PAS-101(3):555–563, March 1982. doi:10.1109/TPAS.1982.317268. (cited on pages 39, 40)

[IEE16] IEEE. IEEE recommended practice for excitation system models for power system stability studies. *IEEE Std 421.5-2016 (Revision of IEEE Std 421.5-2005)*, pages 1–207, Aug 2016. doi:10.1109/IEEESTD.2016.7553421. (cited on pages 16, 42)

[Ind] Inductive automation. What is SCADA. Technical report. (cited on pages xi, 61)

[J.D11] T.J. Overbye J.D.Glover, M. S. Sarma. *Protection of Electrical Networks*. Cengage Learning, 2011. (cited on page 18)

[JSP16] M. K. Jena, S. R. Samantaray, and B. K. Panigrahi. Supervisory control based wide area back-up protection scheme for power transmission network. In *2016 National Power Systems Conference (NPSC)*, pages 1–5, Dec 2016. doi:10.1109/NPSC.2016.7858869. (cited on page 74)

[JSP17] M. K. Jena, S. R. Samantaray, and B. K. Panigrahi. A new wide-area backup protection scheme for series-compensated transmission system. *IEEE Systems Journal*, 11(3):1877–1887, Sep. 2017. doi:10.1109/JSYST.2015.2467218. (cited on pages 74, 75)

[JZLZ13] X. Jing, J. Zhong, S. Lin, and C. Zhan. A novel overcurrent protection method based on wide area measurement in smart grid. In *2013 IEEE Grenoble Conference*, pages 1–6, June 2013. doi:10.1109/PTC.2013.6652187. (cited on page 78)

[KDS10] R. Kumar, M. L. Dewal, and K. Saini. Utility of SCADA in power generation and distribution system. In *2010 3rd International Conference on Computer Science and Information Technology*, volume 6, pages 648–652, July 2010. doi:10.1109/ICCSIT.2010.5564689. (cited on page 62)

[KHL04a] D. Karlsson, M. Hemmingsson, and S. Lindahl. Wide area system monitoring and control - terminology, phenomena, and solution implementation strategies. *IEEE Power and Energy Magazine*, 2(5):68–76, Sep. 2004. doi:10.1109/MPAE.2004.1338124. (cited on pages 10, 58)

[KHL04b] D. Karlsson, M. Hemmingsson, and S. Lindahl. Wide area system monitoring and control - terminology, phenomena, and solution implementation strategies. *IEEE Power and Energy Magazine*, 2(5):68–76, Sep. 2004. doi:10.1109/MPAE.2004.1338124. (cited on page 54)

[KINO98] Y. Katsube, K. Ise, K. Nagami, and Y. Ohba. Study on ATM label switching network architecture. In *1998 IEEE ATM Workshop Proceedings. 'Meeting the Challenges of Deploying the Global Broadband Network Infrastructure' (Cat. No.98EX164)*, pages 43–50, May 1998. doi:10.1109/ATM.1998.675114. (cited on page 72)

[KK10] J. Kabouris and F. D. Kanellos. Impacts of large-scale wind penetration on designing and operation of electric power systems. *IEEE Transactions on Sustainable Energy*, 1(2):107–114, July 2010. doi:10.1109/TSTE.2010.2050348. (cited on pages x, 7, 8)

[KOF+15] C. G. Kaloudas, L. F. Ochoa, I. Fletcher, B. Marshall, and S. Majithia. Investigating the declining reactive power demand of UK distribution networks. In *2015 IEEE Power Energy Society General Meeting*, pages 1–5, July 2015. doi:10.1109/PESGM.2015.7286464. (cited on page 5)

[KP15] P. Kundu and A. K. Pradhan. Online identification of protection element failure using wide area measurements. *IET Generation, Transmission Distribution*, 9(2):115–123, 2015. doi:10.1049/iet-gtd.2014.0276. (cited on page 71)

[Kra15] D. Krambeck. An introduction to SCADA systems. Technical report, 2015. (cited on page 62)

[KT11] B. Kasztenny and M. J. Thompson. Breaker failure protection — standalone or integrated with zone protection relays? In *2011 64th Annual Conference for Protective Relay Engineers*, pages 385–395, April 2011. doi:10.1109/CPRE.2011.6035639. (cited on page 39)

[KWK10] H. Kuehn, M. Wache, and R. Krebs. Wide area monitoring with synchrophasors German experiences. In *IEEE PES General Meeting*, pages 1–5, July 2010. doi:10.1109/PES.2010.5588087. (cited on pages xv, 64, 65)

[LBD+16] R. Li, C. Booth, A. Dyśko, A. Roscoe, H. Urdal, and J. Zhu. A systematic evaluation of network protection responses in future converter-dominated power systems. In *13th International Conference on Development in Power System Protection 2016 (DPSP)*, pages 1–7, March 2016. doi:10.1049/cp.2016.0063. (cited on page 46)

[LBI+17] C. Lu, T. Bi, M. Ilic, K. Tomsovic, and X. Wang. Guest editorial: New trends in wide-area monitoring and control of power systems with large scale renewables. *IET Generation, Transmission Distribution*, 11(18):4403–4405, 2017. doi:10.1049/iet-gtd.2017.1698. (cited on pages xi, 67)

[LH14] J. Liao and C. He. Wide-area monitoring protection and control of future power system networks. In *2014 IEEE Workshop on Advanced Research and Technology in Industry Applications (WARTIA)*, pages 903–905, Sep. 2014. doi:10.1109/WARTIA.2014.6976419. (cited on page 68)

[LSWS15] C. Lu, B. Shi, X. Wu, and H. Sun. Advancing China? smart grid: Phasor measurement units in a wide-area management system. *IEEE Power and Energy Magazine*, 13(5):60–71, Sep. 2015. doi:10.1109/MPE.2015.2432372. (cited on pages 10, 57)

[LTY12] L. Luo, N. Tai, and G. Yang. Wide-area protection research in the smart grid. In *2012 International Conference on Future Energy, Environment, and Materials*, volume 16, pages 1601–1606, 2012. (cited on page 63)

[LYY+17] Y. Liu, S. You, W. Yao, Y. Cui, L. Wu, D. Zhou, J. Zhao, H. Liu, and Y. Liu. A distribution level wide area monitoring system for the electric power Grid–FNET/GridEye. *IEEE Access*, 5:2329–2338, 2017. doi:10.1109/ACCESS.2017.2666541. (cited on pages xi, 54, 55)

[LYZH13] Z. Li, X. Yin, Z. Zhang, and Z. He. Wide-area protection fault identification algorithm based on multi-information fusion. *IEEE Transactions on Power Delivery*, 28(3):1348–1355, July 2013. doi:10.1109/TPWRD.2013.2247638. (cited on page 80)

[LZV16] X. Liu, X. Zhang, and V. Venkatasubramanian. Distributed voltage security monitoring in large power systems using synchrophasors. *IEEE Transactions on Smart Grid*, 7(2):982–991, March 2016. doi:10.1109/TSG.2015.2410219. (cited on page 68)

[Mar16] S. Marx. An introduction to symmetrical components, system modeling and fault calculation. Technical report, 2016. (cited on pages x, 20, 21, 23)

[Mata] Mathworks. Overview of matlab product suite. Technical report. URL: https://uk.mathworks.com/products/Matlab.html. (cited on page 168)

[Matb] Mathworks. Simscape Electrical. Technical report. URL: https://uk.mathworks.com/products/simscape-electrical.html. (cited on page 169)

[MGSX16] P. Mei, Y. Guowen, S. Su, and L. Xiangning. A novel algorithm of wide-area protection based on protection priority. In *2016 IEEE International Conference on High Voltage Engineering and Application (ICHVE)*, pages 1–4, Sep. 2016. doi:10.1109/ICHVE.2016.7800818. (cited on page 82)

[MLT16] J. Ma, C. Liu, and J. S. Thorp. A wide-area backup protection algorithm based on distance protection fitting factor. *IEEE Transactions on Power Delivery*, 31(5):2196–2205, Oct 2016. doi:10.1109/TPWRD.2015.2504128. (cited on page 81)

[MSW09] S. Mohagheghi, J. Stoupis, and Z. Wang. Communication protocols and networks for power systems-current status and future trends. In *2009*

IEEE/PES Power Systems Conference and Exposition, pages 1–9, March 2009. doi:10.1109/PSCE.2009.4840174. (cited on pages xi, 62)

[Muk14] S. Mukhopadhyay. Indian experience with smart grid applications - transmission sector. Technical report, 2014. (cited on page 57)

[MyT16] MyTechInfo. Sequence impedance of power system elements. Technical report, 2016. URL: http://www.mytech-info.com/2016/07/sequence-impedance-of-power-system.html. (cited on page 21)

[Nag16] Y. Nagarjun. Application of synchrophasors in power plants incorporated with condition monitoring systems. Technical report, 2016. (cited on page 59)

[NAP17] NAPSI. Synchrophasors & The Grid, 2017. Technical report, 2017. (cited on page 69)

[NAS17] NASPI Control Room Solutions Task Team. Using synchrophasor data for oscillation detection. Technical report, 2017. (cited on pages xi, 67)

[Nat11] National Grid. Application and protection setting policy for the national grid uk transmission system. Technical report, 2011. (cited on pages 7, 36, 38, 42, 94)

[Nat14] National Infrastructure Commission. Smart power. Technical report, 2014. URL: https://assets.publishing.service.gov.uk/government/uploads/system/uploads/attachment_data/file/505218/IC_Energy_Report_web.pdf. (cited on pages x, 3)

[Nat15a] National Grid. Future energy scenario. Technical report, 2015. URL: http://media.nationalgrid.com/media/1169/future_energy_scenarios_2015.pdf. (cited on pages x, xi, 2, 6, 43, 44, 45, 46, 47, 48)

[Nat15b] National Grid. GC0062 – Fault Ride Through. Technical report, 2015. URL: https://www.nationalgrideso.com/document/13246/download. (cited on page 8)

[Nat15c] National Grid. System operability framework 2015. Technical report, 2015. URL: https://www.nationalgrideso.com/

insights/system-operability-framework-sof. (cited on pages x, xiii, 4, 6, 9, 201, 202)

[Nat15d] National Grid. The Grid Code. Technical report, 2015. (cited on pages 48, 50)

[Nat17] National Grid Electricity Transmission plc. The Grid Code, Issue 5, Revision 21. Technical report, 2017. URL: https://www.nationalgrideso.com/document/34091/download. (cited on page 6)

[Nat18] National Grid. Enhanced frequency control capability (EFCC). Technical report, 2018. (cited on pages xi, 67)

[Nat19] National Grid ESO. Zero carbon operation of Great Britain's electricity system by 2025. Technical report, 2019. URL: https://www.nationalgrideso.com/news/zero-carbon-operation-great-britains-electricity-system-2025. (cited on page 201)

[NGR17] NGR. The large costs of even the smallest power outage and tools to prevent them. Technical report, 2017. (cited on page 58)

[Nor11] North American Electric Reliability Corporation. Reliability guideline, transmission system phase backup protection. Technical report, 2011. (cited on pages 36, 37, 42, 47)

[Nor14] North American Synchrophasor Initiative (NASPI). PMUs and synchrophasor data flows in North America. Technical report, 2014. (cited on pages xi, 57)

[NPB14] P. K. Nayak, A. K. Pradhan, and P. Bajpai. Wide-area measurement-based backup protection for power network with series compensation. *IEEE Transactions on Power Delivery*, 29(4):1970–1977, Aug 2014. doi:10.1109/TPWRD.2013.2294183. (cited on page 71)

[NPT18] NPTEL. Sequence networks of a loaded synchronous generator. Technical report, 2018. URL: https://nptel.ac.in/courses/108107028/module4/lecture7/lecture7.pdf. (cited on pages x, 20, 21, 34)

[NR15] M. K. Neyestanaki and A. M. Ranjbar. An adaptive PMU-based wide area backup protection scheme for power transmission lines. *IEEE Transactions on Smart Grid*, 6(3):1550–1559, May 2015. doi:10.1109/TSG.2014.2387392. (cited on page 69)

[Par11] Parliamentary Office of Science and Technology. UK electricity networks. Technical report, 2011. URL: https://researchbriefings.parliament.uk/ResearchBriefing/Summary/POST-PN-163#fullreport. (cited on page 24)

[Par12] J. Parmar. Delta-star transformer connection overview. Technical report, 2012. URL: https://electrical-engineering-portal.com/delta-star-transformer-connection-overview. (cited on page 100)

[PB13] Y. Paithankar and S. Bhide. *Fundamentals of power system protection*. PHI Learning Private Limited, 2013. (cited on pages x, 17)

[PMR+15] F. Palone, M. Marzinotto, M. Rebolini, S. Gentili, G. M. Giannuzzi, M. Schembari, and S. Lauria. Impact of renewable generation on commutation failures in multi-infeed HVDC systems: a real case study. In *11th IET International Conference on AC and DC Power Transmission*, pages 1–7, Feb 2015. doi:10.1049/cp.2015.0049. (cited on page 5)

[Pow12] Power Grid Corporation of India LTD. Unified real time dynamic state measurement. 2012. URL: http://www.cea.nic.in/reports/committee/scm/allindia/agenda_note/1st.pdf. (cited on page 10)

[Pow14] Power Standard Lab. MicroPMU. Technical report, 2014. (cited on page 10)

[Pre06] C. Preve. *Protection of Electrical Networks*. ISTE Ltd, 2006. (cited on page 17)

[Pri08] Richard Price. System events of 27th May. DSWG meeting, 2008. (cited on page 45)

[PVV16] C. Pisani, A. Vaccaro, and D. Villacci. Conceptualization and experimental deployment of an adaptive synchronized sensing system for power line ther-

mal monitoring. *IEEE Transactions on Industrial Informatics*, 12(6):2158–2165, Dec 2016. doi:10.1109/TII.2016.2601063. (cited on pages xi, 67)

[PWDV16] A. Phadke, P. Wall, L. Ding, and V.Terzija. Improving the performance of power system protection using wide-area monitoring systems. *Journal of Modern Power Systems and Clean Energy*, 4(3):319–331, July 2016. (cited on page 68)

[QUA17] QUANTA Technology. PMU deployment for enhanced protection and control. Technical report, 2017. (cited on page 57)

[QWHL11] L. Qin, Y. Wang, C. Hao, and M. Li. Multi-agent system wide area protection considering distributed generation impact. In *2011 International Conference on Advanced Power System Automation and Protection*, volume 1, pages 549–553, Oct 2011. doi:10.1109/APAP.2011.6180462. (cited on page 72)

[RAB13] A. J. Roscoe, I. F. Abdulhadi, and G. M. Burt. P and M class phasor measurement unit algorithms using adaptive cascaded filters. *IEEE Transactions on Power Delivery*, 28(3):1447–1459, July 2013. doi:10.1109/TPWRD.2013.2238256. (cited on pages 183, 209)

[RBJD] H. Renner, B.Heimbach, and title =Power quality and electromagnetic compatibility: special report, session 2 url = https://biblio.ugent.be/publication/6878660 J. Desmet, year=2015. Technical report. (cited on page 5)

[RBM01] M. A. Redfern, Z. Q. Bo, and D. Montjean. Detection of broken conductors using the positional protection technique. In *2001 Power Engineering Society Summer Meeting. Conference Proceedings (Cat. No.01CH37262)*, volume 2, pages 1163–1168 vol.2, July 2001. doi:10.1109/PESS.2001.970229. (cited on page 16)

[Roy] Royal Institute of Technology. SCADA and central applications. Technical report. (cited on page 63)

[San11] L. Santos. The use of synchrophasors for wide-area monitoring of electrical power grids. Technical report, 2011. (cited on pages xi, 67)

[Sch18] Schweitzer Engineering Laboratories. Tutorial on symmetrical components. Technical report, 2018. (cited on page 18)

[Sco17] Scottish Power. Visualisation of real time system dynamics using enhanced monitoring (VISOR). Technical report, 2017. (cited on pages xi, 57, 59)

[Sco18] Scottish Power Energy Networks. Visualisation of real time system dynamics using enhanced monitoring (VISOR). Technical report, 2018. (cited on pages xi, 67)

[SCY+17] Y. Sun, X. Chen, S. Yang, , K. J. Tseng, and G. Amaratunga. Micro PMU based monitoring system for active distribution networks. In *2017 IEEE 12th International Conference on Power Electronics and Drive Systems (PEDS)*, pages 518–522, Dec 2017. doi:10.1109/PEDS.2017.8289180. (cited on page 223)

[SGNP] S.M.Blair, G.M.Burt, N.Gordon, and title=Wide area protection and fault location : review and evaluation of PMU-based methods year=2018 volume= number= pages= month=Mar P.Orr, booktitle=The 14th International Conference on Developments in Power System Protection (DPSP). (cited on pages 65, 68)

[SK00] T. Seegers and E. Krizauskas. Transmission line protective systems loadability. Technical report, 2000. URL: http://www.pes-psrc.org/kb/published/reports/D6_Loadability.pdf. (cited on page 32)

[SKS+00] E. C. Senger, W. Kaiser, J. C. Santos, P. M. S. Burt, and C. V. S. Malagodi. Broken conductors protection system using carrier communication. *IEEE Transactions on Power Delivery*, 15(2):525–530, April 2000. doi:10.1109/61.852979. (cited on page 16)

[SMK+98] Y. Serizawa, M. Myoujin, K. Kitamura, N. Sugaya, M. Hori, A. Takeuchi, I. Shuto, and M. Inukai. Wide-area current differential backup protection employing broadband communications and time transfer systems. *IEEE Transactions on Power Delivery*, 13(4):1046–1052, Oct 1998. doi:10.1109/61.714445. (cited on page 72)

[Sor17] D. Sorensen. Symmetrical components, 2017. (cited on page 100)

[STD11] IEEE standard for synchrophasor measurements for power systems. *IEEE Std C37.118.1-2011 (Revision of IEEE Std C37.118-2005)*, pages 1–61, Dec 2011. doi:10.1109/IEEESTD.2011.6111219. (cited on pages xv, 55, 56)

[T.A] T.Agarwal. Know all about SCADA systems architecture and types with applications. Technical report. (cited on page 60)

[Taw] M. Tawfeeq. Power system protection - overcurrent protective relays. Technical report. (cited on pages x, 38)

[Tec] TechnologyUK. Supervisory control and data acquisition (SCADA). Technical report. (cited on page 60)

[Ter07] V. Terzija. Adaptive underfrequency load shedding based on the magnitude of the disturbance estimation. In *2007 IEEE Power Engineering Society General Meeting*, pages 1–1, June 2007. doi:10.1109/PES.2007.385657. (cited on page 68)

[TGCR17] A. Tahabilder, P. K. Ghosh, S. Chatterjee, and N. Rahman. Distribution system monitoring by using micro-PMU in graph-theoretic way. In *2017 4th International Conference on Advances in Electrical Engineering (ICAEE)*, pages 159–163, Sep. 2017. doi:10.1109/ICAEE.2017.8255346. (cited on pages 11, 223)

[TH15] M. J. Thompson and D. L. Heidfeld. Transmission line setting calculations - beyond the cookbook. In *2015 68th Annual Conference for Protective Relay Engineers*, pages 850–865, March 2015. doi:10.1109/CPRE.2015.7102209. (cited on page 42)

[The17] The SQSS Review Panel. National electricity transmission system security and quality of supply standard. Technical report, 2017. URL: https://www.nationalgrideso.com/codes/security-and-quality-supply-standards. (cited on page 6)

[TVC00] C. W. Taylor, M. V. Venkatasubramanian, and Y. Chen. Wide-area stability and voltage control. *VII symposium of specialist in electric operational and expansion planning*, 1:1–9, 2000. (cited on pages xi, 67)

[Udr14a] E. Udren. Principles for Practical Wide-Area Backup Protection with Synchrophasor Communications. *CIGRE Paris Session*, 2014. (cited on page 68)

[UDR14b] E. UDREN. Principles for practical wide-area backup protection with synchrophasor communications. In *CIGRE 2014*, 2014. (cited on page 68)

[Uni] University of Washington. 14 Bus Power Flow Test Case. Technical report. URL: `http://www.ee.washington.edu/research/pstca/pf14/pg_tca14bus.htm`. (cited on page 169)

[U.S09] U.S. department of Energy. Western Interconnection Synchrophasor Program. Technical report, 2009. (cited on pages xi, 67)

[U.S14] U.S. Department of Energy. Factors affecting PMU installation costs. Technical report, 2014. (cited on pages 56, 57)

[US15] S. Urooj and V. Sood. Phasor measurement unit (PMU) based wide area protection system. In *2015 2nd International Conference on Computing for Sustainable Global Development (INDIACom)*, pages 597–599, March 2015. (cited on page 54)

[UVd+12] K. Uhlen, L. Vanfretti, M. M. de Oliveira, A. B. Leirbukt, V. H. Aarstrand, and J. O. Gjerde. Wide-area power oscillation damper implementation and testing in the norwegian transmission network. In *2012 IEEE Power and Energy Society General Meeting*, pages 1–7, July 2012. `doi:10.1109/PESGM.2012.6344837`. (cited on pages xi, 67)

[VPXP17] V. Venkatasubramanian, P. Panciatici, F. Xavier, and T. Prevost. Oscillation monitoring and control of the RTE power system using synchrophasors. Technical report, 2017. (cited on pages xi, 67)

[WDM+15] P. Wall, P. Dattaray, P. Mohapatra, J. Yu, D. Wilson, S. Clark, M. Osborne, P. Ashton, and V. Terzija. Visor project: Opportunities for enhanced real time monitoring and visualisation of system dynamics in gb. In *2015 PAC World*, 2015. (cited on page 9)

[WSR+06] M. Weibel, W. Sattinger, P. Rothermann, U. Steinegger, and M. Zima. Overhead line temperature monitoring pilot project. In *CIGRE 2006 Session*, Sep 2006. (cited on pages xi, 67)

[WTS+12] Z. Wu, K. Thomas, R. Sun, V. A. Centeno, and A. G. Phadke. Three-phase instrument transformer calibration with synchronized phasor measurements. In *2012 IEEE PES Innovative Smart Grid Technologies (ISGT)*, pages 1–6, Jan 2012. doi:10.1109/ISGT.2012.6175540. (cited on pages xi, 67)

[WZZ+17] D. Wang, S. Zhao, S. Zhang, S. Song, J. Ma, and W. Zhang. Adaptive voltage protection scheme based on wide area information. *The Journal of Engineering*, 2017(13):2508–2513, 2017. doi:10.1049/joe.2017.0779. (cited on page 76)

[XTEK14] W. Xiao, K. Torchyan, M. S. El Moursi, and J. L. Kirtley. Online supervisory voltage control for grid interface of utility-level PV plants. *IEEE Transactions on Sustainable Energy*, 5(3):843–853, July 2014. doi:10.1109/TSTE.2014.2306572. (cited on pages xi, 67)

[XTTE12] Y. Xue, M. Thakhar, J. C. Theron, and D. P. Erwin. Review of the breaker failure protection practices in utilities. In *2012 65th Annual Conference for Protective Relay Engineers*, pages 260–268, April 2012. doi:10.1109/CPRE.2012.6201237. (cited on pages 39, 40, 41)

[XZY18] Y. Xue, X. Zhang, and C. Yang. Commutation failure elimination of LCC HVDC systems using thyristor-based controllable capacitors. *IEEE Transactions on Power Delivery*, 33(3):1448–1458, June 2018. doi:10.1109/TPWRD.2017.2776867. (cited on page 5)

[YSWW10] X. Yang, Y. Song, G. Wang, and W. Wang. A comprehensive review on the development of sustainable energy strategy and implementation in China. *IEEE Transactions on Sustainable Energy*, 1(2):57–65, July 2010. doi:10.1109/TSTE.2010.2051464. (cited on page 2)

[ZAS15] J. Zare, F. Aminifar, and M. Sanaye-Pasand. Communication-constrained regionalization of power systems for synchrophasor-based wide-area backup

protection scheme. *IEEE Transactions on Smart Grid*, 6(3):1530–1538, May 2015. doi:10.1109/TSG.2014.2387051. (cited on pages 69, 77)

[ZCM+17] L. Zhang, H. Chen, K. Martin, A. Faris, M. Vutsinas, T. Bradberry, E. Phillips, B. Abu-Jaradeh, and J. Bui. Successful deployment and operational experience of using linear state estimator in wide-area monitoring and situational awareness projects. *IET Generation, Transmission Distribution*, 11(18):4476–4483, 2017. doi:10.1049/iet-gtd.2016.2028. (cited on pages xi, 67)

[ZLK+05] M. Zima, M. Larsson, P. Korba, C. Rehtanz, and G. Andersson. Design aspects for wide-area monitoring and control systems. *Proceedings of the IEEE*, 93(5):980–996, May 2005. doi:10.1109/JPROC.2005.846336. (cited on pages xi, 63, 67)

[ZLZ+12] X. Zhang, F. Lu, Y. Zhang, F. Deng, and X. Zhang. On-line fault locating method for wide area back-up protection. In *2012 Asia-Pacific Power and Energy Engineering Conference*, pages 1–3, March 2012. doi:10.1109/APPEEC.2012.6307404. (cited on page 72)